CONFIDENTIAL

REFERENCE ONLY

UNIVERSITY OF LONDON THESIS

Degree PhD Year 2005 Name of Author CAFFITE, V.G.H.

COPYRIGHT

This is a thesis accepted for a Higher Degree of the University of London. It is an unpublished typescript and the copyright is held by the author. All persons consulting the thesis must read and abide by the Copyright Declaration below.

COPYRIGHT DECLARATION

I recognise that the copyright of the above-described thesis rests with the author and that no quotation from it or information derived from it may be published without the prior written consent of the author.

LOANS

Theses may not be lent to individuals, but the Senate House Library may lend a copy to approved libraries within the United Kingdom, for consultation solely on the premises of those libraries. Application should be made to: Inter-Library Loans, Senate House Library, Senate House, Malet Street, London WC1E 7HU.

REPRODUCTION

University of London theses may not be reproduced without explicit written permission from the Senate House Library. Enquiries should be addressed to the Theses Section of the Library. Regulations concerning reproduction vary according to the date of acceptance of the thesis and are listed below as guidelines.

A. Before 1962. Permission granted only upon the prior written consent of the author. (The Senate House Library will provide addresses where possible).

B. 1962 - 1974. In many cases the author has agreed to permit copying upon completion of a Copyright Declaration.

C. 1975 - 1988. Most theses may be copied upon completion of a Copyright Declaration.

D. 1989 onwards. Most theses may be copied.

This thesis comes within category D.

☑ This copy has been deposited in the Library of UCL

☐ This copy has been deposited in the Senate House Library, Senate House, Malet Street, London WC1E 7HU.

Design and Synthesis of Self-Assembling Systems with Multiple Hydrogen Bonding Interactions

Valérie Gisèle Hélène Lafitte

A thesis presented to the University of London in partial fulfillment for the degree of Doctor of Philosophy

Department of Chemistry

University College London

June 2005

ProQuest LLC
789 East Eisenhower Parkway
P.O. Box 1346
Ann Arbor, MI 48106-1346

To my parents,

Jean-Paul and Marie-Christine

DECLARATION

I, Valérie Gisèle Hélène Lafitte, hereby state that the following is entirely my own work and has not been for any other degree or examination.

Valérie Gisèle Hélène Lafitte

June 2005

ACKNOWLEDGMENTS

First, I would like to thank my supervisor Dr Helen Hailes for giving me the opportunity to carry out this project, for her guidance and constant support throughout this PhD.

I thank my industrial supervisor Peter Golding at AWE for financial support. I would like to thank Dr Kason Bala and Hemant Desai for their assistance.

I would like to thank Dr Abil Aliev for his useful help in NMR and molecular modelling.

The X-ray crystallography centre at Southampton is thanked for providing the crystallographic structures. In addition I would like to thank Ashley Hulme for his advices in crystals growing.

I would like to thank Jon and Steve from mass spectroscopy and Dave for his kind assistance on repairing some equipment.

This thesis would not have been the same without my friends and colleagues, and for that reason I would like to thank Jonny for the good laugh and sharing with me his "rock" addiction. I thank my "Sex and the City" girls Ana, Mackie and Rosie for their support and positive spirit and the good moments in and out of the lab. I thank John, Firouz and Olivia for the happy moments. Furthermore, I would like to thank Anne-Cécile for her encouragement during all this time.
I would like to thank my dear flatmates over the last three years, in particular Alexandra, Waleed, Elenaor, Philipp, Arnt and Marco for their friendship and good dinners.
I thank my friends Virginie, Jean-François and Stephanie for their constant support.

Finally I would like to thank my parents and grandparents, my brother, Natalia and little Dimitri, Alexandre, Eve and Alexis for their loving support.

Merci à vous tous!

ABSTRACT

Hydrogen bonding is one of the most useful interactions for the self-assembly of molecular subunits into well-defined supramolecular structures. Recent attention has been focused on systems capable of forming strong, directional, and reversible quadruple hydrogen bonds. Meijer *et al.* have made a significant impact in this area with the synthesis of stable DDAA dimers based on ureidopyrimidinones (Upy) with a dimerisation constant greater than 10^7 M^{-1} in chloroform. This work is reviewed in Chapter I of this thesis.

A less attractive feature of the Upy unit is the possibility of up to three tautomeric forms in solution. The nature of the substituents at C-6 has been shown to influence the tautomeric equilibrium. Chapter II of this thesis describes the synthesis of an ureidopyrimidinone compound incorporating an electron-donating group (p-$C_6H_4NH_2$) at the C-6 position, which has led to the formation of the dimeric form DADA in DMSO-d_6. It was the first time that the hydrogen bonded dimeric Upy was observed in such a polar solvent.

Chapter III describes the use of quadruple hydrogen bonded Upy units in the chain extension of various energetic (PolyGlyn) and non-energetic (polyether and polycarbonate based) telechelic polymers, which has led to the formation of supramolecular polymers with increased elastomeric properties. In addition, the development of an alternative synthetic approach avoiding the use of isocyanate has been successfully achieved leading to supramolecular polymers of improved quality.

In addition, the synthesis of bifunctional Upys incorporating small chiral spacers has been achieved and described in Chapter IV. Notably, it was found that the use of diethyl L-tartrate or butane diol led to the formation of extremely stable cyclic dimers in chloroform with a dimerisation constant greater than 10^8 M^{-1}. The formation of new intramolecular hydrogen bonds within the cyclic species was observed in the crystal structure and was found to stabilise the dimeric form in solution.

Finally, the design of a new quadruple hydrogen bonded DDAA array based on cytosine has been successfully achieved *via* a straightforward synthetic strategy (Chapter V). The structure of the linear DDAA/AADD dimer was revealed in the solid state and in solution with a dimerization constant greater than 10^5 M^{-1} in chloroform. The synthesis of the first generation of polymers based on this new unit has been achieved. The obtained results show great potential for the future material applications.

CONTENTS

FIGURES

TABLES

SCHEMES

GRAPHS

ABBREVIATIONS

A: Acceptor (in hydrogen bonding systems)

A: Adenine

Å: Angstroms

AMMO: 3-Azidomethyl-3-methyl oxetane

Ar: Aromatic group

AWE: Atomic Weapons Establishment

BAMMO: 3,3-Bis-(azidomethyl)oxetane

BnBr: Benzyl bromide

BnOH: Benzyl alcohol

BOC: *tert*-Butoxycarbonyl

Bu: Butyl

C: Cytosine

C.A.: Cyanuric Acid

cat.: Catalyst

CBz: Benzyloxycarbonyl

$CDCl_3$: Chloroform, deuterated

CDI: *N,N*-Carbonyldiimidazole

$CHCl_3$: Chloroform

COSY: Correlated Spectroscopy

CPMAS: Cross Polarisation Magic Angle Spinning

°C: Degree Celcius

D: Donor (in hydrogen bonding systems)

D: Diffusion coefficient (NMR)

d: Deformation vibration (IR)

d: Doublet (NMR)

dd: Doublet of doublets (NMR)

ddd: Doublet of doublets of doublets

dt: Doublet of triplets

Da: Daltons

DCC: Dicyclohexylcarbodiimide

DFT: Density Functional Theory

DHP: Dihydropyrane

DMAP: Dimethylaminopyridine

DP: Degree of Polymerisation

DMF: Dimethylformamide

DMSO: Dimethylsulfoxide

DMSO-d_6: Dimethyl Sulfoxide deuterated

DNA: Deoxyribonucleic acid

DSC: Differential Scanning Calorimetry

2D: Two dimensional

3D: Three dimensional

EDCI: 1-(3-Dimethylaminopropyl)-3-ethylcarbodiimide hydrochloride

EtOAc: Ethyl Acetate

EtOH: Ethanol

ES (+): Positive ion spectroscopy

EXSY: Exchange Spectroscopy

FTIR: Fourier Transformation Infrared Spectroscopy

G: Guanine

GAP: Glycidyl Azide

GLYN: Glycidyl Nitrate

Gn: n Generation (for dendrimers)

GPC: Gas Phase Chromatography

h: Hour

Hz: Hertz

HMQC: Heteronuclear Multiple Quantum Coherence

HMBC: Heteronuclear Multiple Bond Correlation

HOBt: Hydroxybenzotriazole

HRMS: High Resolution Mass Spectroscopy

I: Intensity (Fluorescence)

IMCI: Isocyanatomethyl-methylcyclohexylisocyanate

J: Coupling constant (NMR)

J: Joules

K: Kelvin (Temperature)

K_a: Associaction constant

K_{dim}: Dimerisation constant

kJ: Kilo Joules

Leu: Leucine

LG: Leaving Group

M: Molar concentration

M: Melamine

m: Multiplet (NMR)

m/z: Mass to charge ratio

MeOH: Methanol

MHz: Mega Hertz

NIMMO: Nitratomethyl-3-methyl oxetane

MMX: Molecular Mechanics Extended

M_n: Average molecular weight

mol: Mole

mp: Melting point

mono: Monomer (Florescence)

Napy: 2,7 Diamino-1,8-naphtyridine

NHS: *N,N*-Hydroxy succinimide

NMR: Nuclear Magnetic Resonance

NOE: Nuclear Overhauser Effect

NOESY: Nuclear Overhauser Effect Spectroscopy

PBX: Polymer Bonded explosive

PEG: PolyethyleneGlycole

Ph: Phenyl

PIPS: Polymerisation induced phase separation

PPG: PolypropyleneGlycole

ppm: Part per million

Phe: Phenylalanine

Pyr: Pyrene (Fluorescence)

PTS: *para*-Toluene sulfonic acid

q: Quartet (NMR)

r.t.: Room temperature

RNA: Ribonucleic Acid

ROE: Rotating Frame Overhauser Effect

s: Singlet (NMR)

s: Stretching vibration (IR)

Ser: Serine

T: Thymine

t: Triplet (NMR)

TFA: Trifluoroacetic acid

T_g: Glass transition temperature

THF: Tetrahydrofuran

THP: Tetrahydrpyrane

TLC: Thin Layer Chromatography

TMV: Tobacco Mosaic Virus

Upy: Ureidopyrimidinone

v: Volume

Val: Valine

W: Watt

w: Weight

Chapter I

1 Introduction to Supramolecular Chemistry

1.1 Molecular Recognition

As proposed by J.-M Lehn, supramolecular chemistry can be defined as "the chemistry beyond the molecule" or "the chemistry of the non-covalent bond" and involves molecular systems in which the components are held together reversibly by intermolecular forces, as opposed to covalent bonds (Table 1).[1,2,3,4,5] Supramolecular scientists have crossed the traditional boundaries of their disciplines in order to address specific objectives. Indeed, this interdisciplinary field of science has extended its roots from organic chemistry, inorganic, physics and biology, and has provided a large source of inspiration for chemists involved in the building block design, as well as the understanding of supramolecular structures.

	Covalent	**Non-covalent**
Building block	Atoms	Molecules, ions
Target	Molecule	Assembly
Molecular weight	1000 Da	100 kDa
Bond type	Covalent	Ionic, hydrophobic, metal coordination, hydrogen bonds
Bond energy	350-942 kJ mol^{-1}	2-250 kJ mol^{-1}

Table 1: Differences between covalent and non-covalent synthesis

Complimentarity is a fundamental concept in this field. In 1894, Emil Fisher described this idea as the 'Lock and Key principle'.[6] In this context, a 'supramolecule' can be visualised as a 'host-guest complex' where a molecule 'host' or 'lock' is bonded to another molecule 'guest' or 'key' by non-covalent interactions. Supramolecular host-guest compounds were the first structures studied as part of this new field of chemistry also known as molecular recognition. Much supramolecular chemistry has sprung from development in macrocyclic chemistry in the mid-to-late-1960s. Charles Pedersen made an important breakthrough in 1960, while attempting the synthesis of multidentate ligands for copper and vanadium (bis [2-(*o*-hydroxy-phenoxy)ethyl]ether (**1**)). He isolated instead, a macrocyclic compound, commonly known as crown ether today or more precisely Dibenzyl [18] crown-6 (**2**).[7] Later, Pedersen,[8] Lehn[9,10,11] and Cram[12]

shared the Nobel prize in 1987 for their discovery of crown ethers and cryptands (**3**) (3D crown ethers).

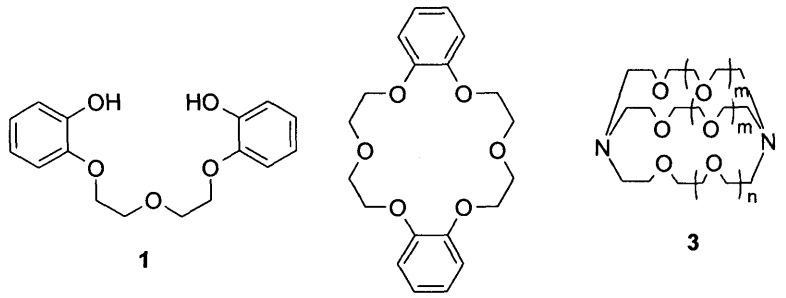

Figure 1: Examples of macrocyclic molecules synthesised by Pedersen, Cram and Lehn

Since the 1980s, several other host-guest systems have been reported.[13,14] Different classes of supramolecular structures exist which depend on the nature of the host and guest, as well as the nature of the interactions between them. Some of the most common macrocyclic structures are listed in Table 2.

Host	Guest	Class	Example
Crown ether (4)	Metal cations	Cavitand	K^+ [18]crown-6
Spherand (5)	Alkyl ammonium cations	Cavitand	Spherand ($CH_3NH_3^+$)
Calixarene (6)	Organic molecules, or cations	Clathrand	*p*-t-butylcalix[4]arene
Cyclodextrin (7)	Organic molecule	Clathrand	α-cyclodextrin.*p*-hydroxybenzoic acid
Cyclophane (8)	Anions or neutral molecules	Cavitand	Cyclophane-durene

Table 2: Classes of macrocyclic molecules

Cavitands are hosts possessing intramolecular cavities, which allow the binding of guests *via* its specific site interactions. Crown ethers (**4**) and Spherands (**5**) are well-known examples for their binding with metal cations (eg. K^+, Na^+, Li^+).[15] Clathrands (**6,7**) are hosts with extra-molecular cavities and are mainly relevant in the solid state. Cyclophanes are generally used as receptors for apolar guests (**8**).

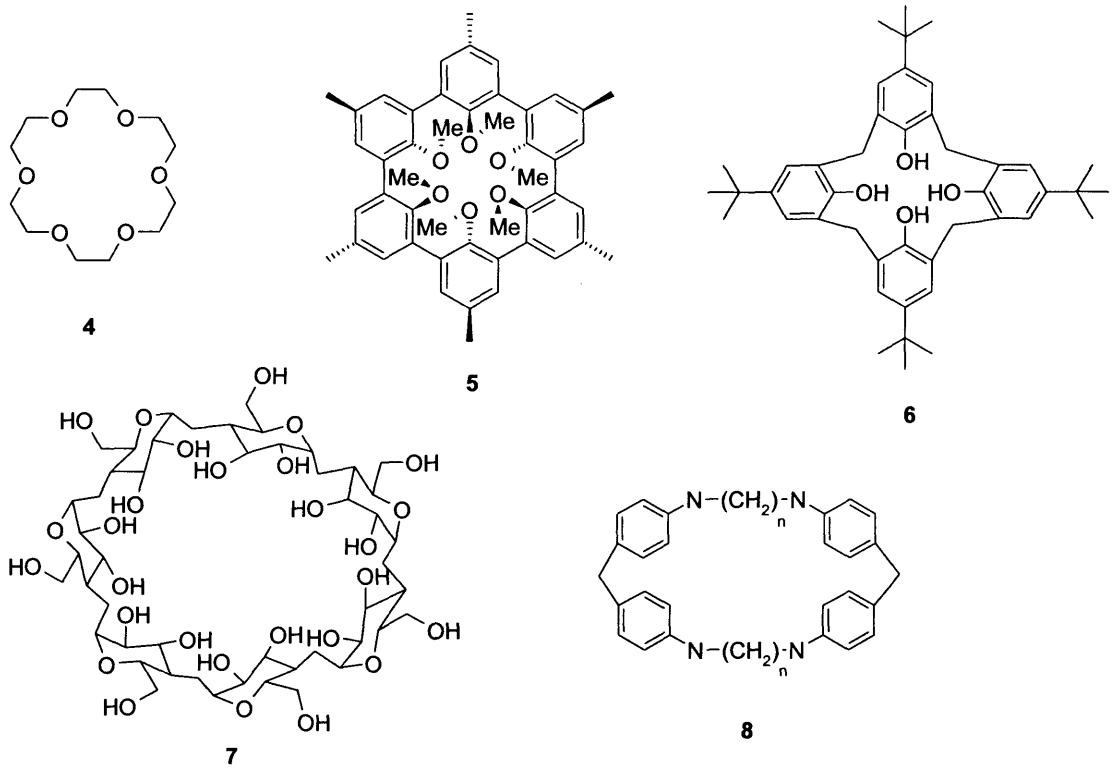

Figure 2: Examples of macrocyclic structures

Host-guest chemistry is not the only area of research as part of this growing field. In the last decade, work has focused on the development of systems that are able to spontaneously self-assemble *via* non-covalent interactions in order to generate large supramolecular architectures.[16]

1.2 Supramolecular Self-Assembly

The term 'self-assembly' is used to describe the thermodynamically controlled ordering that involves atom-specific non-covalent interactions. Self-assembly may lead to finite-sized assemblies (e.g., hydrogen bonded dimers) or may create extended structures (one dimensional chains, two-dimensional sheets and three-dimensional networks). On mixing appropriately designed components (or synthons) in solution, the intermolecular forces that exist between them control their orientation, leading to the reversible assembly of a specific 'supermolecule'.

1.2.1 Supramolecular Interactions

Supramolecular chemistry includes non-covalent bonding interactions. The term 'non-covalent' encompasses an enormous range of attractive and repulsive forces. Several non-covalent interactions have been studied, such as electrostatic interactions (ion-ion, ion-dipole, dipole-dipole), hydrophobic interactions,[17,18] π-π stacking interactions, induction forces (Van der Waals) and hydrogen bonding interactions.

1.2.1.1 *Electrostatic Interactions (100-250 kJ/mol)*[19]

Electrostatic interactions (ion-ion, dipole-ion or dipole-dipole) are based on the Coulombic attraction between opposite charges. Whilst ion-ion interactions do not require directionality of the species, dipole-dipole or ion-dipole interactions must have a suitable alignment for strong binding. Ionic binding is comparable in strength to covalent bonding which makes it a valuable tool for use in supramolecular devices.

1.2.1.2 *π-Interactions (0-50 kJ/mol)*[20a,b,21]

These interactions have long been observed in the crystal structure of aromatic rings and take advantage of the electron rich molecular orbitals of aromatic and vinyl systems. π-Stacking held a prominent place in stabilizing the DNA structure through vertical based pair interaction, as well as for the intercalation of potential drugs within the DNA double helix. There are two general types of π-stacking: face-to-face and edge-to-face (Figure 3). Hunter and Sanders have proposed a simple model to estimate the strength and geometric requirements for π-π stacking interactions. Their model is based on an overall attractive van der Waals interaction, which is proportional to the contact surface area of two π systems. This attraction could be regarded as an attraction between the negatively charged π-electron cloud of one molecule and the positively charged σ–framework of an adjacent molecule. Therefore, the ary-aryl geometry is determined by the electrostatic repulsions between the two negatively charged π-systems. Clearly the ary-aryl interaction is not driven to maximise the orbital overlap.

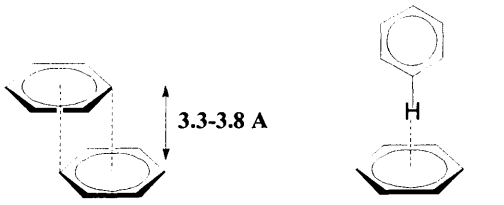

Figure 3: Two examples of π-π stacking interactions

1.2.1.3 *Hydrogen Bonding (4 -40 kJ/mol)*[22,23,24,25]

Because of its relatively strong and highly directional nature, hydrogen bonding has been described as the 'master key' interaction in supramolecular chemistry. Hydrogen bonds connect atoms X and Y that have electronegativities larger than that of hydrogen, generally C, N, O, F, P, S, Cl, Se, Br, and I. The XH group is then referred to as the 'proton donor' (D) and the Y atom as the 'proton acceptor' (A). The strength of a hydrogen bond increases with an increase in the dipole moment of the X-H bond. Therefore, hydrogen bonds can be classified as strong, moderate or weak interactions as shown below in Table 3.

	Strong	**Moderate**	**Weak**
Bond energy (kcal/mol)	15-40	4-15	<4
Bond length (Å)			
H...Y	1.2-1.5	1.5-2.2	>2.2
X...Y	2.2-2.5	2.5-3.2	>3.2
Bond angles (°)	175-180	>130	>90
Examples	Donor: $-O^{+}-H$, Acceptor: F^{-}. $^{-}O-H$	Donor: O-H, N-H Acceptor: C=O, O-	Donor: C-H, Si-H Acceptor: π–electrons

Table 3: Classification of hydrogen bonds

There are different types of hydrogen bonds depending on their geometry (Figure 4). The simplest is a D-H...A arrangement with a favoured angle close to 180°. In some cases one hydrogen atom interacts with more than one acceptor, often called bifurcated arrangement, other cyclic types can also be found as illustrated in Figure 4.

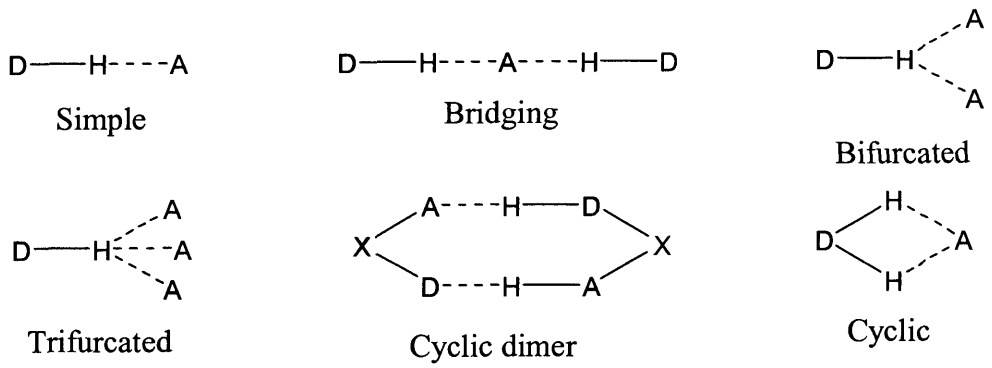

Figure 4: Different hydrogen bond types

1.2.2 Experimental Detection of Hydrogen Bonds

1.2.2.1 *^{1}H NMR Spectroscopy*[26]

NMR spectroscopy is probably one of the most useful tools for the determination of the supramolecular structure. The electron density decreases significantly at the proton involved in hydrogen bonding, leading to a shift of the corresponding NMR signal towards higher frequencies.[27,28] The magnitude of this chemical shift is indicative of the strength of the hydrogen bonding involved. The sensitivity of ^{1}H NMR spectroscopy to changes in electronic environments make it a useful probe for the detection of hydrogen bonds from weak donors, such as S-H and C-H and weak acceptors, such as multiple bonds and aromatic rings. Due to the complexity of hydrogen bonding in solution, the use of routine 1D NMR spectroscopy is limited. To overcome these limitations, new NMR techniques have been developed such as EXSY, which involves measurements of the exchange rates. Furthermore, 2D NMR techniques such as NOESY, COSY and TOCSY, have greatly facilitated the characterisation of hydrogen bonded assemblies. Also, dilution experiments are often a good way to measure the association constant of the binding system, by monitoring the changes in chemical shifts or other parameters (e.g. diffusion rates) due to variation of the strength of hydrogen bonding.

1.2.2.2 *Vibrational Spectroscopy*

Infrared spectroscopy is a straightforward technique to establish the existence of hydrogen bond since the presence of such interactions induces an important large red

shift (>100 cm^{-1}) of the fundamental X-H stretching vibration, and occurs as a consequence of the elongation of the X-H bond. The magnitude of the red shift is directly proportional to the hydrogen bonding strength (Badger-Bauer relation).[29] The strength of the intermolecular hydrogen bond is directly related to the intensity of the observed peak.

1.2.2.3 *Diffraction Methods: X-Ray and Neutron Diffraction*

Single crystal structure analyses have a special role in the study of hydrogen bonds because they provide direct information on their stereochemistry and local environment. This technique coupled with vibrational spectroscopy is an excellent tool for distinguishing the nature of the hydrogen bonds, whether they are strong, moderate or weak.

1.2.2.4 *Theoretical*

This approach includes semi-empirical and empirical calculations, and the use of modelling. This field is continuously growing, with the development of more powerful and efficient ways of calculation.[26]

Conclusions

Non-covalent bonding interactions define and direct the self-assembly process that leads to the formation of new supramolecular architectures, and also govern any dynamic process that occur within the structure. Due to the reversibility and directionability of hydrogen bonds they become an essential 'glue' for the assembly of small molecules into larger aggregates. The formation and properties of hydrogen bonded supramolecular structures will be discussed in the next section.

1.3 Hydrogen Bond Directed Self-Assembly

1.3.1 Biological Self-Assembling Systems

1.3.1.1 *DNA Double helix*

The idea of building supramolecular species originates from nature[30,31] and especially from biological aggregates like the DNA double bond helix.[32] The pairing of nucleic acid strands is perhaps the most elegant example of self-assembly in nature.[33] Two anti-parallel strands are held together *via* complimentary hydrogen bonds betweens pairs of bases forming the natural polymer (Figure 5). The nucleic acid bases are arranged such that cytosine (C) forms three hydrogen bonds with guanine (G) (**9**) while adenine (A) forms two complamentary hydrogen bonds with thymine (T) (**10**).

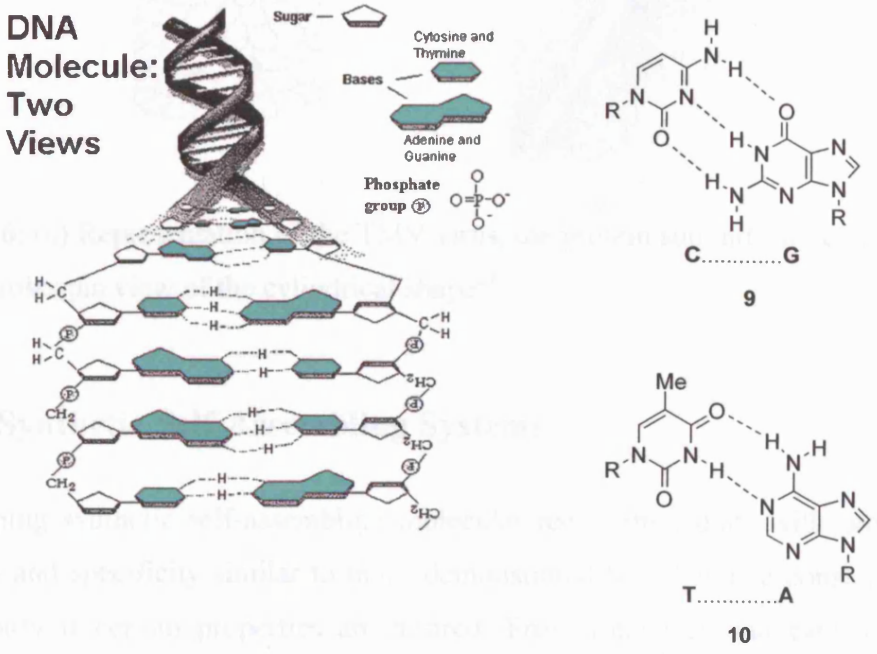

Figure 5: Structure of DNA and complimentary bases[33a]

DNA is certainly the most studied 'strict self-assembly' example, meaning that the final compound is produced directly and spontaneously when the right subunits are mixed together under the appropriate conditions. Any error that may occur will be automatically corrected.

1.3.1.2 *Tobacco Mosaic Virus*

Another well known and widely described example of self-assembly is the tobacco mosaic virus (TMV) (Figure 6), the first macromolecular system purified and the first to be shown to self-assemble in vitro.[27,34] The viral particle is composed of 2130 identical subunits, each comprising 158 amino acids which form a helical sheath around a single strand of RNA (6390 base pairs in length). The helical virus particle is 300 nm long and possesses a diameter of 18 nm. This example shows the potential of biological systems to create super-structures with molecular order, from originally small units through the self-assembly process.

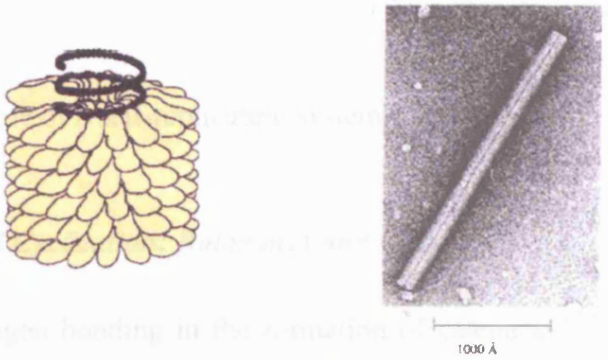

Figure 6: (a) Representation of the TMV virus, the protein subunits are coloured yellow (b) Microscopic view of the cylindrical shape[27]

1.3.2 Synthetic Self-Assembling Systems

Developing synthetic self-assembling molecular recognition units with programmable strength and specificity similar to those demonstrated by DNA is a constant challenge particularly if certain properties are desired. From rotaxanes and catenanes to self-replicating systems, advances in the understanding of the intermolecular forces have provided successful design of complex self-assembling systems.[35] Here, some examples of creative synthetic strategies are considered.

1.3.2.1 *Templed Synthesis: Self-Replicating Molecular Systems*

Based on the concept of auto-replication found in nature, chemists have successfully designed molecules that can self-replicate *via* autocatalytic processes. A synthetic system that replicates in a polar solvent has been reported by Terfort and von

Kiedrowski[36] where the product acts as a catalyst for its own formation. Strong hydrogen bonding between the carboxylate and amidinium (K_a = 350 M^{-1} in DMSO) results in close proximity of the molecules allowing the reaction to proceed (Scheme 1).

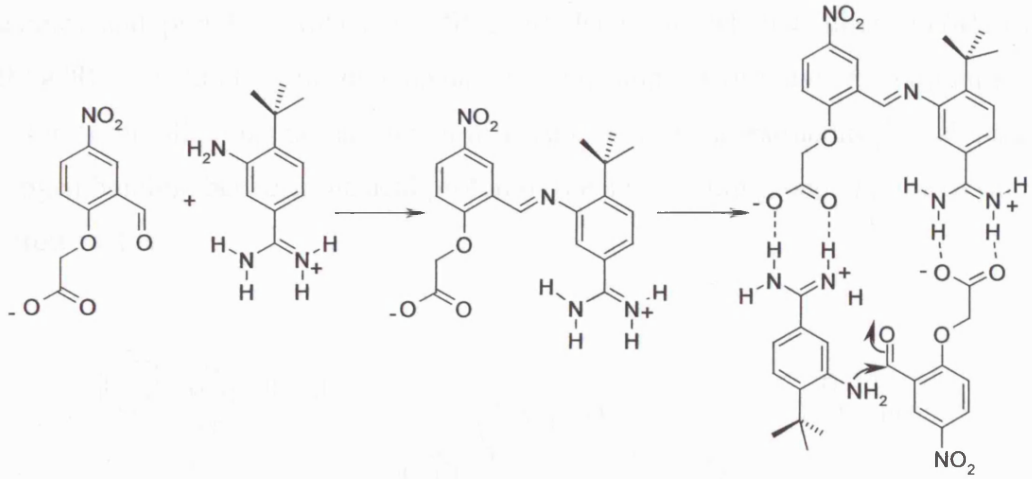

Scheme 1: Example of a self-replicating system

1.3.2.2 *Templed Cyclisation: Rotaxanes and Catenanes*

The use of hydrogen bonding in the formation of catenanes[37,38,39] and rotaxanes[40] has recently shown significant potential for the design of new 'interlocked' compounds. The formation of catenanes involves a template effect where a macrocycle complexes with its linear precursor to enhance the formation of the catenane. Leigh *et al.* have achieved the synthesis of a [2]-catenane through the reaction between acid chlorides and amines to form the amide bonds.[41,42] In this reaction, eight molecules must combine together to form the desired product. Hydrogen bonding between the amide groups is the driving force to generate the interlocked molecule and a total of six hydrogen bonds were revealed by X-ray crystallography as shown in Figure 7.

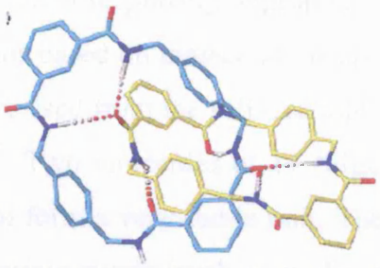

Figure 7: Crystal structure of catenane[42a]

Stoddart's strategy was based on the initial discovery by Pedersen that crown ethers can complex organic and cationic molecules, notably ammonium salts.[43,44] This has led to an efficient templated synthesis based on hydrogen bonding towards the formation of rotaxanes and pseudo[2]-rotaxanes. Stoddart demonstrated that dibenzo-[24]crown-8 (DB24C8) can bind both dibenzylammonium and bis(n-butyl ammonium) in a pseudorotaxane-like manner as shown in Figure 8. The superstructure is stabilised *via* hydrogen bonding between the acid proton of the ammonium group and the oxygens of the crown ether.

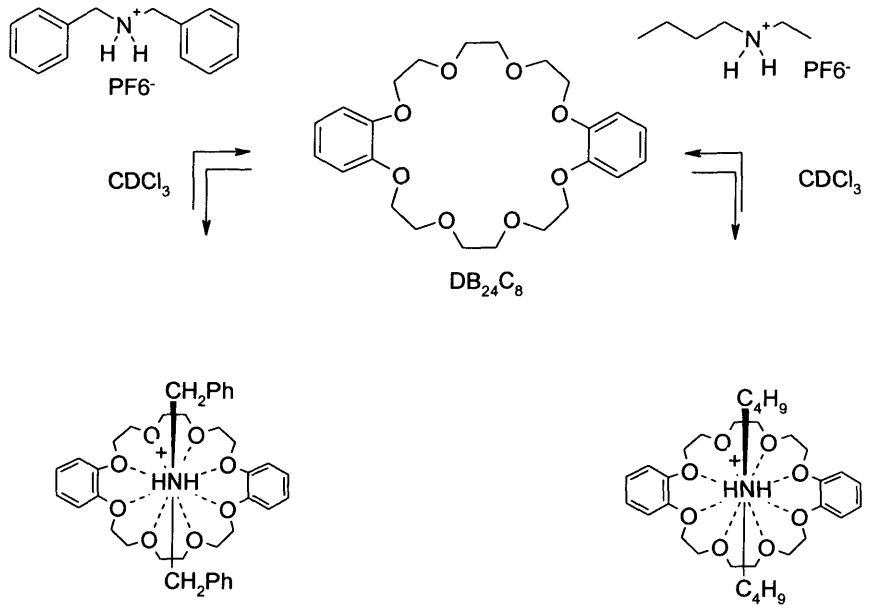

Figure 8: Crown ether binding ammonium salts in a pseudorotaxane manner

1.3.2.3 *Self-Assembled Capsules*

Molecular capsules are formed by the self-assembly of complimentary hydrogen bonding units, with the subunits displaying appropriate 'curvature'. Rebek *et al.* have developed numerous systems based on molecular encapsulation.[45] A key example is the so called 'tennis ball' synthesised from the self-assembly of two molecules of glycouryl with durene tetrabromide.[46] Two molecules of **11** (Figure 9) self-assemble in solution *via* eight hydrogen bonds to form a very stable unit. The molecular capsule formed can then act as a host for appropriate guests (such as methane or ethane) and bring them into a well defined nano-environment.

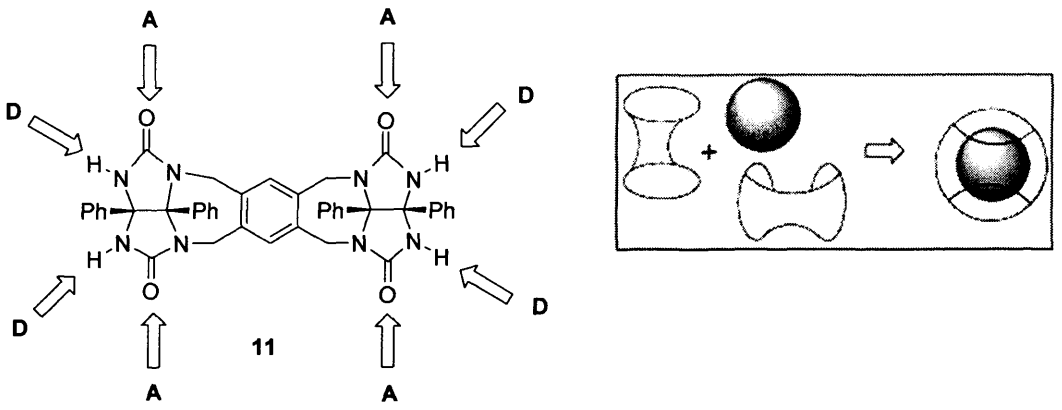

Figure 9: Self-assembled capsules: an example of the 'tennis ball'

For these tennis ball structures, the cavity size can reach 61 $Å^3$ and decrease to 37 $Å^3$ when the phenyl spacer is replaced by ethylene. Much longer spacers can be used as well, leading to a 'soft-ball' capsules of larger size (313 $Å^3$), such as found in compound **12** (Figure 10).[47]

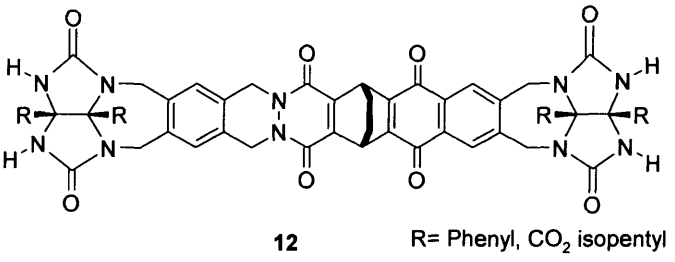

Figure 10: Example of the 'soft-ball' capsule

1.3.2.4 *Cylindrical Structure: Peptide Nanotubes*

A significant breakthrough in self-assembly of nano-devices was made by Ghadiri *et al.*, when they designed organic nanotubes from cyclic peptides.[48,49,50,51] The nanotube consisted of hydrogen bonded stacking of cyclic peptides with an even number of alternating D/L amino acids with a conformation such that the C=O and N-H of the amide moieties are oriented perpendicular to the plane of the macrocycle[52] (Figure 11). Control of the size of the cyclic peptide influences the pore size of the nanotube. Nanotubes were found to be very robust and stable over a wide pH range and in different solvents. These nano-devices have significant potential applications in the transport of ions and small molecules. Recent studies have shown that such nanotubes

can stack inside the cell membrane of the bacteria, leading to cell permeability, and ultimately to the death of the cell, highlighting their potential as antibiotics.

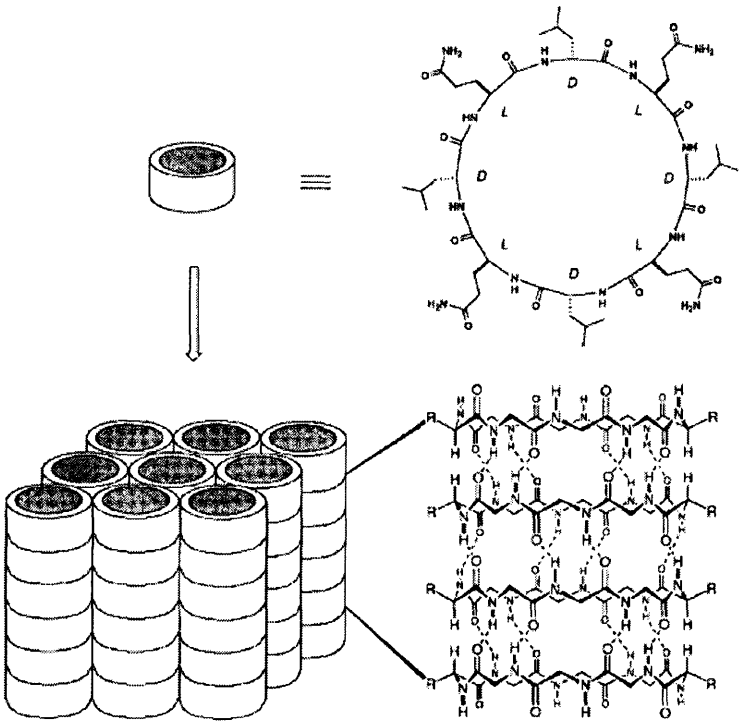

Figure 11: Schematic view of Ghadiri's peptide nanotube[48]

This last example illustrates one of the strategies used to increase the stability of the hydrogen bonded assembly where individual hydrogen bond recognition motifs are covalently connected to give multidentate modules that can associate *via* multiple hydrogen bonds. This approach has been investigated by Hunter *et al.*[53,54,55] for the synthesis of molecular zipper complexes (Figure 12), with an association constant (K_a) of up to 10^3 M^{-1}.

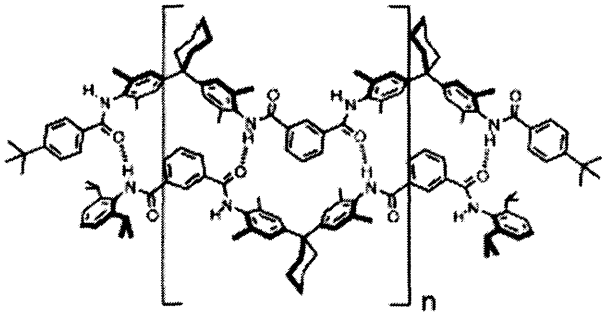

Figure 12: Example of a molecular zipper[55]

Similarly, Gong *et al.* have described the synthesis of an extremely stable hydrogen bonded duplex held together *via* six hydrogen bonds, such as shown in duplex **13** (Figure 13).[56,57,58]

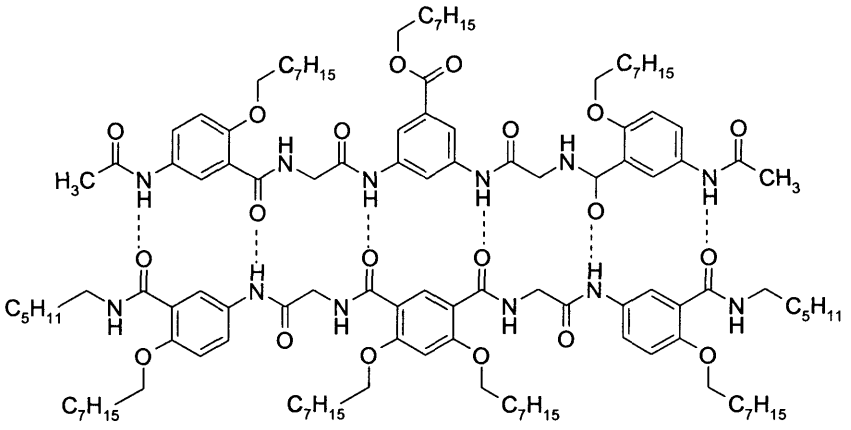

13 $K_a > 10^9 M^{-1}$

Figure 13: Stable duplex *via* six hydrogen bonds

Another approach taken in order to increase the stability of the self-assembly, is the use of hydrogen bonded complexes based on rigid linear arrays of multiple donor (D) and acceptor (A) sites for hydrogen bonding. This strategy has received by far the largest application in material science in recent years and will be discussed in detail in the following section.

1.4 The Self-Assembly of Supramolecular Architectures Using Hydrogen Bonding Modules

The development of rigid heterocyclic modules that can dimerise *via* hydrogen bonding interactions has developed over the last ten years into a unique tool for the synthesis of supramolecular structures. In the following section, various examples of basic modules are considered, which are grouped based on the number of hydrogen bonds formed.

1.4.1 Double Hydrogen Bonded Systems

A large number of organic functionalities can dimerise *via* the formation of two hydrogen bonds. Dimeric assemblies are widely found as heterodimers (DD-AA, with D = Donor and A = Acceptor) and homodimers (DA-AD), in carboxylic acids,[59] amides[60] and ureas.[61] Sartorius and Schneider[62] predicted a low dimerisation constant of ~ 60 M^{-1} for DA-AD in chloroform, which is unfortunately too low to be useful for the synthesis of supramolecular polymers. Dimerisation constants were found to be higher for heterodimers DD-AA, with dimerisation constants reaching 10^2 M^{-1} in $CDCl_3$. The dimerisation constant could be increased further to 3×10^3 M^{-1} with the formation of 'bifurcated' hydrogen bonds such as found in compound **14** (Figure 14). One way of increasing the stability of such dimeric assemblies is to connect multiple modules *via* covalent bonds. Following this strategy Wuest *et al.*[63,64,65] connected two 2-pyridones using a rigid linker. Depending on the arrangement of the pyridone moiety, very stable cyclic dimers could be obtained in $CDCl_3$ ($K_a > 60000$), as well as in the solid state, such as dimer **15**. However, a polymeric aggregate (**16**) was obtained, where the orientation of the amide bond favoured a linear shape.

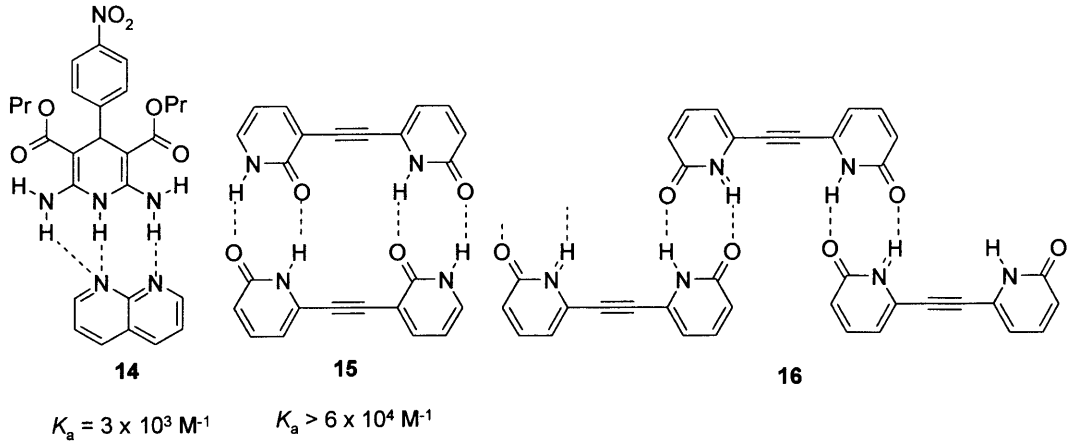

Figure 14: Examples of double hydrogen bonded systems

Although the strength of a double hydrogen bond is not sufficient enough to generate materials with polymeric properties, the use of such synthetically accessible systems inside a polymeric matrix, enhances the material properties. Stadler *et al.* extended this concept, by studying the properties of polybutadienes functionalised with hydrogen bonded phenylurazole units (**17**) (Figure 15).[66,67] The elastomeric polybutadiene transformed into a thermoplastic elastomer upon functionalisation with the reversible units.

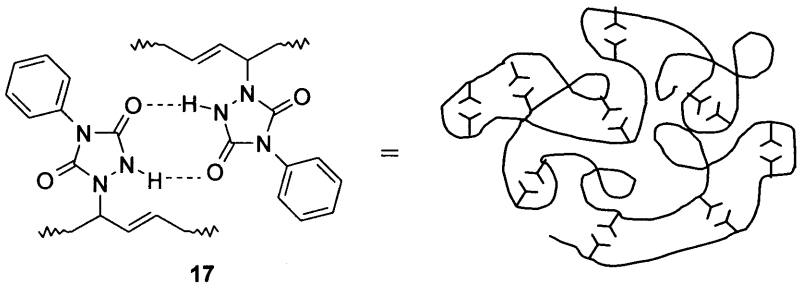

Figure 15: Hydrogen bonded phenylurazol unit incorporated into polybutadiene

Following this significant contribution in the field of supramolecular polymers, further efforts were made towards the development of multiple hydrogen bonding systems that could dimerise with higher dimerisation constants.

1.4.2 Triple Hydrogen Bonded Systems[68]

Triple hydrogen bonding is potentially more suitable for the generation of stronger dimeric units. Three combinations of array can be envisaged, all of them being hetero-complimentary (Figure 16). Heteroaromatic compounds have several advantages, foremost of which is the geometrically well-defined, often linear array of hydrogen-bond donor and acceptor groups present. However, a key disadvantage of using heteroaromatic modules in self-assembly is their poor solubility in organic solvents, which makes it difficult to measure the association constant. Another drawback is that the tautomeric behaviour of heteroaromatic modules is often solvent dependant.

Figure 16: Three possible combinations for triple hydrogen bonded systems

The arrangement of the donor and acceptor in the array has a crucial influence on the dimerisation constant. A few examples of triple hydrogen bonded systems are described in the following section.

1.4.2.1 *DAD and ADA Heteroaromatic Modules* [69,70,71,72]

The most common DAD-ADA hydrogen bonding array is found in the base pair between 2-aminoadenine (A') and thymine (T)[73] (e.g dimer **a**, Figure 17). Such complexes have been shown to increase the dimer stability and specificity relative to adenine.thymine (AT) base pairs (K_a = 90 M^{-1} in chloroform for AT compared to 210 M^{-1} for A'T).[74] One of the most useful ADA arrays contains the pyrimidine-2,4-dione unit as shown in Figure 17 below. The *N*-alkylation of thymine with allyl halide provides a simple method to functionalise this molecule. Example of DAD-ADA complexes and their corresponding K_a values in chloroform are shown in Figure 17.

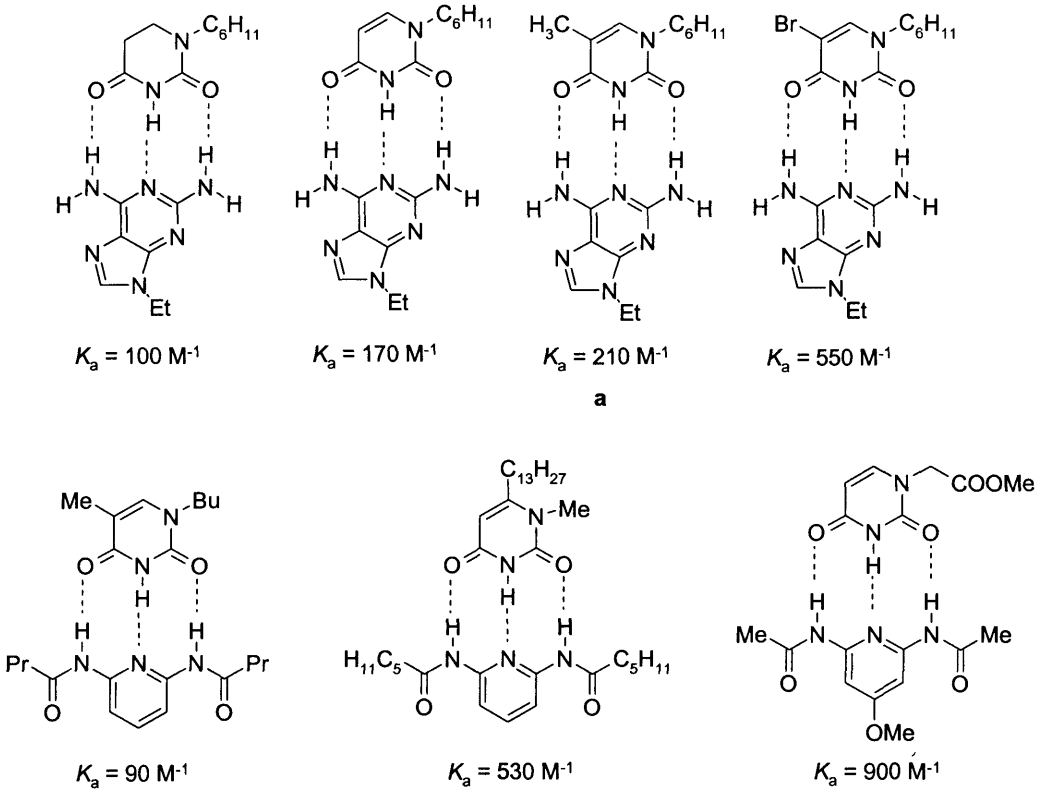

Figure 17: Examples of some triply hydrogen bonded heteromodules based on the DAD-ADA arrangement

1.4.2.2 *DDA and AAD Heteroaromatic Modules*[75,76,77]

A typical example of this system is the cytosine-guanidine base pair. These bases are commercially available and can be derivatised in numerous ways. The association constants presented in Figure 18 lies in the 10^4-10^5 M^{-1} ranges, which are two or three orders of magnitude higher than those observed for the ADA-DAD arrays.

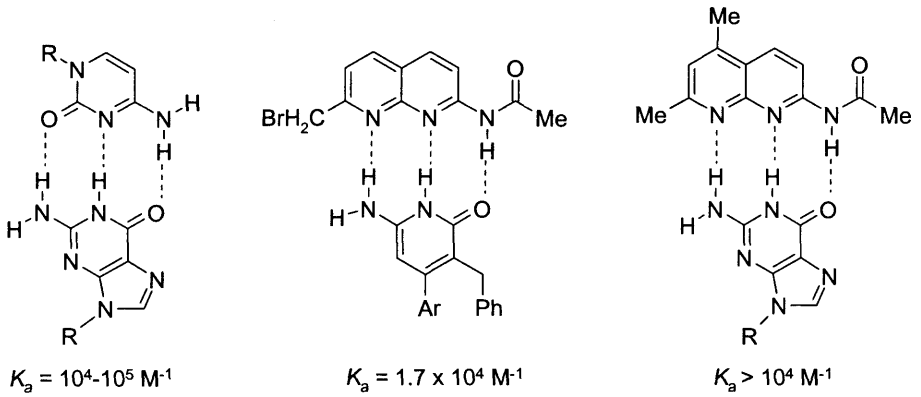

Figure 18: Example of DDA and AAD heteroaromatic modules

1.4.2.3 *DDD and AAA Heteroaromatic Modules*

Few examples of such modules have been reported in the literature. However, one of the most cited examples is the 1,9,10-anthyridine moiety (**18**, Figure 19) with an association constant greater than 10^5 M^{-1} in chloroform with its AAA complimentary unit dihydropyridine **19** (Figure 19).[78,79]

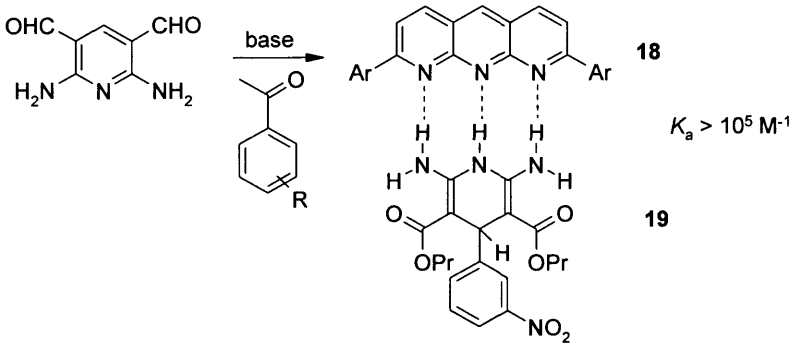

Figure 19: Synthesis of the diaryl-1,9,10-anthyridine module (AAA) **18** and its association with dihydropyridine **19** (DDD)

1.4.2.4 *Variations in Association Constants*

In the late eighties, Jorgensen *et al.* attributed the differences in association constants to the attractive and repulsive secondary interactions within the assembly.[80,81] Stabilisation can arise from the electrostatic attractions of positively and negatively polarised atoms in the adjacent hydrogen bond, whereas destabilisation results from electrostatic repulsions between two positively or negatively charged atoms (Figure 20).

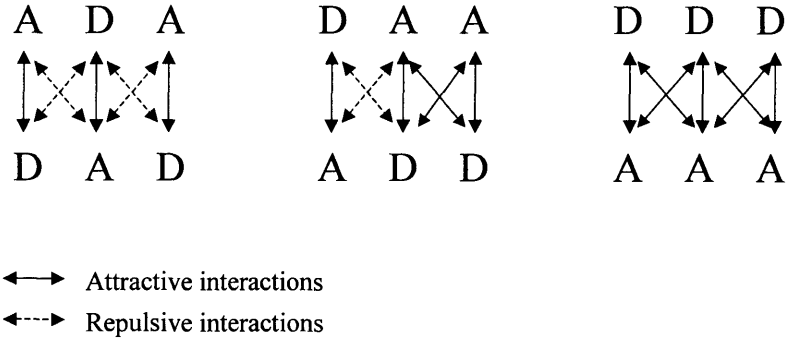

Figure 20: Electrostatic interactions in different triple hydrogen bonded arrays

Complexes formed from the DAD-ADA array show a K_a in the range of 10^2-10^3 M^{-1} in chloroform, whilst the DAA-ADD array has a K_a of 10^4 M^{-1} and exceeds 10^5 M^{-1} for the AAA-DDD complex. In the DAD-ADA complex, the number of repulsive secondary interactions is at a maximum, which destabilises the system, leading to the lowest association constant. In contrast, the AAA-DDD array exhibits the highest association constant because the four secondary interactions are all attractive, which then stabilises the structure.

1.4.2.5 *Supramolecular Assemblies Based on Triple Hydrogen Bonding*

Considerable progress has been made in the last decade on the development of triple hydrogen bonded supramolecular assemblies,[82] in particular for the synthesis of discrete cyclic molecules as well as the development of the first generation of linear supramolecular polymers.

1.4.2.6 *Cyclic Oligomers*

Zimmerman *et al.* have described the synthesis of a stable hexameric disk-shaped aggregate containing 18 hydrogen bonds in total, formed by the association of complimentary DDA and AAD sites.[83] The design of this particular motif allows the formation of particularly stable cyclic assemblies (**20**, Figure 21) over polymeric aggregates.

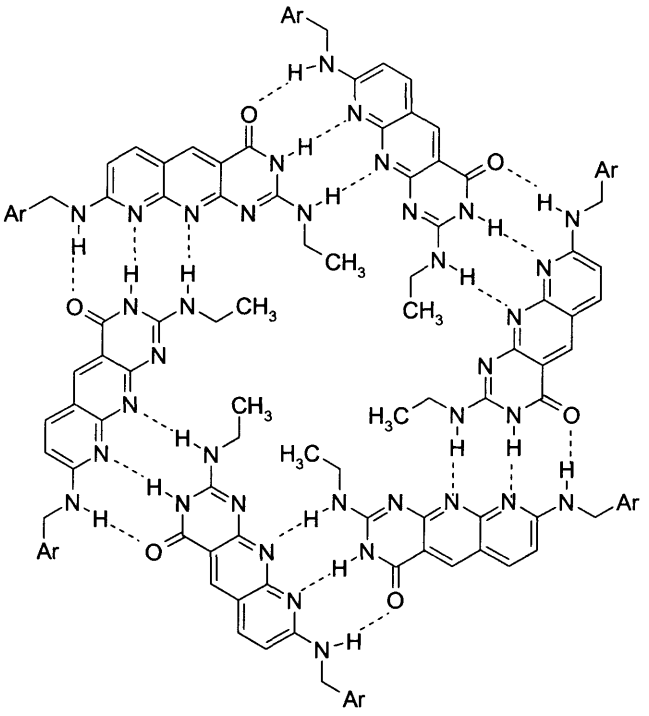

20

Figure 21: Formation of a stable cyclic assembly

1.4.2.7 *Cyclic Multimers and Linear Systems: Rosettes and Ribbons*

Another interesting system is the self-assembly of melamine with cyanuric acid units. Whitesides *et al.* have extensively studied various rosette type molecules.[84] When equimolar amounts of melamine **21** and cyanuric acid **22** were mixed together, an insoluble polymeric complex precipitated from the solution leading to a rosette like arrangement as shown in Figure 22.

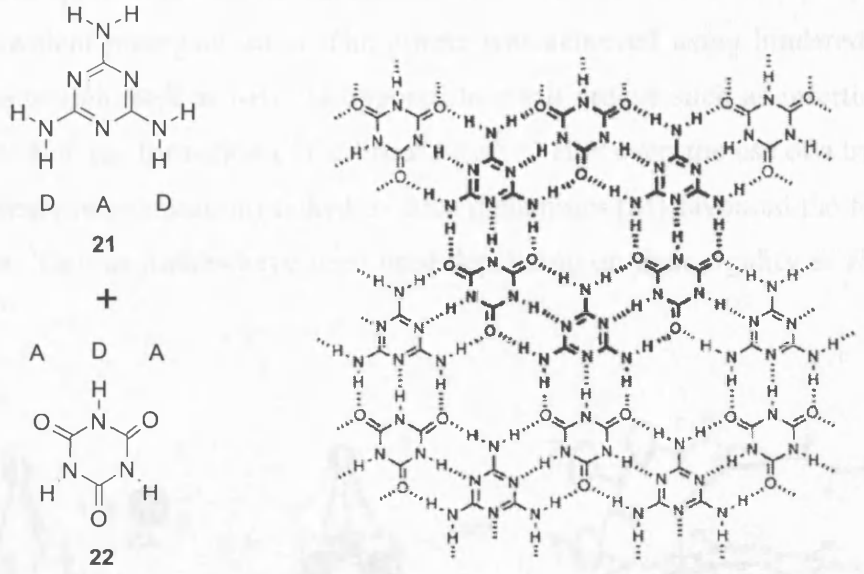

Figure 22: Formation of cyanuric acid-melamine complex[84]

From NMR and GPC studies, it was established that the rosette motif was not the only one present in the solid state The complex displayed three motifs in the solid state including the 'linear tape', the 'crinkled tape' and the 'rosette' motif (Figure 23).[85,86]

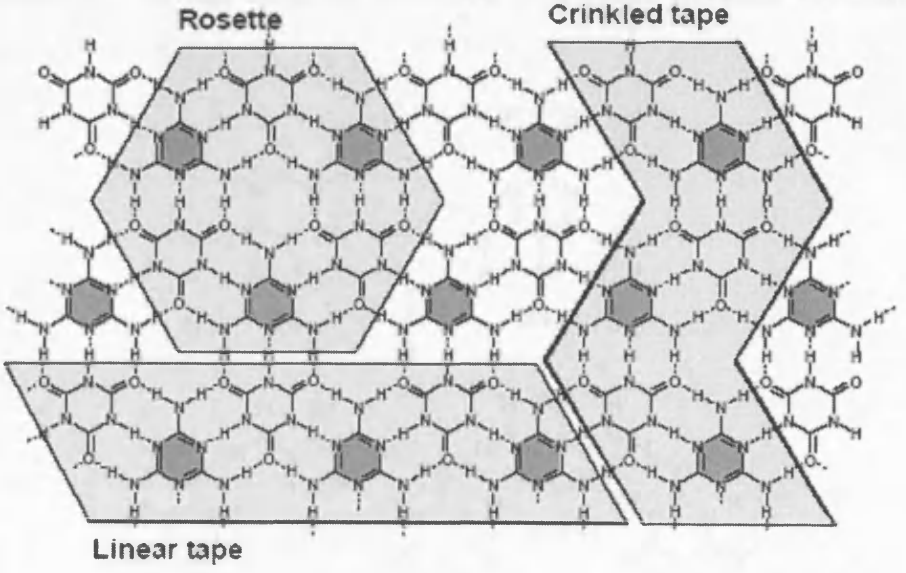

Figure 23: Three motifs formed in the complex of cyanuric acid and melamine[86]

Structural modification of the acid or amine influenced the stability of the linear or wrinkled tape. In order to favour the formation of the rosette motif, Whitesides used two

different approaches: the introduction of stereochemical control by peripheral crowding and covalent preorganisation. The primer was achieved using hindered groups on the melamine unit such as *t*-Bu, as opposed to small groups such as insertion of F or CH_3 that leads to the formation of the linear tape.[87,88] However, the use of a trigonal template (covalent preorganisation) linked to three melamines (M) favoured the formation of the rosette. Various linkers have been used depending on their rigidity as shown in Figure 24.[89,90]

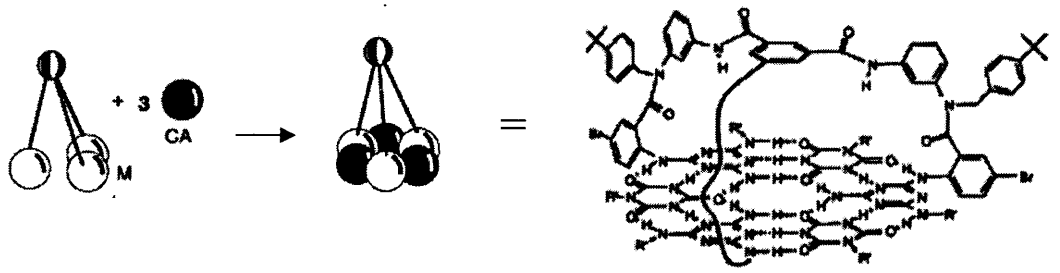

Figure 24: Preorganisation using a rigid linker. M (melamine), CA (cyanuric acid)[89]

Due to their hydrogen bonding capability, derivatives of barbituric acid (**23**) and melamine (**24**) have been also used by Lehn *et al.* for the synthesis of molecular ribbons (**25**, Scheme 2).[91] In this case, the formation of a cyclic hexamer structure was not observed.

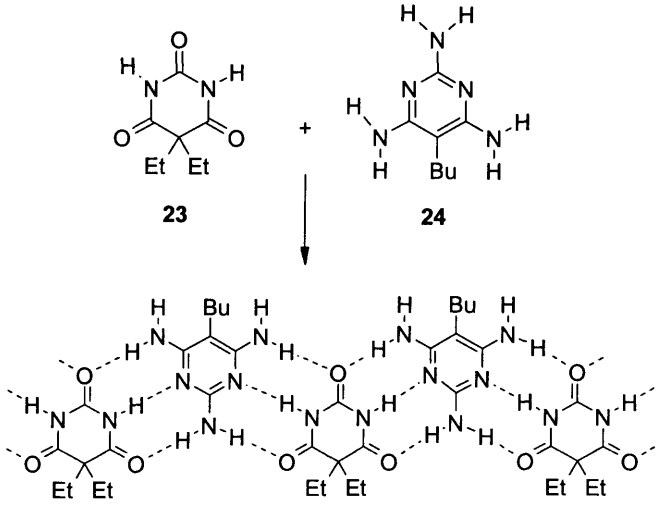

Scheme 2: Formation of molecular ribbons

Triple hydrogen bonding arrays were also synthesised based on 4,6-diamino -5-octylpyrimidin-2 (1H)-one (**26**), and 2-amino-5, 5-dibutylpyrimidine-4,6 (1H)-dione

(**27**) which are complimentary to each other, as well as self-complimentary (Scheme 3). The hetero-association of **26** and **27** lead exclusively to the formation of macrocyclic ring (**30**), while the self-assembly of either **26** or **27** generated only molecular ribbons (**28** or **29**).

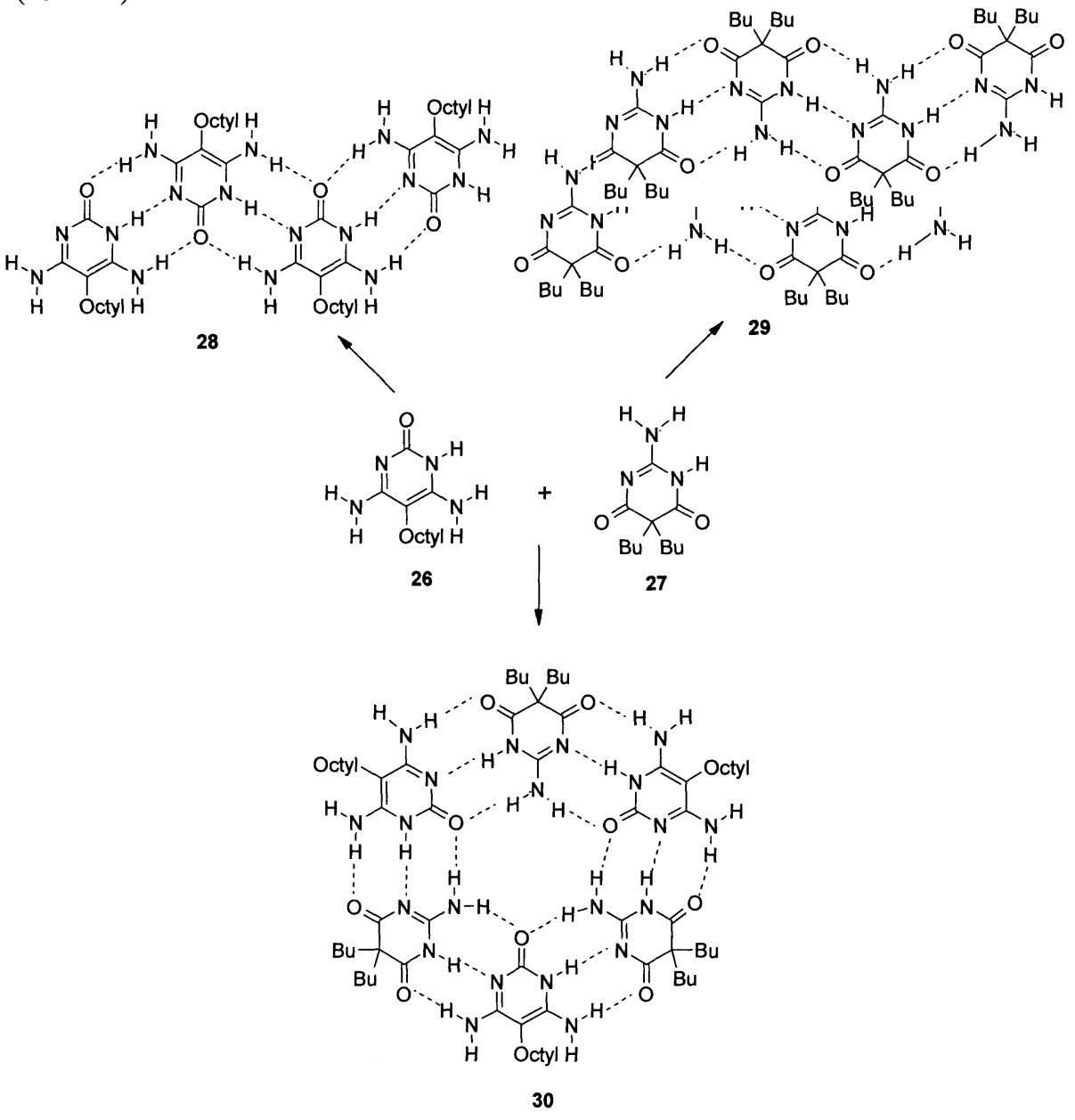

Scheme 3: Formation of macrocyclic ring and molecular ribbons[91]

Molecular ribbons have been classed as the first generation of 'supramolecular polymers', where the length of the ribbon was directly controlled by the strength of the hydrogen bond. Although called supramolecular polymers these ribbons did not show a high degree of polymerisation (DP) due to relatively weak hydrogen bonding interactions. The recent advances in the field of self-assembly have stimulated the

design of a new generation of supramolecular polymers based on strong hydrogen bonding.

1.4.2.8 *Supramolecular Polymers Based on Triple Hydrogen Bonding*

In supramolecular polymers[92,93,94] which are formed by the reversible association of bifunctional monomers, the average degree of polymerisation is dependant on the concentration of the solution, as well as the association constant of the end groups.[95] A schematic representation of DP versus K_a at two different concentrations 1 M and 0.05 M (in the absence of cyclisation) is shown in Graph 1.

From this graph, a single hydrogen bond with $K_a \sim 10^1$ M^{-1} leads to the formation of very low DP, and only association constants greater than 10^5 M^{-1} result in DP greater than 100.

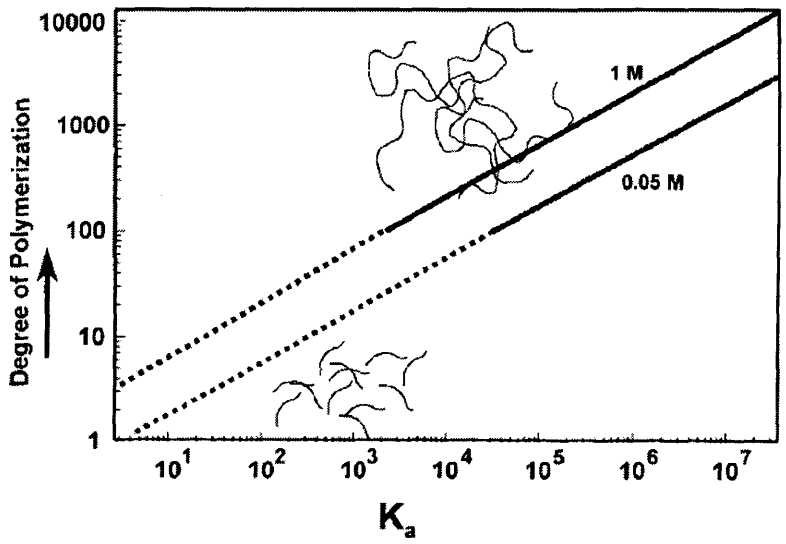

Graph 1: Variation of the degree of polymerisation as a function of K_a [95]

When multiple hydrogen bonding sites are combined together in a functional unit comprising triple hydrogen bonding, the interaction can be strong leading to a supramolecular polymer with unique properties in the bulk. Lehn *et al.* synthesised hetero dimers of bifunctional diaminopyridines (**31**) and difunctional uracil (**32**) held together *via* triple hydrogen bonding (DAD-ADA) (Scheme 4). The 1:1 ratio of the two units displayed liquid crystallinity over a broad range of temperatures while the pure compound (**33**) was solid and melt without displaying a liquid crystalline phase.[96] The

presence of the chiral spacer induced biased helicity as observed by electron microscopy.

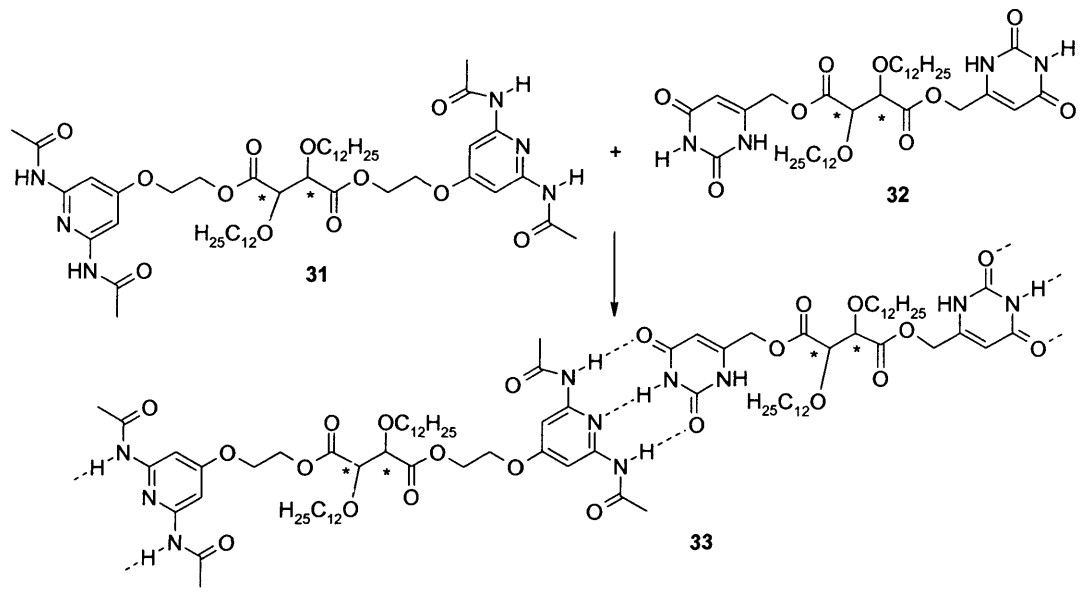

Scheme 4: Formation of linear supramolecular polymers

Liquid crystalline polymers were then prepared by introducing a rigid core composed of 9,10 dialkoxyanthracene between the hydrogen bonding units (**34**, Figure 25).[97,98]

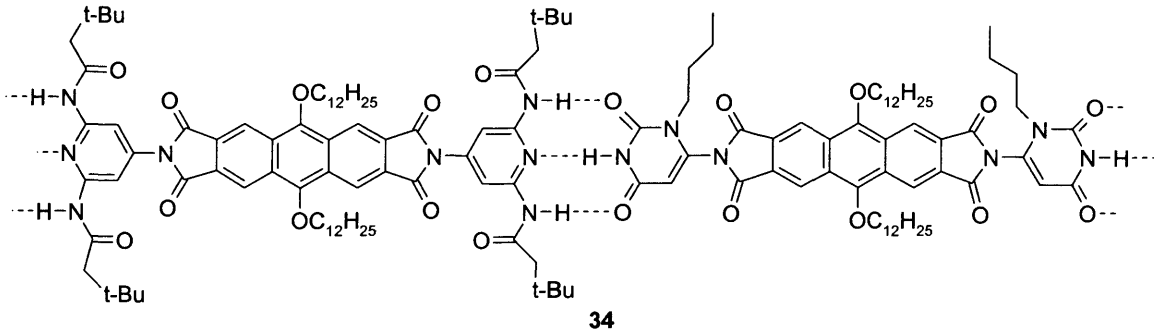

Figure 25: Liquid crystalline polymer made from rigid linker

Compound **34** was not a thermotropic liquid crystal as in the previous case, but lyotropic meaning that the liquid crystalline properties were induced in the presence of apolar solvents. Despite the presence of three hydrogen bonds with association constant K_a of 10^3 M^{-1}, the complex generated was unfortunately not strong enough to induce

true polymer properties in solution. Indeed, the DP was 15 for a 0.05 M solution of polymer **34**. Therefore a stronger hydrogen bonding unit is necessary in order to achieve polymeric properties in solution.

One way of achieving this is to increase the number of hydrogen bonds. Using this approach, Lehn *et al.* synthesised a supramolecular material based on the self-association of two homoditopic hetero-complimentary monomers such as **35** and **36** (Figure 26) through DAD-ADA hydrogen-bonding arrays.[99] The polymer **37** formed fibers (a schematic representation of the linear polymerisation is shown in Figure 27).

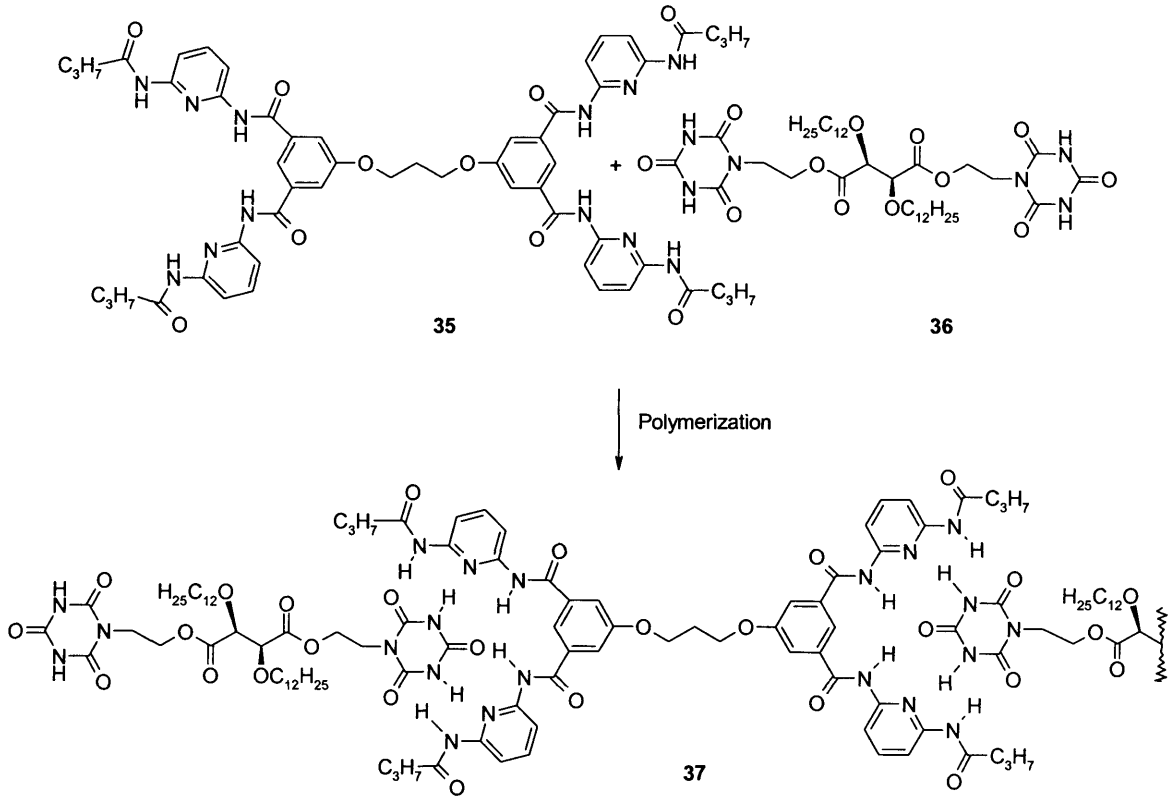

Figure 26: Synthesis of supramolecular polymer **37**

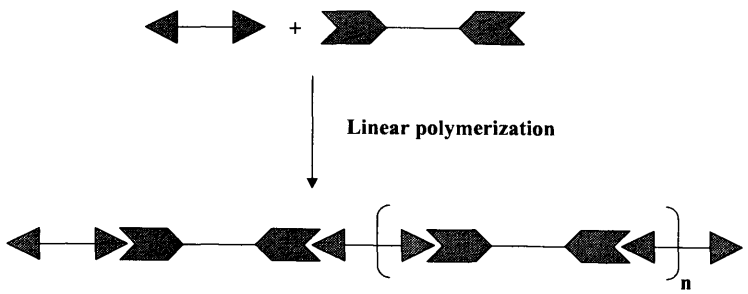

Figure 27: Self-organisation of complamentary monomeric building blocks

As illustrated by the work of Lehn and others, the use of multiple hydrogen bonding systems increased the strength of the desired self-assembly. Recently linear quadruple hydrogen bonding systems have shown significant potential for the synthesis of linear supramolecular polymers.

1.4.3 Quadruple Hydrogen Bonded Systems[100,101]

From a combination of donors and acceptors, six quadruple hydrogen bonded dimers can be envisaged, two containing self-complimentary units (DDAA and DADA) as shown in Figure 28.

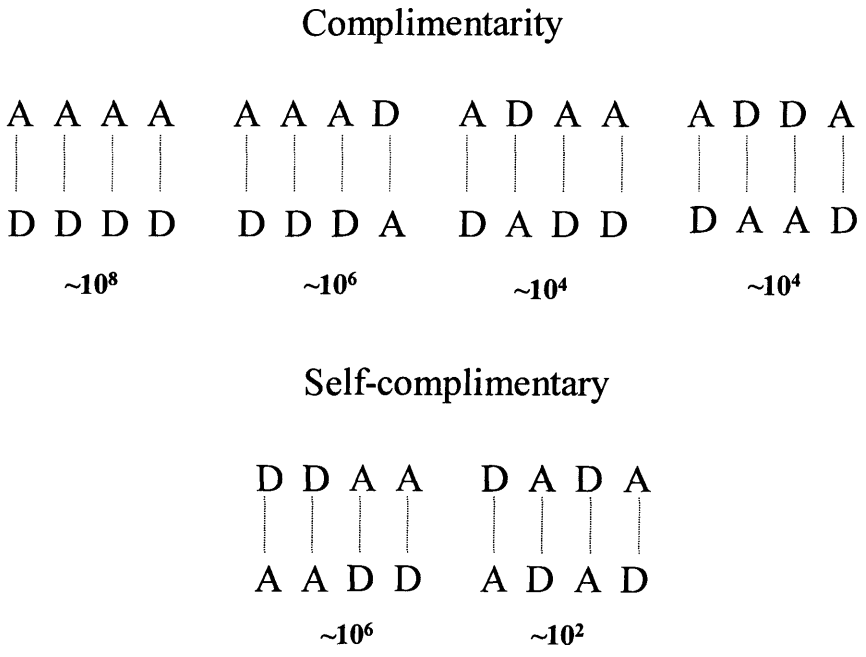

Figure 28: Quadruple hydrogen bonding arrays. Orders of magnitude of the predicted stability constants (in M^{-1}) in $CDCl_3$ are also indicated [100]

The differences in K_a observed can be explained by the Jorgensen model as described previously. Among the hetero-complamentary arrays, AAAA-DDDD is the strongest with six secondary attractive interactions. The self-complimentary array DDAA-AADD also has a high K_a, with four attractive and two repulsive secondary interactions.

1.4.3.1 *Complimentary Arrays*

The use of quadruple hydrogen bonding complimentary arrays is still under investigation and few examples are cited for the DAAD/ADDA array, which was first reported in 1998 when Zimmerman *et al.* described the existence of a very stable complex with $K_a > 10^7$ M^{-1} in solution (**38**, Figure 29).[102] Also, the bis-pyridylurea **39** was described by Lüning with a K_a of 2×10^3 M^{-1}.[103] The low stability was attributed to the presence of an intramolecular hydrogen bond in the pyridyl urea monomer which must break in order to form the linear DAAD array.

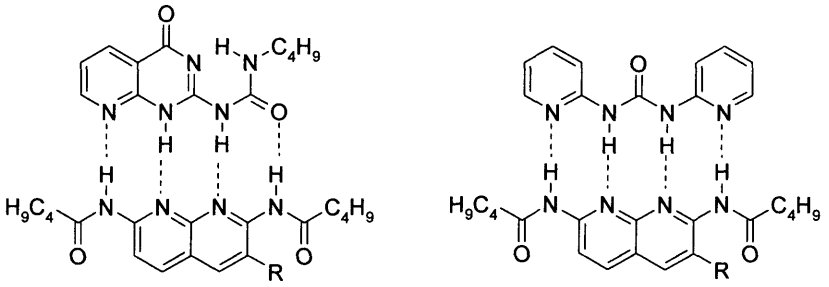

38 $K_a > 3 \times 10^7$ M^{-1} **39** $K_a = 2000$ M^{-1}

Figure 29: Examples of complimentary arrays (ADDA-DAAD)

Recently Li *et al.* have reported the synthesis of a complimentary ADDA-DAAD system based on hydrazide derivative,[104] with an association constant of 4.7×10^4 M^{-1} in chloroform.

A more complex array is the DDAD/AADA hetero-dimer. Meijer *et al.* attempted the synthesis of the module AADA, using a dipyridin-2-ylamine derivative (Figure 30) with the possibility of shifting the tautomeric form of **41** to the corresponding AADA module **40** by complexation with a complimentary DDAD array.[105] Unfortunately, only the tautomer **41** was found to be present both in solution and in the solid state.

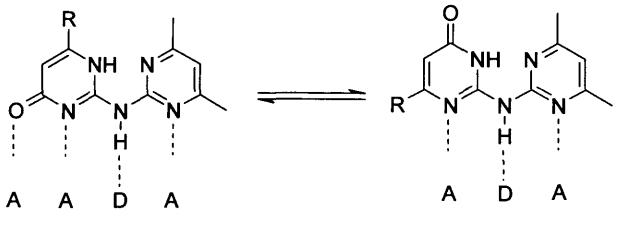

40 **41**

Figure 30: Tautomeric equilibrium of compound **40**

In 2002, Lüning's group reported the synthesis of an AADA/DDAD dimer (**42**, Figure 31).[106,107] The low association constant (K_a = 110 M^{-1}) was explained by the possible formation of an intramolecular hydrogen bond in the DDAD unit that needed to be broken prior complexation (**43**).

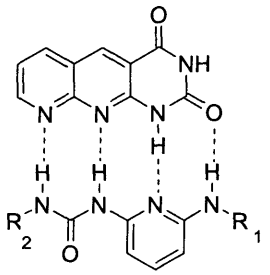

42

K_a = 110 M^{-1}

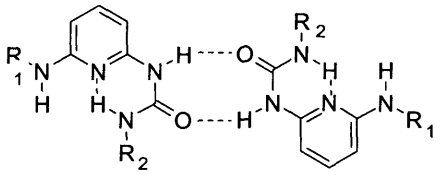

43

Figure 31: Example of a DDAD/AADA system (left) and self-association of the DDAD unit in the folded conformation (right)

1.4.3.2 *Self-Complimentary Arrays*

The development of self-complamentary arrays stems from their potential use in supramolecular polymers and 'intelligent materials'. These are particularly useful class of systems that offer considerable simplification of the supramolecular design. In the following, some of the typical and most widely used modules are considered.

1.4.3.3 *DADA Array*

Meijer *et al.* have shown that acylation of both diamino-triazines and diaminopyrimidines generates a DADA motif.[108] The construction of this motif can be achieved by a simple addition of an acceptor group to a DAD array. Although the DADA array is expected to be the least stable of the quadruple hydrogen bonding motif due to secondary repulsions based on the Jorgensen model, the synthesis of strong dimers with $K_a > 10^5$ M^{-1} have been reported. The increase in the K_a for molecule **44** or **46** (Figure 32) has been possible by the synthesis of preorganised molecules **45** and **47**. The new intramolecular hydrogen bond fixes the array in a planar conformation resulting in a dimerisation constant of 2×10^4 M^{-1} for **45** and 2×10^5 M^{-1} for **47**.

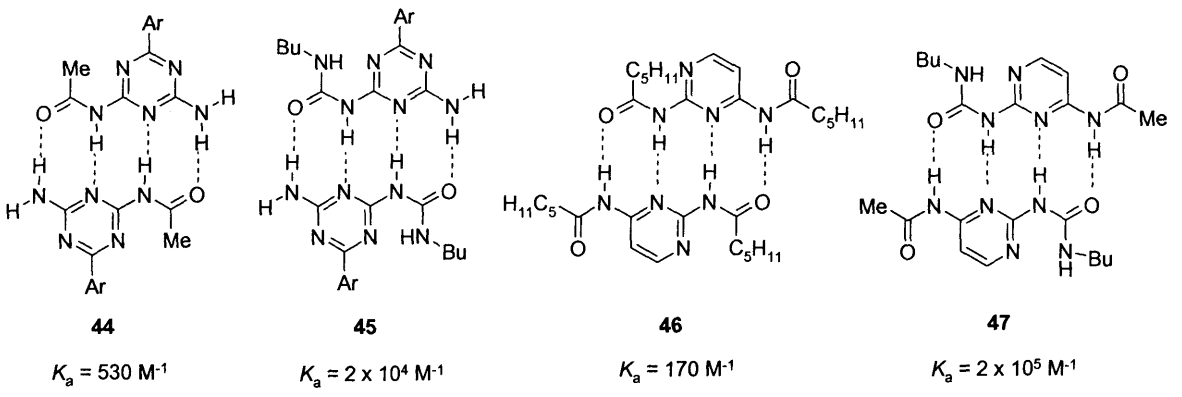

Figure 32: Examples of DADA quadruple hydrogen bonded arrays

1.4.3.4 *Supramolecular Polymers Based on DADA Array*

The straightforward preparation of ureidotriazines[108] as well as the relatively strong dimerisation constant in $CHCl_3$ is an attractive feature for its use in the formation of linear supramolecular polymers. For this purpose, Meijer *et al.* have combined solvophobic interactions and hydrogen bonding in a bifunctional trialkoxyphenyl ureidotriazine derivative **48** (Figure 33).[109]

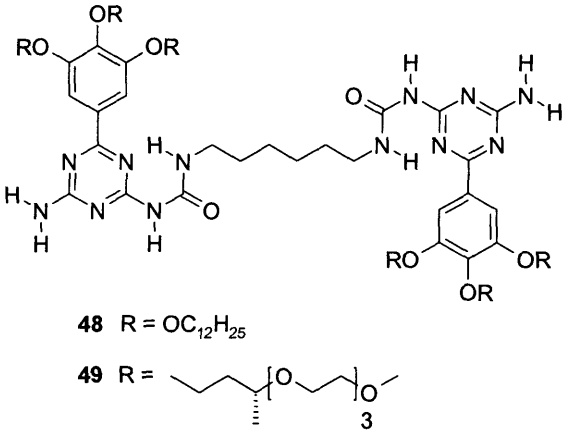

Figure 33: Bifunctional ureidotriazines

The nature of the resulting compound **48** was highly dependant on the solvent. Indeed, in dodecane (apolar solvent), compound **48** organised into a helical columnar polymer (Figure 34), while in chloroform, where the solvophobic interactions were weaker, the final compound formed a random coil polymer. In DMSO, a highly polar solvent, the hydrogen bonds were broken and the compound existed as a monomeric unit. The length of the column was directly linked to the concentration of the solution: for a 0.2 wt.% solution the length is found to be 100 Å, while for a 1.0 wt.% solution the length increased to 190 Å. Compound **49**, containing a chiral oligoethylene unit instead of an

alkyl side chain was soluble in water and surprisingly the hydrogen bonding array was not disrupted due to the hydrophobic environment by the stacking of the planar trialkoxyphenyltriazine moieties.

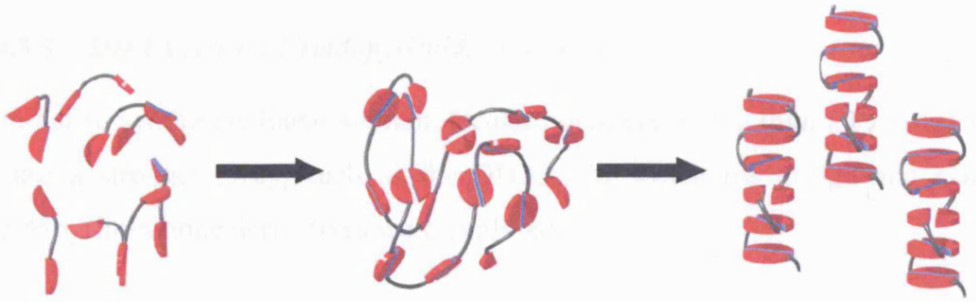

Figure 34: Representation of the random coil polymer and helical columnar aggregate[109]

Recently, Sijbesma *et al.* described the synthesis of ureidotriazine π-conjugated oligo (*p*-phenylene vynilene) groups for the use in electronic devices[110] (Figure 35).

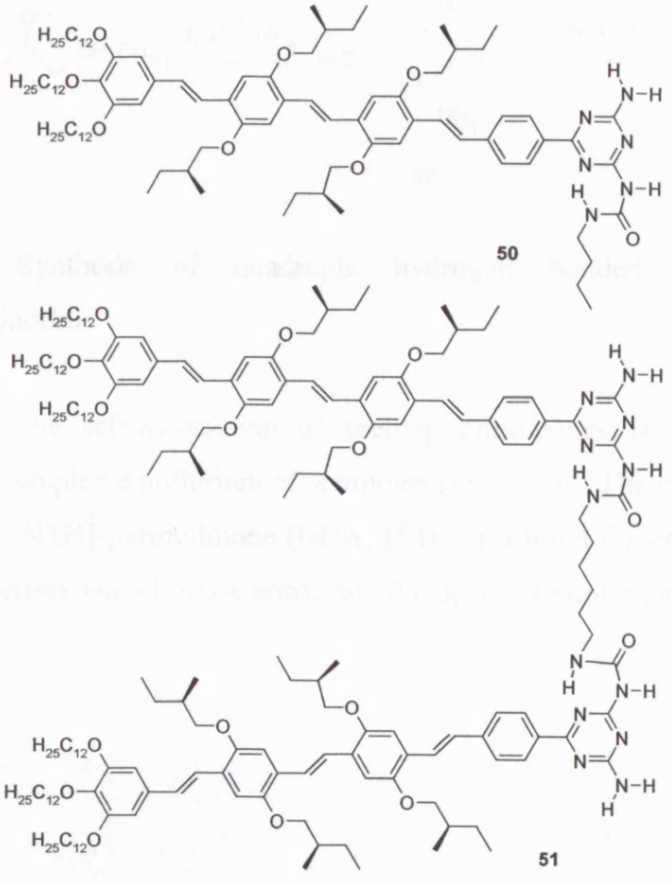

Figure 35: Examples of ureidotriazine π-conjugated systems

Both compounds **50** and **51** formed columnar architectures in dodecane, but **51** was less ordered due to steric effect of the long chain imposed by the linker and the stacking interactions.

1.4.3.5 *DDAA Array: Ureidopyrimidinone (Upy)*

In order to synthesise linear supramolecular polymers with a high DP, it was important to use a stronger array, such as the DDAA for which the design and synthesis of ureidopyrimidinone derivatives were explored.

Ureidopyrimidinone units can readily be synthesised *via* a two step synthesis starting from the condensation of β-keto ester with guanidine, affording the corresponding isocytosine (**52**). Reaction with an alkyl isocyanate affords the quadruple hydrogen bonding system **53** (Scheme 5).[111]

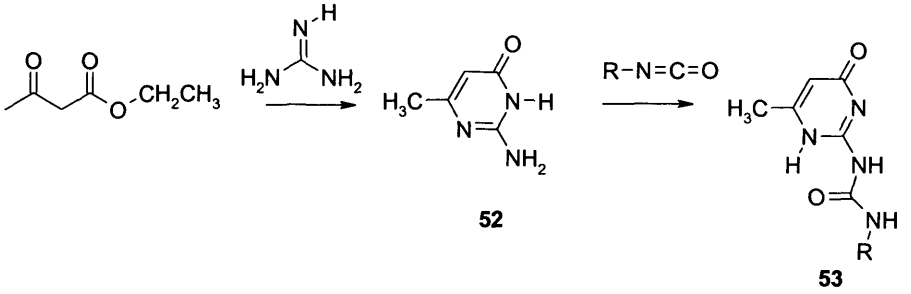

Scheme 5: Synthesis of quadruple hydrogen bonded system based on ureidopyrimidinones

Unfortunately, the self-association of ureidopyrimidinones is complicated by the existence of a complex equilibrium of tautomers (Figure 36). Three forms can exist, one of which is the 6[1H]-pyrimidinone (DDA) (**54**) that cannot dimerise. The pyrimidinol form (**56**) dimerises *via* a DADA array, and the 4[1H]-pyrimidinone (**55**) dimerises *via* DDAA.

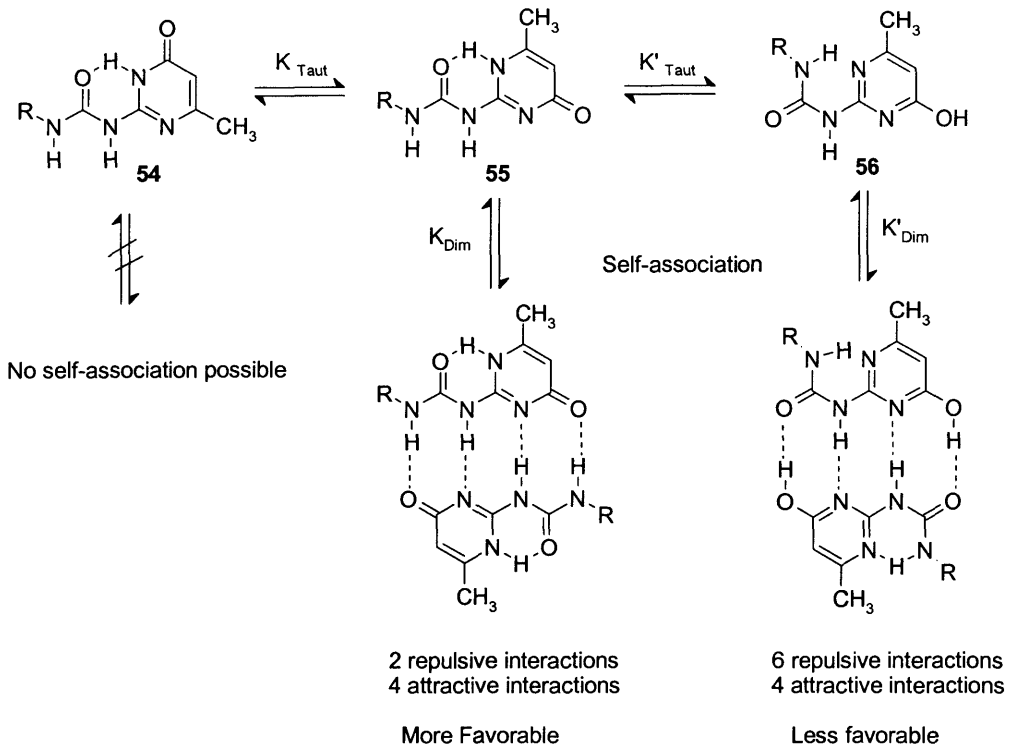

Figure 36: Tautomeric and dimeric equilibria in ureidopyrimidinones

The occurrence of the tautomers was observed to be highly dependant on the polarity of the solvent as well as the concentration and the nature of the substituents at the C-6 position. Remarkably, the pyrimidinone with alkyl groups (such as CH_3) at C-6, existed in $CDCl_3$ as the DDAA tautomer (99%). In order to build supramolecular polymers based on pyrimidinone units, it is important to have a high dimerisation constant as well as a unique tautomer present in solution, otherwise the system can become highly complex.

The crystal structure of **57** (R = C_4H_9, R' = CH_3, Figure 35), revealed the existence of a linear quadruple hydrogen bonding array (DDAA), stabilised by an intramolecular hydrogen bonding between the carbonyl of the urea and the pyrimidine (N-H). The array deviated slightly from linearity with D (N...N) = 2.97 Å (θ = 175°) and D (N...O) = 2.76 Å (θ = 163°).

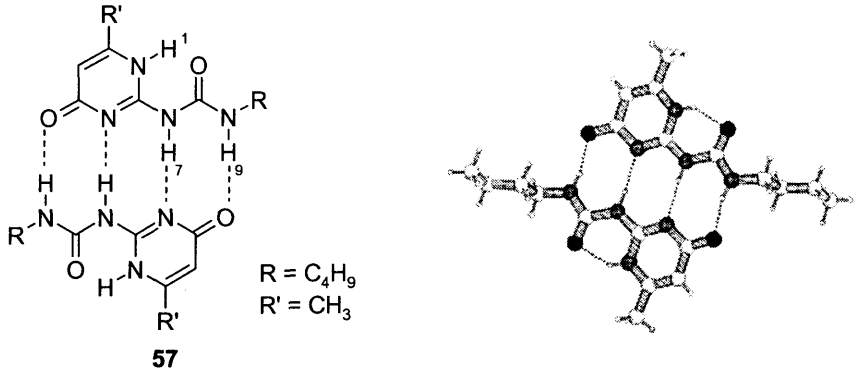

Figure 37: Schematic representation and structure of **57** in the solid state[111]

FTIR measurements (in the solid state and $CHCl_3$) revealed the existence of the DDAA array in solution. NMR studies of compound **57** showed deshielded signals for the NH protons characteristic of strong hydrogen bonding at 13.15, 11.86 and 10.15 ppm for 1-H, 7-H and 9-H, respectively, with a chemical shift for the vinylic proton at 5.88 ppm. In order to measure the dimerisation constant K_{dim}, NMR dilution experiments were performed, but no chemical shift changes of the hydrogen bonded protons were observed, even near the detection limit of a high field instrument operating at 750 MHz. This result was very encouraging and demonstrated that the dimerisation constant was very high, greater than 10^6 M^{-1}.

Meijer *et al.* then used a fluorescence technique[112] with pyrene labelled compound **58** in order to measure K_{dim} (Figure 38). On dimerisation a strong excimer fluorescent signal was observed at 478 nm, and upon dilution, signals of the monomer appeared around 370-400 nm.

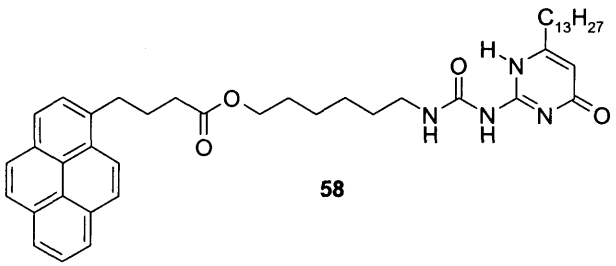

Figure 38: Pyrene labelled compound **58**

Using this technique, the dimerisation constant of the DDAA array was found to be ~ 6 × 10^7 M^{-1} in chloroform, 10^7 M^{-1} in wet chloroform and 6 × 10^8 M^{-1} in toluene.

Ikegami and Arai have used an anthracenyl labelled Upy compound **59** (Figure 39), which exhibited exiplex emission at concentration below $10^{-5}\,M^{-1}$.

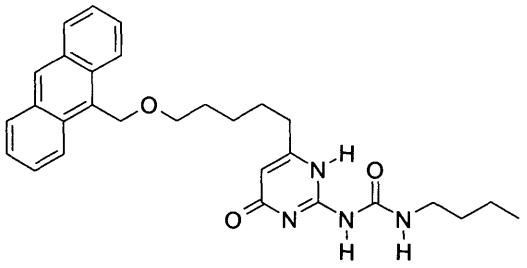

59

Figure 39: Anthracenyl labelled compound **59**

1.4.3.6 *Supramolecular Polymers using Ureidopyrimidinone (Upy)*

Bifunctional Upys

Because of their high dimerisation constant, recently ureidopyrimidinones have been used in the synthesis of high molecular weight polymers. The first supramolecular polymer based on Upy was prepared using a bifunctional Upy derivative. The synthesis of the monomer involved the reaction of a diisocyanate with the isocytosine. Two possible synthetic routes were envisaged as shown in Scheme 6, one where the linker is between the urea bond (**60**), and the other where the linker is connected *via* the C-6 position (**61**).[113]When these monomers were dissolved in chloroform a highly viscous solution was obtained.

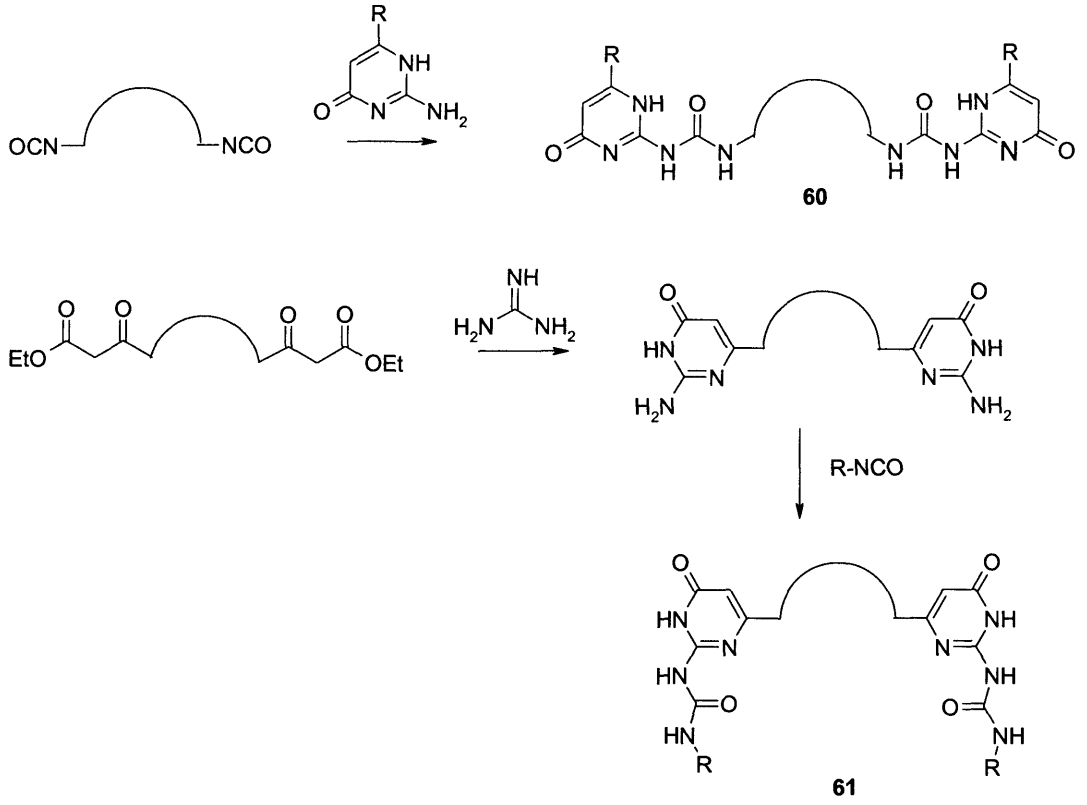

Scheme 6: Two strategies towards the synthesis of supramolecular polymers based on the Upy modules.

In order to obtain information on the DP in solution, a small amount of the mono functional unit was added to an extremely pure solution of the polymer **62**, resulting in a dramatic drop of the viscosity. The monofunctional unit played the role of a polymerisation stopper, which then decreased the DP and thus the viscosity of the solution.[114] Based on viscosity studies and taking into consideration the dimerisation constant of the Upy unit, Meijer *et al.* estimated a DP of 3000 for a pure solution of **62** (Figure 40).

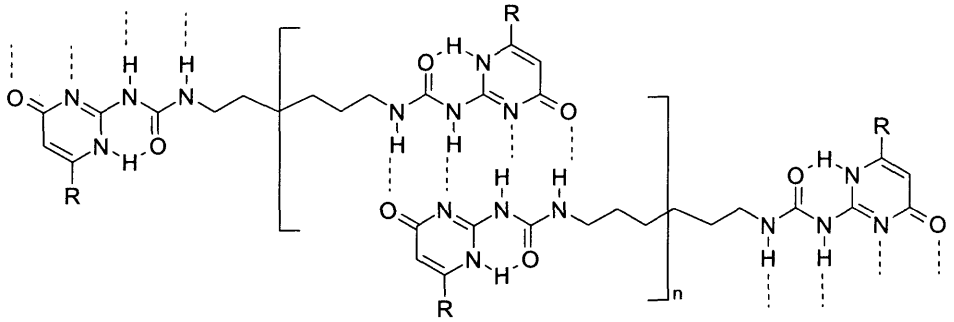

62

Figure 40: Supramolecular polymer **62**

The stopper used can also be in the form of a photolabile nitrobenzyl ether (**63**) that forms a DDA array and cannot compete with Upy. Under photolytic cleavage of the protecting group the carbonyl group is liberated and form an AADD motif (**64**), which can then start the de-polymerisation as shown in Figure 41. This process is unfortunately not reversible.

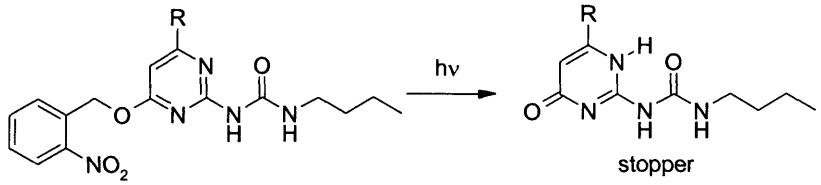

63 64

Figure 41: Photolytic cleavage of compound **63**

In order to take advantage of the high degree of polymerisation offered by the Upy groups in the synthesis of new materials, Meijer *et al.* used long linkers between the Upys, such as telechelic polymers (polysiloxanes), poly(ethylene/butylenes) (**66**), polyethers (**67**), polyesters (**68**) and polycarbonates (**69**) (Scheme 7).[115] It is then possible to combine the mechanical properties of covalent polymers with the low melt viscosity of the hydrogen bonding units. At high temperatures the end groups can dissociate and the viscosity decreases. Such advanced materials are of great interest for many applications, such as thermoplastic elastomers.

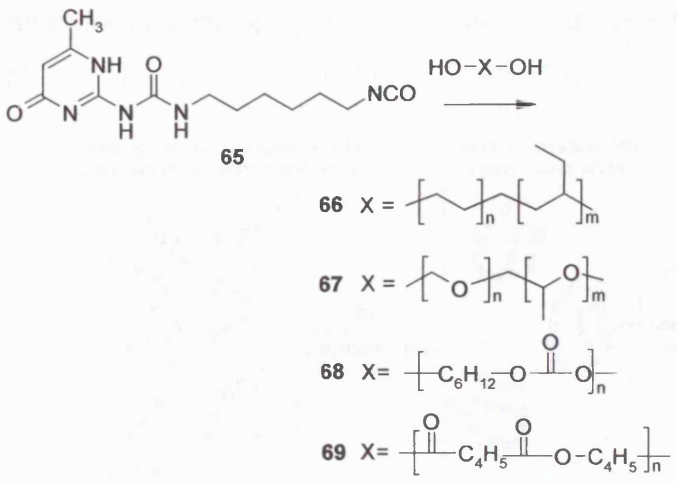

Scheme 7: Functionalisation of telechelic polymers with ureidopyrimidinone

Compound **65** was first synthesised using 6-methyl isocystosine in hexyl diidocyanate and was further reacted with hydroxyl terminated polymers in chloroform in the presence of a tin catalyst. The final supramolecular polymers exhibit improved properties as a result of the self-association. For example, the functionalisation of telechelic poly(ethylene/butylene) copolymer (**66**) resulted in interesting mechanical properties. Whilst the telechelic polymer is a viscous liquid, the Upy end-group modified polymer was an elastomeric solid (Figure 42). It was shown that these novel materials can combine the robustness of traditional covalent macromolecules with the responsiveness of reversible supramolecular polymers.

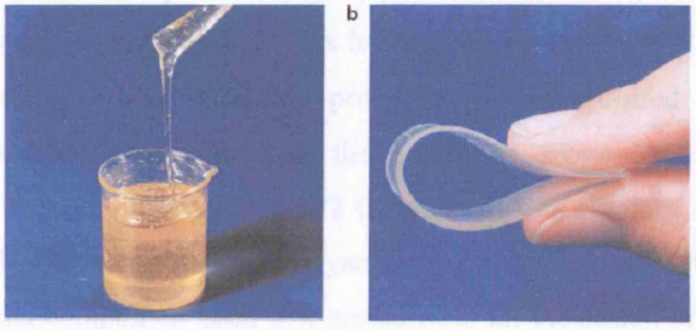

Figure 42: Telechelic polyethylene/butylene, b) telechelic polyethylene/butylene functionalised with Upy[115]

Supramolecular polymers based on telechelic polymers have also recently been used in polymerisation induced phase separation (PIPS). Here a polymer is dissolved in a

monomer matrix, which upon polymerisation causes a phase separation, resulting in two polymeric phases with certain morphologies (Figure 43).

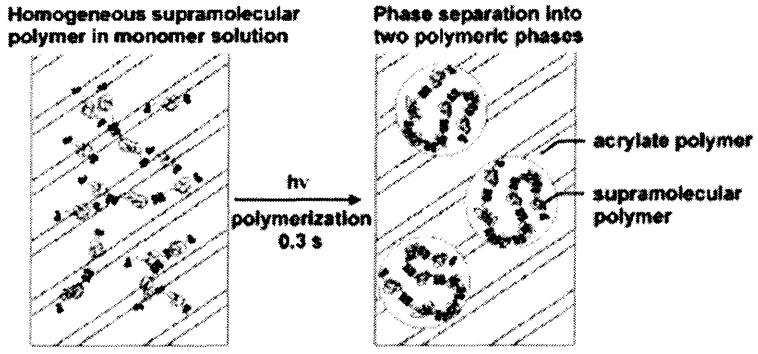

Figure 43: Schematic representation of polymerisation induced phase separation[116]

A big advantage of using PIPS is that it is a solvent free polymerisation process, leading to multi-phases of composite materials. Using this concept, Meijer *et al.* designed an efficient and fast PIPS using telechelic polymers such as poly-THF (M_n ~ 1000 g/mol) and poly-carbonate (M_n ~ 2200 g/mol) dissolved in a mixture of acrylate and diacrylate monomers.[116] Advantage is the formation of two polymeric phases in one polymerisation step. Experiments revealed that the amount of diacrylate was an important factor in the morphology development. The mechanical properties of the films containing the supramolecular polymer were comparable to standard films containing covalent high molecular weight polymers.

These results achieved by combining the low molecular weight telechic polymers and reversible hydrogen bonding networks has led to numerous applications. In particular, Meijer has combined the electronic properties of π-conjugated moieties of oligo(π-vinylenephenylene) oligomers with the polymeric properties offered by the Upy units.[117,118] For example, compound **72** (Scheme 8) was obtained in 45% yield *via* the reaction of diisocytosine **70** with isocyanate **71** in pyridine at 90 °C. It was shown that this and similar compounds open new possibilities for the design of electronic materials.

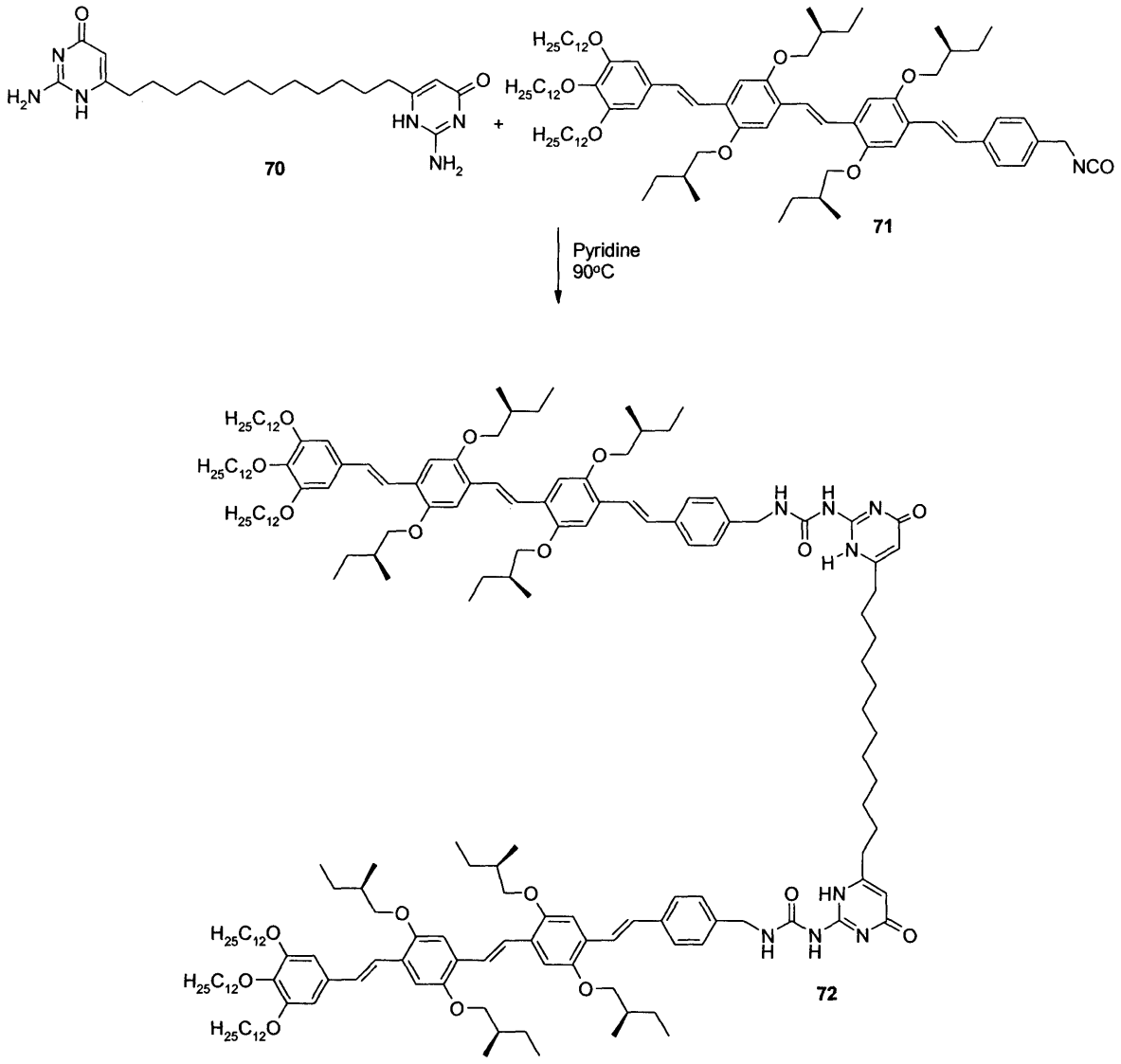

Scheme 8: Synthesis of supramolecular polymer incorporating oligo(π-vinylenephenylene) moieties

More recently, Hummelen's group has synthesised a supramolecular polymer (**73**, Figure 44) based on fullerene C_{60} for use in photovoltaic applications.[119,120,121]

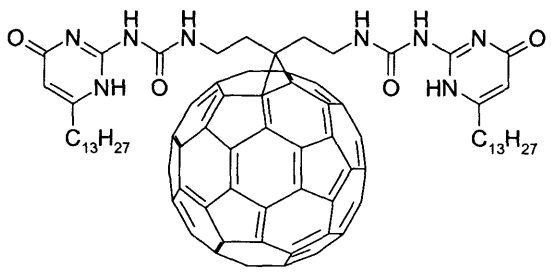

73

Figure 44: Supramolecular polymer incorporating a fullerene moiety

Coates *et al.* have also reported the use of 2-ureido-4[1H]-pyrimidinone derivatives as reversible cross-links in polyolefin elastomers.[122] The incorporation of olefenic 2-ureido-4[1H]-pyrimidinone **74** (Scheme 9) within a main chain amorphous polyolefin was achieved through a coordination polymerisation route using a nickel based brookhart catalyst.

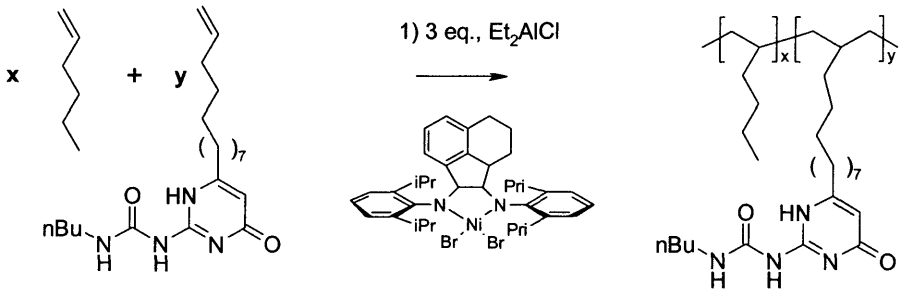

74

Scheme 9: Synthesis of compound **74**

The use of 3 equivalents of monofunctional Upy was necessary in order to prevent precipitation of the growing polymer. The resulting copolymer showed distinctive mechanical properties compared to the homopolymer of 1-hexene. Due to the reversibility of the hydrogen bonding network, the solution viscosity of the copolymer showed strong concentration dependence as opposed to the homopolymer. Furthermore, while the homopoplymer was a viscous liquid, polymer **74** showed elastomeric properties at room temperature.

In an attempt to produce a strong and elastic material, Guan *et al.* have recently reported the incorporation of Upy within a linear polyurethane polymer.[123] For this purpose the diol **78** was prepared *via* a three step synthesis (Scheme 10). The protected precursor **77**, was used to prepare control polymers, which cannot dimerise. Modular polymer A and control polymer B were then prepared *via* the reaction with isocyanate terminated polyurethanes. Due to the loops formed, polymer A shows increased tensile strength and elasticity compared to polymer B.

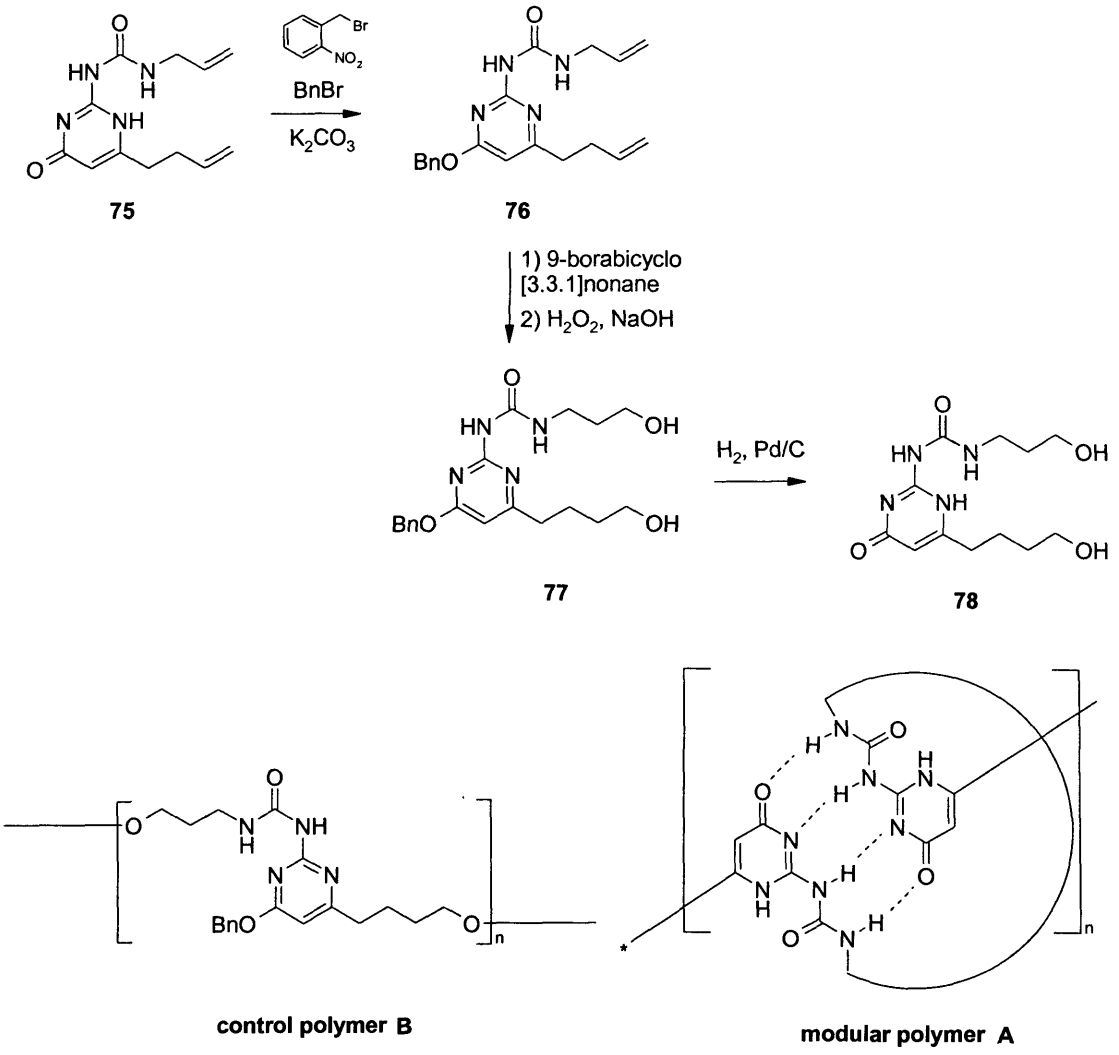

Scheme 10: Synthesis of compounds **77** and **78**

Trifunctional Upy Derivatives

Like the synthesis of linear bifunctional supramolecular polymers, it is possible to form a supramolecular network, based on trifunctional molecules. For example, polymer **79** (Figure 45) was found to form highly viscous solutions in $CDCl_3$, twice as viscous than the bifunctional polymer, and did not lead to gelation, due to the reversibility of the network.

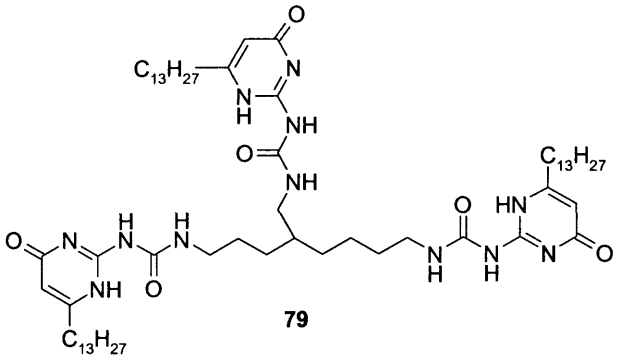

Figure 45: Trifunctional derivative **79**

Meijer *et al.* described the first 3D network supramolecular polymer based on the functionalisation of trifunctional block copolymers of propylene oxide and ethylene oxide (Scheme 11).[124] In order to link the Upy and the copolymer, a reactive and selective coupling agent was necessary. For this purpose, the diisocyanate (4)-isocyanatomethyl-methylcyclohexylisocyanate (IMCI) was used for its selectivity (one primary and one secondary isocyanate in the molecule) and reactivity. The telechelic polymer **80** can first react with the primary isocyanate functionality of IMCI, followed by the reaction of isocytosine with the secondary isocyanate moiety. Crosslinked polymer **81** formed viscoelastic reversible networks, while its analogue **82** was a liquid. Supramolecular polymer network possesses the property of "self-healing", i.e., they can reassemble to form the thermodynamically most favourable state, leading to dense and strong networks.

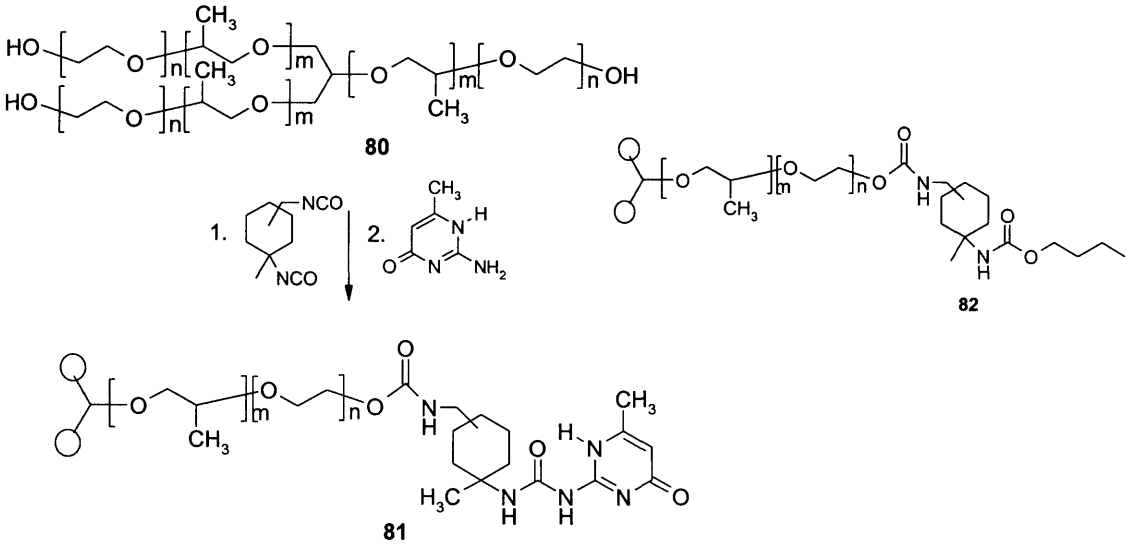

Scheme 11: Synthesis of compound **81**

1.4.3.7 *Polymeric Versus Cyclic Species*

In any polymerisation process (covalent or non-covalent), cyclisation is often observed, although it has been ignored for a long time. The presence of cyclic aggregates in the polymer can considerably affect the mechanical properties of the final material. The formation of cyclic species tends to increase in dilute solutions where the ring formation is favoured over chain extension. Jacobson and Stockmayer predicted the existence of a critical concentration,[125] below which the equilibrium composition of the system consists exclusively of rings, and above which the concentration of rings become constant and all additional material is composed of polymers.

Like other traditional polymers, supramolecular polymers based on Upys are in dynamic equilibrium with cyclic species. The isolation and characterisation of cyclic species is difficult due to the reversibility of the process. However, methods such as NMR diffusion and viscometry have been developed recently in order to measure the presence of cyclic species in supramolecular polymers.

Meijer *et al.* have studied the cyclisation of hetero-dimers between **83** and **84** (Figure 46). The bifunctional compounds **83**, **84** and **85** possess short linkers (max n = 12) to restrict homo-cyclisation.[126,127] Indeed, the latter will require a folding of the molecule since the Upy units have to be in an anti-parallel conformation in order to self-assemble.

Viscometry studies revealed that compounds **83** and **85** behave as polymers, but in an equimolar solution in chloroform the presence of cyclic heterodimers below a critical concentration of 7 mM (**86**) was observed. A quantitative analysis of the cyclic species was possible using the NMR chemical shift of the vinylic proton in the Upy ring, which shows separate signals for the cyclic and polymeric aggregates.

Cyclic species are not favourable products in polymerisation process, however they can be particularly useful as supramolecular assemblies for the host-guest chemistry. For example, in the case of 'Rosette and Ribbon' described previously, the steric effect and preorganisation direct the product distribution towards the rosette shape by decreasing the entropy penalty for cyclisation. This principle has been applied to the Upy system. In order to generate cyclic species in solution, a more preorganised linker has been used, either with a rigid spacer or with a bulky substituted linker.

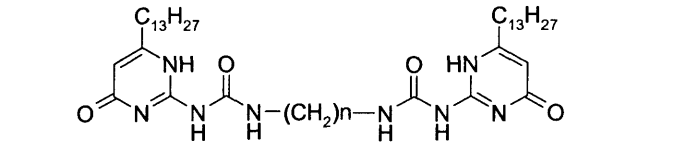

83 n =12
84 n = 6

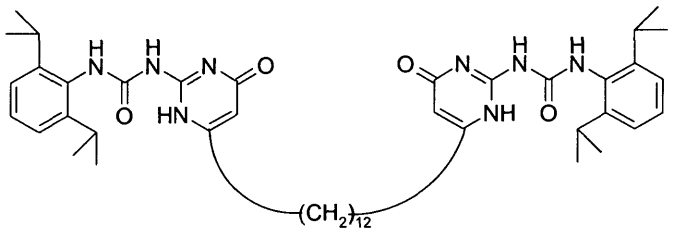

85

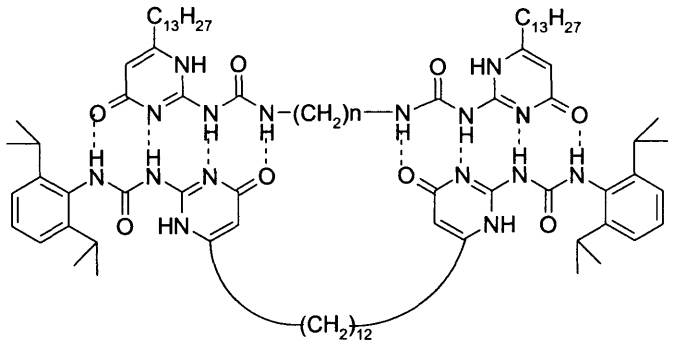

86

Figure 46: Formation of the cyclic structure **86**

Preorganisation Using a Rigid Spacer

Meijer *et al.* have reported the synthesis of bifunctional Upys connected by a tetramethyl *m*-xylene linker (**87**, Figure 47).[128] These molecules appeared to form extremely stable cyclic dimers in solution ($CDCl_3$) and in the solid state and even for a saturated solution no traces of polymeric aggregates were observed. At least three different isomers of the bifunctional Upy derivative exist, and the X-ray analysis revealed the presence of two isomers. The first one was a '*syn*' form, where the Upy groups, both in the 4-keto form, are parallel to each other. The second one was '*anti*' with the Upy groups being in an anti-parallel conformation.

Studies in solution showed the presence of a third form, in which one half is the keto tautomer, and the other one the enol form. Measurements of exchange rates were

performed using dynamic NMR studies and the constants of exchange are depicted on Figure 47.

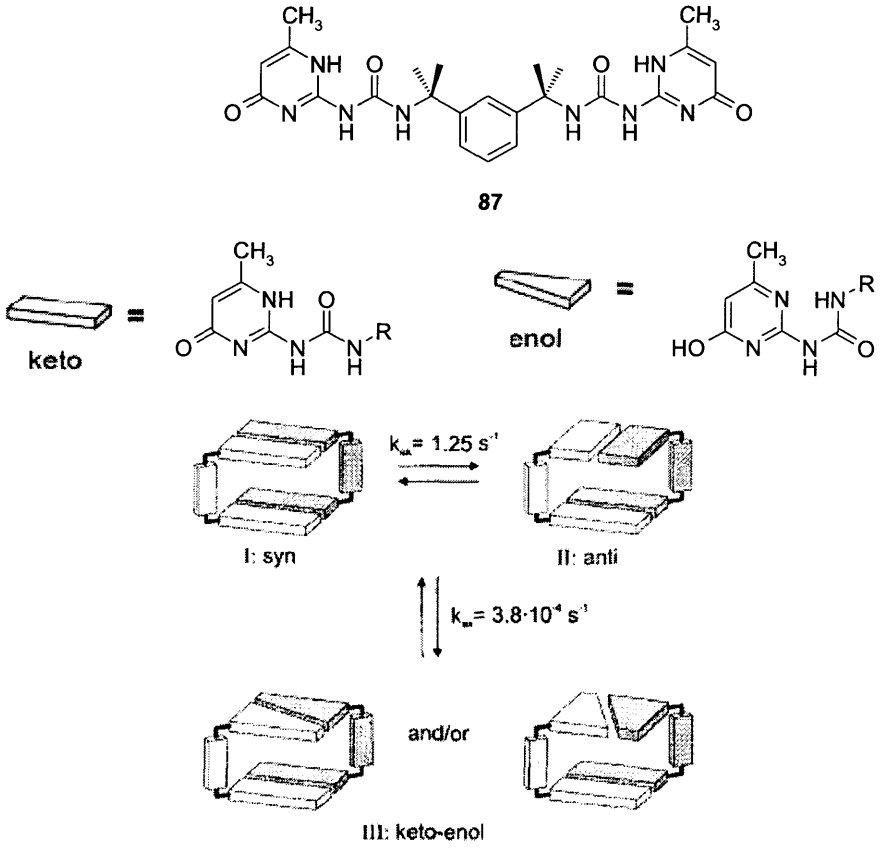

Figure 47: Equilibrium between *syn* and *anti* conformation[128]

Recently, Mendoza *et al.* reported the strong dimerisation of a cyclic dimer preorganised using a rigid calixarene [4] (**88**, Figure 48),[129] which was highly stable in chloroform. The dimerisation constant was estimated to be 2500 M^{-1} and 572 M^{-1} for solutions in chloroform containing 64% and 73% of DMSO, respectively.

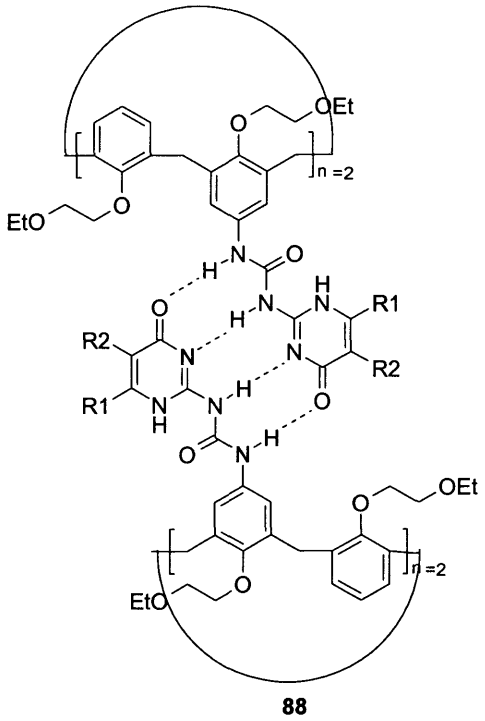

88

Figure 48: Ureidopyrimidinones incorporating calixarene moieties

Another way to favour the formation of cyclic dimers is the use of flexible linkers with bulky substituents.

Preorganisation Using a Biased Linker

Inspired by Hoffman's work[130] on the conformations of alkyl chains substituted by methyl groups, Meijer *et al.* built a bifunctional Upy, linked with a flexible alkyl chain, substituted by methyl groups. It was rationalised that the molecule would prefer adopting a conformation where the methyl groups are in anti-orientation to each other, due to steric effects (Figure 49). This would favour a U-shape conformation promoting cyclisation without loss of flexibility.

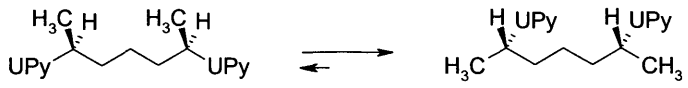

Figure 49: Conformational equilibrium

Several different bifunctional molecules were synthesised with different substituents and their critical concentrations were measured in chloroform.[131] The results are shown in Table 4.

Compounds	Critical concentration (mM)
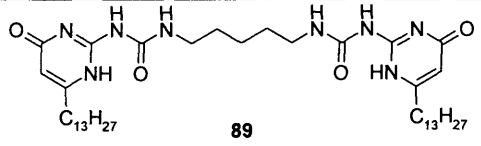 **89**	6
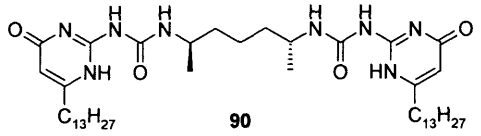 **90**	>300
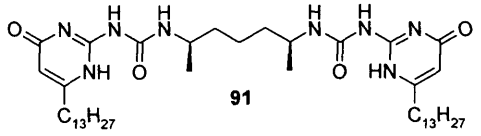 **91**	33
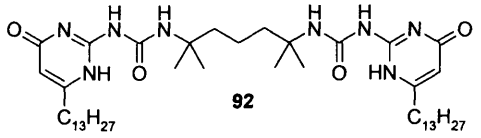 **92**	95

Table 4: Critical concentrations determined by NMR

The results were in accordance with their hypothesis, since methyl substituted linkers promote the formation of cyclic dimers compared to a linear alkyl chain. In the light of these results, methyl groups adopting an *anti* position to each other (**88**) promote the cyclisation.

Controlling the Ring-Chain Equilibrium

Bifunctional units linked by C-5 linkers (Table 4) showed a typical behaviour where the cyclisation is entropically favoured, i.e. on raising the temperature, the equilibrium was shifted towards cyclic species.

Meijer *et al.* found that bifunctional Upys such as compound **93** (C-6, biased trimethyl) showed unexpected entropy-driven polymerisation (Figure 50).[132] On heating, the equilibrium between cyclic and polymeric species was shifted towards the formation of polymer according to viscosity measurements.[133]

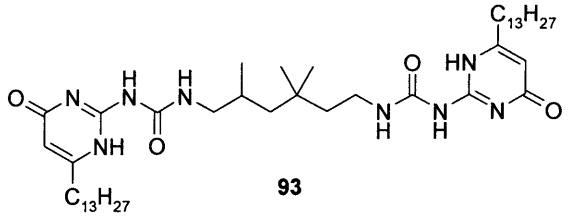

Figure 50: Upy incorporating a biased linker

1.4.3.8 *DDAA Arrays other than Upy*

In an innovative effort to build a DDAA array with tautomeric fixation and very strong self-association, Corbin and Zimmerman developed a new module, which meets these criteria.[134] Compound **94** was synthesised in two steps and dimerised *via* a DDAA regardless of tautomerism (Figure 51). Results showed that compound **94** formed very stable cyclic aggregates in solution (toluene), while polymeric species existed preferably in more polar solvents such as THF. The specific structure that was formed was highly dependent on the size of the dendron and the solvent. The largest nanoscale assembly was hexamer, highly stabilised *via* 30 hydrogen bonds in total, with a molecular mass about 17.8 kDa.

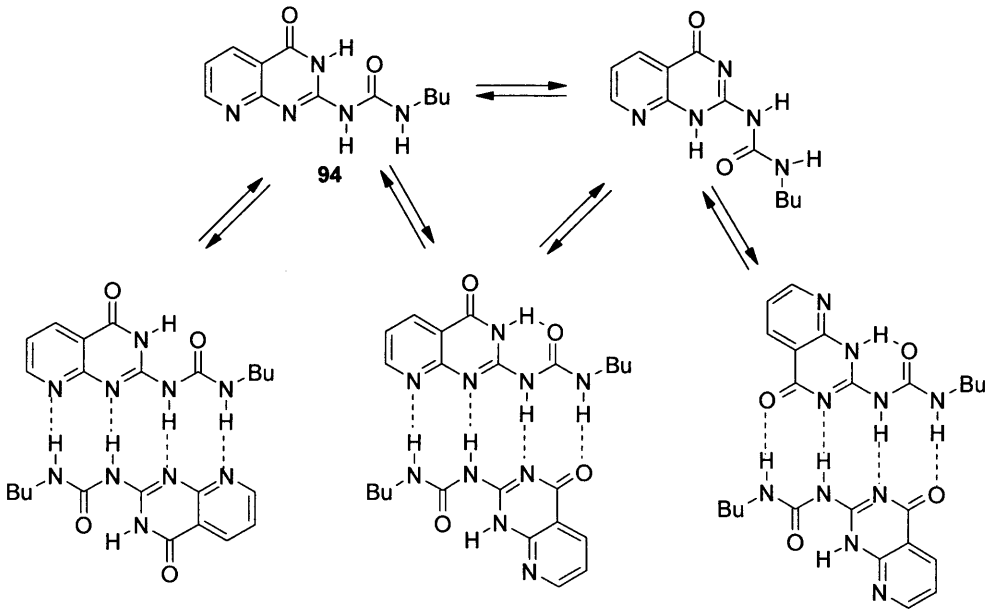

Figure 51: Tautomeric equibria of compound **94**

In order to assess the K_{dim} value in solution, the group used fluorescence measurements. The dimerisation constant was found to be exceptionally high with $K_{dim} > 5 \times 10^8\ M^{-1}$. In order to take advantage of the exceptionally high dimerisation constant for the building block of nano-structure, two units of **94** were linked together *via* a rigid spacer with a first, second and third generation dendron (Gn, **96**). An important characteristic of compound **96** was that the linker could either adopt a symmetrical arrangement (head-to-head) expressing polymeric properties (**95**) or anti-symmetrical (head-to-tail) (**97**), leading to a cyclic aggregate (**98**) (Figure 52).

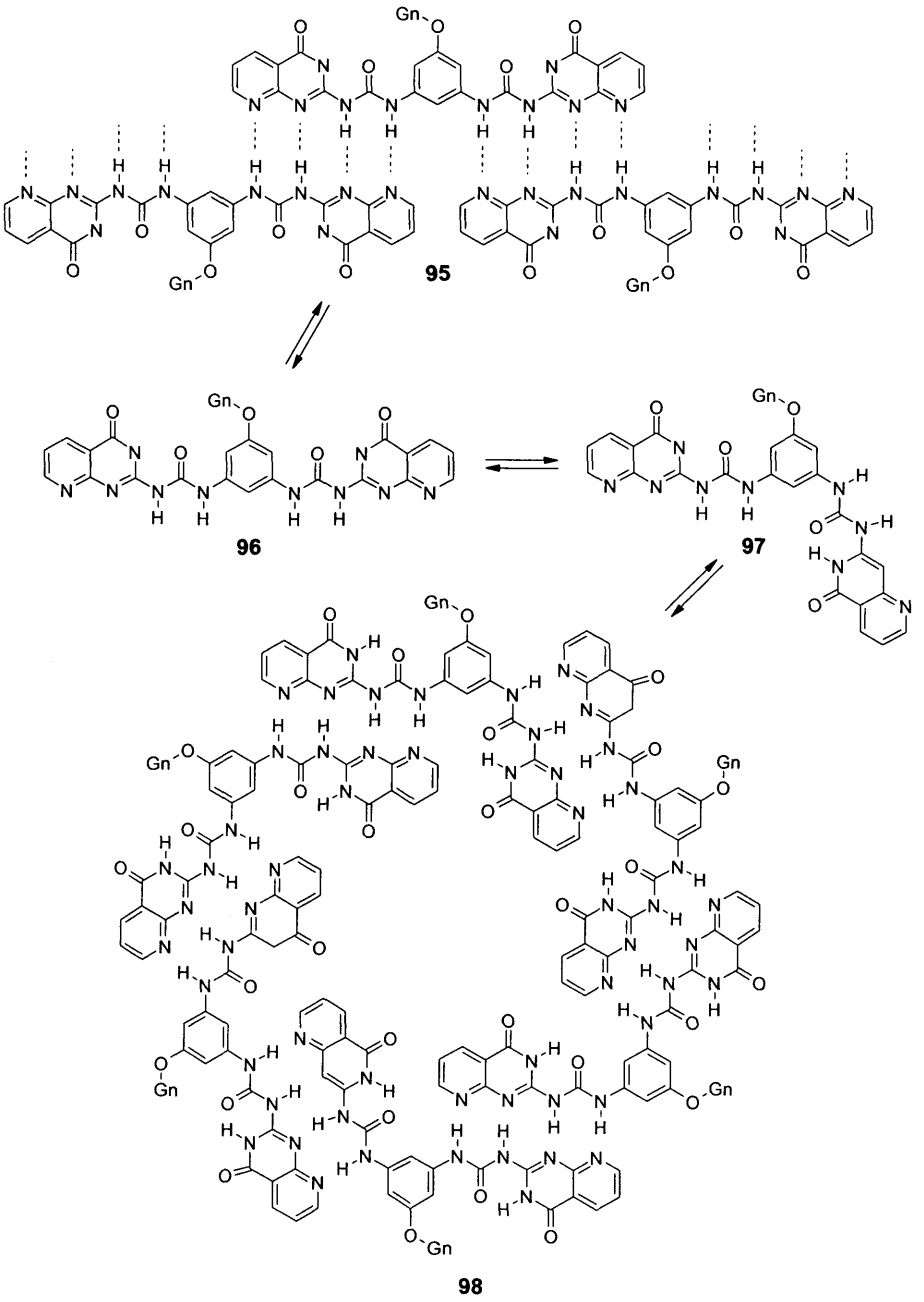

Figure 52: Self-association of compounds **96** and **97**

Unlike the DDAA arrays previously made using triazine, isocytosine or pyrimidine, further research by Davis *et al.* highlighted the use of the *N*-carbamoyl squaramide module (**99**, Figure 53), which dimerises *via* two bifurcated hydrogen bonds.[135]

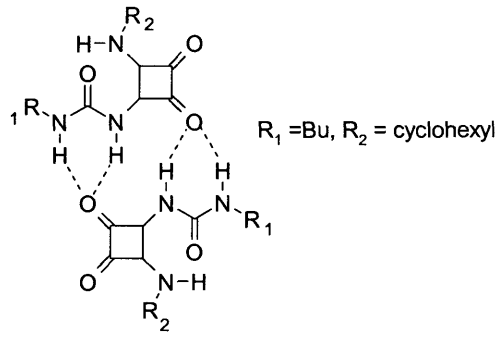

99

Figure 53: Quadruple hydrogen bonding of *N*-carbamoyl squaramide **99**

No signs of dissociation of the dimer in $CDCl_3$ were observed by NMR, down to a concentration of 0.5 mM suggesting a strong dimerisation. A study in a mixture of $CDCl_3$-DMSO (99:1) suggested a dimerisation constant of 180 M^{-1}.

Conclusion

Hydrogen bonding is an essential interaction for the self-assembly of small units into complex supramolecular structures. A significant breakthrough was made in the field of supramolecular polymers, when Meijer synthesised a strong quadruple hydrogen bonding unit (Upy). Since then, many research groups have used the ureidopyrimidinone unit as a building block for the synthesis of new materials, useful in areas such as electronics, cosmetics and drug delivery.

The aim of our research was the use of Upy derivatives for the synthesis of energetic and non-energetic supramolecular polymers, as well as for the synthesis of cyclic assemblies. Upy is a complex system due to the presence of tautomeric forms in solution, and a target was the study of its tautomerism using functionalisable electron-donating groups. In addition, the synthesis of a novel array with different complexing properties that could be useful for the generation of polymeric arrays was of particular interest.

Chapter II

2 Ureidopyrimidinones Incorporating a Functionalisable *p*-Aminophenyl Electron-Donating Group at C-6

2.1 Introduction

Ureidopyrimidinones (Upy) have significant potential for use as building blocks in the synthesis of new supramolecular architectures. The Upy systems have the characteristic features to dimerise in a self-complimentary array of four hydrogen bonds such as DDAA with a very high dimerisation constant (K_{dim}) of approximately 10^7 M^{-1} in $CDCl_3$. Although the synthetic accessibility and strong hydrogen bonding arrays generated highlights the advantages of using Upy, a less attractive but important feature is the presence of up to three tautomeric forms in solution.[111] Depending on the solvent and the concentration used as well as the substituents (R_1 and R_2), the three forms, '6-keto' (**A**), '4-keto' (**B**) and 'enol' (**C**), are in equilibrium (Scheme 12).

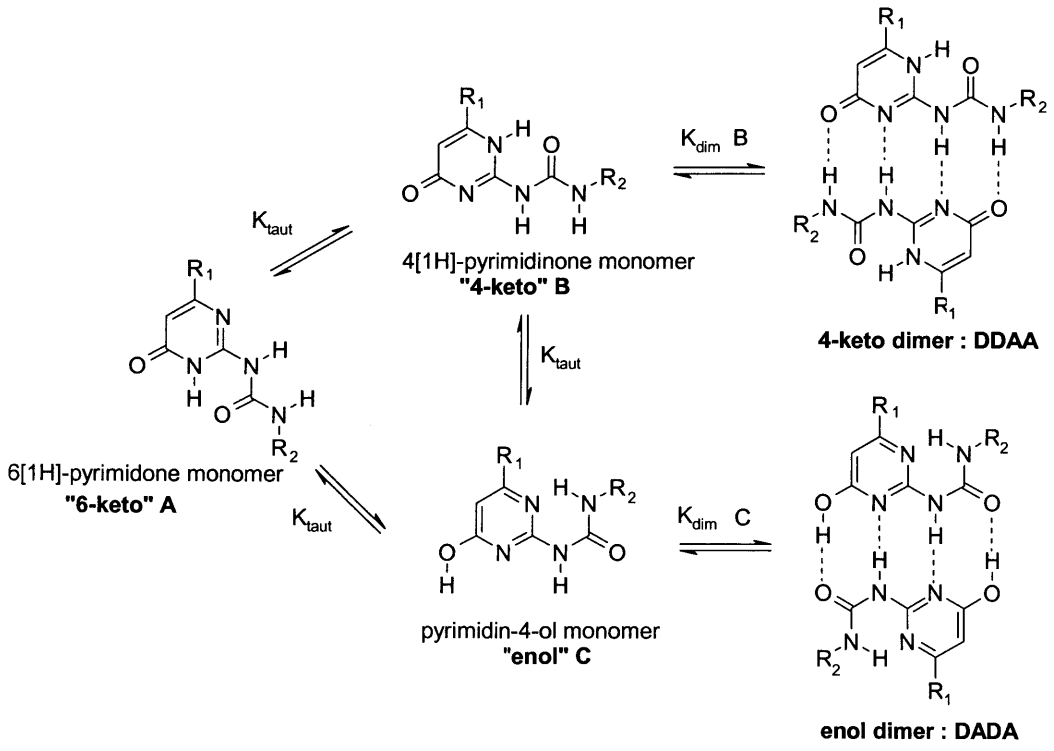

Scheme 12: Three tautomeric forms of ureidopyrimidinones

Two of these tautomers **B** and **C**, strongly dimerise *via* a quadruple hydrogen bonding array possessing an intramolecular hydrogen bond. Both of them have contributed to numerous applications in materials chemistry, including the use for the design of reversible polymers that respond to external stimuli and enhance processability. Unlike tautomers **B** and **C**, the '6-keto' form (**A**) cannot dimerise *via* quadruple hydrogen bonding due to the spatial arrangement of the donor and acceptor groups within the molecule. Therefore, the '6-keto' form (**A**) normally exists as a monomer in solution. Meijer *et al.*, pioneers in this area, have studied the effect of the polarity of the solvent as well as the nature of the substituents, at R_1 and R_2, on the tautomeric equilibrium. Several techniques were used for the characterisation of the tautomeric equilibria, but NMR measurements proved to be most useful. For example compound **100** (Figure 54), which possesses a phenyl group at the C-6 position shows two sets of signals in the ^1H NMR spectrum. One set of N-H signals (87% abundance) at 13.95 ppm (1-H), 12.06 ppm

(7-H) and 10.23 ppm (9-H), which corresponds to tautomer (**B**) and the second one at 13.6 ppm, 11.3 ppm and 10.0 ppm assigned to tautomer (**C**) with an abundance of 13% (Figure 54). The aromatic proton 5-H of tautomer **C** resonates 0.5 ppm downfield to the alkylidene signal found in tautomer **B**. Based on this observation, a series of compounds (**2** to **10**) was studied by Meijer *et al.* and the relative amounts of tautomer **B** and **C** in $CDCl_3$ and toluene were determined by the integration of peaks in the ^1H NMR spectra (Table 5).

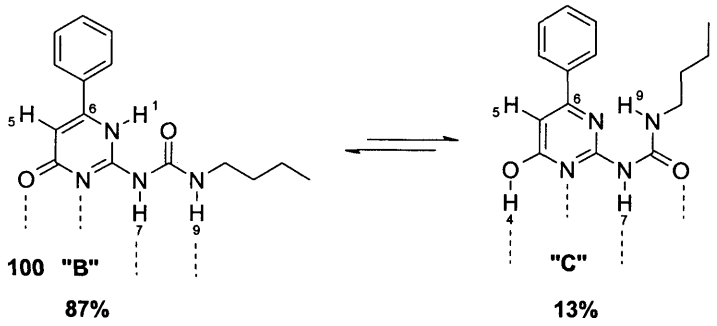

Figure 54: Equilibrium between tautomers **B** and **C**

Compound	R_1	R_2	% tautomer B $CDCl_3$	% tautomer B Toluene-d_8
101	CH_3	*n*-C_4H_9	>99	insoluble
102	$C_{13}H_{27}$	*n*-C_4H_9	>99	87
103	$C_{13}H_{27}$	C_6H_5	>99	98
104	$C_{13}H_{27}$	*p*-$NO_2C_6H_5$	>99	insoluble
105	$C_{13}H_{27}$	*p*-$NEt_2C_6H_5$	>99	97
106	*p*-$NO_2C_6H_5$	*n*-$C_{18}H_{37}$	40	insoluble
107	CF_3	*n*-C_4H_9	<1	-
108	$C_6H_2(OC_{12}H_{25})_3$	*p*-$NO_2C_6H_5$	>99	>99
109	$C_6H_2(OC_{12}H_{25})_3$	*p*-$NEt_2C_6H_5$	85	51

Table 5: The tautomeric ratio of B/C in different solvents as a function of R_1 and R_2 [111]

As apparent from this data, alkyl groups R_1 at the C-6 position (**101-105**) favoured the formation of the 4-keto form (**B**) (> 99%) in both $CDCl_3$ and toluene-d_8 and it was found that the nature of the substituent (R_2) had very little influence on this equilibrium. Interestingly, electron-withdrawing groups at R_1 such as *p*-nitrophenyl (**106**) and trifluoro (**107**) (R_2 = *n*-C_4H_9 and *n*-$C_{18}H_{37}$, respectively) increased significantly the population of tautomer **C** in $CDCl_3$. Indeed, more than 99% of **C** was found for compound **107**, and 60% for compound **106**. This was explained by the electron-withdrawing group at C-6 which tends to decrease the electronic density at the carbonyl group involved in hydrogen bonding, and then reduces the stability of the 4-keto form **B** in favour of the enol form **C**.

For compounds **108** and **109** which possess an aryl electron-donating moiety (C_6H_2-$(OC_{13}H_{27})_3$) at C-6, tautomer **B** dominated in $CDCl_3$, but there was also a significant dependence on the nature of the substituent R_2. In particular, for compound **108** with the electron-withdrawing group (*p*-$NO_2C_6H_5$), the 4-keto tautomer was the predominant form in both solvents studied, whereas the change from *p*-NO_2 in **108** to *p*-NEt_2 in **109** resulted in a significant increase of the enol form **C**. In the case of compound **109**, the dependence of the tautomeric distribution on the nature of the solvent was also apparent. It is clear from these observations that the nature of the substituent at C-6 has a pronounced effect on the tautomeric form adopted by the Upy system in solution. In $CDCl_3$ or toluene-d_8, only dimeric species of tautomers **B** and **C** were present. In mixtures of $CDCl_3$ and DMSO-d_6 compound **101,** which existed almost exclusively as tautomer **B** in pure $CDCl_3$, was in equilibrium with a second tautomer. This second tautomer had one hydrogen bonded NH proton at 11.4 ppm and two non-hydrogen bonded NH protons at 9.4 and 7.2 ppm and was the only tautomer found in pure

DMSO-d_6. This new tautomer was assumed to be the 6-keto monomer (**A**) (Scheme 12). The observation made for compound **101** was further generalised by Meijer *et al.* for the other Upys included in Table 5.

The understanding of such complex tautomeric systems in solution is of critical importance for the synthesis of supramolecular polymers. Indeed, not only a strong hydrogen bonding network is required, but for a predictable recognition process the presence of a single tautomer in solution is desirable. Here, Upys with alkyl groups (**101-105**) and trifluoro (**107**) at R_1 meet these criteria and therefore, Upy units with alkyl groups at C-6 such as CH_3 and $C_{13}H_{27}$ have been widely used for the synthesis of supramolecular architectures.

In order to design new materials with enhanced structural diversity, the incorporation of a functionalisable group at the C-6 position of the ureidopyrimidinone ring has been a key objective in this project. In particular, to assess the influence of functionalisable electron-donating groups on both the dimerisation motif and the tautomeric distribution of isomers, the synthesis of compounds possessing a *p*-aminophenyl group and azo derivatives at C-6 was investigated. A particular interest was the tautomeric distribution, which ultimately could allow tuning properties of this interesting class of materials in a controlled manner. It should be noted that previous studies of Upy derivatives provided only limited data for the characterisation of the tautomers in solution, especially for the 6-keto form. Therefore, considerable effort was put into verification of the results using NMR studies, both in solution and the solid state. The results of these detailed studies are also included in this chapter.

2.2 Synthesis

The synthesis of 6-(*p*-aminophenyl)isocytosine **112** was performed as shown in Scheme 13. For simplicity, all the compounds are represented in the 4-keto form **B**, but it does not reflect the actual tautomeric form adopted in a given solvent or in the solid state.

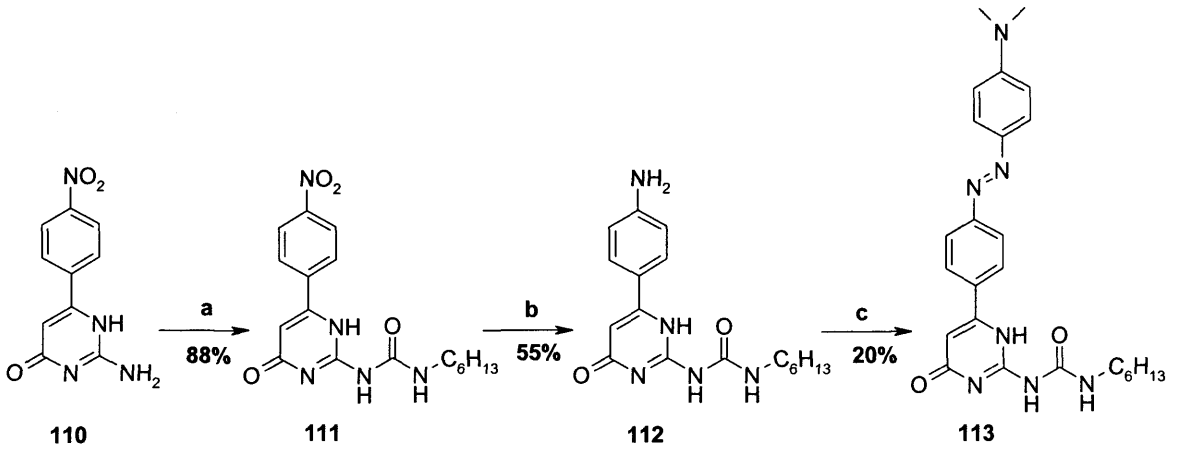

110 111 112 113

Reagents and conditions : **(a)** $C_6H_{13}NCO$, pyridine, reflux, 18h, 88%; **(b)** $SnCl_2$, HCl, EtOH, reflux, 1h, 55%; **(c)** $NaNO_2$, $C_6H_5NMe_2$, 20%.

Scheme 13: Synthetic routes towards the formation of compounds **112** and **113**

Initially, ethyl-*p*-nitrobenzoyl acetate was reacted with guanidinium carbonate to give the 6-subtitutued isocytosine **110** in 32% yield as yellow needles as previously reported.[111] Subsequent coupling with hexyl isocyanate in dry pyridine gave compound **111** in 88% isolated yield. Reduction of the nitro group was first carried out using catalytic hydrogenation[136,137,138] with H_2 over Pd/C in MeOH but was not successful due to the very poor solubility of **111** in organic solvents. Further attempts using other solvents such as THF, EtOH or EtOAc did not show any traces of compound **112** either. Therefore, other reduction methods were investigated and the use of tin chloride (II) in acidified ethanol[139,140] successfully gave **112** in 54% isolated yield. Under such acidic conditions the protonated amine was first isolated which was then washed thoroughly with a basic solution to give the primary amine.

The synthesis of a derivative of **112**, containing an azo moiety as an alternative electron-donating group, was then carried out. Formation of derivative **113** was achieved *via* diazotisation of **112** using sodium nitrite and *N,N*-dimethylaminobenzene in acidic media.[141,142,143] Unfortunately, compound **112** had very low solubility in the reaction solvent (acetic acid) and compound **113** was isolated in 20% yield.

The synthesis of compounds **112** and **113** possessing an electron-donating group at C-6 with an alkyl chain C_6H_{13} at the ureido position (R_2), had been achieved, but the very poor solubility of these two compounds in most organic solvents and particularly in $CDCl_3$ limited their analysis by NMR studies. These compounds were however soluble

in DMSO-d_6 and most of the NMR experiments were then performed in this alternative polar solvent (Table 6).

Initial tautomerism studies were carried out on the amine **112** together with **111** and **114** as control compounds, in $CDCl_3$ and DMSO-d_6. Analogues of **111** and **114** have been previously studied by Meijer *et al.* Compound **114** was synthesised from the reaction between 6-methylisocytoine and hexyl isocyanate in dry pyridine and was obtained in 82% yield (Scheme 14).

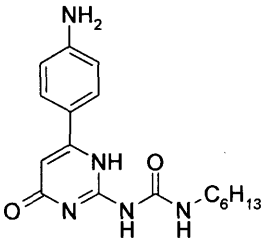

112

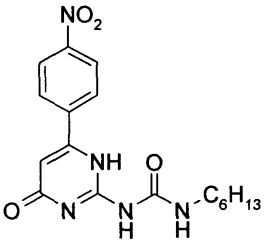

111

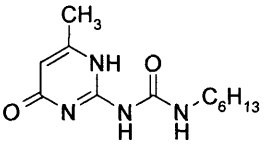

114

Solvents			
$CDCl_3$	very poor solubility	insoluble	soluble
DMSO	soluble	soluble	soluble

Table 6: Compounds **111**, **113** and **114** and their solubilities in $CDCl_3$ and DMSO-d_6

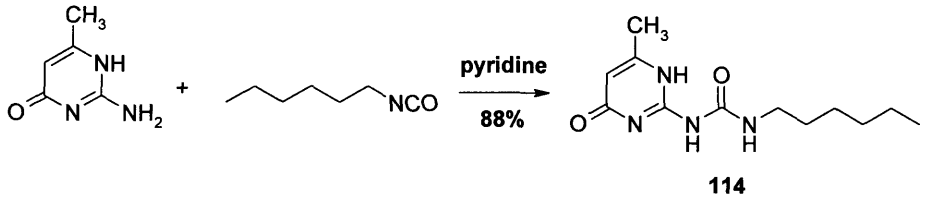

114

Scheme 14: Synthesis of compound **114**

2.3 NMR Spectroscopic Studies in Chloroform

2.3.1 Compound 114

Compound **114** was first studied in $CDCl_3$ in order to establish the full chemical shift assignment and to compare the results with analogous compounds **101-105** (Table 5) reported previously.

The ^{1}H NMR spectrum of **114** showed the characteristic hydrogen bonded protons of tautomer **B** at 13.13, 11.85 and 10.14 ppm for 1-H, 7-H and 9-H, respectively, as well as the vinylic proton 5-H at 5.81 ppm. The hydrogen bonded protons of the enol form **C** were also observed at 13.40, 11.15 and 9.90 ppm, respectively for protons 4-H, 7-H and 9-H (Figures 55 and 56). The chemical shift of proton 5-H in tautomer **C** was shifted downfield to 6.15 ppm as expected. The ratio of tautomer **B/C** was found to be 99/1. Interestingly, the enol form **C** was not identified previously for compound **101** (Table 5), presumably because it was present in only very small quantities. Interestingly, on increasing the temperature from 298 K to 328 K the proportion of tautomer **C** increased from 1% to 5%. This small change highlighted the effect of temperature on the tautomeric equilibrium.

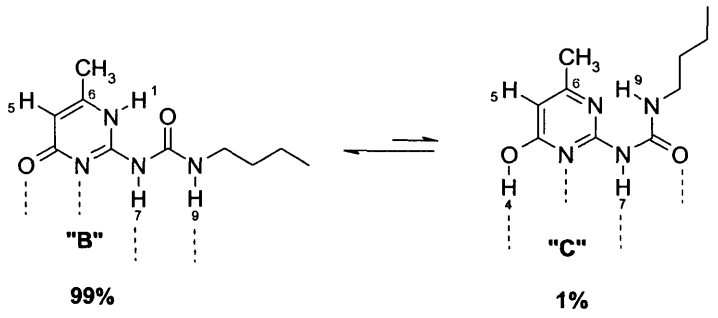

Figure 55: Equilibrium between tautomers **B** and **C**

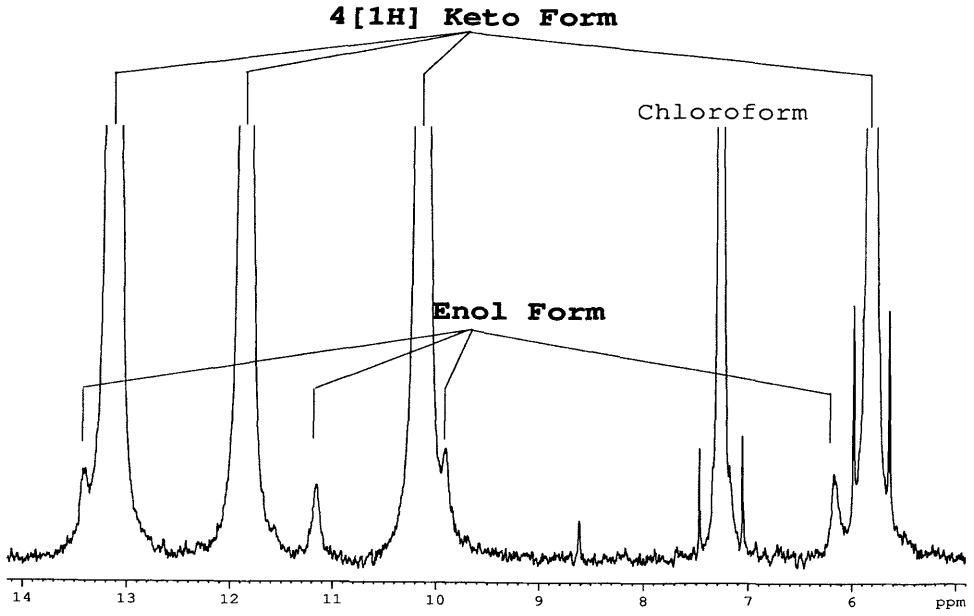

Figure 56: ^{1}H NMR spectrum of **114** in $CDCl_3$ showing the two tautomers **B** and **C**

Other characteristic NMR parameters were also revealed, supporting the 4-keto tautomer **B** as the predominant form. For example, the W type configuration is present

between protons 5-H and 1-H in tautomer **B** (Figure 57). A relatively large value of the long-range $^4J_{HH}$ coupling was therefore expected and the measured value was 1.7 Hz. In addition, $^4J_{HH}$ coupling between protons 5-H and CH_3 was also measured (1.0 Hz).

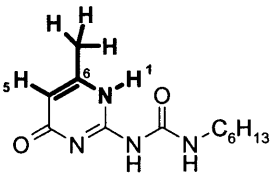

Figure 57: Long range J-coupling paths in the 4-keto form **B**

Further structural information was obtained using NOE measurements. One advantage of this technique is that both the structural and dynamic features can be monitored *via* (usually) positive enhancements corresponding to NOEs due to spatial proximity of protons or negative enhancements if there is an exchange, either inter- or intramolecular, between different species present in solution. An example of results obtained from NOE experiments showing both of these effects is presented in Figure 58. Here, proton 7-H was selectively excited and a positive enhancement of proton 9-H was detected, which confirmed the linear arrangement of these two protons in a DDAA array. The observed negative enhancements between 4-H (**C**), 1-H (**B**), and 7-H (**C**) (-80%, -1% and -130%, respectively) was indicative of an exchange process, between tautomers **B** and **C** (Figure 58).

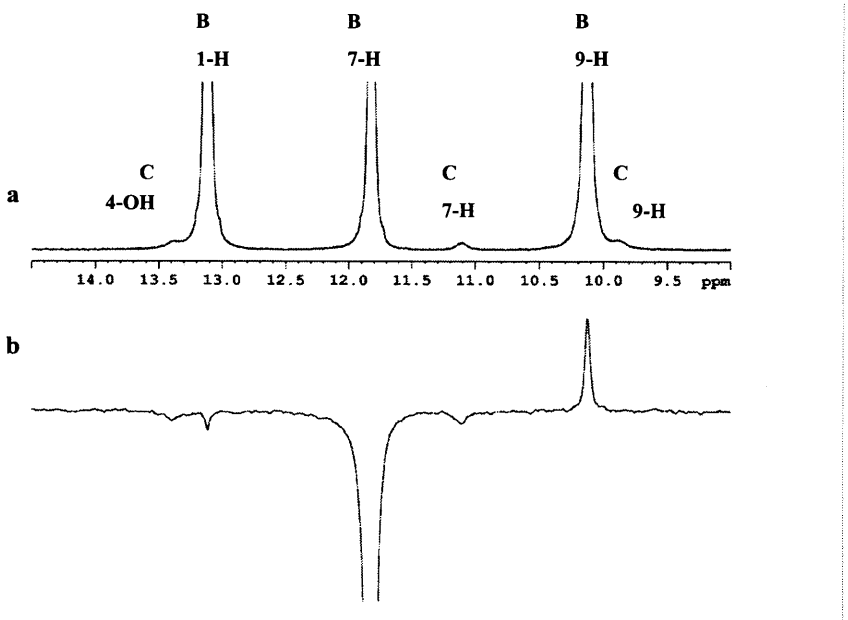

Figure 58: a) ^{1}H NMR spectrum of compound **114**. b) Selective excitation of proton 7-H and enhancements observed.

Carbon-13 NMR spectra were run in $CDCl_3$ at 323 K in order to assign the chemical shifts of the two tautomers present in solution. The temperature used for the experiment was dictated by the increased amount of the enol observed at higher temperatures. ^{13}C chemical shifts were found to vary quite significantly between the two forms **B** and **C** in solution, mainly due to the aromacity of the ring in the enol form **B**. In particular, carbon C-5 shifted upfield from 106.6 ppm in the 4-keto form **B** to 101.7 ppm in the enol form **C**.

In such complex heterocyclic systems where three different tautomers can exist, the use of ^{15}N NMR can be useful for the determination of the tautomeric species in solution and the solid state. For this purpose, ^{1}H, ^{15}N correlation experiments were run in $CDCl_3$ at 298 K using a 70 mM solution of **114**. As expected for tautomer **B** three different chemical shifts characteristic of secondary amines were found at -248.5, -266.0 and -279.9 ppm for N-1, N-7 and N-9, respectively, relative to nitromethane (0 ppm). A signal at -170.1 ppm was assigned to the unprotonated nitrogen N-3 (Figure 59). The assignment of the ^{15}N peaks was made using the cross peaks observed in the ^{1}H, ^{15}N HMQC and HMBC spectra.

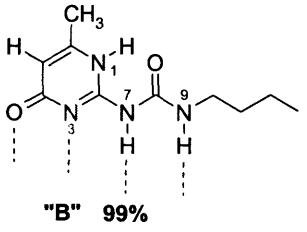

Figure 59: Compound **114** highlighting three secondary N and one tertiary N atoms

In the solid-state the ^{13}C and ^{15}N NMR chemical shifts were measured using the conventional CPMAS technique. Comparison of ^{13}C and ^{15}N chemical shifts data observed in solution and in the solid state was made. In general, such a comparison is a straightforward method for detecting any tautomeric changes that may occur on dissolving a solid sample in a solvent. Compound **114** showed almost identical ^{13}C and ^{15}N chemical shifts in the $CDCl_3$ solution and in the solid state, suggesting that **114** exists predominantly as the 4-keto dimer both in the solid state and in the chloroform solution (Table 7). Some small differences in the ^{15}N chemical shifts (less than 3 ppm) can be attributed either to crystal packing effects or to stronger N1-H...O and N9-H...O hydrogen bonds in the solid state.

Position	^{13}C $CDCl_3$	^{13}C Solid State	^{15}N $CDCl_3$	^{15}N Solid State
1	-		-248.5	**-245.8**
2	154.7	**156.5**		
3	-		-170.1	**-171.5**
4	172.8	**174.7**		
5	106.6	**108.1**		
6	147.9	**148.5**		
7	-		-266.0	**-265.4**
8	156.5	**156.5**		
9	-		-279.9	**-277.4**

Table 7: Comparison of ^{13}C and ^{15}N chemical shifts in $CDCl_3$ and solid state.

To conclude, the experiments carried out on compound **114** confirmed the existence of tautomer **B** in the $CDCl_3$ solution with ~ 1% (at 298 K) of the enol tautomer **C**. Further investigation using solid-state ^{13}C and ^{15}N CPMAS NMR provided evidence for the existence of the same 4-keto form **B** in the solid state.

2.3.2 Study of Compound 112 in $CDCl_3$

As mentioned above, the solubility of compound **112** was very poor in $CDCl_3$, and only trace signals were observed in the ^1H NMR spectrum. Nevertheless, ^1H chemical shifts were measured for a very dilute solution at 328 K and key signals indicated the tautomer adopted in $CDCl_3$: 13.72 ppm (1-H), 12.00 ppm (7-H), 10.17 ppm (9-H) and 6.22 ppm (5-H). From this chemical shift values, and those for **114** and compound **129** (see Table 16), compound **112** adopted the 4-keto form **B** in $CDCl_3$ (Figure 60).

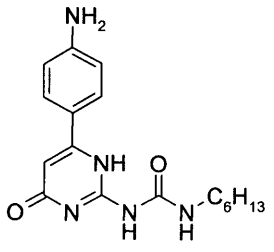

112

Figure 60: Compound **112** and representation of the 4-keto form **B**

Due to the poor solubility in $CDCl_3$, a more detailed study of this compound was then conducted in DMSO-d_6. This solvent was expected to strongly interfere with the hydrogen bonds of the ureidopyrimidinone dimers, but nevertheless could provide

additional means of assessing the strength and nature of the hydrogen bonding and indeed, whether a C-6 functionalised ureidopyrimidinone can exist as a quadruple hydrogen bonded dimer even in a DMSO solution.

Furthermore, very few studies of Upy systems have been made in such a polar solvent and this could be relevant for applications of Upys in polar aqueous media.

2.3.3 Tautomeric Studies in DMSO-d_6

2.3.3.1 *6-Methyl isocytosine*

Preliminary studies of the starting material isocytosine, which is used in the synthesis of compound **114** were carried out initially.

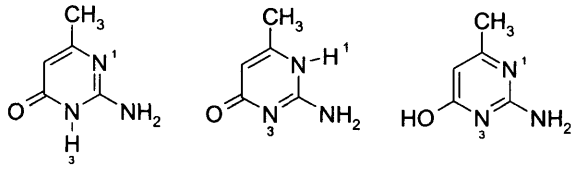

Figure 61: Three different tautomers of isocytosine

Isocytosine has been found to exist as the 4-keto form **B** in the solid state and enol form **C** in the gas phase.[144] Since the tautomeric preference of this compound in DMSO-d_6 solution has not been studied before, multinuclear NMR experiments were conducted in this solvent and in the solid-state. Since the latter was established in the solid state, the ^{13}C CPMAS was run and chemical shifts were measured as 158.2, 173.7, 101.6 and 151.1 ppm for C-2, C-4, C-5 and C-6, respectively. The ^{13}C NMR spectrum was then acquired in DMSO-d_6 and the chemicals shifts were significantly different: 164.0, 100.4, 165.4 and 155.6 ppm. It is evident from this data, that the tautomeric form is not the 4-keto **B** but rather **A** or **C** in DMSO-d_6.

In order to determine the tautomeric form in solution, ^{15}N chemical shifts were measured in the solid state and in DMSO-d_6. The assignment was made using ^{1}H-^{15}N HMBC correlations, and it was clear from the data obtained that the 6-keto tautomer **A** was the one present (Figure 62, Table 8). In particular, one secondary (-232.5 ppm) and one tertiary (-180.6 ppm) N signals were found and a cross-peak between the ^{1}H methyl peak and the ^{15}N peak at -180.6 ppm in the HMBC spectrum (at 298 K for the 170 mM

DMSO-d_6 solution) was detected, suggesting that the closest nitrogen to the Me group was tertiary. In addition, chemical shift of 5-H and its $^1J_{CH}$ coupling constant of 168 Hz were also in favour of the 6-keto form (see discussion below for compounds **111**, **112** and **114**)

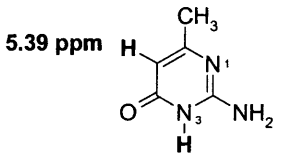

A **11.08 ppm**

Figure 62: ^{1}H NMR chemical shifts found in 6-keto A.

position	^{13}C	^{15}N
1		-180.6
2	155.6	
3		-232.5
4	164.0	
5	100.4	
6	165.4	

Table 8: ^{13}C and ^{15}N NMR chemical shifts in DMSO-d_6

2.3.3.2 *Studies of Compounds 111, 113 and 114 in DMSO-d_6*

The ^{1}H NMR spectroscopic data for the hydrogen bonded protons (1-H, 7-H, 9-H) as well as for the vinylic proton 5-H for compound **111**, **112** and **114** were assessed. Remarkably, the ^{1}H NMR spectra were very similar for compounds **111** and **114** (Figure 63a), but compound **112** gave rise to significantly different chemical shifts, suggesting that a different tautomeric form may be present (Figure 63b).

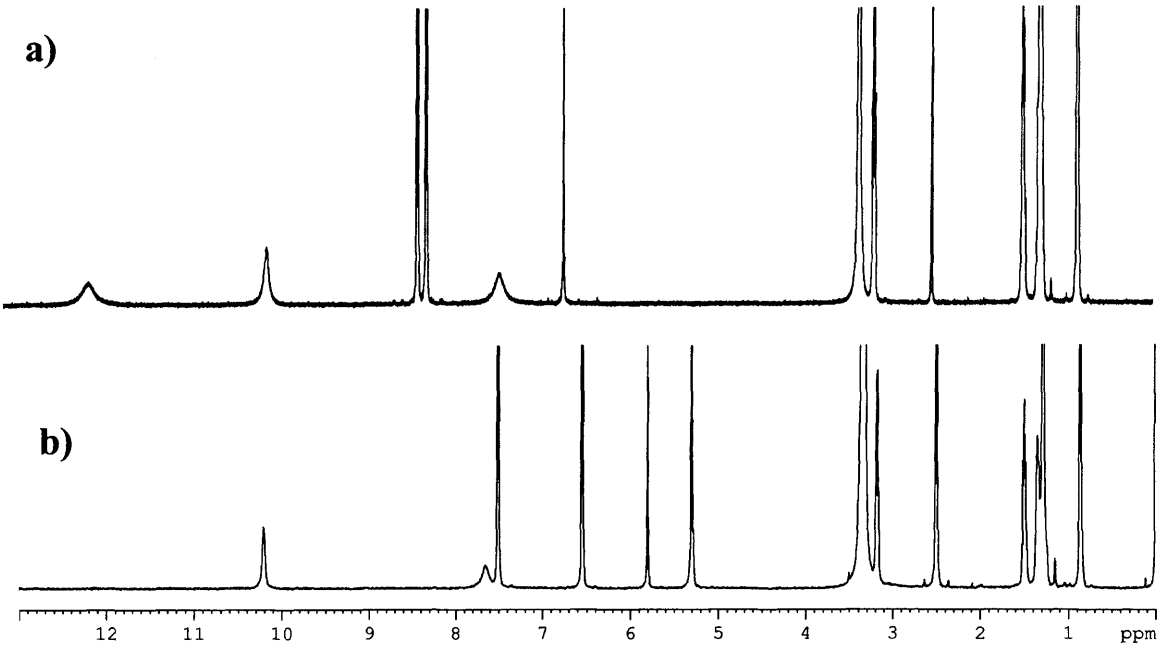

Figure 63: a) ^{1}H NMR spectrum for compound **111**, 298K, b) ^{1}H NMR spectrum of **112**, 298K

Meijer *et al.* have assumed that analogues of **111** and **114**, where $R_1 = p\text{-}NO_2C_6H_4$, $R_2 = C_{18}H_{37}$ and R_1 = Me, $R_2 = C_4H_9$, exist in pure DMSO-d_6 as the monomeric 6-keto form **A**. Examination of the chemical shift data suggested that **111** and **114** adopted the monomeric tautomer **A** in DMSO-d_6, but **112** existed as either tautomer **B** or **C**. Since the ^{1}H NMR spectrum of tautomer **A** has not been fully characterised, compound **114** was studied in detail by NMR in DMSO-d_6. The 6-keto form **A** is an interesting tautomer since it can exist as either conformer **A** or **A'** with intramolecular hydrogen bonding present in both of them (Figure 64).

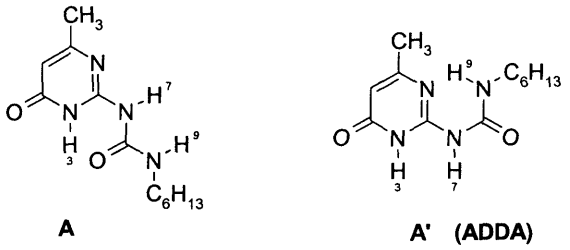

Figure 64: Two possible conformers for 6-keto form **A**

2.3.3.3 *Study of compound 114 in DMSO-d_6*

The assignment of the NH protons were made as following. Proton 9-H was first assigned without difficulty since there is a $^3J_{HH}$ coupling of 5.7 Hz between 9-H and the adjacent methylene protons of the alkyl chain. The determination of 3-H and 7-H was less straightforward but the results obtained from the study of 6-methylisocytosine in DMSO-d_6 suggested that the chemical shift at 11.46 ppm could be attributed to 3-H. From these observations a full ^{1}H NMR spectroscopic data was established for compound **114** (Table 9).

proton	114
3-H	11.46
5-H	5.77
7-H	9.76
9-H	7.44

Table 9: ^{1}H NMR Chemical shifts of **114** (79 mM solution) in DMSO-d_6 at 298 K

The chemical shifts were affected slightly on increasing the concentration of the solution in DMSO: from 11.55 (3-H), 9.65 (7-H) and 7.39 (9-H) ppm in the 14 mM solution to 11.46, 9.76 and 7.44 ppm in the 79 mM solution at 298K. The latter values are in agreement with the monomeric 6-keto tautomer. This conclusion was further supported by diffusion coefficient measurements: at three different concentrations, 28 mM, 14 mM and 7 mM, the D values were 2.66×10^{-10}, 2.65×10^{-10} and 2.63×10^{-10} m^2s^{-1}, respectively, at 298 K. No change of the diffusion rate on increasing the concentration was in favour of monomeric form, which does not dimerise on increasing the concentration.

The distinction between conformer **A** or **A'** was not straightforward. Various NMR experiments were undertaken in an attempt to address the issue of preferred conformer, and some of the NMR results described below tend to suggest that conformer **A'** could be predominant in the DMSO-d_6 solution.

Within the limits of the ^{1}H data, the chemical shift of 9-H could indicate the involvement of this proton in intramolecular hydrogen bonding, the strength of which is considerably weakened due to the high polarity of the solvent used. On the other hand the relatively high frequency shifts of 3-H and 7-H protons may be due to the intermolecular hydrogen bonding with solvent molecules, since DMSO is well known to be a strong hydrogen bonding acceptor (Figure 65).

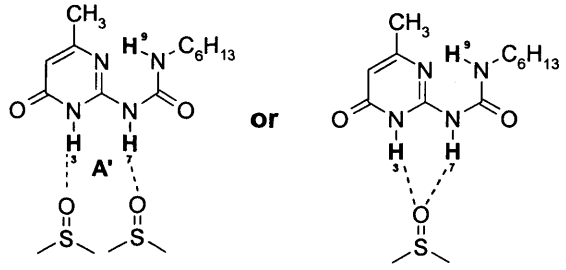

Figure 65: Tautomer **A** and interaction with DMSO molecules

In selective NOE experiments positive enhancements of protons 5-H and 9-H were observed on excitation of protons 6-Me. Qualitatively, the observation of the NOE between proton 9-H and 4-Me is in favour of the 6-keto conformer **A'**. Overall, these results suggest that **A'** is more likely to be the major conformer of the 6-keto form in DMSO. Since compounds **114** and **111** show similar ^{1}H NMR spectra, the conformer of the 6-keto tautomer is also likely to be present in the DMSO-d_6 solution of **111**. Complete assignments of ^{1}H and ^{13}C NMR spectroscopic data have been summarised in Table 10 for compounds **111** and **114**.

carbon	111 ^{1}H NMR (130 mM)	111 ^{13}C NMR	114 ^{1}H NMR (79 mM)	114 ^{13}C NMR
2		152.2		151.3
3	12.05		11.46	
4		161.4		161.1
5	6.66	104.2	5.77	104.5
6		159.1		164.8
7	10.04		9.76	
8		154.5		154.7
9	7.38		7.44	

Table 10: ^{1}H and ^{13}C chemical shifts for **111** and **114** in DMSO-d_6

A simple comparison of the ^{1}H NMR data for **111** and **114** with that of **112** was not sufficient for determination of the tautomeric form adopted by compound **112** in DMSO-d_6, and whether the 4-keto **B** or enol form **C** is favoured. Therefore, further experiments were carried out such as ^{13}C and ^{15}N in solution and the solid state.

The ^{13}C NMR spectral analysis of **112** and **114** highlighted some key differences in the chemical shift values. These differences are shown in Figure 66 (the region between 80 and 180 ppm).

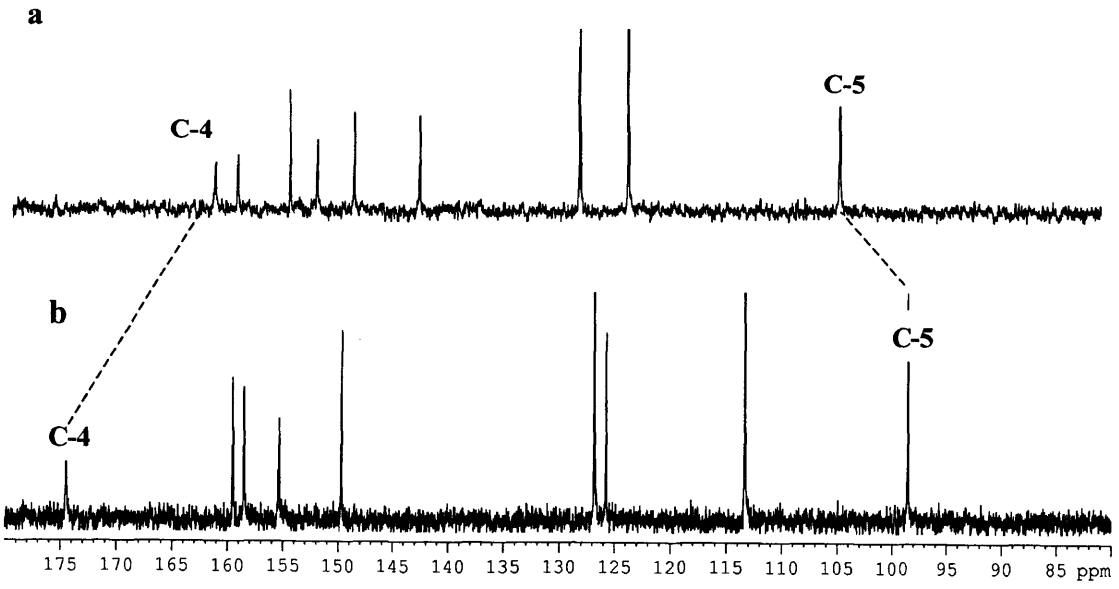

Figure 66: ^{13}C NMR spectra for compound **111** (a) and **112** (b)

Assignments based on the HMQC and HMBC experiments indicated that the vinylic carbon at C-5 has a specific chemical shift of approximately 104 ppm in tautomer **A** and

106 ppm in tautomer **B**. The latter value was determined for compound **114** in $CDCl_3$. For the enol form **C**, an upfield shift is expected due to the aromaticity of the ring. The chemical shift of C-5 for compound **112** was approximately 98 ppm, suggesting that the enol form **C** was present (Figure 67). Similarly, according to the assignments made based on the HMBC experiment, carbon C-4 was found at 161 ppm in the 6-keto form, but for **112** it was observed at 174 ppm.

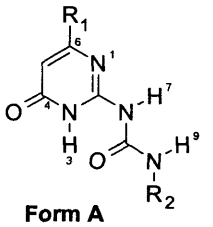

Form A

111: R_1 = *p*-$NO_2C_6H_4$, R_2 = C_6H_{13}
114: R_1 = CH_3, R_2 = C_6H_{13}

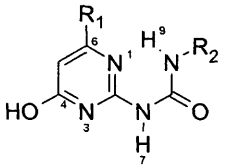

Form C ? to be confirmed

112: R_1 = *p*-$NH_2C_6H_4$, R_2 = C_6H_{13}

Figure 67: Summary of tautomeric forms adopted in DMSO-d_6

Since the number of protonated nitrogens in the enol form **C** is different from that in tautomers **A** and **B**, the use of ^{15}N and ^{13}C experiments in the solid state and in solution were undertaken for the determination of the tautomeric form of **112**.

Unfortunately, the ^{15}N HMQC and HMBC spectra in DMSO-d_6 did not allow detection of all the peaks. Only two peaks at -286 (N-9) and at -320 ppm (NH_2) were detected. In the solid-state, however, the ^{15}N CPMAS spectrum of compound **112** showed all the peaks. In particular, two tertiary N signals were observed at -164.5 ppm and -178.5 ppm and attributed to N-1 and N-3. Resonances around -250 ppm are characteristic for secondary amine groups and corresponded to N-7 and N-9 at -260.4 and -280.5 ppm. The primary amine signal was observed at -324.9 ppm. From this data it is clear that compound **112** exists as the enol form **C** in the solid state, since unlike the enol tautomer, the other two tautomers have only one tertiary nitrogen atom. A direct comparison of the ^{13}C CPMAS spectrum with the ^{13}C spectrum in the DMSO-d_6 solution was then used to determine the preferred tautomeric form of **112** in DMSO (Table 11).

carbons	Solid State Enol C	DMSO (concentrated solution)
C-2	157.2	158.5
C-4	176.4	174.5
C-5	98.3	98.5
C-6	159.3	159.5
C-8	157.2	155.3

Table 11: Comparison of ^{13}C chemical shifts in DMSO-d_6 and in the solid state

Comparison of this data showed a close similarity in ^{13}C chemical shifts, confirming that the enol form **C** was also present in DMSO-d_6 solution. In particular, carbon C-5 is found at 98.3 ppm in DMSO-d_6 and at 98.3 ppm in the solid state, which is an indicator of the aromatic pyrimidinone ring in the enol form **C**.

From these ^{13}C and ^{15}N results, it is evident that compound **112** exists as the enol form both in the DMSO solution and in the solid state. An assignment of the key ^{1}H NMR peaks is shown in Table 12.

proton	112 (saturated)
4-OH	Not observed, very broad
5-H	5.88
7-H	8.01
9-H	10.13

Table 12: ^{1}H NMR of **112** (saturated solution) in DMSO-d_6

In addition, selective NOE measurements were performed for **112** (Figure 68). On selective excitation of the signal due to the aromatic ortho-proton 17-H of the *p*-aminophenyl ring, negative enhancements of -2% for proton 9-H, -9% for the meta proton 18-H on the *p*-amino phenyl ring, and -6% for the 5-H were measured. The existence of the NOE between 17-H and 9-H can serve as another proof of the enol form C in DMSO-d_6.

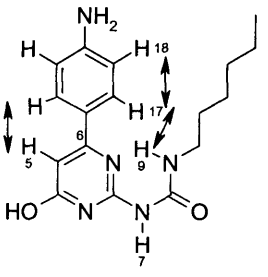

112

Figure 68: NOEs observed for compound **112**

Interestingly, the NOEs were negative, indicating that the effective molecular weight is high (combined with the high viscosity of the solvent), which in turn suggests a probable dimerisation *via* DADA-ADAD.

Once the type of the preferred tautomeric form was established for **112**, further studies were undertaken in order to examine the possibility of dimerisation. In this study, NMR diffusion experiments were used in order to determine the dimerisation constant of compound **112** in DMSO-d_6. The diffusion measurement alone cannot be used for distinguishing different tautomeric forms since the monomeric tautomers **A**, **B** and **C** of a given ureidopyrimidinone would be expected to have similar diffusion rates. Therefore, the concentration dependence of some of the proton chemical shifts has been used when identification of the tautomer involved in the dimerisation is of interest.
In particular, NMR studies in the solid state and concentrated solution in DMSO-d_6 revealed that compound **112** exists as the tautomer **C**, which is capable of dimerizing (DADA). Dilution experiments on compound **112** indicated a strong dependence between concentration and the chemical shift of proton 7-H. This was consistent with a hydrogen bonded array, since an increase in the population of the dimer occurs at higher concentrations (Table 13).
By contrast, the chemical shift of 9-H at approximately 10.2 ppm was unaffected, consistent with the presence of tautomer **C** where there is an intramolecular hydrogen bond. Thus it is clear that there is a dimer-monomer equilibrium and that the population of dimer decreases on dilution. The upfield shift for 7-H on dilution is also in favour of the shift of this equilibrium towards the monomeric form.

proton	1.8 mM	25 mM	Saturated
5-H	5.74	5.83	5.88
7-H	7.39	7.78	8.01
9-H	10.33	10.19	10.13

Table 13: Variation of ^{1}H chemical shifts as a function of the concentration in DMSO-d_6

To further establish the tautomeric state of the monomeric form in DMSO-d_6, $^1J_{CH}$-couplings for C-5 were measured from the ^{13}C satellites in ^{1}H NMR spectra. Specifically, from the analysis of compound **111**, **112** and **114**, two distinct values of

$^1J_{CH}$ in the keto and enol forms were found: 160 Hz in tautomer **C** and 170 Hz in tautomers **A** and **B**. This change of $^1J_{CH}$ reflects whether the C-H bond is aromatic (tautomer **C**) or vinylic (tautomer **A** and **B**). The values measured for saturated, 25 mM and 1.8 mM solutions of **112** were 160.9, 160.2 and 159.5 Hz. By comparison, $^1J_{CH}$ was 169.6 Hz for tautomer **A** of **111** in DMSO-d_6.

Based on these results, a simple two-site mono-enol/dimer-enol exchange (Figure 69) for **112** in DMSO-d_6 was considered, rather than a possible three site equilibrium which also includes the monomeric tautomer **A**.

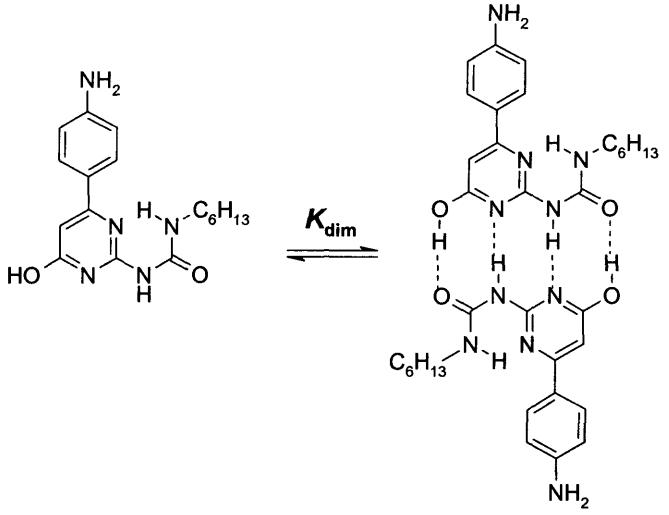

Figure 69: Equilibrium between monomer and dimer (DADA...ADAD) in DMSO-d_6

2.3.3.4 *Diffusion Experiments*

Having determined the nature of the tautomeric species in DMSO-d_6, diffusion experiments were then performed on compounds **111**, **112** and **114**. As expected for tautomer **A** in solution, no significant changes in diffusion coefficient was observed for solutions of **111** and **114**. In the case of compound **112**, the results were in accordance with the presence of the DADA dimer, since a change of diffusion was observed upon decreasing the concentration of the solution, suggesting the presence of dimeric species in equilibrium with monomers. The concentration of **112** in DMSO-d_6 was varied from 1.8 mM to 25 mM at 298 K, and overall seven different concentrations were studied. From the analysis of the diffusion experiments using the non-linear least-squares method, the diffusion coefficients for pure dimer and monomer were derived, which then were used to calculate the ratio of dimer/monomer in DMSO-d_6 (Table 14).

Compound 112	1.8 mM	25 mM	Saturated
Ratio: dimer/monomer	13:87	54:46	95:5

Table 14: The dimer-to-monomer ratio as a function of the concentration

Calculations using the non-linear least-squares method led to a dimerisation constant of 46 M^{-1} for compound **112.**[145,146] The low value is a consequence of the high polarity of DMSO, as well as its capability to act as a strong hydrogen bond acceptor. Therefore, DMSO decreases the strength of hydrogen bonding in the DADA motif. However, in this case, the high polarity of the solvent is not sufficient to disassemble the DADA array.

2.3.3.5 *Study of Compound 113*

NMR measurements were also carried out on compound **113** in DMSO-d_6. ^{13}C chemical shifts revealed some very close similarities with compound **112**. Specifically, carbons C-5 and C-4 resonated at 98.5 and 174.5 ppm, respectively, which is characteristic for the enol tautomer. By analogy with **112**, the low frequency shift of 5-H on dilution (from 6.13 ppm at 35 mM to 6.05 ppm at 5mM) indicated a fast mono-enol/dimer-enol exchange (Figure 70). Thus, both the tautomeric and dimeric behaviour of compound **113** were similar to that of **112**.

atom	^1H NMR 5 mM	^1H NMR 35 mM	^{13}C NMR 35 mM
2		-	158.5
3		-	-
4		-	174.5
5	6.05	6.13	98.5
6	-	-	159.5
7	7.65	8.02	-
8	-	-	155.4
9	10.19	10.06	-

Table 15: ^1H and ^{13}C chemical shifts at 298K in DMSO-d_6

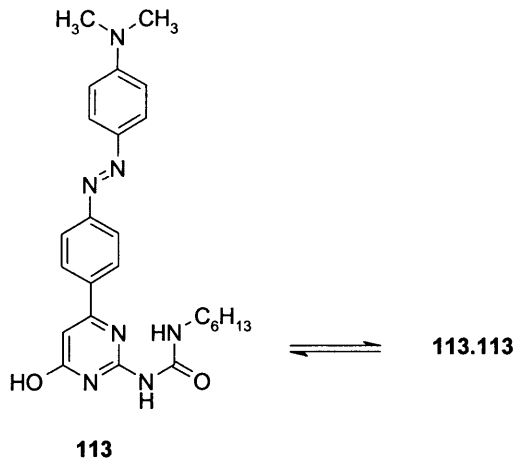

Figure 70: Dimerisation of compound **113**

2.4 Rationalisation

Meijer *et al.* have reported that pyrimidinones possessing electron-withdrawing groups at C-6 favour the enol form **C** in $CDCl_3$ and the 6-keto form **A** in DMSO-d_6, while alkyl or ether electron-donating groups adopt the 4-keto form **B** in $CDCl_3$ and again the monomeric form **A** in DMSO-d_6. It was shown for the first time in this work that the introduction of electron-donating groups at the C-6 position (compounds **112** and **113**, $PhNH_2$ and azo derivative, respectively) lead to a DADA dimeric form in DMSO. In compound **112**, the solvent DMSO-d_6, which is a strong hydrogen bonding acceptor, has the capability of forming stabilizing hydrogen bonds with the NH_2 of the amine group which may enhance the formation of the DADA array. Solvation of the amine in DMSO through hydrogen bonding could enhance the polarisation of the amine nitrogen, increasing the basicity of the oxygen atom and N-1and N-3 of the pyrimidinone moiety (as indicated in the zwitterionic mesomeric representations in Scheme 15). The preferred formation of tautomer **C**, rather than **A** for compound **112** may therefore be due to a combination of factors: higher basicity of the oxygen atom with respect to N-1 and N-3, a more pronounced aromatic stabilisation of the enol form with respect to the pyrimidinone moiety, and a favourable intramolecular hydrogen bond between the urea side chain and N-1 (Scheme 15). A similar rational can be invoked with the azo compound **113**.

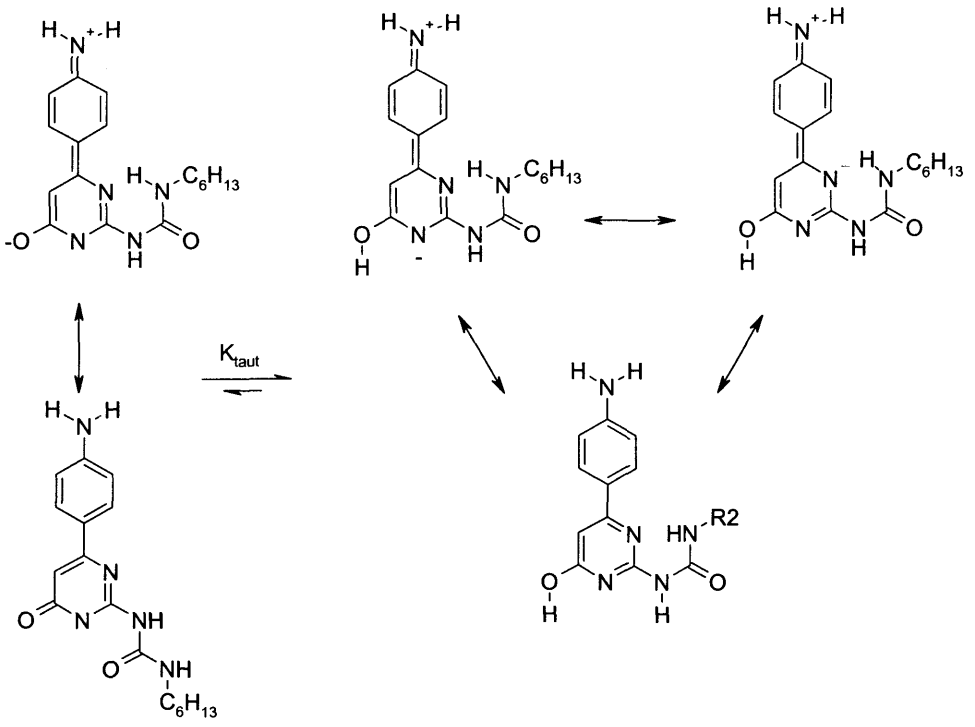

Scheme 15: Mesomeric representations of tautomers **A** and **C**

2.5 Synthesis of Novel Ureidopyrimidinone Incorporating a PEG chain at the Ureido Position (R_2)

Since the solubility of compounds **112** and **113** were low in a range of organic solvents, the introduction of a hydrophilic side chain at R_2 was attempted in order to enhance the solubility and assess the effect of a hydrophobic versus hydrophilic side chain at R_2 on the tautomeric distribution (Figure 71). For this purpose, the use of a short PEG chain was initially explored.

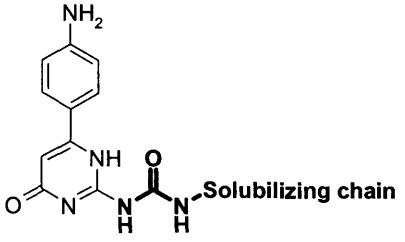

Figure 71: Targeted molecule

2.5.1 Synthesis of PEG-amine

Initially the conversion of PEG_3OMe into a PEG_3OMe terminated amine (**115**) was explored (Scheme 16).

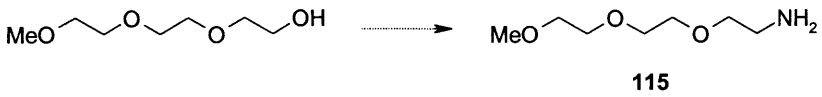

115

Scheme 16: Synthetic strategy

Vidya Sagar Reddy *et al.* recently described a novel, facile one-pot synthesis for the conversion of alcohols to azides and amines using sodium azide and triphenyl phosphine in a mixture of CCl_4-DMF (1:4).[147] In this procedure, the treatment of two equivalents of PPh_3 compared to sodium azide was used which afforded amines in excellent yields (85-95%), whereas the addition of only one equivalent of triphenyl phosphine afforded the azide exclusively in good yields (Scheme 17).

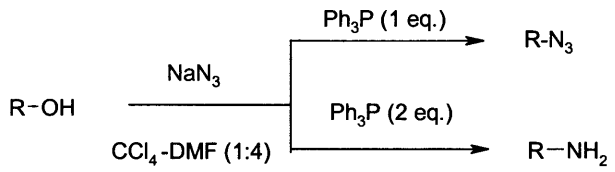

Scheme 17: Conversion of alcohol into azide or amine

Following this procedure, PEG_3OMe was reacted with sodium azide (1.5 eq) and triphenylphosphine (3 eq) in the solvents mixture (CCl_4: DMF). Unfortunately, under these reaction conditions the desired compound **115** was not formed (Scheme 18).

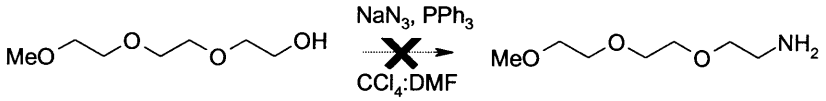

Scheme 18: Towards the synthesis of 2-[2-(2-Methoxy-ethoxy)-ethoxy]-ethylamine (**115**)

The reaction was repeated using 2 equivalents of sodium azide and 4 equivalents of triphenyl phosphine which afforded 10% of the amine **115** after purification. However, traces of the bi-product triphenyphosphine oxide were difficult to separate completely from the amine. This method was not efficient as expected for this substrate, and therefore the conditions of the reaction were not optimised further.

Therefore a less direct route *via* the mesylate (**116**) and azide (**117**) was explored as depicted in Scheme 19.

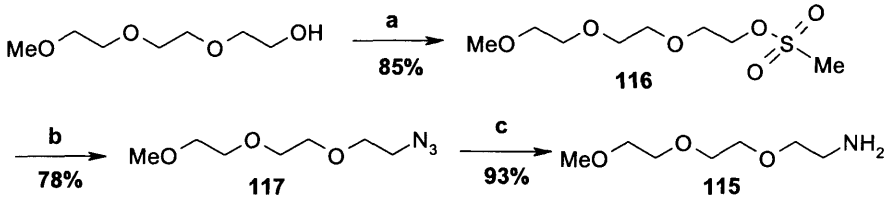

Reagents and conditions: **(a)** $MeSO_2Cl$, Et_3N, CH_2Cl_2, 85%; **(b)** NaN_3, DMF, 78%; **(c)** H_2, Pd/C, EtOH, 93%.

Scheme 19: Towards compound **115**

PEG_3OMe was first mesylated using methane sulfonyl chloride in the presence of Et_3N in CH_2Cl_2.[148] After a couple of hours, the reaction was complete and led to the isolation of compound **116** in 85% yield. The product was dried by the azeotropic removal of water with toluene, and used directly in the next step. Formation of the azide was achieved using sodium azide in dry DMF for five days at room temperature.[149] The crude product **117** was obtained in 78% yield and used directly in the next step without further purification. Reduction of the azide group was first attempted *via* the Staudinger reaction using triphenylphosphine in THF and water.[150] The reaction mixture was stirred at room temperature for three days and then purified using flash chromatography. Unfortunately, the separation of products was complicated again by the presence of triphenylphosphine oxide and once again only a small amount of the amine **115** was recovered after purification. Azide derivatives are generally reduced to primary amines using $LiAlH_4$ [149] or other reducing agents including Pd/H_2.[151] To avoid the formation of undesirable by-products the reduction of the azide was then carried out using catalytic hydrogenation over Pd/C in ethanol. After two days, the azide was quantitatively reduced and afforded the amine **115** in 93% isolated yield after purification.

In order to attach the PEG chain to the ureidopyrimidinone, transformation of the amine into the corresponding isocyanate was necessary (Scheme 20).

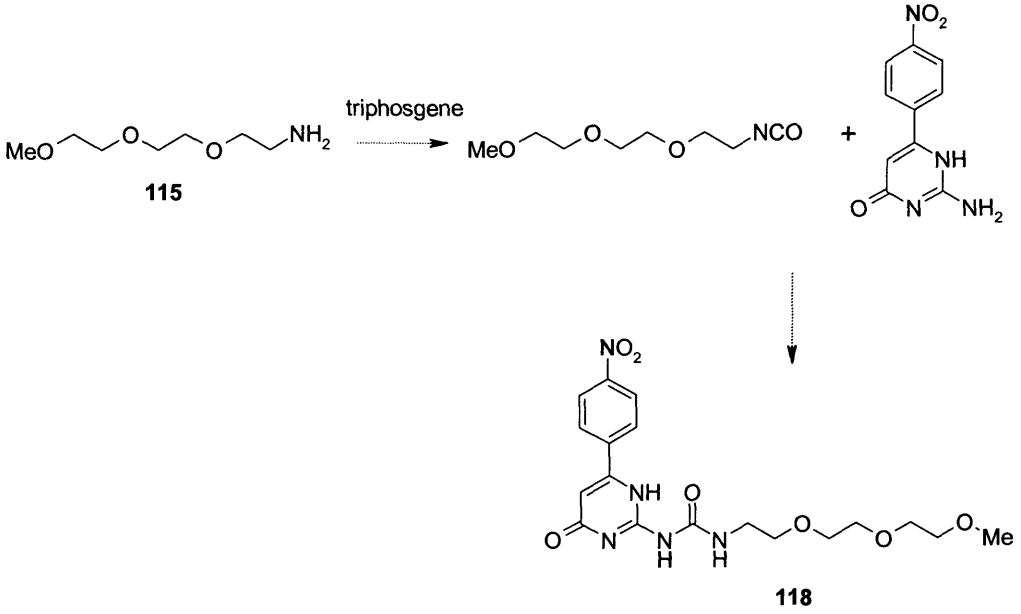

Scheme 20: Synthetic route towards **118**

In general amines can react easily with phosgene or triphosgene to afford isocyanates. PEG amines have been less studied in this regard and very few reports have described the synthesis of PEG isocyanates. One of the few examples encountered in the literature and described by Strazewski *et al.*[152,153] is the synthesis of diisocyanates from tetraethylene glycol in a five step synthesis (Scheme 21).

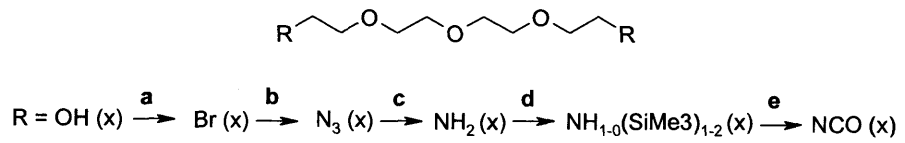

Scheme 21: Synthesis of PEG diisocyanate in five steps

The use of *N*-trimethylsilylation in the last step has been previously described by Mironov et *al.*[154] for the smooth conversion of amines into isocyanates. In this case, the isocyanate was obtained in 65% yield. Previous attempts using phosgene or triphosgene/Et_3N directly with the amine led to a certain degree of polymerisation.

Compound **115** was however initially reacted directly with triphosgene and triethylamine. The reaction was followed using IR spectroscopy. After a couple of hours a band characteristic of the asymmetric vibration NCO at ~ 2270 cm^{-1} appeared in the IR spectrum and compound **110** was then added to the solution, but unfortunately no reaction occurred, and the starting material was recovered. Further attempts altering the reaction conditions were also unsuccessful. This could have been due to the poor solubility of **110** in CH_2Cl_2, or instability of the PEG isocyanate in the reaction mixture. Since this synthetic approach appeared unsuccessful, another method towards the synthesis of PEG isocyanate was explored starting from the 2-[2-(2-methoxyethoxy)ethoxy]ethanoic acid (Scheme 22) using the Curtius rearrangement, which has the advantage of avoiding the use of phosgene based reagents.

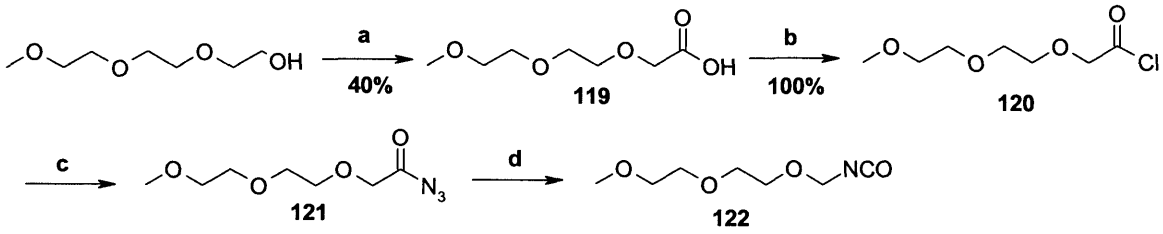

Reagents and conditions: **(a)** $KMnO_4$, KOH, H_2O, 40%; **(b)** $SOCl_2$, CH_2Cl_2, 100%; **(c)** NaN_3, acetone; **(d)** Toluene, heat.

Scheme 22: Synthesis of 1-[2-(2-Isocyanato-ethoxy)-ethoxy]-2-methoxy-ethane *via* the Curtius rearrangement

The alcohol was first oxidised following Heimann and Voegtle's procedure[155] using alkaline solution and potassium permanganate as the oxidizing agent. Because of the high solubility of the acid in aqueous media, only 40% of compound **119** was recovered after distillation.

The carboxylic acid was then converted quantitatively into the corresponding acid chloride using neat thionyl chloride under reflux conditions for two hours. Completion of the reaction was monitored using IR spectroscopy (band characteristic of COCl at 1803 cm^{-1}). The acid chloride (**120**) was not isolated and was used directly in the next step. Reaction in DMF with a large excess of sodium azide[156] (added slowly, exothermic) to the cooled solution gave an orange solution, which was stirred at room temperature over night. The resulting mixture was then diluted with water and extracted with chloroform, and IR spectroscopy revealed the appearance of a new band at 2108

cm^{-1} consistent with the formation of azide. This compound was then heated in toluene under reflux conditions but after 18h no IR signal characteristic of the NCO group was detected. Toluene used was replaced by xylene and the solution heated under reflux for 16 h. Once again no rearrangement was observed. Further modification of the method was carried out and the acid chloride (**120**) was dissolved in dry acetone and then added to an aqueous solution of sodium azide.[157] Extraction of the aqueous solution with chloroform afforded an acid azide as shown by the IR signal, which this time was at 2142 cm^{-1}, slightly higher than the signal observed previously. The azide (**121**) was not isolated and was diluted in toluene which was directly heated under reflux conditions. The evolution of gas was observed suggesting generation of nitrogen. After 10 min, the evolution of gas ceased, and IR spectroscopy showed the disappearance of the CON_3 band and the appearance of an NCO band (2252 cm^{-1}). The isocyanate (**122**) was redissolved in dry pyridine along with compound **110** and the solution was heated at 90 °C for another 16 h (Scheme23). The desired compound **123** was finally obtained after purification in 28% yield (yield calculated from the carboxylic acid **119**).

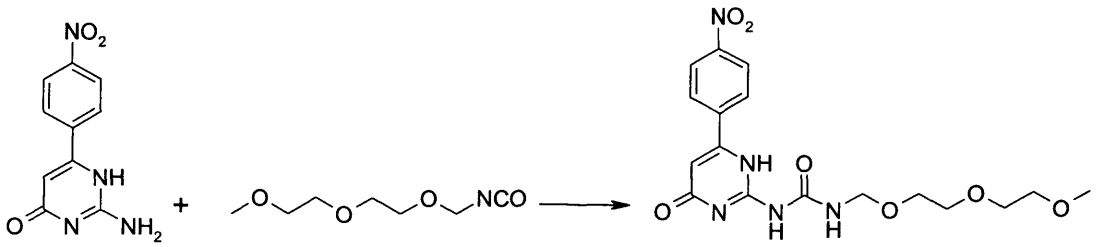

110 **122** **123**

Scheme 23: Synthesis of compound **123**

Attempts to reduce the nitro group to the corresponding amine (**124**) under acidic conditions using tin chloride and hydrochloric acid led to cleavage of the PEG chain, presumably due to the close proximity of the urea and PEG oxygen moiety. Other methods such as catalytic hydrogenation were also unsuccessful, due to the low solubility of **123** in the solvents used (Scheme 24).

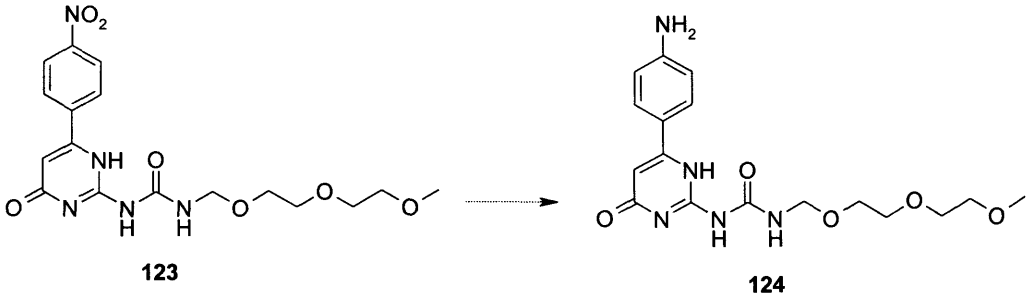

123 **124**

Scheme 24: Towards the formation of compound **124**

2.5.2 Introduction of an Alternative Solubilizing Moiety

A new strategy was explored involving the synthesis of an isocyanate incorporating a phenyl group. The selected compound **127** (Figure 72) inserted a benzyl spacer adjacent to the urea, which could be more stable to the acidic reducing conditions required.

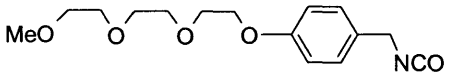

127

Figure 72: 1-Isocyanatomethyl-4-{2-[2-(2-methoxy-ethoxy)-ethoxy]-ethoxy}-benzene

Preliminary test reactions were performed using a hexyl chain attached to the benzyl group as described in Scheme 25 below. No tautomeric studies were performed on these compounds. The synthesis will be described in the experimental section.

2.5.2.1 *Synthesis*

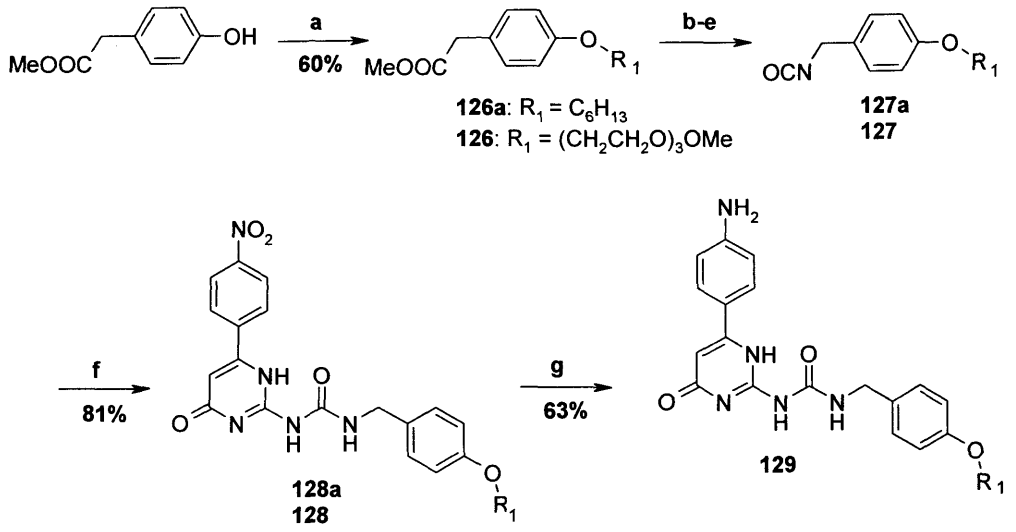

Reagents and conditions: (a) 126a: BrC_6H_{13}, K_2CO_3, DMF, 100°C, 16 h, 70%; **126**: $Br(CH_2CH_2O)_3OMe$, K_2CO_3, MeCN, reflux, 2d, 60%; **(b)** NaOH, 1N, MeOH, reflux, 55%; (a)NaOH 1N, MeOH, reflux, 70%; **(c)** $SOCl_2$, 100%; **(d)** NaN_3, acetone; **(e)** Toluene, heat; **(f) 128**: 110, pyridine, 77%; **128a**, pyridine; 81%; **(g)** $SOCl_2.2H_2O$, HCl, EtOH, reflux, 1h, 63%.

Scheme 25: Synthetic route towards the formation of compound **129**

First the activated PEG chain **125** was synthesised in two steps *via* the formation of the mesylate **130**. Substitution of the mesylate with lithium bromide afforded compound **125** in an overall 66% yield after purification using flash chromatography (Scheme 26).[158] Reaction of methyl-4-hydroxyphenylethanoate with 1-(2-bromoethoxy)-2(2-methoxyethoxy)ethane (**125**) and potassium carbonate in acetonitrile gave **126** in 60% yield.

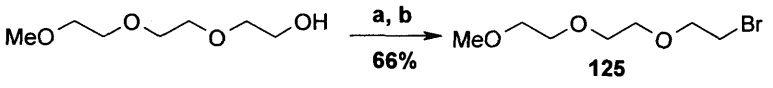

Reagents and conditions: **(a)** MsCl, Et_3N, CH_2Cl_2; **(b)** LiBr, acetone, reflux, 66%

Scheme 26: Synthesis of 1-[2-(2-Bromo-ethoxy)-ethoxy]-2-methoxy-ethane in two steps

Hydrolysis of the ester **126** under basic conditions gave the corresponding acid in a ~ 70% isolated yield. Reaction of the carboxylic acid with thionyl chloride gave the acid

chloride, which was used directly in the following step. The formation of the acid azide was achieved *via* the reaction of acyl chloride with sodium azide in dry acetone. The product was not isolated and was heated at 90 °C in toluene in order for the Curtius rearrangement to occur. The reaction was monitored by IR spectroscopy and the NCO band at 2270 cm^{-1} was observed after 30 min. The solvent was evaporated and the residue was redissolved in dry pyridine. A solution of the nitro compound **110** in pyridine was added to the isocyanate solution (**127**), and the mixture was heated at 90 °C for 16 h, affording compound **128** in 81% isolated yield (from compound the carboxylic acid). Reduction to the corresponding amine was successfully achieved using tin (II) chloride in acidified ethanol, with retention of the PEG chain, in 63% yield. Interestingly, compound **129** (R_1 = PEG_3OMe) had an improved solubility in organic solvents and in particular in $CDCl_3$, compared to **112** and **113**. Attempts to convert the amine **129** into the corresponding azo derivative (**130**, Scheme 27) led to the formation of an inseparable mixture of compounds.

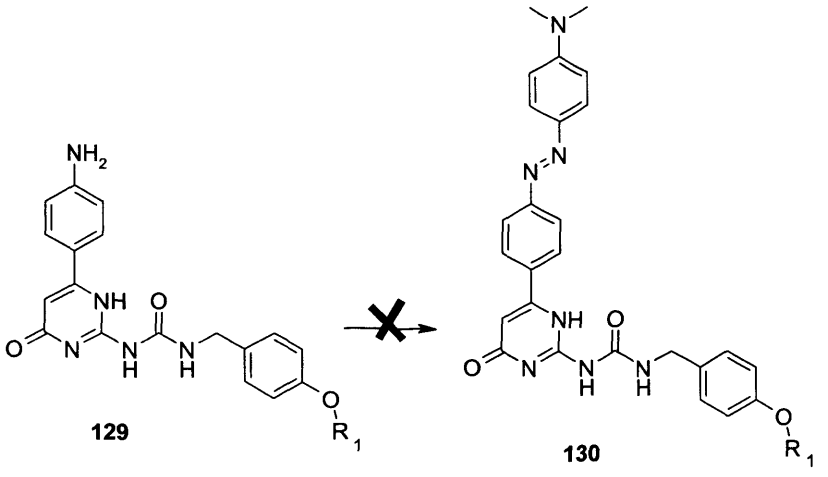

Scheme 27: Towards the synthesis of the azo derivative

2.5.2.2 *Tautomeric Studies*

Compound 128

The solubility of the nitro compound **128** did not improve in $CDCl_3$ with the introduction of the PEG chain and only studies in DMSO-d_6 were then possible. As expected, the spectrum observed in DMSO was similar to that of compound **111** (R_1 =

$PhNO_2$, $R_2 = C_6H_{13}$), suggesting the presence of the 6-keto form **A**. A comparison of the chemical shifts for these two compounds is shown in Table 16.

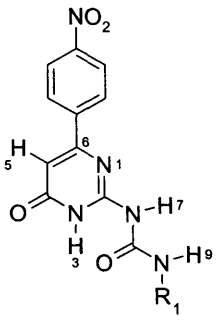

111 : $R_2 = C_6H_{12}$
128 : $R_2 = CH_2PhO(CH_2CH_2O)_3Me$

position	128 ^{1}H 298K	111 **^{1}H 298K**	128 ^{13}C 298K	111 **^{13}C 298K**
1	-	-	-	-
2	-	-	152.2	**152.1**
3	12.05	**11.92**	-	-
4	-	-	161.9	**161.6**
5	6.66	**6.67**	104.0	**104.2**
6	-	-	159.1	**159.1**
7	10.04	**10.07**	-	-
8	-	-	154.5	**154.5**
9	7.38	**7.74**	-	-

Table 16: Comparison of ^{1}H and ^{13}C chemical shifts for compounds **128** and **111**

Both the ^{1}H and ^{13}C chemical shifts were almost identical for these two compounds. A small difference of 0.36 ppm was observed for proton 9-H, probably due to the change in the R_2substituent.

Compound 129

The introduction of the lateral chain $PhO(CH_2CH_2O)_3Me$ improved significantly the solubility of the amine **129** in $CDCl_3$. The proton ^{1}H NMR spectrum was first run in $CDCl_3$ at 298 K, which revealed the presence of two sets of peaks with chemical shifts characteristic for tautomers **B** and **C** (Figure 73).

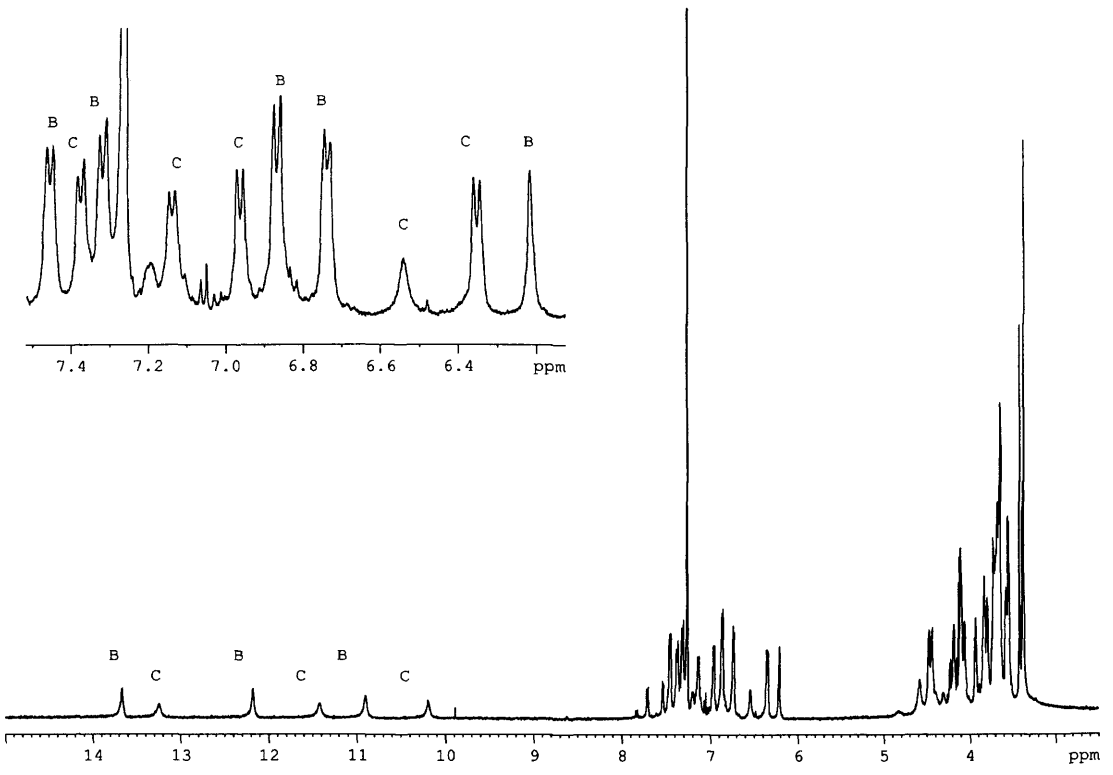

Figure 73: ^{1}H NMR spectrum of compound **129** in $CDCl_3$ at 298 K

Based on the previous results found for compound **112** in $CDCl_3$, as well as similar results obtained by Meijer *et al.*, the assignment of peaks was straightforward. Nevertheless, 2D correlation techniques were additionally used in order to verify the assignment of the ^{1}H and ^{13}C peaks. A summary of the selected proton chemical shifts are presented in Table 17.

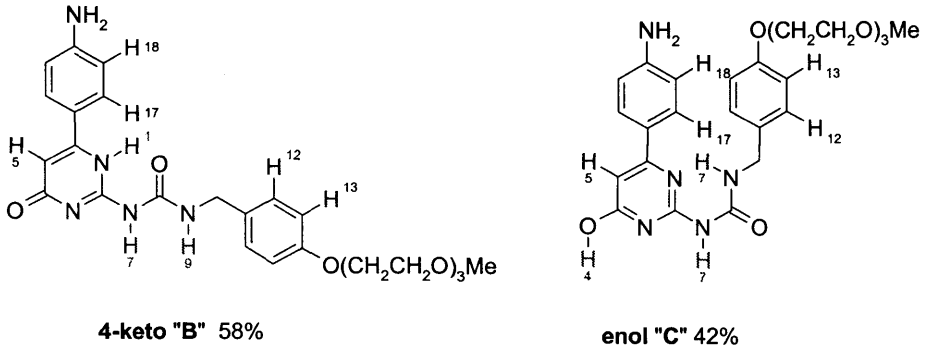

Figure 74: Structure of tautomer **B** and **C** for compound **129**. Populations in % were measured at 298 K in $CDCl_3$.

Position/ppm	4-keto B 58 %	Enol C 42%
1	13.66	13.24
5	6.21	6.54
7	12.17	11.41
9	10.89	11.00
12	7.31	7.37
13	6.87	6.96
17	7.45	7.14
18	6.73	6.35

Table 17: ^{1}H chemical shifts for tautomer **B** and **C** in $CDCl_3$ at 298 K

As expected for the enol form, proton 5-H showed a shift towards the higher frequency by about 0.3 ppm compared to the 4-keto form **B**. Interestingly, on decreasing the temperature from 298 K to 258 K, the relative population of enol form increases from 42% to 52%.

The ^{13}C NMR spectra gave the chemical shift of carbon C-5 at 101.7 ppm for the 4-keto form **B** and at 95.1 ppm for the enol tautomer. These values were lower than those already observed for the 4-keto form in $CDCl_3$ (e.g., compound **112**). Such a change may be due to the redistribution of the electronic density in the pyrimidinone ring on introduction of the $PhNH_2$ substituent.

The presence of a relatively high proportion of the enol form **C** in $CDCl_3$ was surprising since electron-donating groups at C-6 such as alkyl groups or ethers have favoured almost exclusively the 4-keto tautomer **B** in $CDCl_3$.

However, these results indicated that not only electron-withdrawing groups favour the enol form as mentioned by Meijer *et al.*, but an electron-donating group such as $PhNH_2$ can also shift the equilibrium towards the DADA dimeric species.

To conclude, the synthesis of compound **112** incorporating an electron-donating group as C-6 has encouraged the formation of the dimeric form DADA in DMSO-d_6. It was the first time that a dimeric form of Upy was observed in such a polar solvent. The results obtained for compound **129** in $CDCl_3$ highlighted the complexity of these ureidopyrimidinones in solution in terms of tautomeric distribution. Overall, the prediction of the tautomeric forms still remains difficult since many factors such as polarity of the solvent, the nature of substituents, temperature and concentration, can influence the tautomeric behaviour of Upys.

Chapter III

3 The Synthesis of Supramolecular Polymers Based on Ureidopyrimidinones

3.1 Introduction

The use of ureidopyrimidinone units for the synthesis of supramolecular polymers has led to a new class of polymers where the reversibility of the non-covalent bonds between the monomers gives rise to novel material properties. The high dimerisation constant of the Upy dimer in chloroform means they can be used in the generation of high molecular weight polymers. In most cases, ureidopyrimidinones possessing an alkyl chain at the C-6 position, such as CH_3 or $C_{13}H_{27}$ have been used since they exhibit almost exclusively the 4-keto form B in chloroform, as described in Chapter II. There are many ways to synthesise these materials but generally the linker has been connected to the Upy units at the urea functionality. Three synthetic strategies X, Y and Z could be envisaged in order to form the urea bonds, as described in Figure 75.

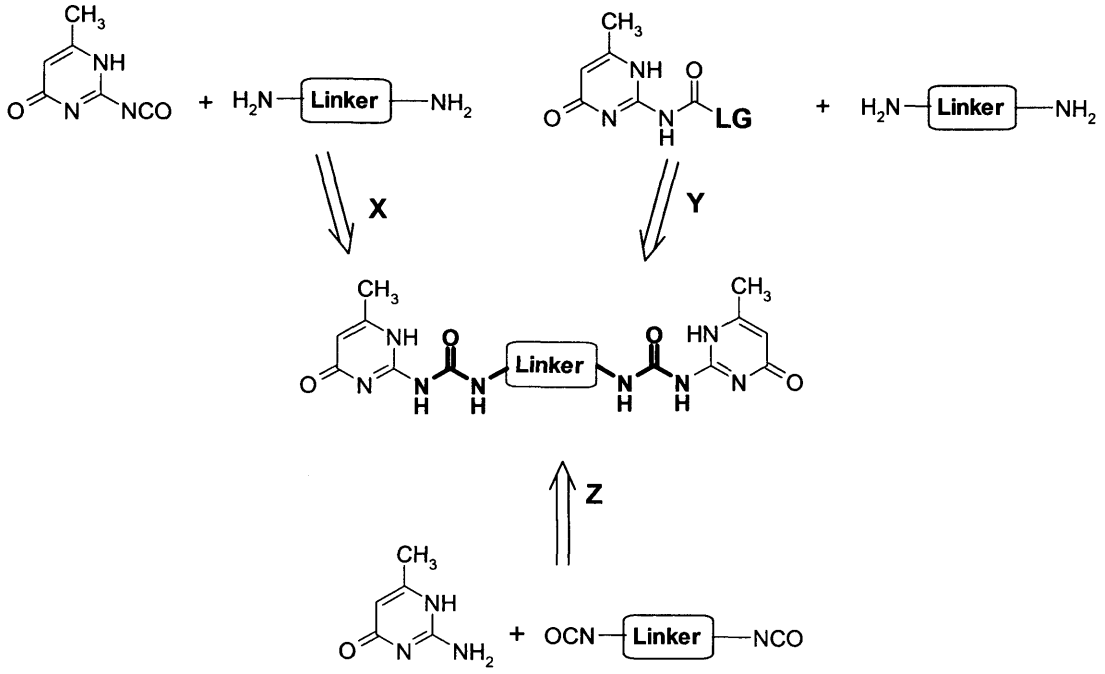

Figure 75: Three possible routes for the formation of linear supramolecular polymers; LG stands for the leaving group

A conceptually straightforward strategy involves the reaction between an isocytosine isocyanate with a linker possessing amine terminated groups (route **X**). Unfortunately, this method is problematic since the formation of the isocytosine isocyanate cannot be achieved easily. Gizycki et *al*[159] demonstrated that the reaction of pyridines and pyrimidines with diphenyl carbonate led to the formation of dimeric ureas. More recently Meijer *et al.* have attempted the synthesis of isocytosine with phosgene, but only a covalent dimer was obtained (Scheme 28). This method was therefore not used and the other routes Y and Z have been mainly investigated.

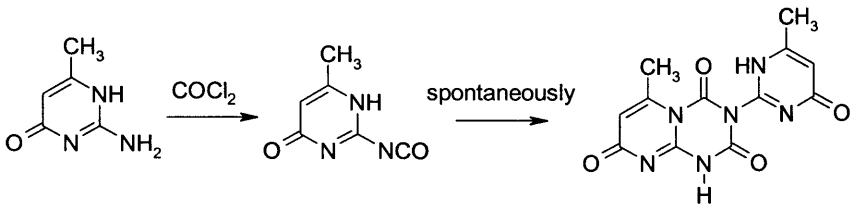

Scheme 28: Formation of isocytosine dimers

Strategy **Y** involves the activation of isocytosine with the use of a leaving group such as 1,1'-carbonyldiimidazole (CDI)[160,161] giving an activated amide that can react smoothly with both aliphatic and aromatic amines to give the corresponding ureidopyrimidinone derivatives in fairly good yield (Figure 76). This is an attractive method for industry since it does not require the use of isocyanates whose toxicity can be sometimes very high.

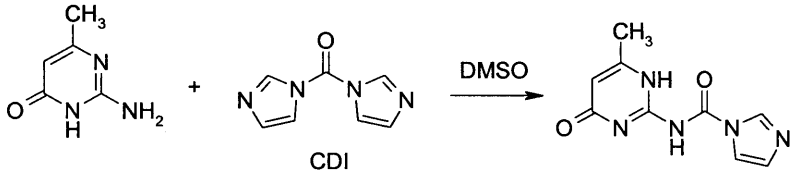

Figure 76: Synthesis of activated isocytosine; the tautomeric form of the activated isocytosine is drawn as the 4-keto form **B**

Strategy **Z** is the most frequently used method for the synthesis of linear supramolecular polymers.[127] It involves the reaction of isocytosine with a linker terminated with an isocyanate group. This approach has disadvantages however, since the amino group of

the isocytosine has a low reactivity towards aromatic diisocyanates leading to incomplete functionalisation with a spacer.

This problem is less of an issue with aliphatic diisocyanates. Indeed the use of an excess of hexyl diisocyanate afforded the monoisocyanate **131** in 80% yield (Scheme 29).

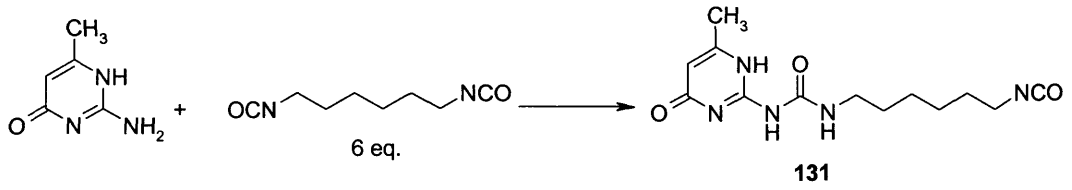

Scheme 29: Synthesis of monofuntionalised Upy terminated with isocyanate

The isocyanate **131** is reasonably stable under anhydrous conditions and can react smoothly with linkers possessing alcohol or amine terminated functionalities, as well as with telechelic polymers (Scheme 30).

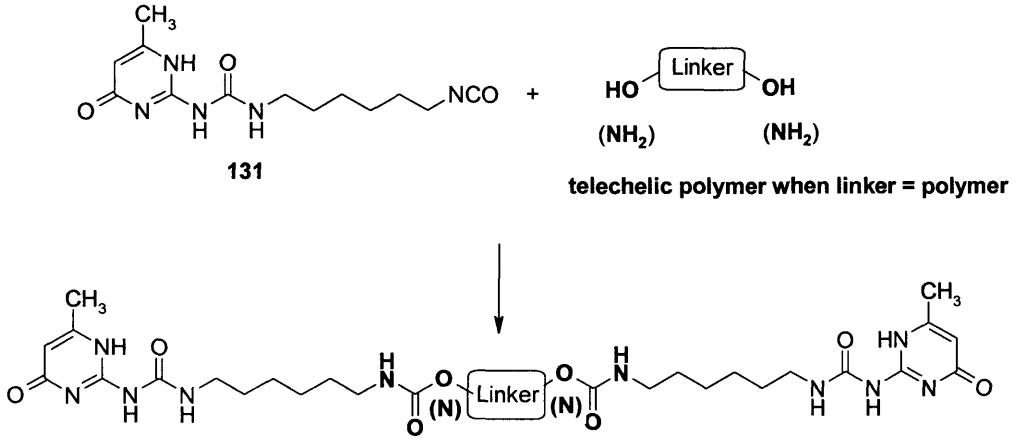

Scheme 30: Synthesis of supramolecular polymers

Meijer *et al.* have developed this method for the synthesis of supramolecular polymers incorporating various polymers and copolymers such as polyethylene-polypropylene, or polyesters and polyethers as linkers. A key advantage of this approach is that many polymers are commercially available with hydroxyl terminated groups (telechelic polymers), and the synthesis is then rather straightforward and relatively cheap. Examples of such supramolecular polymers have been presented in Chapter I.

One of the aims of this thesis was the synthesis of supramolecular polymers incorporating polyethers and polycarbonates and assessment of their properties, as well as the development of supramolecular polymers following a synthetic strategy avoiding the use of isocyanates. These results are presented in detail in the first part of this chapter. The second part will introduce the area of energetic polymers and the synthesis of energetic precursor derivatives of ureidopyrimidinones will be discussed.

Part I: The synthesis of Non-Energetic Materials:

3.2 Functionalisation of Polyethylene Glycol with UPys

Different polyethyleneglycols were selected with molecular weights between 280 and 3300 g/mol for reaction with synthon **131** as shown in Scheme 31.

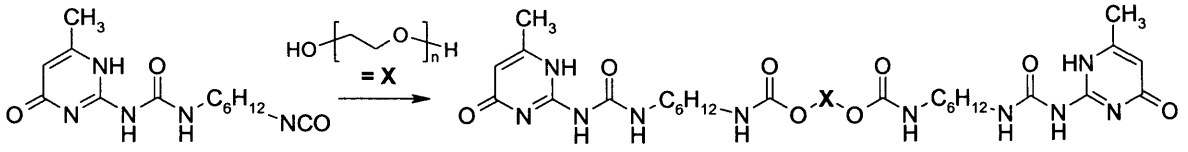

131

132: n = 6
133: n = 12
134: n = 33
135: n = 77

Scheme 31: Functionalisation of PEG chains

The characteristics of the PEG telechelic polymers inserted are shown below in Table 18.

Length of PEG chain	M_n (g/mol)	Physical appearance
n = 6	282	Liquid
n = 12	570-630	Moist solid
n = 33	1450-1550	Waxy solid
n = 77	3250-3550	Powder

Table 18: Properties of PEG chains

The supramolecular polymers **132** to **135** (n = 6, 12, 33 and 77, respectively) were prepared following Meijer's procedure.[127] A solution of the polyethyleneglycol in dry chloroform was heated under reflux conditions together with a four-fold excess of the isocyanate **131** and with a 0.5% (w/w PEG) of the catalyst tinbutyldilaurate. The reaction between isocyanates and hydroxyl groups are known to be rather slow, thus requiring the use of a catalyst for the reaction to proceed. The conversion of the reaction was followed by ^{1}H NMR spectroscopy, and after 16 h, the reaction was complete. Polymers **132** to **135** were obtained after a work up procedure involving filtration of the excess of isocyanate **131**. Any residual isocyanate was then removed by reaction with silica gel in the presence of small amount of catalyst (~ 1 h under reflux conditions). Removal of the silica gel by filtration and then evaporation of the filtrate afforded the desired supramolecular polymer. Further precipitation of the polymer from chloroform in hexane allowed removal of any remaining catalyst.

When dissolved in chloroform, polymers **132** and **133** did not show any increase in viscosity. However, when the length of the polyethylene glycol increased (polymers **134** and **135)** the formation of a highly viscous solution was then observed in chloroform.

The thermal properties of these polymers were assessed by Differential Scanning Calorimetry (DSC) in order to measure the glass transition temperature (T_g) and the melting point (mp). The results are shown in Table 19.

PEG chain	**Glass transition (T_g, °C)**	**Melting point (mp, °C)**
n = 6	-26.7	5.8
n = 12	-24.9	15.3
n = 33	-44.0	22.5
n = 77	Not well defined	Not defined

Table 19: Differential scanning calorimetry results and measurement of melting points

The melting point transition is a first order transition where the transfer of heat between the system and surrounding medium undergoes an abrupt change of volume. The glass transition is a second order transition since there is no transfer of heat. The volume does not change abruptly as it reflects a change in the free volume between the polymer chains (Figure 77).

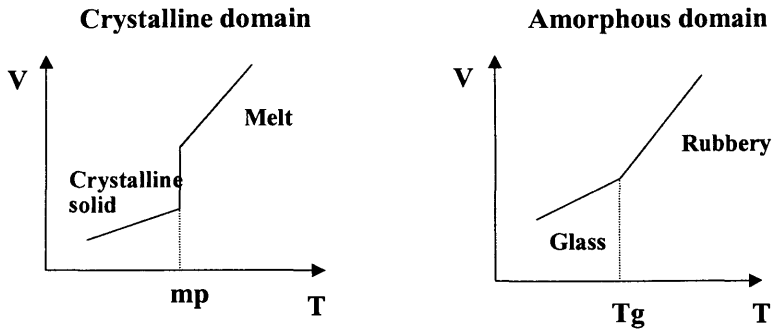

Figure 77: Differences between the crystalline and the amorphous domains

3.2.1 Results

The presence of both a melting point and a glass transition temperature suggested that the materials were semi-crystalline solids. For all the polymers the T_g values were found below room temperature, which indicated that the mechanical properties are close to those found in elastomers, as opposed to plastics where the glass transition temperature is above room temperature. Furthermore, the results indicated that the glass transition temperature of the final polymer was dependent on the length of the PEG chain: the longer the PEG, the lower the T_g. Unfortunately, for the material with very long chain (n = 77) no clear glass transition was detected. Overall, these results were in accordance with the observation that when the chain of the polymer increases, there is improvement of flexibility of the material which is translated into a decrease in T_g. Polymers containing only an amorphous domain exhibit very interesting elastomeric properties and therefore preparation of such a polymer with a T_g near -50 °C has been one of the targets of this research (Note: The target of -50 °C is British requirement for binders used in guns and rocket propellants). One factor that could influence the glass transition is the introduction of side chains within the telechelic polymer and flexible pendant groups such as alkyl groups, which may act as plasticiser. Pendant groups can increase the free volume between polymer chains leading to a lower T_g of the final supramolecular polymer. Following this approach the use of block polymers of

polyethylene glycol such as polyethylglycol-polypropyleneglycol-polyethyleneglycole (PEG-PPG-PEG) were investigated.

3.3 Functionalisation with a Branched Polymer

The synthesis of supramolecular polymers incorporating block polymers PEG-PPG-PEG, has been achieved following a similar procedure as described previously. For our study two commercially available telechelic polymers were chosen:

136: $M_n \sim 2000$ g/mol, ca 10% PEG

137: $M_n \sim 2900$ g/mol, ca 40% PEG

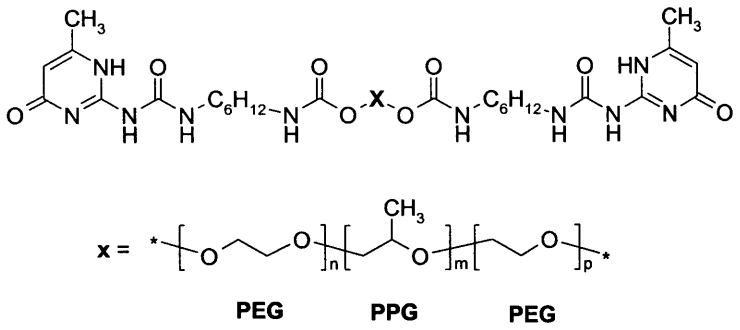

Figure 78: Functionalisation of PEG/PPG/PEG block polymers with Upy

The supramolecular polymers synthesised showed interesting flexibilities upon analysis, which suggested that the T_g values were certainly lower as intended. Indeed, glass transitions at -60.4 °C and -63.7 °C were measured together with melting points at -29.1 °C and 6 °C for **136** and **137**, respectively. The low glass transition temperatures reflected the elastomeric properties of the final materials, however the presence of a melting point for both supramolecular polymers suggested that some crystalline domains were still formed.

To conclude, the functionalisation of PEG chains revealed that the longer the PEG polymer the lower the T_g. Furthermore, with block polymers containing branched polypropylene glycol, the T_g decreased to ~ -60 °C, with the presence of some crystalline domains. These studies have demonstrated the influence of the nature of telechelic polyethers on the glass transition of the final material. In an effort to synthesise other novel materials, the functionalisation of a polycarbonate polymer was undertaken.

3.4 Functionalisation of poly (polytetrahydrofuran carbonate) diol

The commercially available telechelic polymer (M_n ~ 2000 g/mol) was functionalised according to a similar procedure described previously (Figure 79).

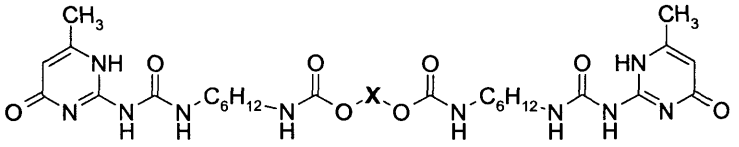

138 = $-(OCH_2CH_2CH_2CH_2)_3[OCO(OCH_2CH_2CH_2CH_2)_3]_7-$

Figure 79: Functionalisation of poly(polytetrahydrofuran carbonate)diol

The material generated was surprisingly rubbery and even less brittle than the polymers synthesised with block polymers PEG/PPG/PEG. The DSC analysis revealed a low T_g at -64.5 °C. Remarkably, no melting point was observed, suggesting that no significant crystalline domains were formed.

The polymer was further characterised using NMR spectroscopy. The proton NMR spectrum in $CDCl_3$ was recorded and is shown in Figure 80. In addition, ^{13}C (see experimental part) and ^{15}N (Figure 81) NMR chemical shifts were also measured. According to the results previously described (Chapter I), the ^{1}H, ^{13}C and ^{15}N NMR chemical shifts were consistent with the 4-keto tautomer B in $CDCl_3$.

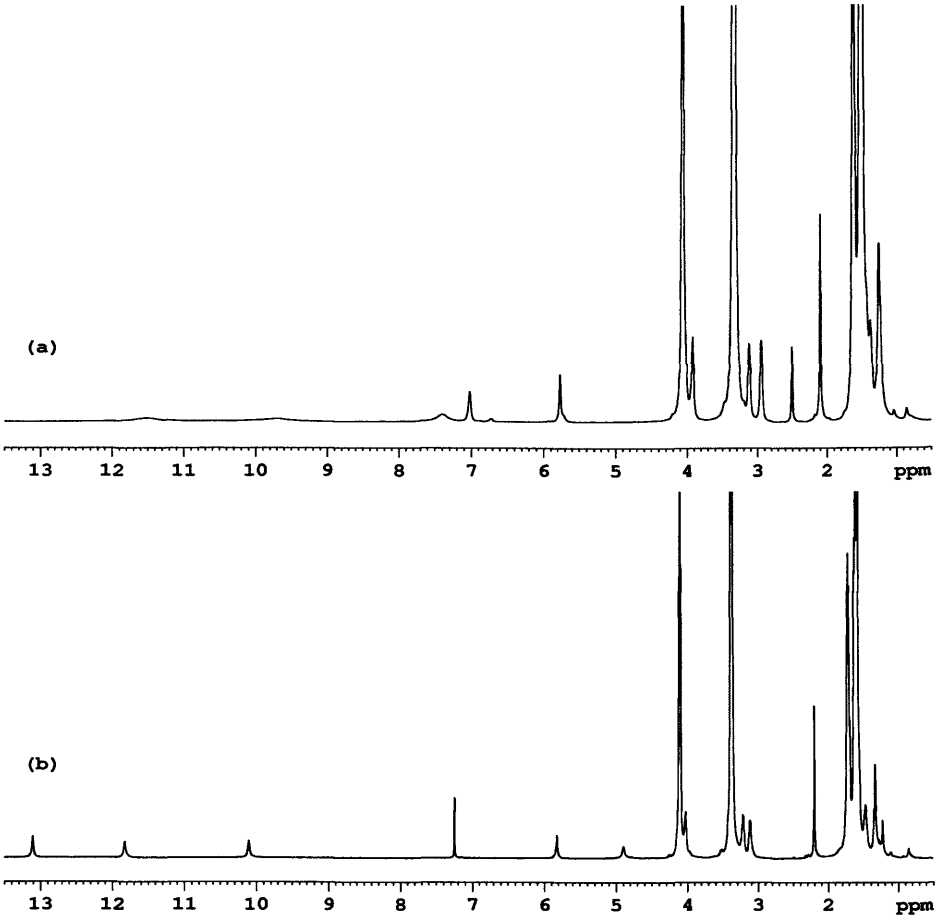

Figure 80: ^{1}H NMR spectra of polymer **138** at 298 K in (a) DMSO-d_6 and (b) $CDCl_3$

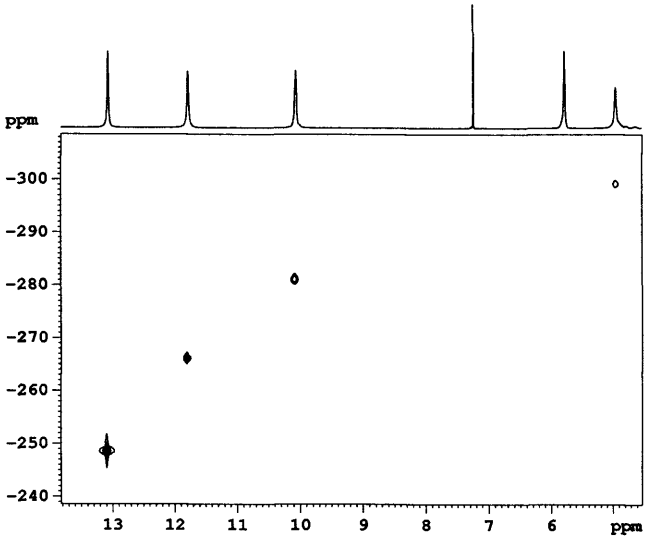

Figure 81: $^{1}H,^{15}N$ HMQC spectrum of **138** in $CDCl_3$. The ^{15}N chemical shifts were at -248.5 (N-1), -266.1 (N-7), -280.7 (N-9) and -299.1 (NH-COO) ppm. The N-3 site with no directly attached protons was not detected in this spectrum. The chemical shifts are similar to those measured for **114** (Chapter I), and are in favour of the 4-keto form.

When dissolved in DMSO-d_6 the hydrogen bonding system in the polymer was disrupted and a change of tautomer from 4-keto B to 6-keto A occurred. The latter tautomer **A** exists as monomer in the DMSO-d_6 solution. Interestingly, proton 17-H, which is part of the carbamate moiety (N*H*COO), was found at 7.02 ppm while it was found at 4.97 ppm in $CDCl_3$. The significant shift (ca. 2 ppm) towards higher frequencies in DMSO-d_6 reflects the relatively strong hydrogen bonding between the solvent and 17-H. The diffusion coefficient in DMSO-d_6 solution was 3.20×10^{-11} m^2/s. The relatively slow diffusion of **138** in DMSO-d_6 is indicative of the high molecular weight of the monomeric unit (2616 g/mol), as well as high viscosity of the solvent. Based on the Stokes-Einstein equation, the diffusion coefficient is inversely proportional to the viscosity (η) of the solvent. Thus, on the assumption that the solvation shells in two different solvents do not affect diffusion rates significantly, the ratio of η (DMSO) / $\eta(CHCl_3)$ = 3.93 was used to estimate the diffusion coefficient of the monomer in $CDCl_3$ and the value obtained was 1.26×10^{-10} m^2/s. Further diffusion NMR studies were undertaken in $CDCl_3$ solution where the diffusion coefficient was measured to be 2.18×10^{-11} m^2/s for a 19 mM solution, which is in agreement with a high molecular weight polymer. By comparison, the diffusion coefficient of a dimer such as **114** (Chapter I) in $CDCl_3$ was 6.19×10^{-10} m^2/s, significantly higher than that measured for polymer **138**. Additional diffusion NMR measurements were undertaken for dilute solutions in $CDCl_3$. Diffusion coefficients were 1.00×10^{-10} m^2/s and 1.29×10^{-10} m^2/s for the 3.1 mM and 1.5 mM solutions. These are considerably faster than that measured for the 19 mM solution. In fact, the value measured for the 1.5 mM solution is close to that estimated for the 6-keto monomer in $CDCl_3$ based on the measurement in DMSO-d_6 (1.26×10^{-10} m^2/s, see above). From this, polymer **138** dissociates on dilution in $CDCl_3$. It should be noted that the NMR solvent used was not dried and therefore contained some water. It is likely that the increase of the water content relative to that of polymer on dilution may facilitate dissociation of the polymer.

To conclude, the synthesis of supramolecular polymers has been achieved following a synthetic route involving the use of isocyanate. The physical properties of the final materials have been significantly improved after functionalisation of the telechelic polymers with Upy. This strategy has proved to be very effective for the synthesis of new materials, and therefore it will be used for the synthesis of energetic materials as described in part II of this chapter. The accessibility of the starting materials is a clear advantage of the synthetic approach described above. However, the use of isocyanates is

a less attractive feature especially in view of possible industrial exploitation. With this prospect in mind, a more 'environmentally friendly' approach has been developed for the synthesis of supramolecular polymers.

3.5 Alternative Methods for the Synthesis of Supramolecular Polymers

The novel strategy involved the synthesis of a supramolecular polymer with an ester linker as opposed to a carbamate linker as previously described (Figure 82). The ester bond could lead to increased flexibility of the chains, and therefore enhance elastomeric properties within the final material. More importantly, the synthesis of such polymer does not require the use of isocyanate.

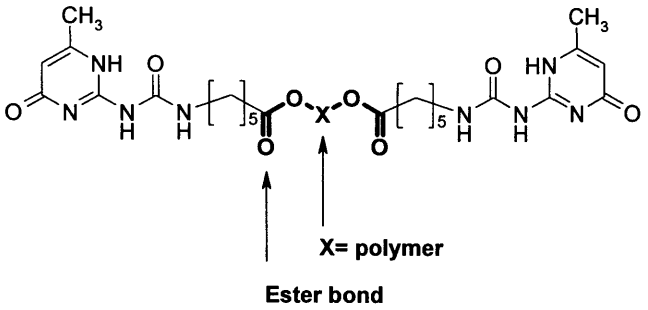

Figure 82: Supramolecular polymer with ester linkage

The strategy involved a five step synthesis as shown in Scheme 32.

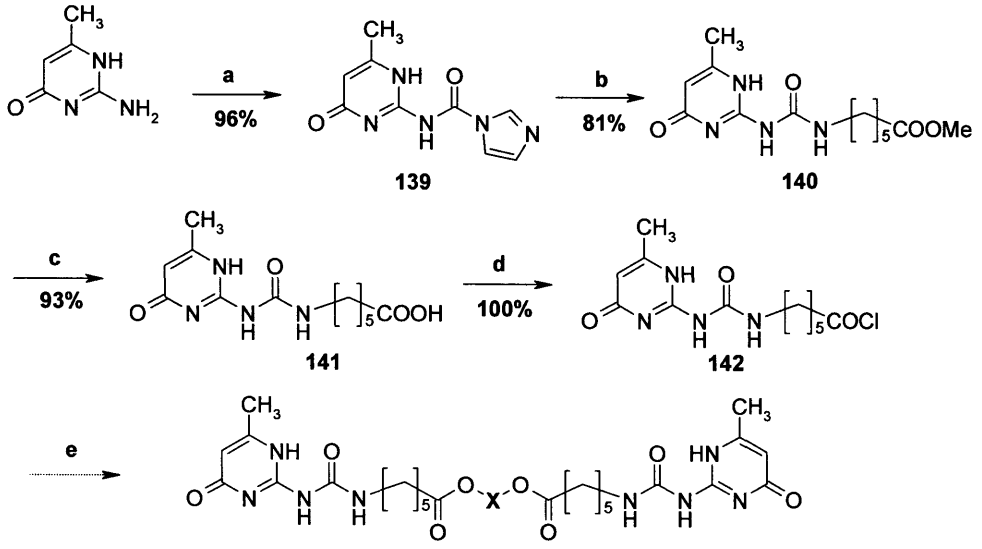

Reagents and conditions: **(a)** CDI, DMSO, 60 °C, 2 h, 96%; **(b)** 6-aminohexanoic methylester chloride, Et_3N, THF, reflux, 81%; **(c)** HCl (2N), THF, reflux, 4 h, 93%; **(d)** $SOCl_2$, CH_2Cl_2, 40 °C, 100%.

Scheme 32: Synthetic route towards a supramolecular polymer

The starting material 6-methyl isocytosine was first activated with carbonyldiimidazole in DMSO at 60 °C for 2 h affording compound **139** in 96% yield after drying *in vacuo* at 50 °C for 16 h.[131] Compound **143** was prior obtained in 58% yield *via* the reaction of 6-amino hexanoic acid with thionyl chloride in dry methanol at -10 °C (scheme 33).[162] Compound **139** was then reacted with 6-amine hexane methyl ester hydrochloride (**143**) in the presence of triethylamine under reflux conditions in dry THF, affording compound **140** in 81% yield.

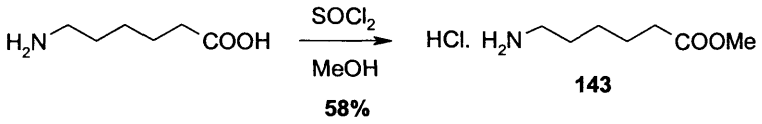

Scheme 33: Synthesis of 6-amino hexane methyl ester hydrochloride

Hydrolysis of **140** under basic conditions (KOH / MeOH) led to cleavage of the urea moiety. In contrast, the use of acidic conditions (2 N hydrochloric acid) afforded the corresponding carboxylic acid derivative **141** in 91% yield. Compound **141** was then reacted with thionyl chloride, which led to the formation of acid chloride **142** in quantitative yield. Compound **142** was reacted with 1,4-butanediol with a small amount of Et_3N, as a test reaction for the synthesis of supramolecular polymers (Scheme 34). The bifunctional compound **144** was successfully isolated in 46% isolated yield.

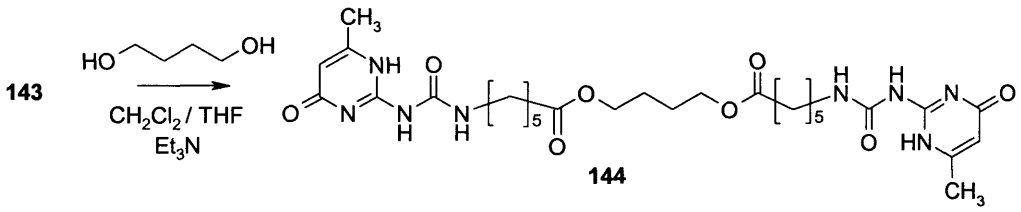

Scheme 34: Functionalisation of 1,4-butanediol

The ^1H NMR spectrum confirmed the formation of the bifunctional Upy system. In particular, peaks in the high-frequency region were characteristic of the hydrogen bonded NH protons. In addition, the integration and chemical shifts of the peaks (Figure 83) were consistent with the expected structure.

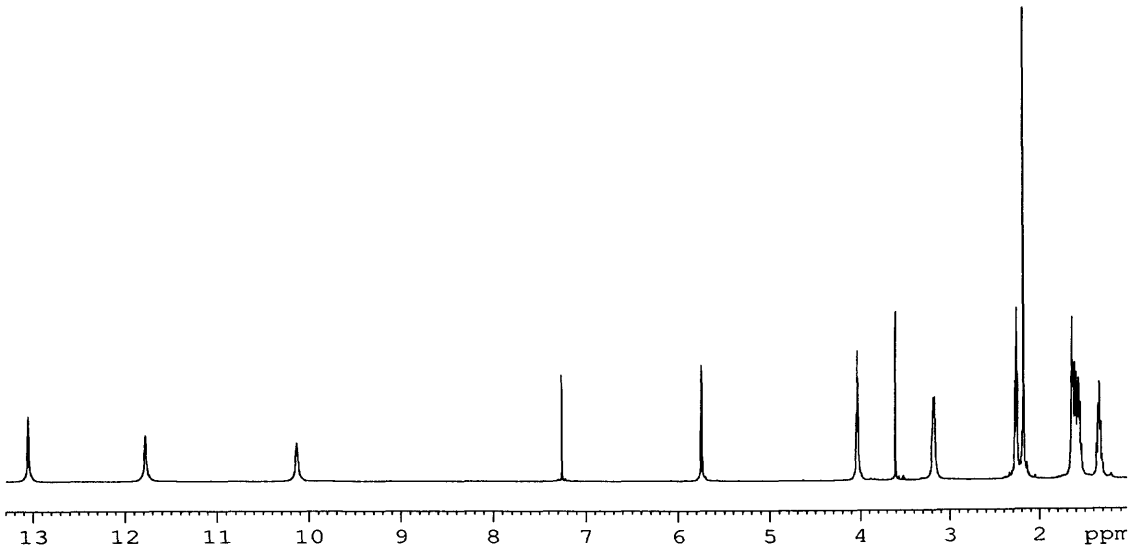

Figure 83: ^{1}H NMR spectrum of **144** in $CDCl_3$ at 298K

An estimation of the diffusion coefficient was made in chloroform at 298 K for a 66 mM solution of **144** and was found to be 1.17×10^{-10} m^2/s. Dilution of this solution to 24 mM led to a significant increase of the diffusion coefficient up to 3.60×10^{-10} m^2/s. Further low-temperature ^{1}H NMR measurements at 258 K of **144** in $CDCl_3$ (24 mM) revealed the presence of two new species with relatively small populations (Figure 84). From the line fitting of the 5-H region, the ratio of the peaks at 5.82, 5.79 and 5.75 ppm was approximately 15:77:8. Diffusion measurements at 258 K showed that the corresponding species diffused at significantly different rates: 1.05×10^{-10} m^2/s (5.82 ppm), 1.26×10^{-10} m^2/s (5.79 ppm) and 2.68×10^{-10} m^2/s (5.75 ppm). Based on the relationship used between diffusion coefficient and the molecular weight ($D_{pol} \sim M^{0.62}$)[163] the corresponding peaks at 5.82, 5.79 and 5.75 ppm could be assigned to trimeric, dimeric and monomeric species. These must be cyclic, as the corresponding NH protons resonate in the high-frequency region characteristic for the 4-keto quadruply hydrogen bonded array.

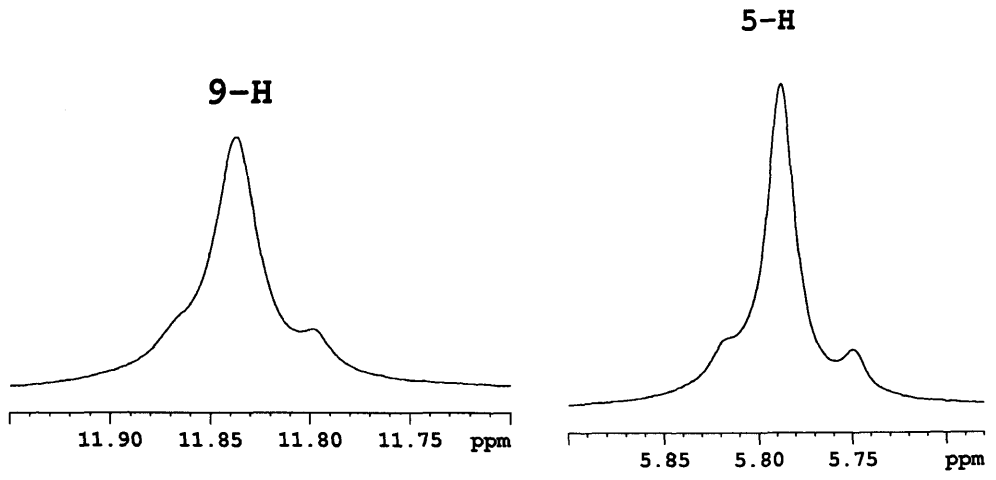

Figure 84: Peaks corresponding to protons 9-H and 5-H in the ^{1}H NMR spectrum of **144** in $CDCl_3$ at 258 K

This result suggested that at lower concentrations the linear polymer chains were disrupted and certainly recombined into smaller oligomeric species or even cyclic species. Meijer *et al.* have already described similar observation for some bifunctional Upy systems but with shorter linkers between the Upys (e.g Chapter I). Some other bifunctional Upy derivatives studied in this work showed a similar behaviour on dilution and these results will be discussed in more detail in the next chapter.
Following this result, the telechelic block polymer PEG-PPG-PEG (M_n ~ 2900 g/mol) was functionalised using the same reaction conditions as previously described. ^{1}H NMR spectrum confirmed the presence of the desired bifunctional material. The compound was dried under vacuum for two days and submitted for further DSC measurements (under investigation at AWE).

To conclude, the synthesis of new polymeric materials *via* an alternative synthetic route has been achieved. One of the ultimate goals for AWE would be application of this strategy for the synthesis of energetic supramolecular polymers.

PART II: Towards the Synthesis of Hydrogen Bonded Energetic Materials

One of the major targets for the AWE is the preparation of supramolecular polymers with energetic formulations for the use in explosives, propellants or pyrotechnics and to generate novel supramolecular architectures, which may be repeatedly processed and recycled. These materials would have great advantages in terms of safer handling, the reduction of waste of expensive ingredients and aid demilitarisation programmes.

3.6 Introduction

3.6.1 Energetic Polymers and Plasticisers for Explosives Formulation

The design of future energetic systems requires the use of explosive and propellant formulations having enhanced performance and reduced vulnerability (storage and transportation). Some important criteria such as mechanical properties, the lifetime, ease of disposability and environmental impact in manufacture and use have to be taken into consideration for the design of such materials. In particular, extensive programmes have been set up worldwide for the development of Insensitive Munitions (IM), that satisfy the performance expectation and that assure a reduced risk to unplanned hazardous stimuli.

One of the responses to this research has been the development of cast-cured polymer bonded explosives (PBX) in which the explosive ingredient is suspended in a polymeric binder, cured in situ into a tough elastomeric rubber which absorbs and dissipates the energy from hazardous stimuli. Binders are typically cross-linked polymers, and one of the earliest binders in energetic materials was nitrocellulose in nitroglycerine, where the nitrocellulose was used to thicken the nitroglycerine to reduce any impact and friction risk. Nowadays, the explosive is encapsulated in a binder, such as a telechelic polymer (Hydroxy Terminated Polybutadiene (HTPB, Figure 85), Hydroxy Terminated Polyethers (HTPE)) crosslinked with isocyanate, and containing a plasticiser such as Dioctyl Adipate (DOA).

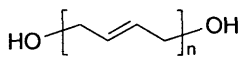

Figure 85: Hydro Terminated Poly Butadiene (HTPB)

The advantages of these binders are the excellent physical properties and reduction of the vulnerability of the explosive charges, however they are inert and decrease the overall energy output of the explosive. One solution to overcome this problem has been the use of polymers/plasticisers that contribute to the overall energy of the composition. This could be easily improved by incorporating some energetic functional groups, such as nitro (C-nitro, O-nitro, N-nitro) but also azido and the difluoroamine group along the polymer backbone. Recent energetic binders that satisfy these criteria include azide functional polymers such as glycidyl azide (GAP) or the nitrato polyethers such as poly(3-nitratomethyl-3-methyloxetane) (polyNIMMO) and poly(glycidyl nitrate) (PolyGLYN). Other binders include fluoropolymers and polynitroaromatic.

3.6.2 Classification of the Most Common Energetic Polymers[164]

3.6.2.1 *Glycidyl Azide Polymer*

Azido-functionalised polymers such as glycidyl azide polymer (GAP) (Figure 86) were intensively used in the early 1980s, as the safety characteristics of GAP loaded with explosive entities are similar to those made with inert HTBT binders.

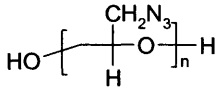

Figure 86: Glycidyl azide polymer (GAP)

Such polymers were first synthesised in 1972 by Vandenburb *via* the reaction of sodium azide in DMF with polyepichlorohydrin, PECH-triol. The functionalisation of GAP has been studied in order to obtain a tough and elastomeric rubber. For this purpose Frankel *et al.* patented a process where linear GAP is terminated with isocyanate groups to give an α,ω-diisocyanate functionalised GAP (Figure 87).

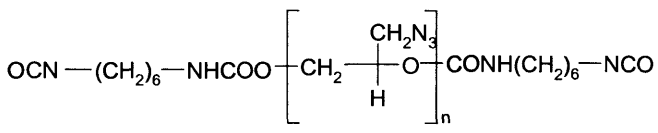

Figure 87: α,ω-diisocyanate functionalised GAP

3.6.2.2 *GAP Properties*

The physico-chemical properties of the polymers depend on the degree of polymerisation and the method of preparation. GAP has a relatively low glass transition temperature (-45 °C), and this results in an energetically favourable binder system. However, GAP is hard and brittle at low temperatures due to the rigid, conjugated N_3 groups, limiting the flexibility of the polymer backbone. Another problem is that GAP functionalised with isocyanates liberates carbon dioxide when the isocyanate reacts with moisture. Carbon dioxide is then trapped in the cross-linked binder and results in decreased mechanical properties and safety. The energetic properties are a function of the decomposition of the azide group, which generates nitrogen. Also, the high concentration of carbon atoms results in a high combustion potential.

3.6.2.3 *Oxetane Polymers*

Energetic polyoxetanes were first synthesised by Manser using the monomers 3-nitratomethyl-3-methyl oxetane (NIMMO, 3,3-bis-(azidomethyl)oxetane (BAMO) and also 3-azidomethyl-3-methyl oxetane (AMMO) (Scheme 35).

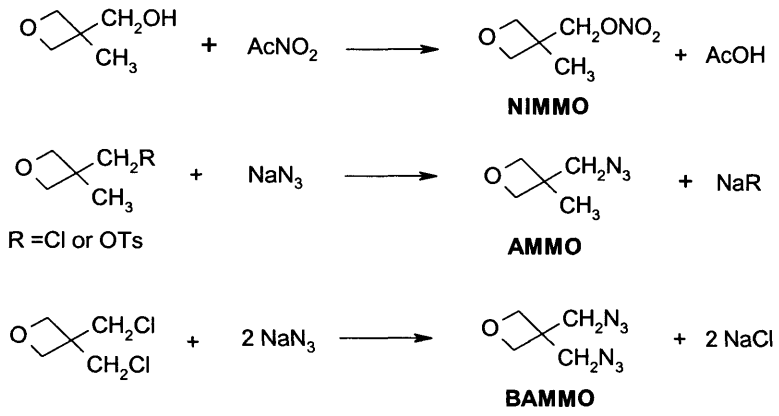

Scheme 35: Synthesis of oxetanes

3.6.2.4 *Synthesis and Properties of PolyNIMMO*

The polymerisation of NIMMO has been achieved *via* a cationic polymerisation employing initiators (commonly diols) and catalyst (Lewis acid). If the initiator is a diol such as 1,4-butanediol then the polyNIMMO prepared is bifunctional (Figure 88).

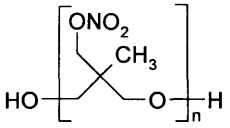

Figure 88: PolyNIMMO

Having a primary hydroxyl terminated alcohol is a great advantage in terms of the high reactivity towards isocyanate. PolyNIMMO has interesting properties, as the glass transition temperature is around -35 °C, and can be readily cured with conventional isocyanates upon heating.

3.6.2.5 *Oxirane Polymers*

Oxirane polymers differ from the oxetane polymers by the number of methylene groups in the repeating unit. Glycidyl nitrate (GLYN) is a monomer used for the polymerisation. Slow addition of the monomer solution (GLYN) to the initiator solution (tetrafluoroboric acid etherate) generates an activated monomer unit, which combines with the difunctional alcohol (glycerol) in a ring opening process (Scheme 36).

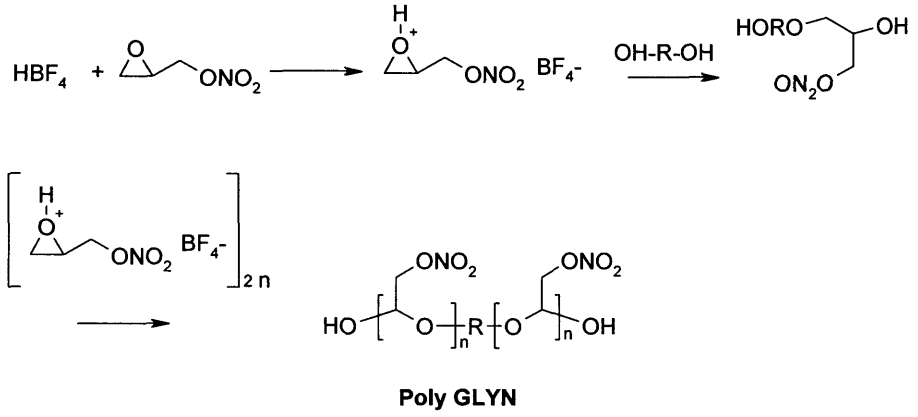

Scheme 36: Polymerisation of PolyGLYN

PolyGLYN can also be functionalised with isocyanate leading to polyGLYN cured rubbers as shown in Figure 89.

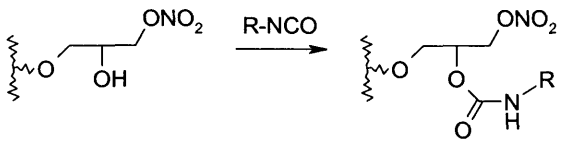

Figure 89: Cured PolyGLYN

When cured with isocyanates, the resulting polyurethane rubbers show poor stability. Indeed degradation of the network can occur due to the labile proton (Figure 90).

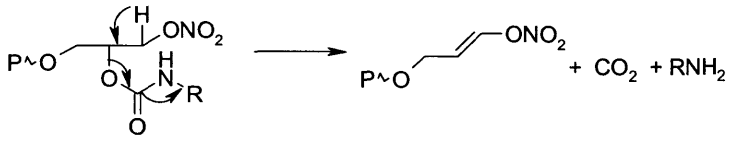

Figure 90: Degradation of the cured polyGLYN

This problem has been overcome by modification of the chain ends to give a primary hydroxyl terminated polyGLYN.

3.6.2.6 *Properties of PolyGLYN*

PolyGLYN is a clear, yellow liquid, with a low T_g (-30 °C). As with PolyNIMMO, its sensitivity is too low to be classified as a class 1 explosive in the UK.

One of the exciting challenges would be the functionalisation of energetic polymers such as PolyGLYN or PolyNIMMO with Upy groups, to form an energetic supramolecular polymer. The combination of an energetic source and elastomeric properties could make them excellent energetic binders for future high energy applications. Furthermore, the presence of non-covalent interactions would afford an easy way of decommissioning the materials.

3.7 Synthesis of Energetic Supramolecular Materials

3.7.1 Functionalisation of PolyGLYN with Upy unit

PolyGLYN (M_n ~ 2000 g/mol) was reacted with synthon **131** under the same conditions as described in Part I (Figure 91). However, the final material was not dried *in vacuo* to

avoid any possible decomposition reactions. Since the chemical hazards were not fully assessed, only DSC analysis were performed at AWE.

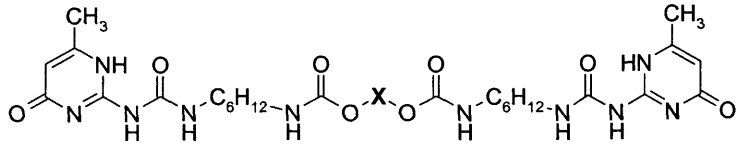

X = PolyGlyn, 2000 g/mol

Figure 91: Functionalisation of PolyGLYN

3.7.1.1 *Results*

The final material was a white opaque compound, and the DSC analysis showed a T_g at ~ -22 °C and no distinctive melting point, which suggested that the final supramolecular polymer contained only amorphous domains. A decomposition run was performed showing an exotherm at 196.8 °C with an energy of -1057 J/mol (ΔH). The decomposition process of an energetic polymer starts with the degradation of the nitrato group. For polyGLYN the decomposition mechanism of the energetic group is as following:

$$-CH_2\text{-}O\text{-}NO_2 \longrightarrow CH_2O^{\bullet} + {}^{\bullet}NO_2$$

From these results a comparison of the physical properties of polyGLYN and the functionalised polymer is presented in Table 20.

Polymer	T_g (°C)	Decomposition Temperature (°C)	Decomposition Heat (J/g)
PolyGLYN	-31.5	204	2000
PolyGLYN+ UPy	-22	196	1057

Table 20: Comparison of physical properties of PolyGLYN and its Upy derivative

It is apparent that the presence of the Upy units has an effect on the glass transition temperature, which is increased. This was probably due to the addition of rigidity in the final polymer by the introduction of heterocyclic rings. The decomposition temperature was not significantly affected, however the decomposition heat was much lower, which reflects an overall decrease in the energetic composition due to the presence of Upy groups and the C_6 chain spacer within the supramolecular polymer.

3.8 Synthesis of Energetic Precursor of Ureidopyrimidinones

In order to synthesise Upy systems, which possess potential energetic sites, derivatives of Upy incorporating one or two hydroxyl groups at the C-6 position were synthesised with the objective of introducing energetic group such as NO_2 after its synthesis (Figure 92).

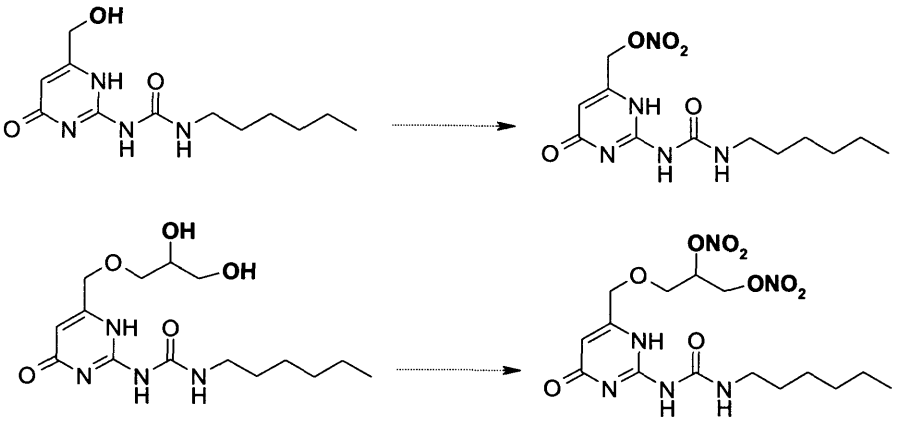

Figure 92: Introduction of energetic groups at the C-6 position of the Upy unit

3.8.1 Synthesis 1

The first synthesis was carried out following Scheme 37 shown below.

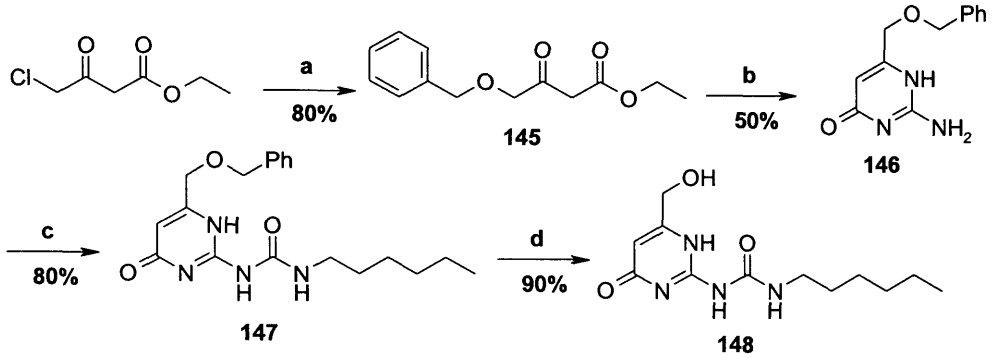

Reagents and conditions: **(a)** BnOH, NaH (60%), toluene, r.t, 80%; **(b)** guanidine carbonate, EtOH, reflux, 50%; **(c)** $C_6H_{13}NCO$, pyridine, 100 °C, 80%; **(d)** BCl_3, CH_2Cl_2, -78 °C, 90%.

Scheme 37: Synthesis of compound **148**

Following Yasohara *et al.*,[165] cloroacetoacetate was first reacted with benzyl alcohol in the presence of sodium hydride (60% in oil) in dry THF. The mixture was stirred at r.t. for 16 h. Unfortunately, the desired product was not isolated, and it was clear by TLC analysis that many products were formed. Dry toluene was then used as previously described by Beck *et al.*[166] and this time the reaction was successful and the desired compound **145** was isolated in 80% yield after purification by flash chromatography. The reaction of **145** with guanidine carbonate in ethanol under reflux conditions afforded the desired isocytosine **146** in 50% yield after precipitation from the solution. The product was dried thoroughly under pressure, and reacted further with hexylisocyanate in dry pyridine at 100 °C for 16 h. Addition of hexane to the cooled solution resulted in the precipitation of compound **147** in 80% yield. Finally, removal of the benzyl group was first attempted using catalytic hydrogenation over Pd/C in THF/ MeOH (5:1). Compound **147** was insoluble in most organic solvents and the reduction could not be achieved, even when heating at 50 °C. The use of an alternative method was then considered using the Lewis acid BCl_3 in CH_2Cl_2 at -78 °C,[167,168] which successfully led to the deprotected compound **148** in 90% yield after purification. The final compound was unfortunately insoluble in $CDCl_3$ and could only be studied by NMR in DMSO-d_6. This material is currently being tested at AWE.

3.8.2 Synthesis 2

The synthesis was carried out as shown below:

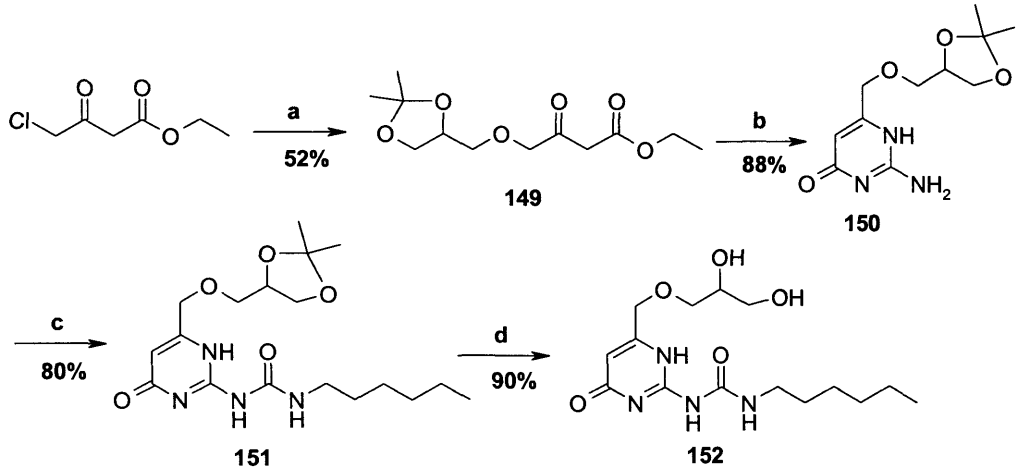

Reagents and conditions: **(a)** Solketal, NaH (60%), toluene, r.t., 52%; **(b)** guanidine, EtOH, reflux, 88%; **(c)** $C_6H_{13}NCO$, pyridine, 100 °C, 80%; **(d)** HCl (1N), MeOH, THF, 90%.

Scheme 38: Synthetic route towards compound **152**

To prepare a more functionalised substrate, cloroacetoacetate was first reacted with solketal in the presence of sodium hydride (60% in oil) to give **149** in 52% yield after purification. The reaction of **149** with guanidine carbonate in ethanol under reflux conditions afforded the isocytosine **150** in 88% isolated yield. Further reaction between **150** and hexyl isocyanate in pyridine at 100 °C, followed by the addition of hexane led to the precipitation of pure compound **151** in 80% yield. The acetal protecting group was finally removed under acid conditions (1 N HCl) in a mixture of methanol and THF (2:1) under reflux conditions for 30 min. The product **152** was isolated in 90% yield. Once again, the final compound had low solubility in most organic solvents and is under further investigation at AWE.

Conclusion

The functionalisation of non-energetic and energetic telechelic polymers with ureidopyrimidinones has been achieved, opening up a new area for energetic binders. The development of an alternative synthetic approach for the synthesis of such supramolecular polymers, avoiding the use of isocyanates, has proved to be efficient although less straightforward. This method could lead to further development for industrial purposes. In all cases, a linear supramolecular polymer of high molecular weight was obtained over a range of concentrations. Interestingly, the linear polymer chain was dissociated into smaller oligomeric species upon dilution. The hydrogen bonding system still persisted in solution according to the ^{1}H NMR chemical shifts, but it was more likely that cyclic species were then formed. Indeed, the bifunctional monomer was sufficiently long enough to form an intramolecular quadruple hydrogen bonding and generate a cyclic monomer ('head-to-tail'). Since the concentration under which the oligomeric species are formed is relatively low (~ 5-10 mM), this does not affect the industrial applications of these materials. The equilibrium between polymeric chains and cyclic species will be further discussed in the following chapter.

Chapter IV

4 Cyclic Dimers of Bifunctional Ureidopyrimidinones

4.1 Introduction

The use of bifunctional ureidopyrimidinone systems has been investigated for the synthesis of linear supramolecular polymers incorporating linear alkyl chains (**62**) or various polymers and co-polymers (**66**).[115] In addition, Meijer *et al.* have studied intensively the use of rigid linkers (**87**) and biased linkers found in compounds **90** and **93** on the formation of stable cyclic dimers over polymers (Chapter I).[126,128]

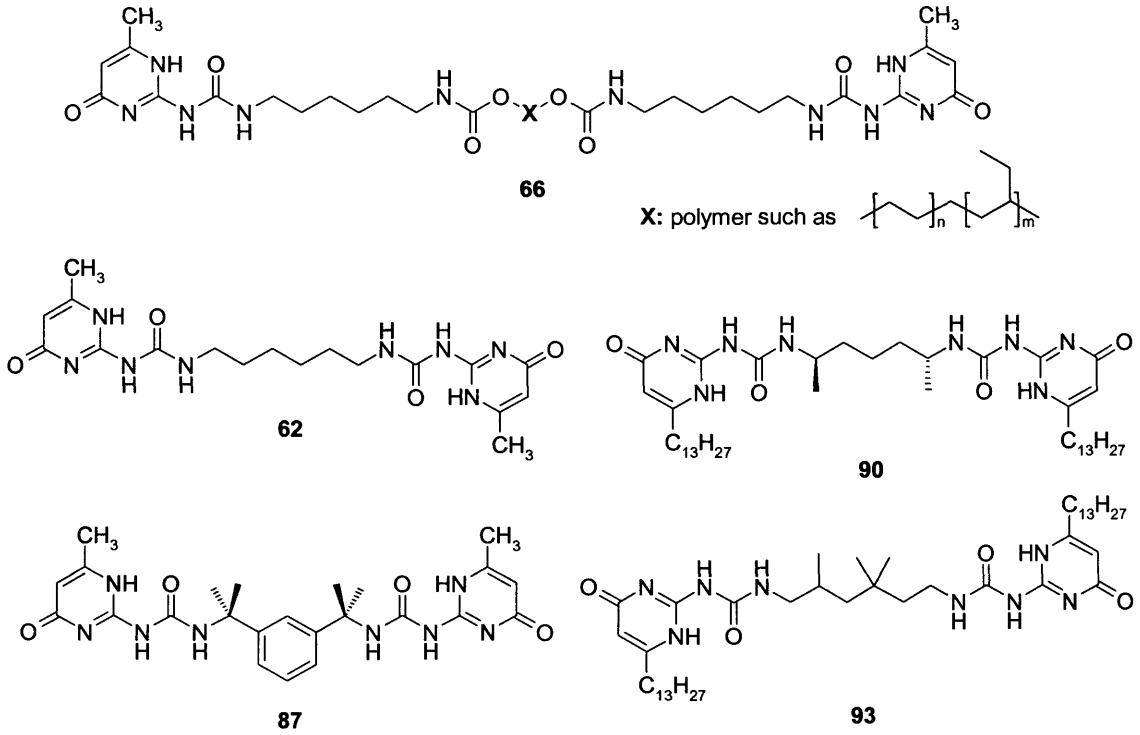

Figure 93: Examples of bifunctional Ureidopyrimidinone systems

These examples reflected the importance of the nature of the spacer (flexible, rigid or biased) between two Upy units on the conformation of the final supramolecular structure (polymer/cyclic dimer) (Chapter I). Interestingly, ureidopyrimidinones incorporating small chiral units at position '**X**' (see compound **66**, Figure 93) have not been reported so far. To this end, analogues of compound **66** were designed to open up potential for a new type of materials with greater structural diversity (Figure 94).

Primarily, we were interested in assessing whether larger cyclic dimers could be generated using these new arrays and consequently study the cyclic/polymeric interconversion of these supramolecular systems.

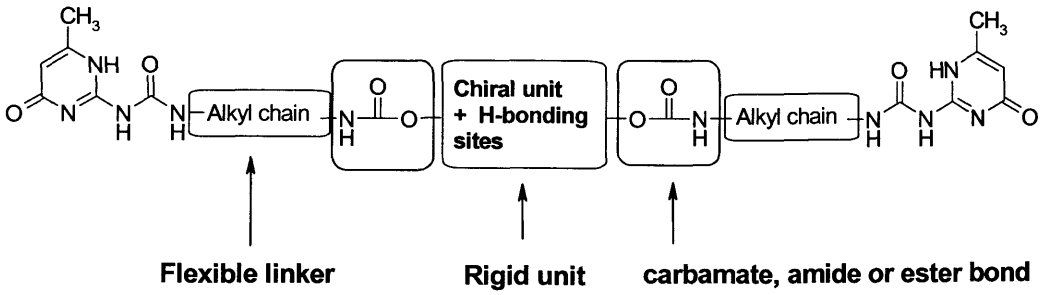

Figure 94: Design of new arrays, analogues of compound **66**

The desired characteristics of the new hydrogen bonded array are as followed:

- A small chiral unit: the presence of chirality has already been shown to induce helicity into polymers, and therefore could lead to interesting new supramolecular structures.
- Potential capability of hydrogen bonding sites within the chiral unit to generate further intramolecular hydrogen bonds and enhance the overall stability of the array.
- A flexible alkyl chain where the length could be varied to alter structural properties.
- A linker such as carbamate, amide or ester depending on the synthetic route used.

The insertion of a cyclic dipeptide as well as tartrate derivatives were then investigated.

4.2 Incorporation of a Cyclic Dipetide

The cyclic dipetide (**153**) derivative of L-serine was first selected since it combines rigidity and chirality as well as the capacity to form intramolecular hydrogen bonds such as **a** and **b** as shown below (Figure 95), using a carbamate linker.

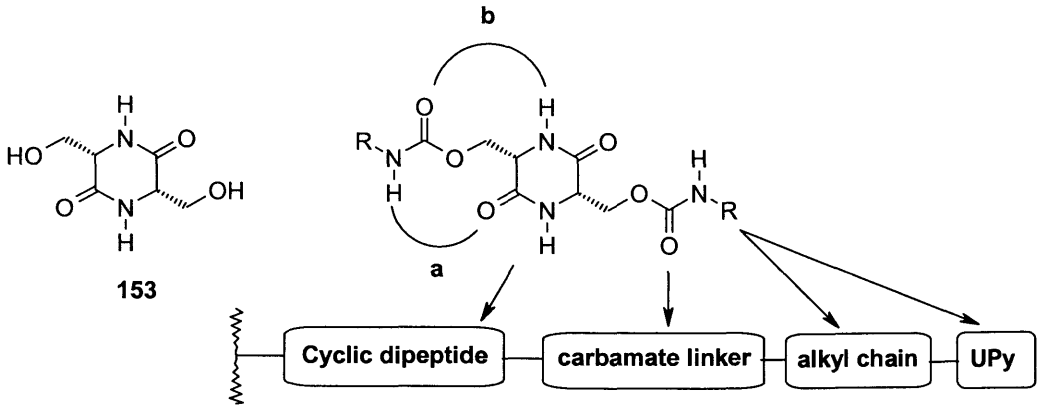

Figure 95: Structure of the cyclic dipeptide and schematic view of the array generated

4.2.1 Towards the Synthesis of the Cyclic Dipeptide

The synthesis of cyclic dipeptides has been reported using several methods such as those described by Fisher and Nitecki.[169] Both methods have advantages and disadvantages in terms of the yields achieved and degree of racemisation observed. It has been shown that the Fisher method involving the aminolysis of the dipeptide ester in methanolic ammonia, lead to appreciable racemisation. Nitecki *et al.* have described a different procedure *via* the deprotection of a Boc-dipeptide ester using formic acid and the subsequent reflux of the deprotected ester formate with a mixture of *s*-butyl alcohol and toluene. This method lead to reduced racemisation within the final compound, however the yield is not particularly high as a result of competing side reactions (40% for L-Ser-L-Ser-).

It has also been reported that dipeptide esters can be spontaneously cyclised by the hydrogenolysis of a benzyloxycarbonyl protecting group. Cyclic peptides were obtained by refluxing a solution of the deprotected dipeptide esters in methanol. A comparison of these methods in terms of yield and racemisation for some cyclic dipeptides is shown in Table 21.

Compound	Yield (Racemisation)		
	Fisher	Nitecki	MeOH-Reflux
Cyclo(-L-Leu-L-Leu-)	70% (1.5%)	71% (5.5%)	76% (1.2%)
Cyclo(-L-Val-L-Val-)	20% (0.9%)	58% (0.4%)	64% (0.6%)
Cyclo(-L-Ser-L-Ser-)	53% (2.7%)	40% (1.5%)	63% (1.4%)
Cyclo(-L-Phe-L-Phe-)	86% (0.6%)	89% (0.6%)	93% (0.1%)

Table 21: Comparison of Fisher, Nicketi and MeOH/Reflux methods for the cyclisation of dipeptides[169]

To ensure as little racemisation as possible, the MeOH-reflux method was initially followed (Scheme 39).

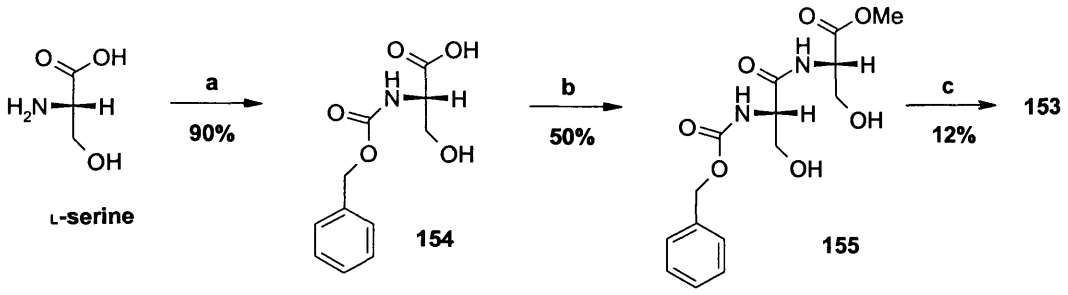

Reagents and conditions: **(a)** $PhCH_2OCOCl$, $NaHCO_3$, 90%; **(b)** L-serine-OMe, HCl, PPh_3, CCl_4, NEt_3, CH_3CN, 50%; **(c)** H_2, Pd/C, MeOH, reflux, 8d, 12%.

Scheme 39: Synthesis of the cyclic dipeptide

CBz-protected serine **154** was synthesised from L-serine and benzylchloroformate in a saturated aqueous carbonate solution.[170] Protected L-serine was recovered as a white solid in 90% yield and was used directly in the next step. Peptide couplings are commonly carried out using carbodiimides such as DCC with either DMAP or triethylamine, however this procedure did not afford the desired product. An alternative method is the use of triphenylphosphine, carbon tetrachloride and triethylamine which can prevent side chain reactions with primary hydroxyl functional groups present in the peptide.[171]

The coupling reaction between **154** and L-serine methyl ester chloride using this method gave **155** as a white powder in 50% yield after purification.

The next step involved removal of the CBz protecting group using catalytic hydrogenation over Pd/C black in methanol. In order to achieve the cyclisation, the deprotected dipeptide L-serine-L-serine was heated at reflux in methanol for 8 days (repeat experiments have highlighted the necessity of using a dilute reaction conditions in order to generate the product). The first successful attempt gave the cyclic dipeptide in only 12% yield.

In order to generate the supramolecular array (**156,** Figure 96) the reaction between hexyl diisocyanate **131** and cyclic dipeptide **153** was carried out in $CHCl_3$ under reflux conditions using the method previously described by Meijer *et al.* and involving the use of tinbutindilaurate as a catalyst for the reaction (Scheme 40).[115]

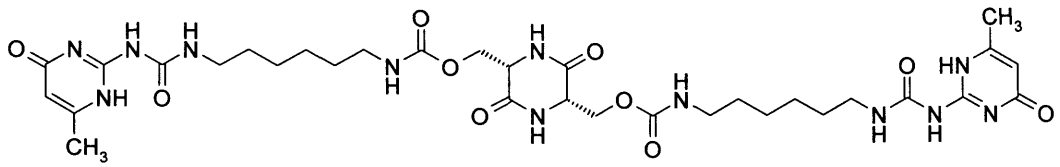

156

Figure 96: Bifunctional ureidopyrimidinone incorporating a cyclic dipeptide

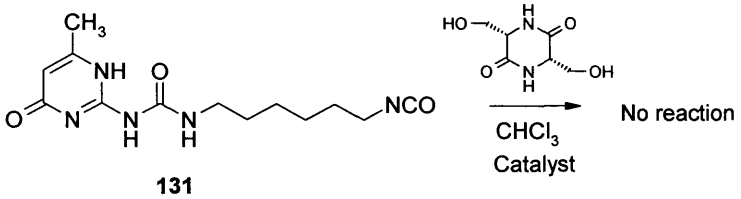

Scheme 40: Towards the synthesis of compound **156**

Compound **153** was however sparingly soluble in organic solvents and an initial attempt in chloroform under reflux conditions was unsuccessful. A second attempt using 10% DMSO in chloroform also led to the isolation of the starting material. The reaction was then conducted using 60% DMSO in chloroform. However, this method failed to yield the desired product.

Due to the poor solubility of the cyclic peptide in organic solvents, an alternative chiral unit was then considered. Previously Lehn *et al.* have reported the synthesis of

supramolecular polymers incorporating tartaric acid derivatives, which induced helical orientation of the polymeric chains (Chapter I).[96] Based on this idea, molecule **157** (Figure 97) was selected incorporating a chiral tartaric unit linked through an amide bond to an alkyl chain of variable length. Other than the chirality within the molecule, the free hydroxyl groups of the tartaric unit can act as hydrogen bonding donors. They could also be further functionalised to form new derivatives.

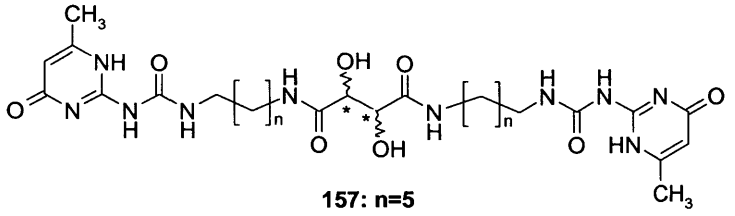

Figure 97: New supramolecular array targeted

4.3 Incorporation of Tartaric Acid

The synthesis of **157** could be carried out through the condensation of **139** with the corresponding amine salt **158** (Scheme 41).[172]

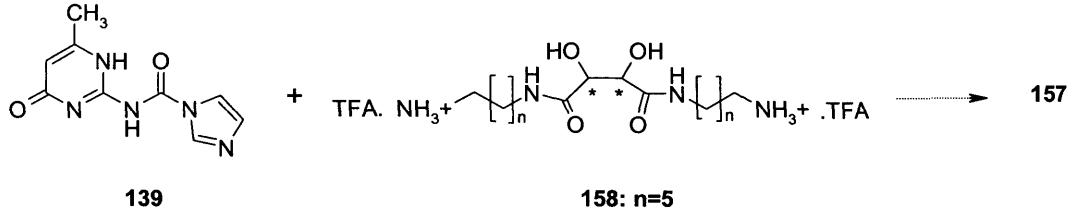

Scheme 41: Synthetic strategy for compound **157**

Tartaric acid can be converted to tartramide when reacted with an amine (Scheme 42). The formation of the amide bond required the use of a coupling reagent such as DDC or EDCI/HOB*t*. An alternative method requires the use of microwave activation, which enables the use of solvent free reaction conditions.

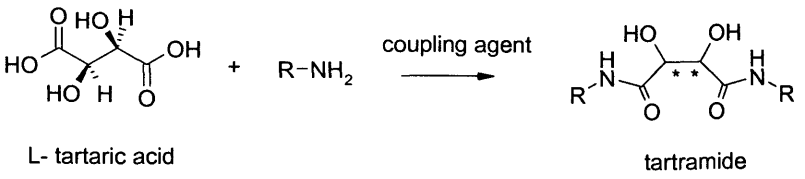

L- tartaric acid

tartramide

Scheme 42: Synthetic strategy for tartramide compounds

Following this procedure, Massicot *et al.* have synthesised tartramides in good yield (70%) from benzylamine and aliphatic primary amine (12 min, 20-180 °C).[173] In order to study this reaction and investigate the best procedure for the coupling step, butylamine (R = C_4H_9) was used in test reactions under the conditions shown in Table 22. In order to avoid any intermolecular side reactions with DCC as a coupling agent, EDCI was first chosen, as it is well known for its high reactivity towards primary amines. In particular, Marastoni *et al.* have described an efficient method using EDCI/HOBt to give tartramides in good high yields (~ 70%).[174]

Method	Yield
A) EDCI/HOBt/CH_2Cl_2	0%
B) EDCI/HOBt/DMF	45%
C) Microwave, 180 °C, 34 W, 9 min.	60%

Table 22: Different conditions used for the reaction between L-tartaric acid and butylamine

From these results it appeared that the microwave reaction was the most efficient method, giving the highest yield in the shortest time. When using EDCI, no reaction occurred in CH_2Cl_2, while in DMF 45% of pure product was isolated. Following these preliminary test reactions, the microwave activation was then applied for the synthesis of tartramide **160** (Scheme 43) between tartaric L-acid and compound **15.**[175] However the desired compound was not isolated.

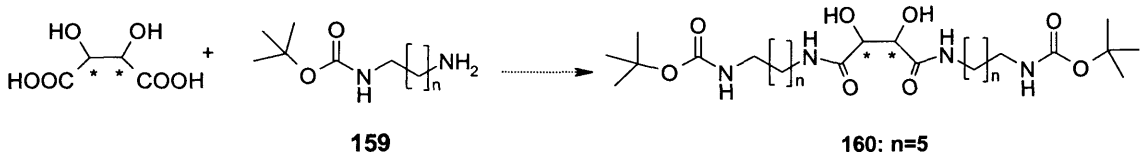

159 **160: n=5**

Scheme 43: Synthesis of tartramide derivative **160**

A decrease in the reaction temperature of the microwave reactor did not improve the reaction. It was then rationalised that the Boc protecting group was unstable under the microwave conditions, and subsequent decomposition of the molecule was observed.

Unfortunately, this method proved to be ineffective with this particular substrate and the reaction between tartaric acid and compound **159** with EDCI/HOBt in DMF was then carried out and **160** was isolated in 76% yield. Deprotection of BOC protecting group in TFA/CH_2Cl_2 (1:1, v/v) afforded the corresponding salt **158** in quantitative yield (Scheme 44).

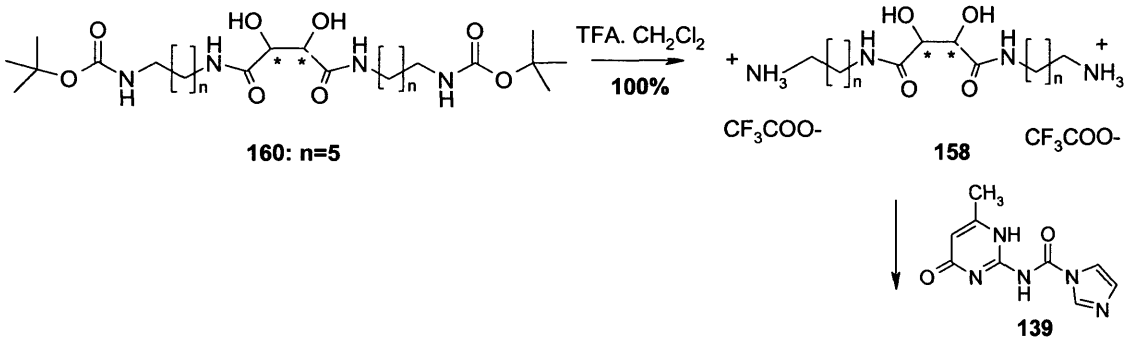

160: n=5 **158** **139**

Scheme 44: Deprotection of the tartramide protected compound **160** and subsequent reaction with compound **139**.

Compound **158** was unfortunately insoluble in organic solvents such as THF, $CHCl_3$ or acetonitrile. However, it was reacted with **139** in the presence of triethylamine in dried THF under reflux conditions. Meijer *et al.* reported a similar reaction procedure for the synthesis of compound **90**.[172] Unfortunately the reaction did not afford the desired product **157**, which is likely to be due to solubility problems as the imidazole derivative **139** also had low solubility in organic solvents.

Once again the synthetic approach was reconsidered, as the very poor solubility of such chiral units appeared to be a major problem.

4.4 Incorporation of Diethyl Tartrate

A low cost derivative of tartaric acid is the L or D diethyl tartrate, commercially available in both pure enantiomeric forms (Figure 98). One interesting characteristic is the presence of ester moieties that should increase the solubility, and the carbonyl groups could take part in additional hydrogen bonding within the final molecule. The use of diethyl tartrate was explored, one key advantage being the facile coupling reaction between the hydroxyl groups and the isocyanate **131** to generate a carbamate linker. When taking into account all these factors, this molecule appeared to be an excellent candidate for this study.

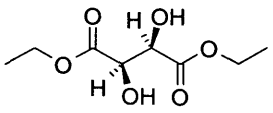

(R, R)-Diethyl L-tartrate

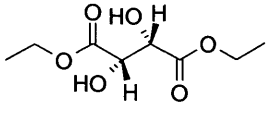

(S, S)-Diethyl D-tartrate

Figure 98: Diethyl tartrate derivatives

4.4.1 Synthesis

The isocyanate **131** was reacted with diethyl L-tartrate (the same with D) in dry chloroform with a drop of tin dibutyldilaurate using a similar method as that described previously (Scheme 45). Unfortunately the ^{1}H NMR spectrum showed a mixture of the products **161** and **162** in a ratio 1:9, but not the desired bifunctionalised compounds. Two doublets at 5.42 ppm and 4.69 ppm (J = 2 Hz) were attributed to the non-equivalent CH protons found in compound **161**. Further verification of the presence of **161** was provided by mass spectroscopy (ES+) with a molecular ion m/z at 500. Determination of the structure of compound **162** was however less straightforward together with rationalisation of its formation.

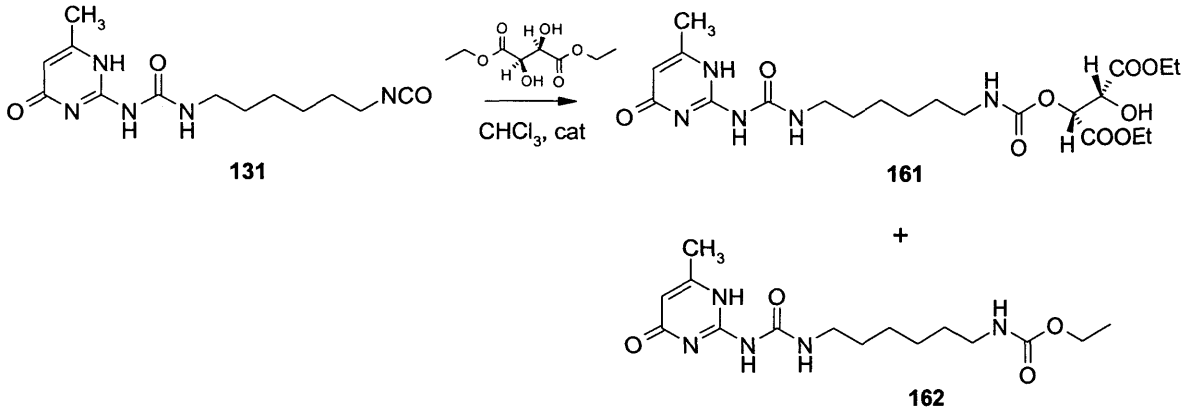

Scheme 45: Reaction of isocyanate **131** with diethyl L-tartrate

A quartet at 4.12 ppm and a triplet at 1.10 ppm were observed showing a ^{1}H-^{1}H coupling and were attributed to the $COOCH_2CH_3$ groups. A broad signal around 4.50 ppm was assigned to the NH proton of the carbamate group. In addition, the mass spectrum of the mixture showed a peak at 340.32, with an abundance of 100%, corresponding to **162**. Further confirmation was provided from the reaction of **131** with ethanol, and as expected the spectroscopic data were identical to that of compound **162**. The rational for the reaction of **162** was unclear at first. Two sources of ethanol were envisaged: either the 0.5-1% ethanol present in chloroform used as a stabiliser, or possibly from the hydrolysis of the diethyl ester moieties of the tartrate unit under the reaction conditions. In order to establish this, an experiment was conducted between **131** and diisopropyl L-tartrate (Scheme 46).

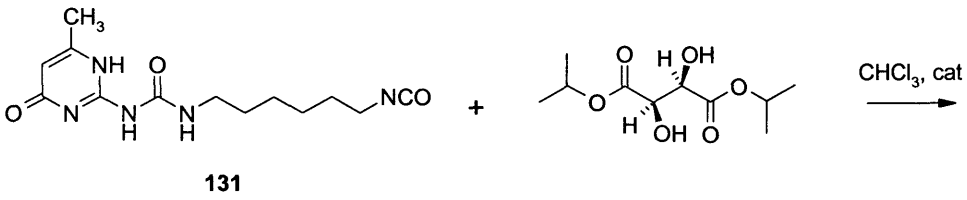

Scheme 46: Reaction between **131** and diisopropyl L-tartrate

Once again the quartet and the triplet at 4.12 ppm and 1.10 ppm, respectively, were observed and no traces of isopropanol that could have been generated from the ester moieties were observed. This confirmed that the source of ethanol was coming from the chloroform used. Although Meijer *et al.* never reported this problem in the synthesis of supramolecular polymers, in this present case ethanol did play a crucial role and

appeared to be a competing reagent. In order to avoid this side reaction in future, chloroform stabilised with amylenes was used.

The reaction was then repeated using an approximately 18.2 mM solution of the diethyl L-tartrate (Scheme 47) and ^{1}H NMR spectroscopy was used to monitor the progress of reaction over 96 h.

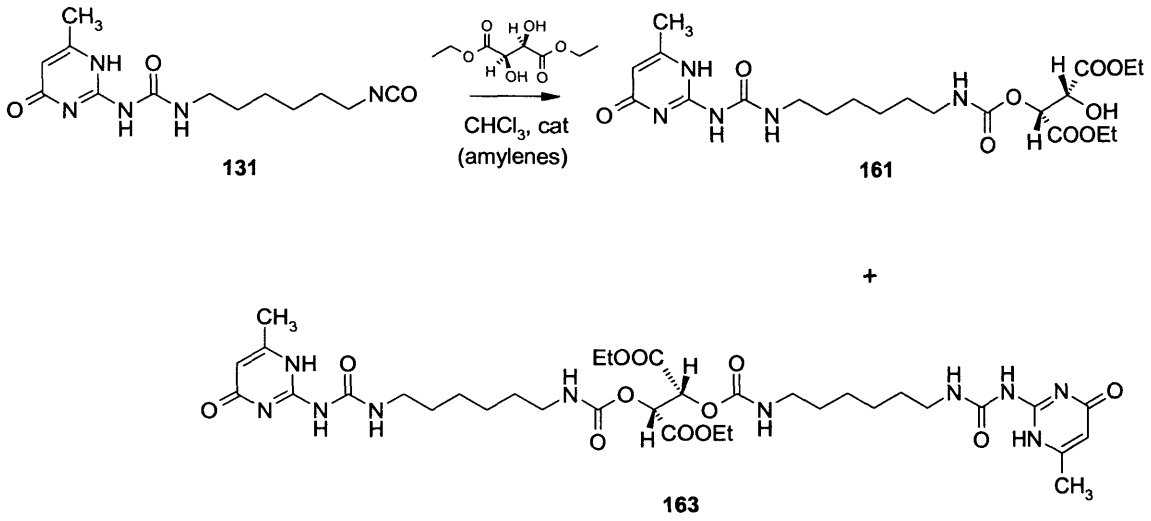

Scheme 47: Reaction between **131** and diethyl L-tartrate using reaction conditions

After an hour the presence of mono functionalised **161** was observed (indicated by # in Figure 99), along with starting materials (diethyl L-tartrate, marked as SM in Figure 99). Verification using mass spectrometry showed a peak corresponding to compound **161**. Interestingly, after approximately 5 h, an additional set of signals was observed in the ^{1}H NMR spectrum (marked by arrows in Figure 99). Additional MS analysis indicated a peak at 793 corresponding to compound **163**. The reaction appeared to be relatively slow, and even after 72 h, there was still a substantial amount of **161** present with the ratio **163**:**161** ≈ 2:3 (Figure 99, top trace).

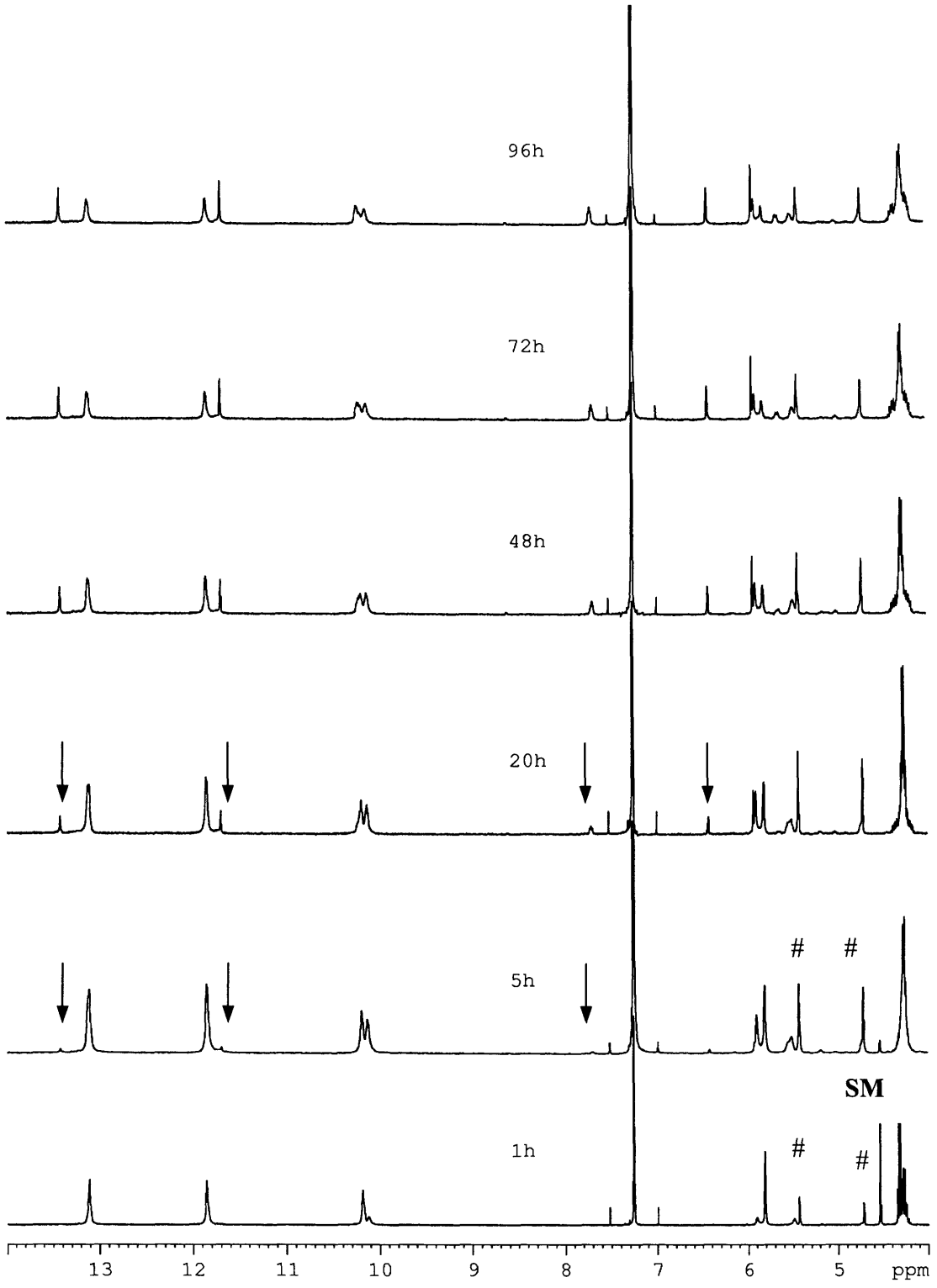

Figure 99: Advance of the reaction of **131** with diethyl L-tartrate (18.2 mM solution) followed by ^{1}H NMR as a function of time.

In order to increase the rate of the reaction and drive it to completion, parameters such as the concentration of the solution can be altered. In this study, increasing the concentration of diethyl L-tartrate from 18.2 mM to 55 mM had a significant effect on the rate of the reaction. After 1 h almost all the diethyl L-tartrate has reacted forming predominantly **161**. After 5 h, significant amount of **163** was already observed, and after about 20 h compound **163** was the major product (Figure 100).

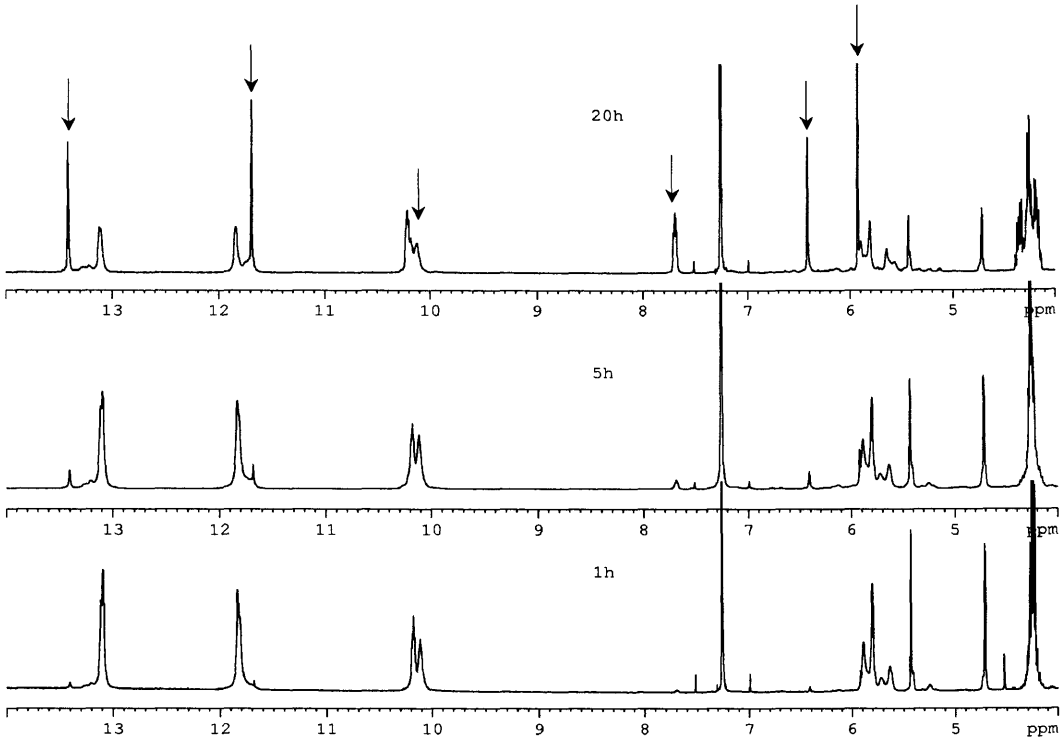

Figure 100: Advance of the reaction of **131** with diethyl L-tartrate (55 mM solution) followed by ^{1}H NMR as a function of time. Arrows indicate some of the key peaks due to the bifunctional Upy **163**.

Even more satisfactory results were observed when the solvent of the reaction was left to evaporate slowly. In this case almost no traces of **161** were observed by ^{1}H NMR spectroscopy. Compound **163** was purified *via* flash silica chromatography and isolated in 30% yield.

4.4.2 Determination of the Structure of Compound 163

Having isolated **163** the conformation of the supramolecular structure was explored to assess whether a polymer (**a**) or a cyclic form (**b**) was generated (Figure 101).

a **b**

Figure 101: Representation of a linear supramolecular polymer (**a**) and a cyclic dimer (**b**)

4.4.2.1 *NMR Studies of 163*

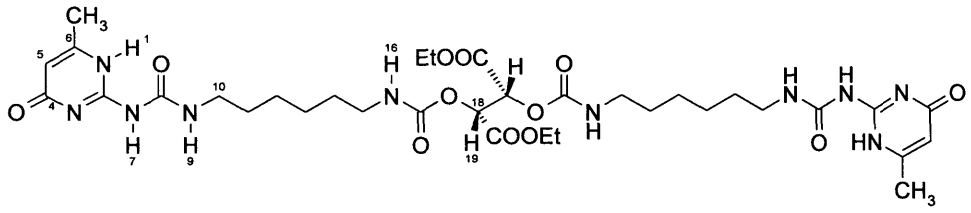

163

Compound **163** was initially studied in solution ($CDCl_3$) using NMR spectroscopy. The ^{13}C NMR chemical shifts of C-4 and C-5 at 174.0 ppm and 107.0 ppm (Figure 102a), indicated that the Upy units adopted the 4-keto form **B** and no enol form **C** was present (Chapter II). In Figure 102b, ^{1}H NMR chemical shifts and their assignments are shown. ^{15}N NMR chemical shifts were also measured using heteronuclear correlation experiments (Figure 103).

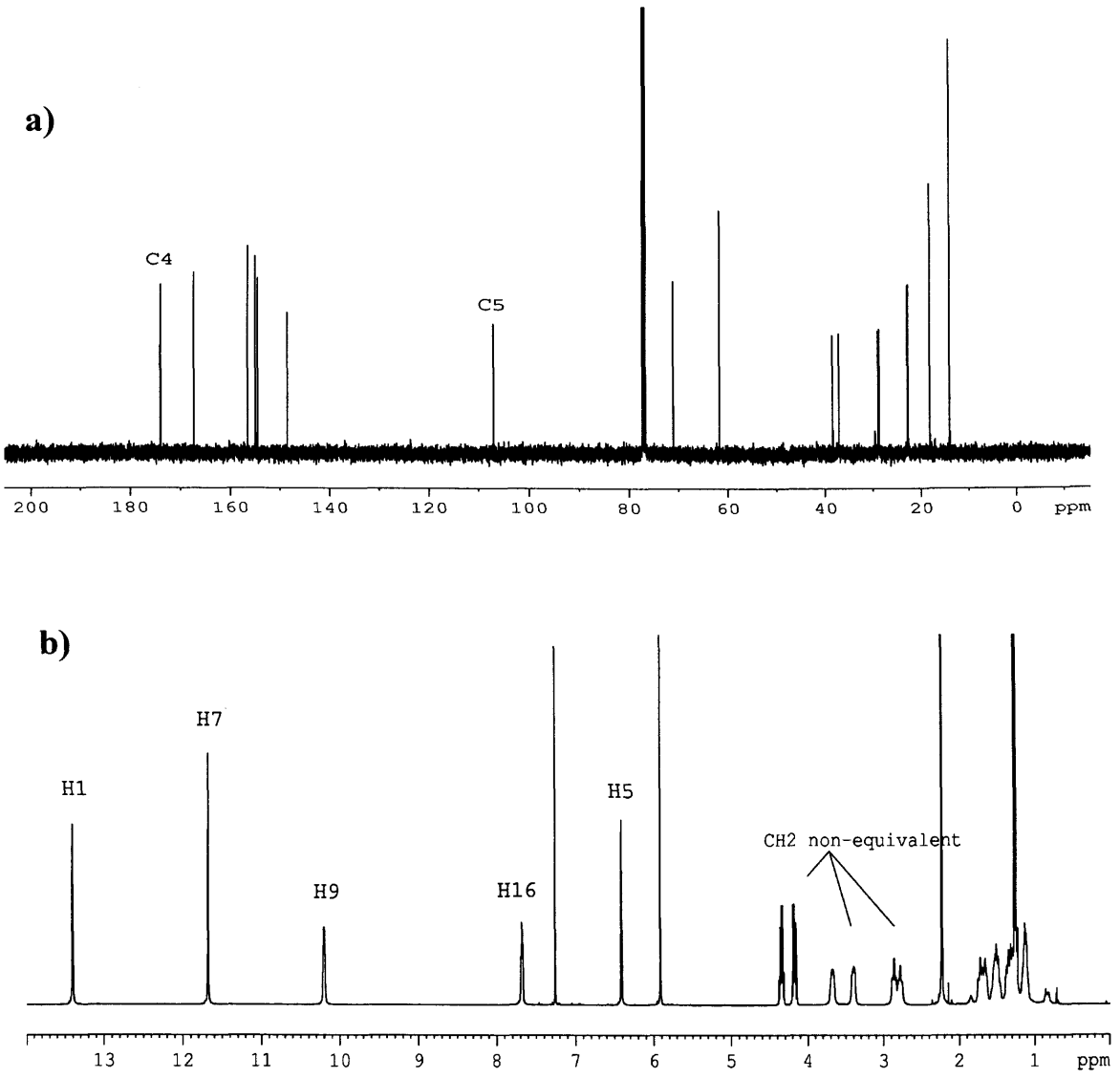

Figure 102: a) ^{13}C spectrum and b) ^{1}H spectrum of compound **163**

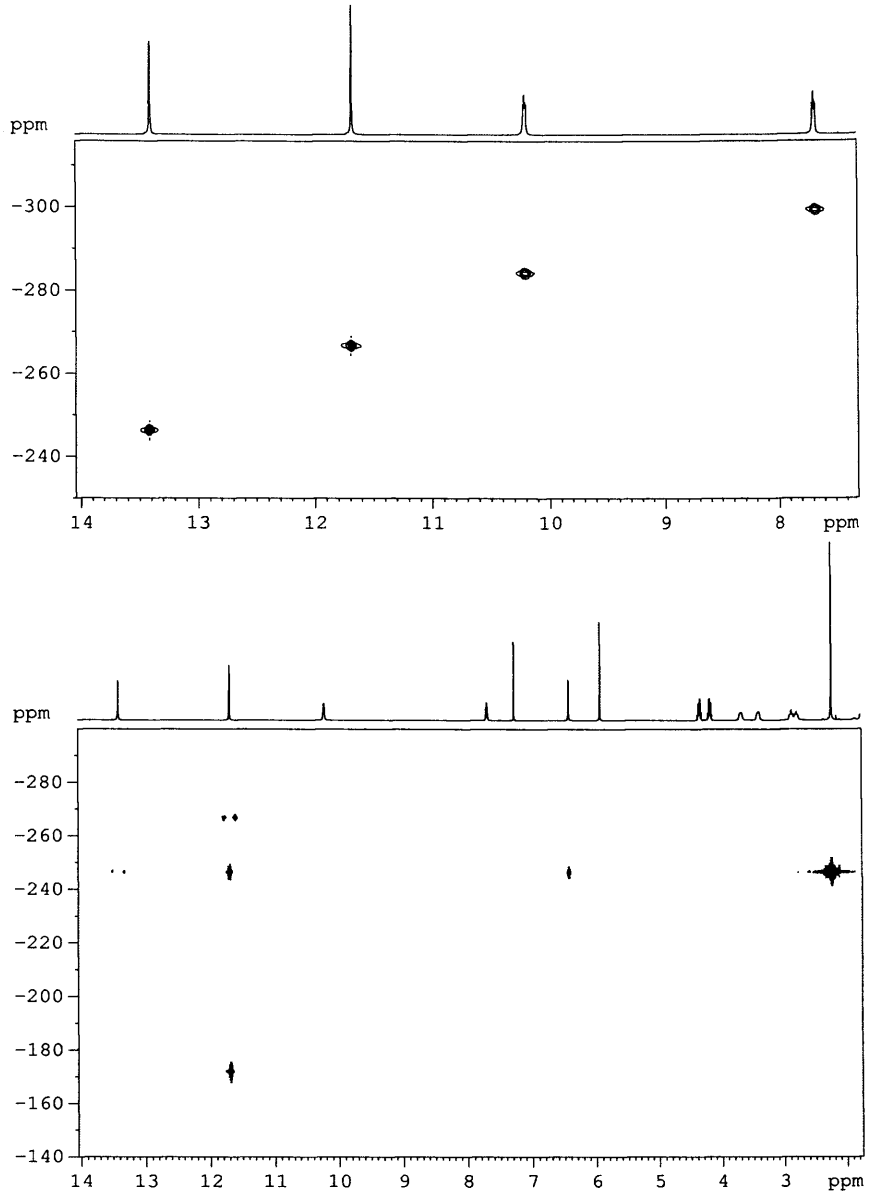

Figure 103: $^{1}H,^{15}N$ HMQC (top) and HMBC (bottom) spectra of **163** in $CDCl_3$. The ^{15}N chemical shifts were: -172.2 (N-3), -246.3 (N-1), -266.5 (N-7) and -284.1 ppm (N-9). Similar chemical shifts were also measured in the solid state: -172.1 (N-3), -245.9 (N-1), -266.4 (N-7) and -283.8 ppm (N-9)

Interestingly, the CH_2 protons adjacent to the linkers, as well as the CH_2 protons of the tartrate moiety were non-equivalent (Figure 104) in the ^1H NMR spectrum.

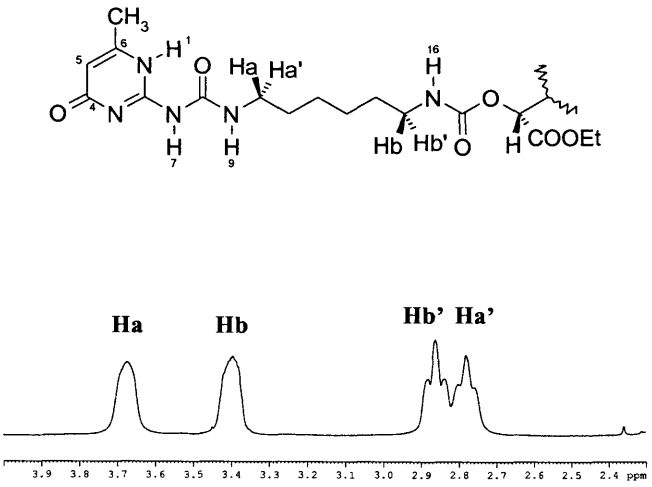

Figure 104: Part of the ^1H NMR spectrum showing the peaks due to non-equivalent CH_2 groups

This first observation, showing the non-equivalence of the hexyl chain indicated that compound **163** could adopt a cyclic structure. For comparison, in polymer **138** (Chapter III) corresponding protons H_a and $H_{a'}$ are chemically equivalent with the chemical shift of 3.20 ppm, which corresponds to the averaged position of protons H_a and $H_{a'}$ in Figure 104.

Compound **163** was dissolved in DMSO-d_6 and as expected, the DDAA hydrogen bonding network was disrupted. The 6-keto form **A** was shown to be present in solution, according to ^1H and ^{13}C NMR chemical shifts (Table 23). In particular, the ^{13}C NMR chemical shifts of C-4 and C-5 at 161.85 ppm and 104.64 ppm and the $^1J_{CH}$ coupling of C-5 (168 Hz) were in favour of the 6-keto form **A**. Since the substituent at C-6 is a methyl group, the tautomer **A** was expected in DMSO-d_6 based on the previous results (Chapter II).

Atom position	^1H $CDCl_3$ 298K	^1H DMSO-d_6 303K	^{13}C $CDCl_3$ 298K	^{13}C DMSO-d_6 303K
4	-	-	**174.03**	**161.85**
5	**6.41**	**5.78**	**107.06**	**104.64**
($^1J_{CH}$)	**(173.6 Hz)**	**(168 Hz)**		
7	11.68	9.8	-	-
9	10.21	7.44	-	-
16	7.68	7.38	-	-

Table 23: Comparison of ^1H and ^{13}C chemical shifts in $CDCl_3$ and DMSO-d_6

A comparison of the proton chemical shifts observed in $CDCl_3$ with those of the linear polymer **66** previously reported is shown in Table 24.

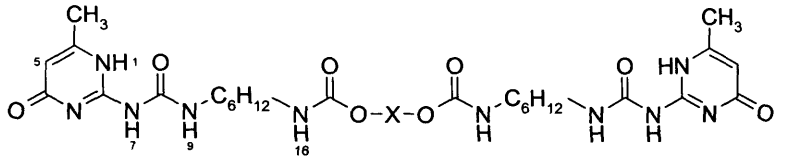

66=

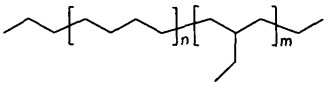

Protons	Linear polymer 66	Compound 163
1-H	13.09	13.41
5-H	5.83	6.41
7-H	11.82	11.68
9-H	10.08	10.21
16-H	4.87	7.68

Table 24: Comparison of ^1H NMR chemical shifts observed for the linear polymer and compound **163**

Substantial deshielding effects were observed for 1-H, 5-H and 16-H in compound **163** compared to the polymer. The drastic downfield chemical shift of 2.7 ppm at 16-H strongly suggested that it was involved in hydrogen bonding. These results revealed that the electronic environment around these protons had been modified, possibly by the formation of cyclic species in solution.

To assess potential hydrogen bonding between 16-H and the carbonyl group of the ester tartrate moiety within a molecule free of Upy units, hexyl isocyanate was reacted with diethyl-L tartrate to afford **164** in 56% yield (Scheme 48).

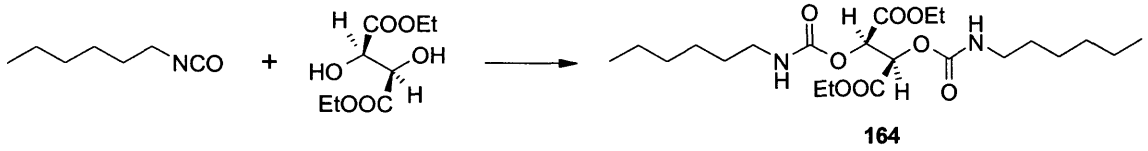

164

Scheme 48: Reaction between hexyl isocyanate and diethyl L-tartrate

The ^{1}H NMR spectrum of **164** showed a triplet at 5.9 ppm characteristic of the NH proton. If the NH group formed a hydrogen bond with an ester moiety, then the chemical shift of the NH proton should be close to the one found in compound **163**. The shift of 5.9 ppm indicated that the Upy units in **163** could act as acceptors for the formation of hydrogen bonds with 16-H.

To further investigate spatial arrangement of protons in **163**, NOE and ROE measurements were performed in the $CDCl_3$ solution (Figure 105). On selective excitation of proton 5-H the strongest NOE of -0.6% was found for proton 16-H. The corresponding ROE was 5.0%. These measurements were in favour of close spatial proximity of protons 16-H and 5-H, which in turn is in agreement with the large high frequency shifts observed for protons 16-H and 5-H. In addition, a small negative NOE of -0.2% (0.6% ROE) was found between 16-H and 9-H indicating that 16-H is in close proximity of the DDAA array.

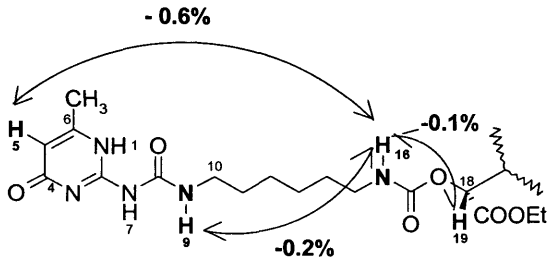

Figure 105: Some of the NOEs in **163**

4.4.2.2 *Proposed Structure*

The relative ratio of the NOEs were used to estimate some of the unusual proton proximities described above : 2.81 Å for (5-H, 16-H), 4.32 Å for (5-H, 9-H) and 3.26 Å for (9-H, 16-H). In the force field geometry optimisations using MMX, which is the extended version of the MM2 force field,[176] these internuclear separations were used as distance constraints. Additional torsional constraints were also imposed in order to retain a planar arrangement of the two quadruple hydrogen bonded UPy fragments. The energy minimisation led to a cage type structure shown in Figure 106. The distances highlighted in Figure 106 agree with the existence of the hydrogen bonding between 16-H and 4-O (N16-H…O), although these are longer than those for N9-H…O bond in the force-field optimised geometry.

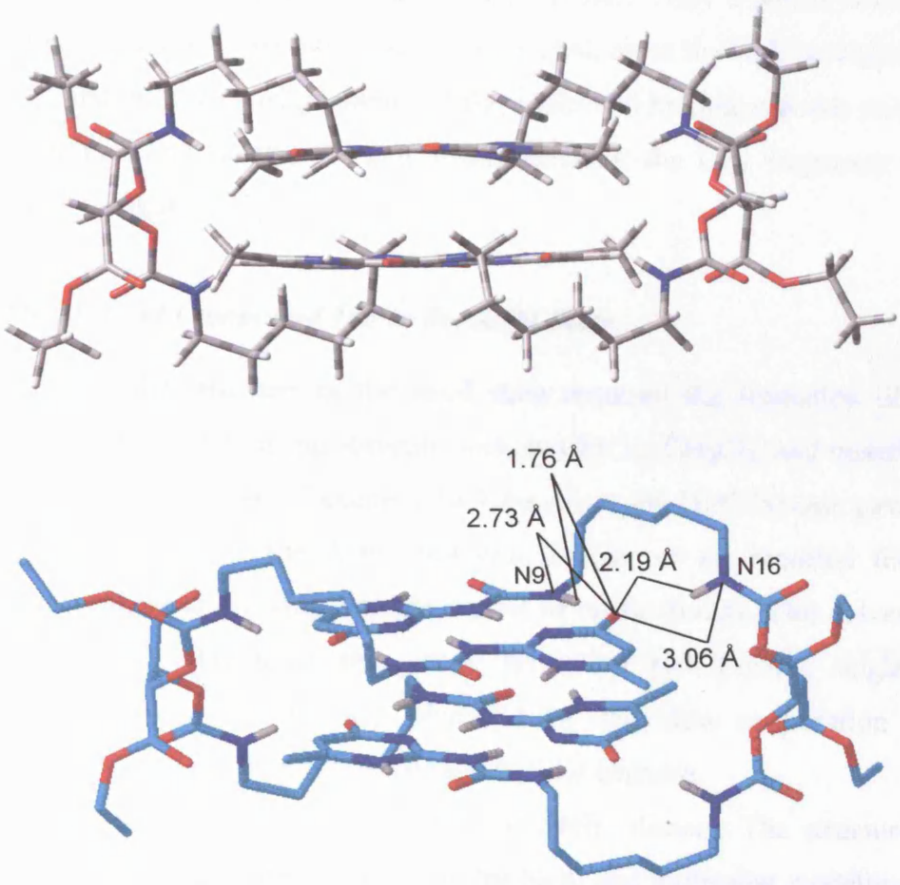

Figure 106: Top: the MMX force field geometry of **163** using fixed distances from NOE measurements. Bottom: the upper side view of the above without the protons attached to carbons. The shown distances from the carbonyl oxygen compare the two hydrogen bonds, N9-H…O and N16-H…O

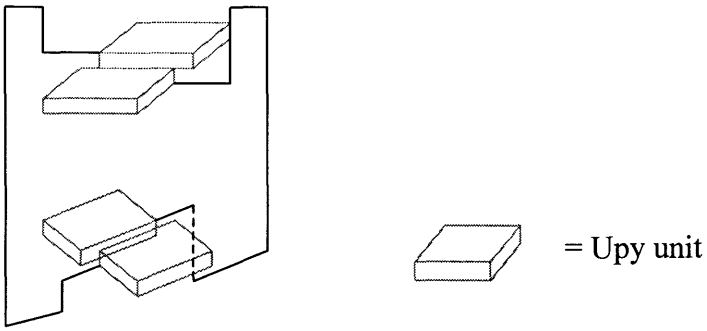

Figure 107: Schematic presentation of the anti-arrangement of the cyclic dimer.

Minimisation of the energy for other possible side chain orientations revealed that the ester moieties of the tartrate units prefer to be on the outside of the cavity rather directed towards the space between the two Upy planes. Only a model where the two Upy were in an anti-conformation could be elucidated, since the high preorganisation of the molecule and the preferred geometry of the additional hydrogen bonds restricted the syn conformation. For clarity, the anti arrangement of the Upy fragments is shown schematically in Figure 107.

4.4.2.3 *Structure of Compound 163 in the Solid State*

Determination of the structure in the solid state required the formation of a single crystal. Numerous attempts using solvents such as $CHCl_3$, CH_2Cl_2, and mixed solvents such as $CHCl_3$/hexane, CH_2Cl_2/hexane, $CHCl_3$/parafine and DMF/hexane gave crystals of insufficient quality for the X-ray analysis. Meijer *et al.* reported the use of DMSO/acetic acid when growing a single crystal of cyclic dimers. This solvent system however was not suitable to grow a single crystal of **163**. Finally, single crystals (colourless slabs) were successfully produced by the slow evaporation at room temperature of a mixed solution of dichloroethane and heptane.

Crystallographic data revealed the existence of cyclic dimers. The structure was in agreement with the one already proposed by the NOE and molecular modelling (Figure 108). Data were transferred into Mercury software and representation of the cyclic structure is depicted below. Details of crystallographic measurements are included in Appendix A.

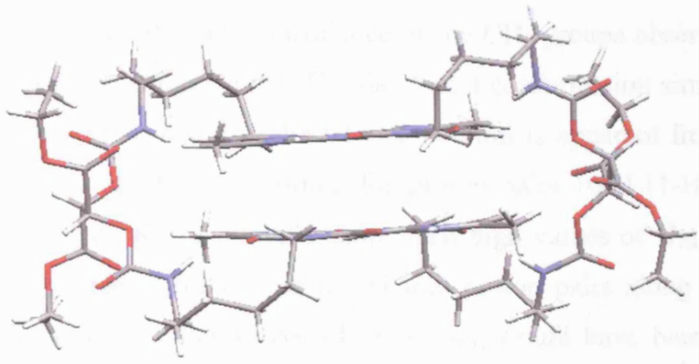

Figure 108: The molecular structure of compound **163** in the solid state

Analysis revealed that the cyclic dimer was maintained through a total of 16 hydrogen bonds in which eight were from the two DDAA-AADD arrays, four of them are the intramolecular hydrogen bonds in each DDAA unit, and four are the new hydrogen bonds formed between 16-H and the carbonyl oxygen at C-4 (Figure 109).

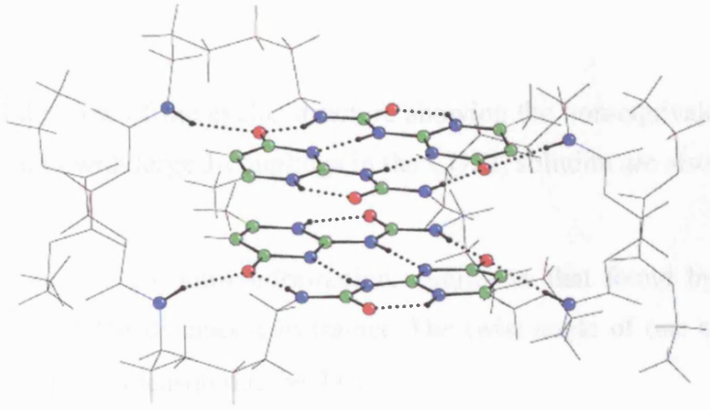

Figure 109: The view of the cyclic structure with the highlighted hydrogen bonds

The C_6 chain spacer appeared to form a loop to the outside of the Upy dimers planes which clearly explained the non-equivalence of the CH_2 groups observed previously in the ^1H NMR spectrum (Figure 110). The fact that a conformation similar to that in the solid state is also predominant in the $CDCl_3$ solution is apparent from the large $^3J_{HH}$ couplings of 11.5 and 11 Hz measured for proton pairs 10-H,11-H and 14-H,15-H, respectively. Based on Karplus relationship, such high values of $^3J_{HH}$ are in favour of ~180° torsional geometry for one of the vicinal proton pairs along C-10,C-11 or C-14,C-15. Significantly smaller values of these $^3J_{HH}$ would have been observed in the case of conformational flexibility in solution about the C-10,C-11 or C-14,C-15 bonds.

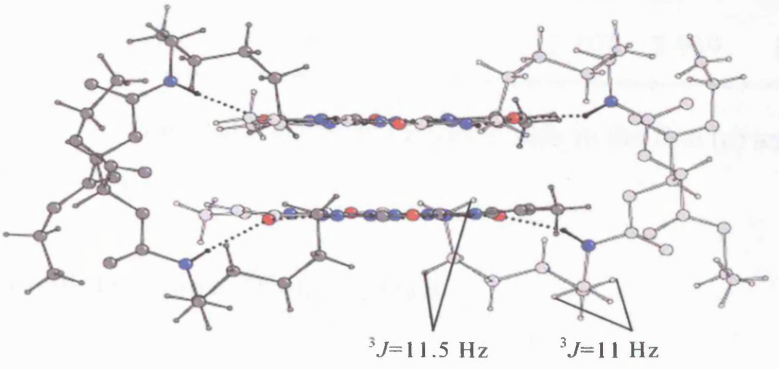

Figure 110: Side view of the cyclic structure showing the non-equivalence of the alkyl chain. Proton pairs with large J-couplings in the $CDCl_3$ solution are also shown

The two Upy were in an anti-conformation, similar to that found by the force field calculations using NOE distance constraints. The twist angle of one of the Upy plane relative to another was measured to be 73°.

The distances and angles of the hydrogen bonds in the cyclic dimer are given in Table 25. The cyclic dimer is not fully symmetrical as revealed by the differences in bond lengths and angles between the two dimers DDAA/AADD in the cyclic structure. For example, O…N-H bond varies from 1.842 Å in dimer (a) to 1.877 Å in dimer (b) while the angle changes from 173.4° to 170.0°. The new hydrogen bonds formed between 4-O and 16-H are short (~2.0 to 2.1 Å) and in the same order of magnitude as the NH…N bonds found in the Upy dimers. The distance between the two parallel planes of Upy dimers is approximately 3.3 Å suggesting a possible stacking of the two Upy planes.

H-bond	A...HD (Å)[a]	A...D (Å)[a]	θ (AHD) (°)[a]	A...HD (Å)[b]	A...D (Å)[b]	θ (AHD) (°)[b]
CO...HN	1.841	2.717	173.4	1.877	2.749	170
N...HN	2.07	2.948	175.4	2.04	2.919	176.6
NH...N	2.068	2.946	175.9	2.105	2.974	169.7
CO...HN	1.889	2.745	163.8	1.923	2.796	171.4
Intra CO...HN	1.799	2.496	134.6	1.862	2.541	132.6
Intra CO...HN	1.884	2.561	132.4	1.889	2.55	130.6
$C_4O...H_{16}N$	2.051	2.849	150.3	2.021	2.844	155.3
$C_4O...H_{16}N$	2.124	2.988	167.2	2.101	2.959	165

Table 25: Distances and angles of the hydrogen bonds in the first (a) and the second (b) DDAA/AADD arrays

Comparison with the Dimer DDAA-AADD

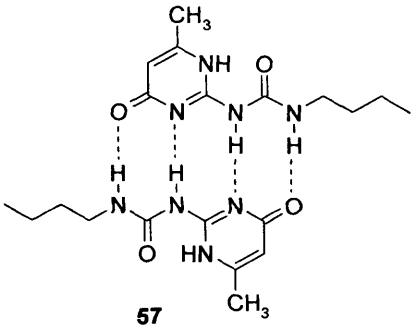

57

Figure 111: Representation of a DDAA-AADD dimer

DDAA/AADD	A...HD (Å)	θ (°)
CO...HN	1.877	175
N...HN	2.086	163

Table 26: Bond lengths and angles of the dimer

The bond lengths and angles found for the DDAA-AADD dimer **57** (Table 26) are very similar to those measured in the cyclic dimer **163.** This indicated that the strength of the DDAA-AADD dimers is conserved in the cyclic structure and possibly increased due to potential stacking between the two parallel Upy planes.

Comparison with a cyclic dimer

Recently Meijer has described the structure of a cyclic dimer with 12 hydrogen bonds formed by a short linker (**91**) between two Upy units (Figure 112).[177]

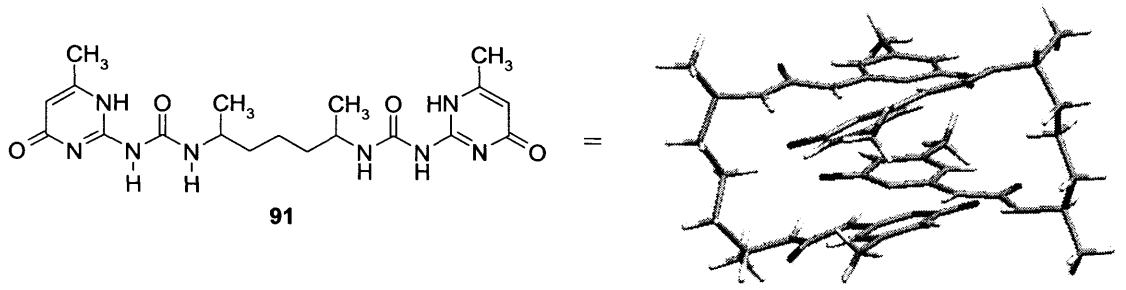

91

Figure 112: The X-ray structure of compound **91**

The short linker induces more strain in the ring and because of the reduced flexibility the two Upy dimers units are not parallel to each other, but significantly deviated from one to the other in order to assemble into a stable cyclic dimer. This distortion leads to an elongation of the O...H-N bond compared to compound **163**. As observed for compound **163,** the cyclic dimer **91** was not symmetrical (Table 27).

DDAA/AADD	A...HD (Å)	θ (AHD) (°)	A...HD (Å)	θ (AHD) (°)
O....HN	1.959	176.3	2.016	176.7
N....HN	2.023	172	2.125	177.7
NH....N	2.062	176.3	2.057	178.3
O....HN	1.982	176.1	1.945	171.6
O...HN (intra)	1.902	137.3	1.955	133.1
O...HN (intra)	1.806	138.4	1.874	139.1

Table 27: Bond lengths and angles found in cyclic dimer **91**

4.4.2.4 *Solid State NMR*

Solid-state NMR data was then acquired to confirm whether the solution conformation in $CDCl_3$ was the same as that in the solid. As shown in Table 28, the chemical shifts are almost identical in both cases confirming that the cyclic dimer is present in $CDCl_3$.

Carbon	δ_c (ppm), $CDCl_3$	δ_c (ppm), solid state
C-4	174.0	174.4
C-5	107.1	107.5
C-6	154.5	155.0
C-10	38.4	37.8
C-15	37.2	37.8

Table 28: Comparison of ^{13}C NMR chemical shifts in $CDCl_3$ and in the solid state

In summary, this is the first time that an ureidopyrimidinone cyclic dimer, stabilised with 16 hydrogen bonds has been observed both in solution and in the solid state. The novel approach of combining a flexible alkyl chain with an ester functionality has proved to be particularly effective for the formation of the cyclic dimer. Stacking *via* π–π interactions seems to be another stabilising factor. The role of the small chiral unit, however, is less clear. Other questions related to the cyclisation remain, such as what is the main driving force behind the dimeric cyclisation of bifunctional Upy's. Also, how stable is the cyclic structure and is the cyclisation enantioselective.

4.4.2.5 *Stability of the Cyclic Dimer*

As previously described in the introduction, the supramolecular rings and polymers are normally in equilibrium and the presence of polymeric species often occurs above a critical concentration, or in some cases with an increase in temperature.
Concentration dependence studies were undertaken to assess the possibility of polymer formation for **163**. No changes in ^1H NMR chemical shifts were observed on varying the concentration in the range from 1 mM to 500 mM in $CDCl_3$ at 298 K. Diffusion experiments were also performed in $CDCl_3$ on two samples at different concentrations: 10 mM and 135 mM and diffusion coefficients were 4.5×10^{-10} m^2/s and 4.4×10^{-10} m^2/s, respectively. Furthermore, upon increasing the concentration up to 500 mM there was still no sign of polymer that could be detected by ^1H NMR. This result suggested that the cyclic structure was extremely stable in solution with a critical concentration (if any) above 500 mM.

The dimerisation constant of the cyclic dimer was also assessed and for this purpose dilution experiments were performed in $CDCl_3$ down to 1.4 μM. No changes of the ^1H

chemical shifts were observed. The dimerisation constant was therefore estimated to be greater than 1.3×10^8 M^{-1}. This estimate was derived from K_{dim}= [d]/[m]^2 and [t] =2[d]+[m] relationships, where [t] is the total initial concentration, [d] and [m] are the concentrations of dimer and monomer, respectively. It was assumed that at the lowest concentration examined there is 5% of monomer that is not detected by NMR chemical shift measurements. This data highlighted the very high stability of the cyclic dimer in solution.

Temperature studies were also performed in toluene-d_8 in order to study the thermal behaviour of compound **163** and the possibility of polymer formation at higher temperatures. The results are summarised in Table 29.

Proton	296 K	363 K	378 K
1-H	13.72	13.51	13.45
7-H	11.85	11.67	11.64
9-H	10.30	9.98	9.92
17-H	7.91	7.28	7.09

Table 29: Variation of ^{1}H NMR chemical shifts in toluene-d_8 as a function of temperature

No traces of the polymer were observed on raising the temperature from 296 K to 378 K, however, a change in the hydrogen bonding behaviour was detected with all hydrogen bonded protons shifting upfield. The largest shift was for 17-H, suggesting that the corresponding hydrogen bond is the weakest in the cyclic dimer.

4.4.2.6 *Is the Cyclisation Enantioselective?*

Meijer *et al.* have described the formation of cyclic aggregates with high selectivity between homochiral and heterochiral cyclic species.[176]

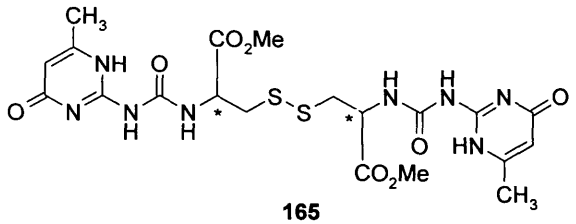

165

In Meijer's study the enantioselective dimerisation, (R,R)-**165** and (S,S)-**165** were synthesised from pure cystine methyl esters and solutions of the enantiomers were compared to solutions of the racemic mixture and studied by ^{1}H NMR dilutions (Figure 113). At 30 mM, the ^{1}H NMR spectrum of the racemic mixture was identical to that of pure enantiomers, showing that only homochiral cyclic species were formed in solution. The four peaks observed for the pyrimidinone alkylidene 5-H were all assigned to cyclic assemblies.

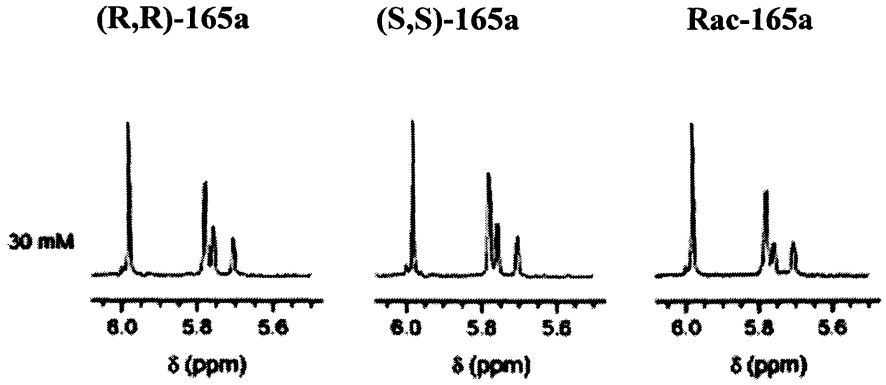

Figure 113: Alkylidene region of ^{1}H NMR spectra of **(R,R)-165a**, **(S,S)-165a** and a racemic mixture in $CDCl_3$[176].

Following the same idea, cyclic compounds **163a** and **163b** were then synthesised using (R,R) diethyl L-tartrate and (S,S) diethyl D-tartrate, respectively. The ^{1}H NMR spectra were identical for these two molecules and were compared to a solution of the racemic mixture in $CDCl_3$. In this case, the ^{1}H NMR spectrum displayed a new set of peaks indicating the presence of a heterochiral cyclic assembly along with the homochiral species **(R,R)-163a** and **(S,S)-163b**. The ratio of these three cyclic assemblies was close to 1:1:1 (Figure 114)

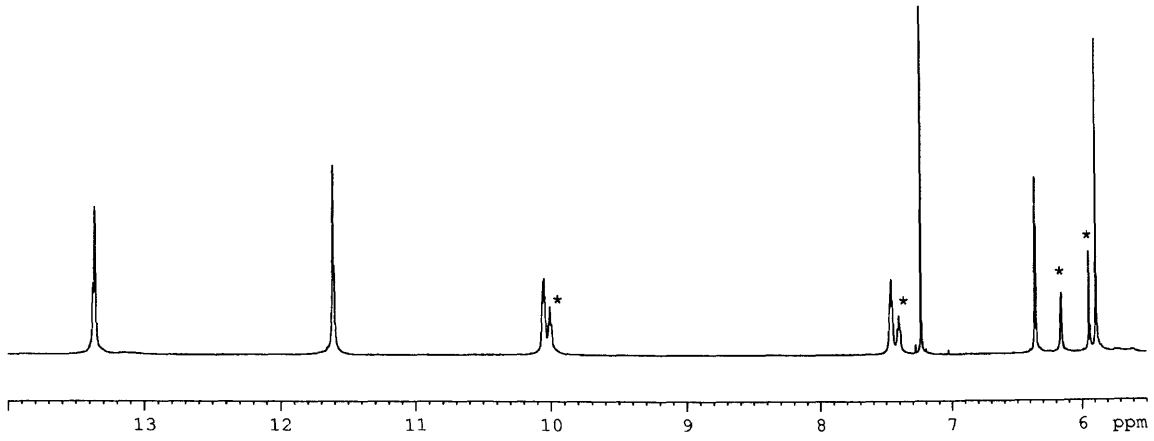

Figure 114: ^{1}H NMR spectrum of a racemic mixture of **163** in $CDCl_3$ at 298K. Asteriks denote peaks assigned to heterochiral cyclic assembly

The presence of heterochiral cyclic assembly in solution confirmed the fact that no enantioselective cyclisation was observed for **163**. Thus, there is no pronounced selectivity between homochiral and heterochiral cyclic species, although the cyclic dimer is very stable in solution. However, this result is not surprising since this kind of phenomenon usually takes place in the crystalline state.

4.4.3 Other Analogues of Cyclic Dimer 163

In order to gain a greater understanding of the preference for cyclisation, derivatives of compound **163** were synthesised using an analogous synthetic procedure as for **163**. Initially, a mimic compound of **163** was prepared, this time with the (2R,3R) butanediol as the chiral unit, and leading to compound **166** (Figure 115). Based on the NMR data the cyclic dimer was the only product isolated but was formed in a low yield (20%) reflecting the poor solubility of **166** in chloroform.

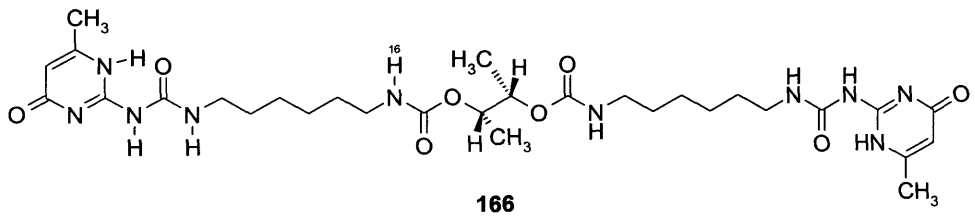

166

Figure 115: Structure of compound **166**

The ^{1}H NMR spectrum was very similar to that of **163** highlighting the presence of cyclic dimer in solution. The 16-H intramolecular hydrogen bonded proton was found this time at 7.13 ppm slightly shielded as compared to 7.63 ppm found in compound **163**. This result suggested that a change in the substituent on the chiral unit, from an ester to a methyl group, did not have a significant effect on the structure of the final molecule. In a different approach, the use of a ring substituent on the chiral unit, was explored. For this purpose, the synthesis of a chiral molecule possessing a crown ether (**167**) was carried out (Scheme 49).

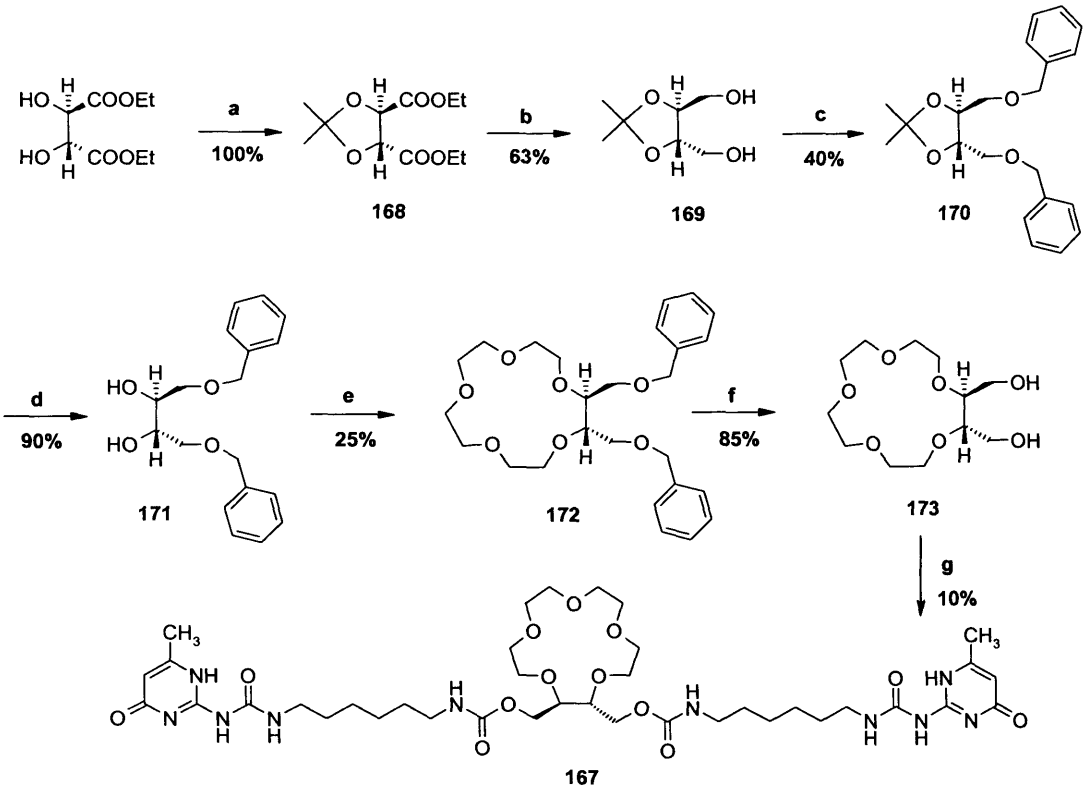

Reagents and conditions: **(a)** $(CH_3)_2CH(OMe)_2$, PTS, azeotrope, 100%; **(b)** $NaBH_4$, EtOH, 63%; **c**: NaH (60%), BnBr, THF, 40%; **(d)** HCl (1N), THF/MeOH,reflux, 90%; **(e)** NaH (60%), bis-tosylate, THF, 3d, reflux, 25%; **(f)** H_2, Pd/C, MeOH, 85%; **(g)**Isocyanate, $CHCl_3$, catalyst, reflux, 10%.

Scheme 49: Synthetic route towards compound **167**

Diethyl L-tartrate was protected using 2,2-dimethoxy propane to form dimethyl 2,3-*O*-isopropylidene L-tartrate **168** *via* the azeotropic removal of toluene-methanol in the presence of a *p*-toluenesulfonic acid catalyst.[178] The reaction was quantitative but trans esterification also occurred giving a mixture of diesters. However this was not a problem since the ester moieties were reduced in the next step. Compound **168** was reduced without further purification with the use of sodium borohydride in anhydrous ethanol and heating at reflux, to give 2,3-*O*-isopropylidene L-threitol **169** in 63% isolated yield.[179] Compound **169** was then protected using benzyl bromide affording

170 in 40% yield after purification.[180,181] Deprotection of the acetal group under acidic conditions gave **171** in 90% isolated yield. Compound **171** was then reacted with bis-toluene-4-sulfonic acid 2-{2-[2-(2-ethoxy)-ethoxy]-ethoxy}-ethylester[182] using sodium hydride in THF under reflux conditions for three days. Previous attempts using bis mesylate (PEG_4) were unsuccessful. This highlighted the fact that the tosylate was a better reagent for this reaction. Few examples have been described in the literature on the synthesis of "chiral" crown ethers, and the synthesis of compound **172** was reported in 50% yield.[183] Purification of **172** was a major problem: a first purification through a neutral alumina chromatography column (petroleum ether/propan-2-ol, 50 :1) was insufficient and a second column (flash silica) using ethylacetate as the eluent appeared to be more effective, however a third column in this system was necessary in order to obtain a pure fraction of compound **172** in only 25% yield. In the following step, the debenzylation of **172** using H_2 on Pd/C in MeOH at atmospheric pressure was carried out to afford **173** in 85% yield. The final step involved the reaction of 3 equivalents of isocyanate **131** (mentioned at the beginning of this chapter) with the free alcohol groups of compound **173** in chloroform. Tinbutyldilaurate was used as catalyst, under the same conditions as previously used for **163**. Due to poor solubility and the small quantities obtained, the separation of products was difficult to perform. From the materials obtained after separation, it was however clear from ^{1}H NMR that a cyclic structure was present, according to the distinctive chemical shifts. Traces of starting material (isocyanate) were also observed (Figure 116).

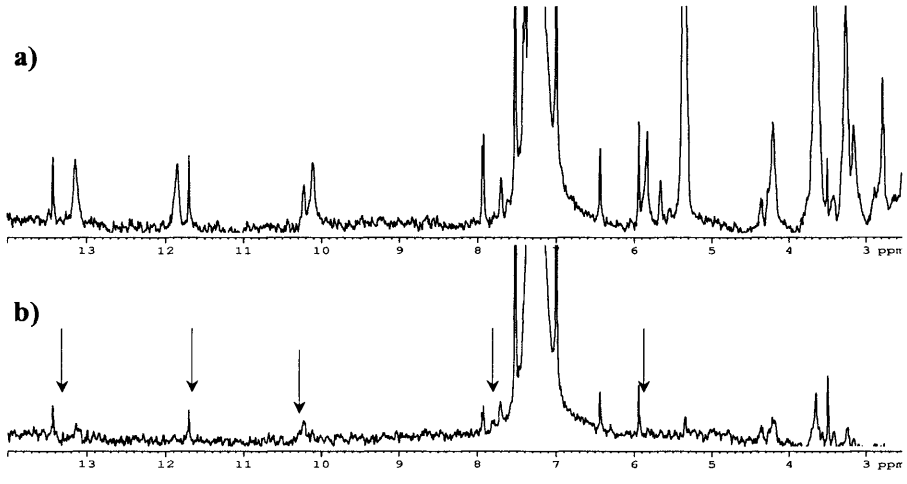

Figure 116: ^{1}H NMR spectra of compound **167** before (a) and after purification (b). The arrows indicate the peaks characteristic of the cyclic dimers.

Although the cyclic species were not as readily formed and easy to isolate after addition of the chiral unit, it was however interesting to observe that cyclisation still did occur despite the use of a sterically crowded diol. Also, with the C4 versus C2 chiral unit inserted little effect on the formation of cyclic species was observed. To assess whether the nature of the substituents might induce cyclisation, the synthesis of compound **174** was attempted from the isocyanate **131** and pinacol using the same reaction conditions as before (Figure 117). Here the small unit was non chiral and possessed four methyl groups.

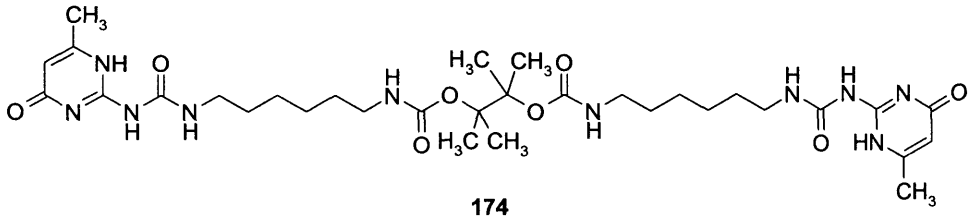

174

Figure 117: Structure of compound **174** incorporating pinacol chiral unit

Unfortunately the reaction only led to the monofunctional derivative **175**, which was probably due to steric reasons that prevent the reaction to proceed further.

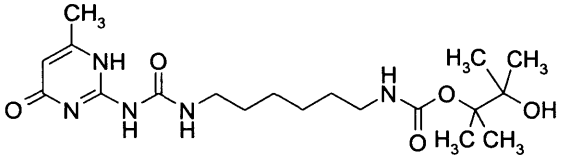

175

4.5 Synthesis of a Supramolecular Array with an Ester Linkage

In order to understand further the formation of the cyclic dimers, ureidopyrimidone derivatives were synthesised with the carbamate moiety replaced by an ester bond (**176,** Figure 118). This would avoid the formation of the intramolecular hydrogen bonding and may suppress the formation of a cyclic structure.

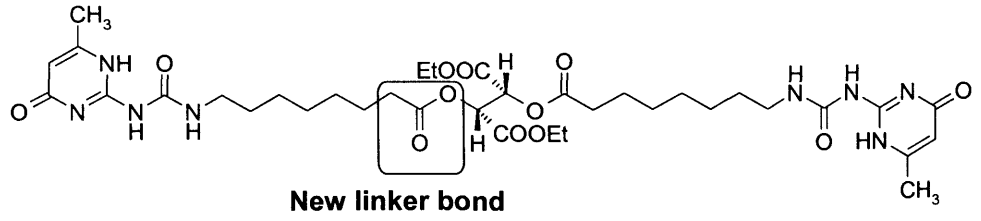

176

Figure 118: Synthesis of a bifunctional ureidopyrimidinone incorporating diethyl L-tartrate using ester linkage

4.5.1 Synthesis

Diethyl L-tartrate was reacted with carboxylic acid **177** (Scheme 51), which was previously synthesised in 50% yield *via* Boc protection of 8-aminooctanoic acid in CH_2Cl_2 (Scheme 50).[184]

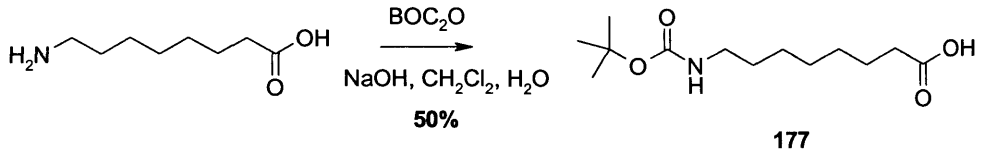

177

Scheme 50: Protection of primary amine with Boc protecting group

Compound **178** was obtained in 50% yield, using DCC as coupling agent, in the presence of DMAP in CH_2Cl_2. The yield was not particularly high, and further optimisation of the reaction could have certainly increased the yield. The amine was then deprotected using TFA in CH_2Cl_2 (1/1, v/v), which afforded the salt **179** in 95% yield. Finally, compound **179** was reacted with **139** in THF under reflux conditions for 16 h in the presence of triethylamine. The final product **176** was isolated in 80% yield.

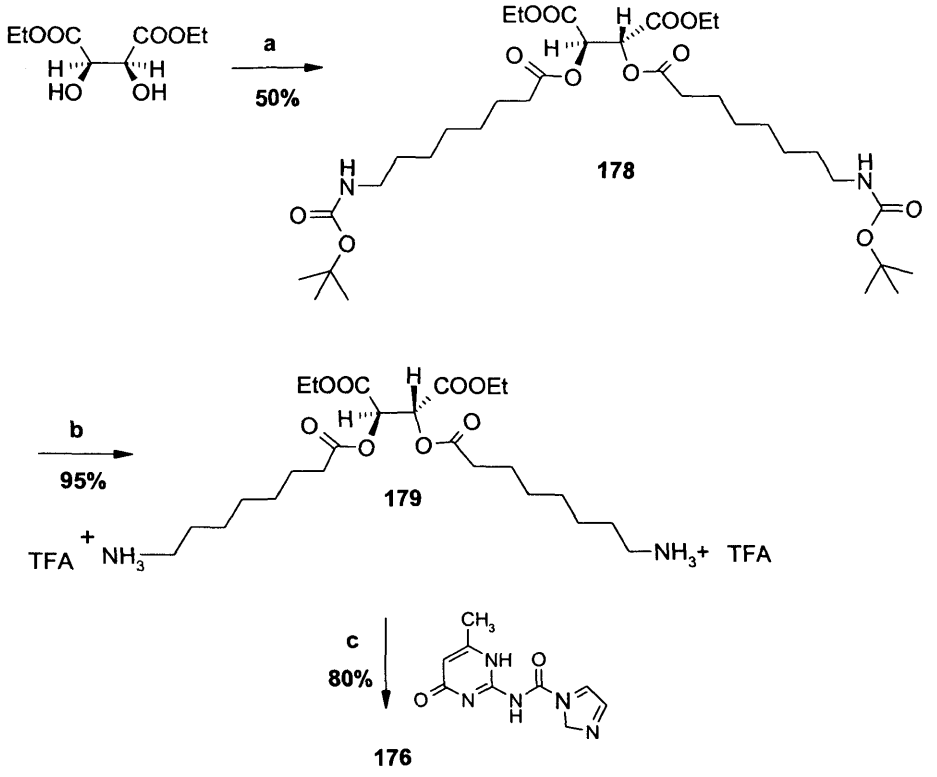

Reagents and conditions: (a) DCC, DMAP, CH_2Cl_2, 50%; (b) TFA, CH_2Cl_2, 95%; (c) Et_3N, THF, reflux, 80%.

Scheme 51: Synthetic route towards compound **176**

4.5.2 NMR studies

To identify the nature of the supramolecular structure, compound **176** was first studied by ^1H NMR spectroscopy in $CDCl_3$ (Figure 119). Diffusion measurements were also performed on a series of diluted samples (Table 30).

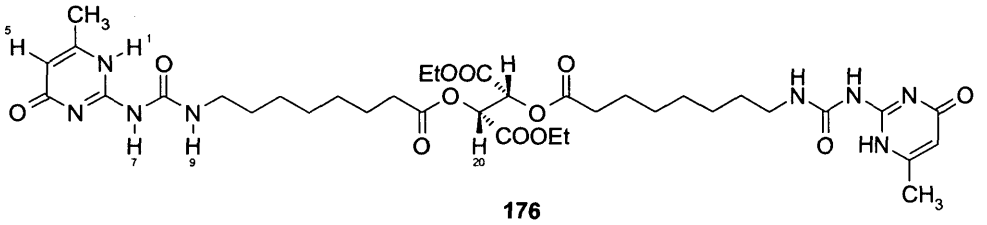

176

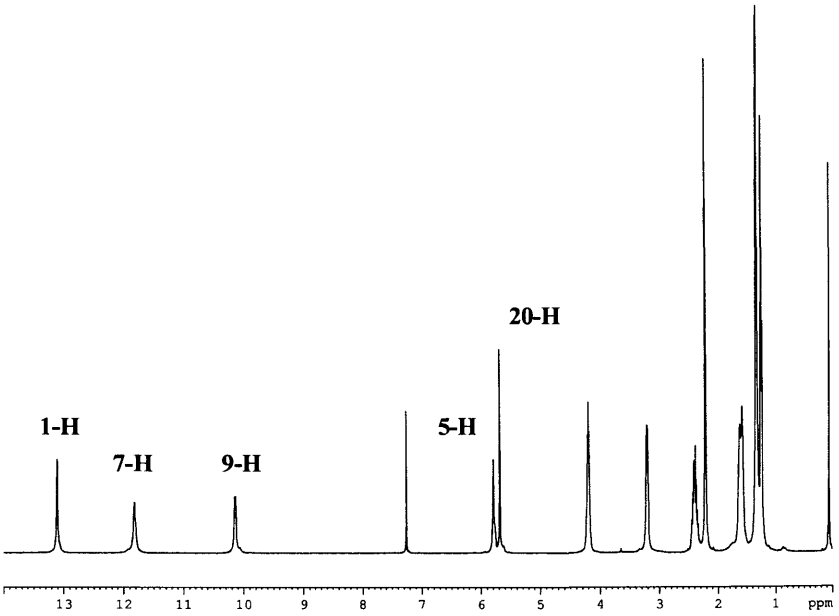

Figure 119: ^{1}H NMR spectrum for compound **176** ($CDCl_3$, 298K) and assignments of protons

Concentration (mM)	Diffusion (m^2/s)
135	1.8×10^{-10}
88	3.1×10^{-10}
41	3.8×10^{-10}
28	4.3×10^{-10}
10	4.8×10^{-10}

Table 30: Diffusion coefficient measurements as a function of concentration of **176** in $CDCl_3$ at 298 K.

These results showed a gradual and significant increase in the diffusion rate upon dilution, suggesting that smaller species had been formed. Since the molecular weight of **176** is almost identical to that of the cyclic structure **163**, a comparison of their diffusion rates was then possible. Interestingly, the cyclic dimer **163** has a diffusion coefficient of 4.5×10^{-10} m^2/s (10 mM solution in $CDCl_3$), which is close to those found for the diluted solution of **176** (10 mM). This data suggested that at low concentration mainly cyclic dimers were present. At higher concentrations (27-135 mM), a considerable slow down of diffusion was detected, which indicated the presence of high-molecular species (denoted as $(\mathbf{176})_{n>3}$). The observed decrease of D on increasing

the concentration can be explained either by the shift of the equilibrium between $(\mathbf{176})_2$ and $(\mathbf{176})_{n>3}$ towards $(\mathbf{176})_{n>3}$, or simply by the increase of n in $(\mathbf{176})_{n>3}$ on increasing the concentration.

In addition, the ^{1}H NMR spectroscopic study revealed some unusual behaviour. After preparation of the sample (10 mM), the ^{1}H NMR spectrum showed four distinct peaks in the region 5.5-6.0 ppm, characteristics of 5-H and 19-H (CH tartrate unit). When the sample was run after 16 hours, mainly two peaks were observed in the same spectral region (Figure 120). No further changes were observed after longer delays.

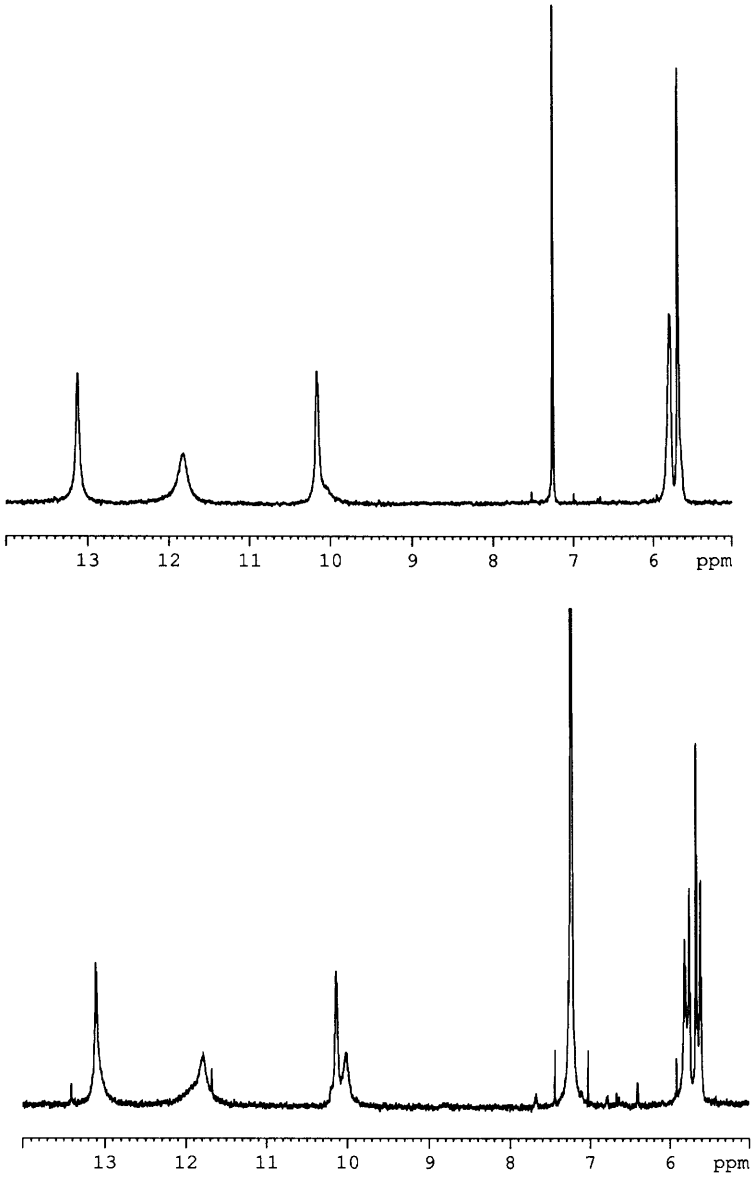

Figure 120: ^{1}H NMR spectrum of **176** in $CDCl_3$ prepared by dilution of the 28 mM solution. Bottom: 20 minutes after dilution. Top: 16 hours after dilution. Both spectra were recorded at 298 K.

Surprisingly the chemical shifts were the same as those for the concentrated sample (135 mM). From these observations it appeared that the exchange between the cyclic dimer and $(\mathbf{176})_{n>3}$ was not at its equilibrium in a freshly diluted sample, i.e., the equilibration process is rather slow. As shown in Table 31, ^{1}H NMR chemical shifts for compound **176** are very close to those found in polymer **66** and dimer **114.**

protons	Compound 176 (135 mM)	Cyclic dimer 163	Linear polymer 66	4-keto dimer 114
1-H	13.11	13.41	13.09	13.13
5-H	5.80	6.41	5.80	5.81
7-H	11.83	11.68	11.81	11.85
9-H	10.15	10.21	10.09	10.14
10-H	3.21	2.78 & 3.68	3.20	3.23
16-H	2.38 & 2.41 (CH_2)	7.68 (NH)	4.94 (NH)	-
20-H	5.69	5.92	-	-

Table 31: Comparison of ^{1}H chemical shifts between compound **176**, and cyclic dimer **163** and linear polymer **66**

The fact that the chemical shifts are identical at low and high concentrations tends to suggest that the same type of species predominate in both solutions. However, based on the diffusion measurements, it is clear that there is dissociation on dilution into smaller assemblies. This behaviour could be explained by the formation of 12 hydrogen bonded cyclic dimer assemblies at low concentrations, which would lead to the proton chemical shifts close or almost identical to those found in the linear polymer.

Conclusions

The formation of high-molecular species with n>3 is favoured when the carbamate bond of **163** is replaced by the ester linkage in **176**. However, due to the flexibility of the alkyl chain, there is a possibility of forming a twelve hydrogen bonded cyclic dimer of **176**, which is predominant at low concentrations in $CDCl_3$. Such behaviour of **176** is common and has been described for other bifunctional Upy systems. From the comparison of **163** and **176**, it is apparent that the presence of intramolecular hydrogen bonds in **163** is critical for the formation of highly stable cyclic dimers, even in the presence of long and flexible linkers. The example or **163** and **176** presented here clearly show how the 'cyclic dimer/polymer' equilibrium can be controlled by only minor adjustments of the structure.

Chapter V

5 The Design of a New DDAA Array

5.1 Introduction

The design of linear multiple hydrogen bonding arrays has been a continuing challenge in the field of supramolecular self-assembly. Particular attention has recently been paid to systems capable of forming strong quadruple hydrogen bonds.[100] Meijer *et al.* have made a significant contribution to this area with the synthesis of strong self-complimentary DDAA and DADA moieties based on ureidopyrimidinones and ureidotriazines. Since the first reports, there have been numerous applications of these arrays in supramolecular polymers and materials synthesis[126] (see Chapter I). Zimmerman *et al.* have also made a significant contribution to the field with the synthesis of a very stable DDAA module, which dimerises regardless of its tautomeric form[134] (see Chapter I). Recently, they have also reviewed the use of heterocyclic compounds in the synthesis of stable quadruple hydrogen bonded dimers *via* self-assembly processes.[68] However, the development of linear supramolecular polymers based on hydrogen bonding units has been mainly restricted to the Upy modules. Therefore, further advances in the field of supramolecular materials require the development of new hydrogen bonding modules. Hence, the synthesis of a new DDAA unit combining rigidity, accessibility and strength has been investigated and the strategy adopted is detailed in this chapter.

5.1.1 From Nature to Molecular Design

Pyrimidines and their various derivatives have been well studied throughout the past century due to their diverse pharmacological properties. In self-assembly they offer great potential due to the presence of heteroatoms acting as donors and acceptors for hydrogen bonding. Inspired by their presence in DNA base pairs, an interesting approach emerged in this work, which uses cytosine as starting point for the synthesis of a novel DDAA motif. Cytosine or 4-amino-1*H* pyrimidin-2-one, was first reported in 1894 when isolated from the calf thymus tissues, and its structure was confirmed in 1903. Since then, an impressive number of derivatives of cytosine and cytidine have

been synthesised for the use in recognition processes, the transfer of genetic information and new therapeutic agents (Figure 121).[185]

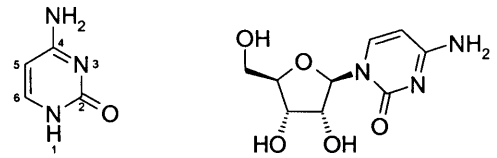

Figure 121: Structure of cytosine and cytidine

5.1.2 The DDAA Building Block

As illustrated in Figure 122, both cytosine and 2-amino-6-methyl-1*H*-pyrimidin-4-one display the same AAD motif in their structures and the reaction of these molecules with an isocyanate leads to the formation of the AADD array. Interestingly, among the wide variety of cytosine analogues encountered in the literature, very few examples have described the functionalisation of the primary amine. This is not so surprising since the amine, a donating group for hydrogen bonding, often plays a major role within the recognition process.

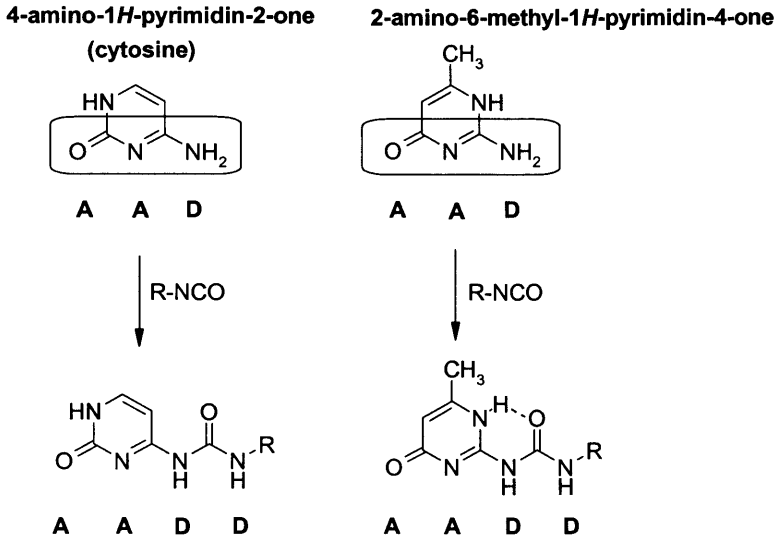

Figure 122: Two approaches to form a DDAA array

The functionalisation of cytosine to give the DDAA array appears to be a straightforward strategy at first sight. However, in reality these heterocyclic compounds

are often more complex due to the presence of a variety of tautomeric forms and conformers in solution and in the solid state which can obscure the formation of the linear DDAA array.

5.1.3 Tautomers

One of the major drawbacks encountered in the design of quadruple hydrogen bonded arrays based on heteroatoms is the presence of several tautomeric forms. As previously described for the Upy systems, tautomeric species can affect dramatically the dimerisation process and are influenced by various factors such as polarity of the solvent, temperature or concentration. One of the goals in the synthesis of new arrays is therefore to limit as much as possible their presence.

Pyrimidines in particular can adopt several tautomeric forms.[186,187] Cytosine has been shown to exist in six different tautomers (Figure 123) with C_1 or C_3 being the most predominant forms in solution.

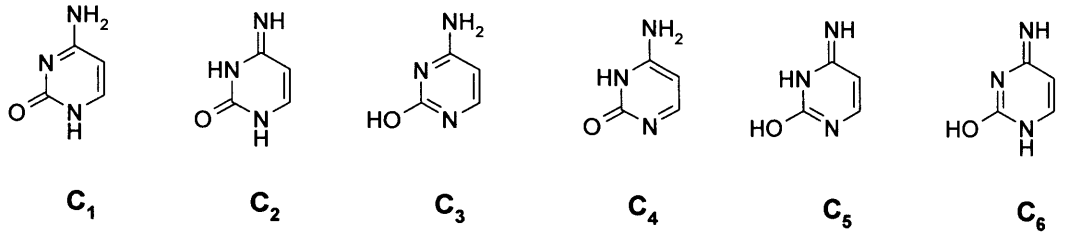

Figure 123: Structures of the 6 tautomeric forms found in cytosine.

When cytosine is functionalised with an isocyanate at the primary amine, the number of tautomers decreases to three, labelled as **180a**, **180b** and **180c** in Figure 124 (a). One is a [2]-keto form (**180a**) that can self-dimerise *via* a DDAA array while the second and third forms can only dimerise with their complimentary arrays such as ADAA and DAAA, respectively, for **180b** and **180c**. The presence of the DADD array is an attractive feature since only few groups have reported its synthesis to date and it is unknown whether the DADD motif will be favoured in solution in the presence of its complimentary ADAA pair.

More interestingly, functionalisation at the N-1 position with a substituent R_2, should result in the formation of compound **181** existing exclusively as the AADD tautomer (Figure 124 (b)). The presence of a single tautomeric form in solution increases

significantly the potential of this array for the use in supramolecular devices and may enhance dimerisation properties. The synthesis and characterisation of analogues of **180** were therefore explored and are described in this chapter.

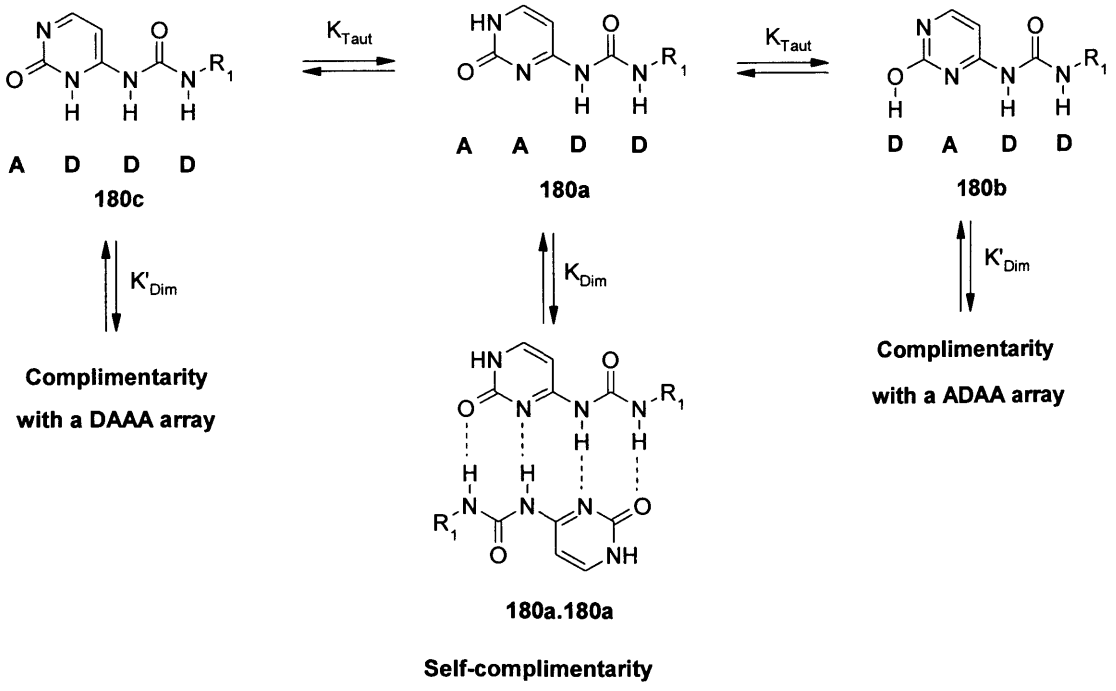

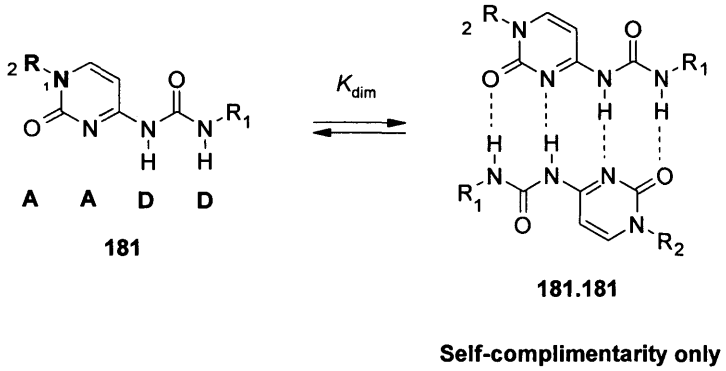

Figure 124: (a) three tautomeric forms for compound **180,** (b) formation of the self-complimentary DDAA array exclusively

In the first instance, conformational aspects of molecule **181** were examined closely in order to assess their possible influence on the dimerisation process.

5.1.4 Conformers

Whilst the geometry of the Upy unit is maintained through the formation of intramolecular hydrogen bonding between 1-H and O-8, there is a possibility of rotation about the C-4-N-7 bond. A lack of controlled geometry at the DDAA hydrogen bonding region could inevitably have serious consequences on the formation and strength of a new DDAA array.

The rigidity in the structure of N^4-acetyl cytidine has been previously studied.[188,189,190] They indicated that the N^4-acetyl group should be proximal to C-5, therefore leading to a preference for conformer **A**. Indeed, the repulsive interactions between N-3 and O-8 found in conformer **B** are expected to destabilise the system, and consequently shift the equilibrium towards **A** (Figure 125).

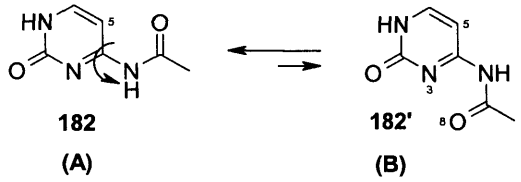

Figure 125: Two possible conformers for compound **182**

Compound **181**, which possesses a urea fragment at C-4 position can also exhibit the same type of rotations, and as indicated above conformer **A** should be favoured over **B**. Interestingly, further rotations along the CO-NH bond lead to a conformer **C** (**181'**) stabilised *via* the formation of an intramolecular hydrogen bond between 9-H and N-3 (Figure 126).

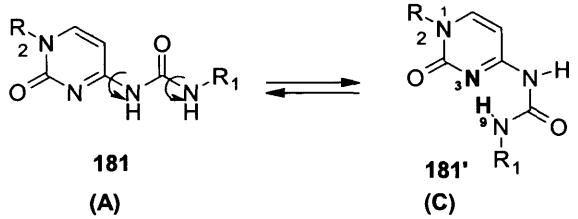

Figure 126: Representation of the unfolded (left) and folded (right) conformers of **181**

A similar type of equilibrium between the two conformers (**A**) and (**C**) has been previously discussed for some pyridyl urea derivatives. Indeed, Zimmerman *et al.* have

reported the dimerisation of a naphthyridinyl urea **183** with a K_{dim} value of 259 M^{-1} (Figure 127).[191] This low value was attributed to various factors including the fact that the linear array **183** is in equilibrium with its conformer **183'** which then needs to unfold in order to dimerise through a DDAA array. It was also found that **183'** could dimerise *via* two hydrogen bonds to form the dimer **(183'.183')** in solution.

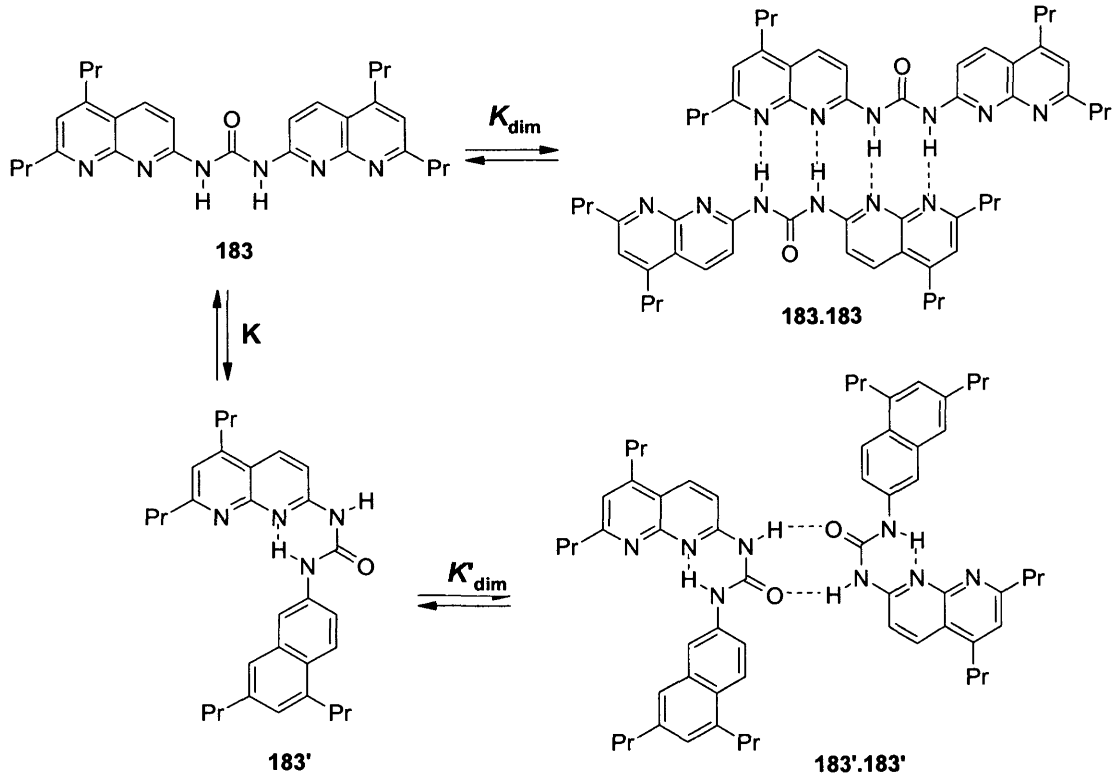

Figure 127: Representation of conformers **183** and **183'** and their dimerisation into **183.183** and **183'.183'**, respectively

It was also shown that bis-ureido naphthyridines **184** exist exclusively in the folded conformer **C (184')** in the solid state and give oligomeric association **(184'.184')$_n$** in the $CDCl_3$ solution (Figure 128).

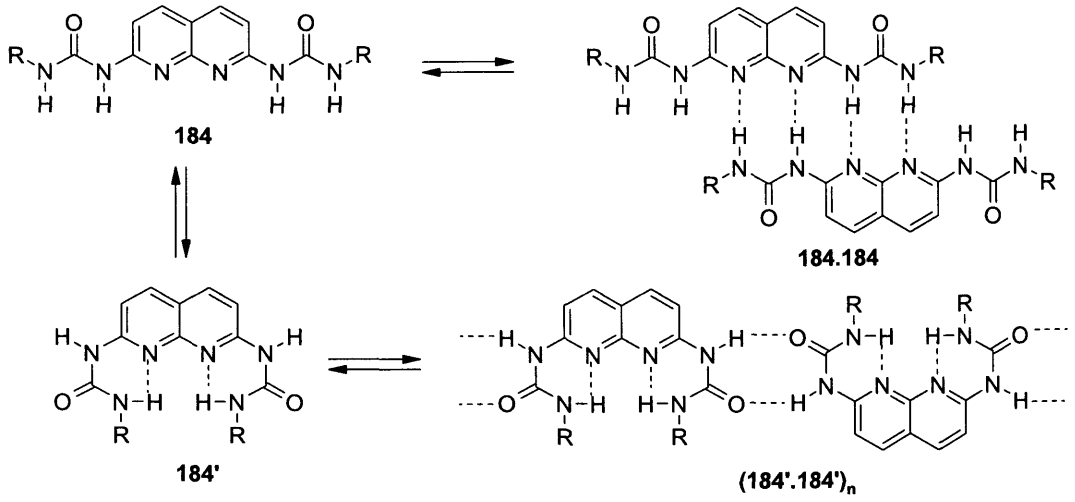

Figure 128: Dimer of **184** and oligomer of **184'**

More recently, Lüning *et al.* have reported the same phenomenon for pyridyl and naphthapyridyl ureas such as compounds **185** and **186**. In both cases a folded conformer (**C**) was observed in the crystal structure and in solution (Figure 129).[106]

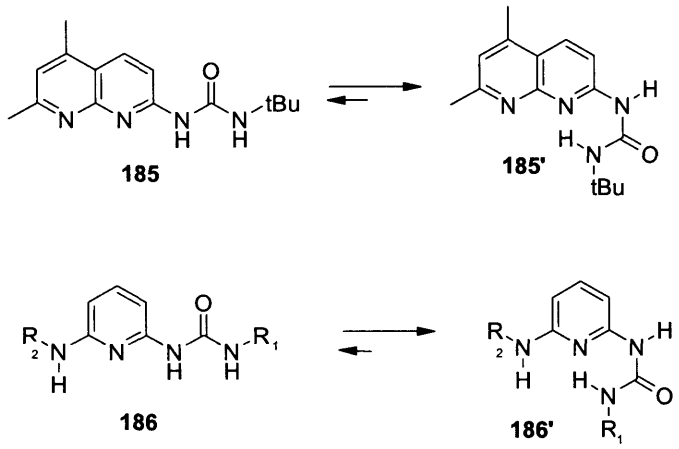

Figure 129: Conformers for compounds **185** and **186**

In all the examples above, the presence of the intramolecular hydrogen bond in the folded structure decreases the dimerisation constant of the quadruple linear array due to the energy cost during the unfolding process. Preliminary calculations in the gas phase using the MMX force field showed that in the case of monomeric cytosine **181** with R_2 = R_1 = Me the folded conformer is more stable than the unfolded conformer by approximately 7 kJ/mol. Similar calculations of the dimeric forms showed that the

quadruple hydrogen bonded dimer of the unfolded conformer is more stable than the double hydrogen bonded dimer of the folded conformer by approximately 14 kJ/mol. Calculated geometries of the two dimeric forms are shown in Figure 130.

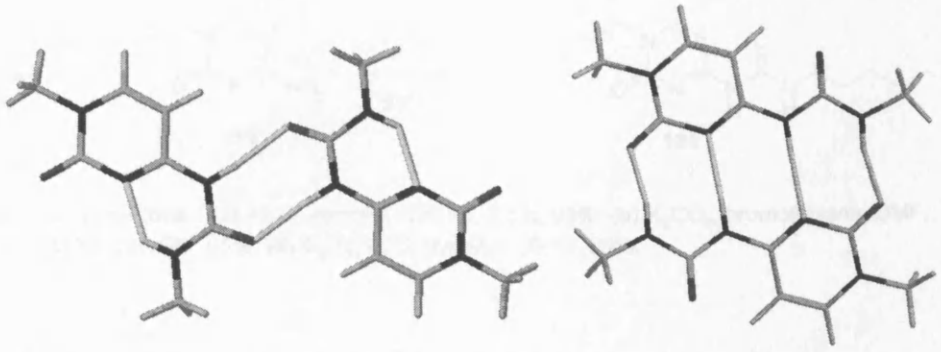

Figure 130: Calculated geometries of dimers of the folded (left) and unfolded (right) conformers. Hydrogen bonds are shown in yellow.

In summary, in the case of compound **181**, a derivative of cytosine, the possibility of a folded conformer may interfere with the formation of the linear DDAA array. Nevertheless, the synthesis of cytosine analogues was still explored, with the expectation that overall the quadruple hydrogen bonding of the unfolded conformer may be more stable than the double hydrogen bonding of the folded conformer.

5.2 Synthesis of Compound 181

Initially the synthesis of compound **181**, where R = C_6H_{13}, was explored (Figure 131 and Scheme 52).

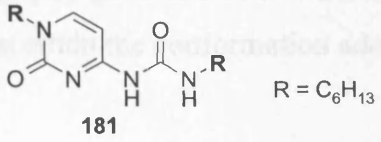

181

Figure 131: Targeted compound

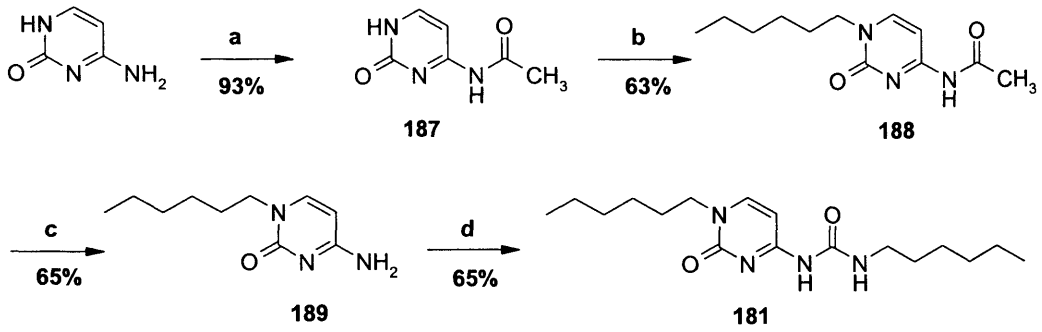

Reagents and conditions : **(a)** Ac_2O, pyridine, 125 °C, 2.5 h, 93%; **(b)** K_2CO_3, bromohexane, DMF, reflux, 63%; **(c)** NH_3/MeOH, 65%; **(d)** $C_6H_{13}NCO$, pyridine, 90 °C, 65%.

Scheme 52: Synthetic strategy towards compound **181**

As outlined in Scheme 52, the primary amine of cytosine was first protected using acetic anhydride in pyridine to give compound **187** in 93% yield.[192] Compound **187** was then reacted with bromohexane in DMF in the presence of anhydride potassium carbonate giving **188** in a 63% isolated yield.[193] The use of sodium hydride instead of potassium carbonate led to reduction in the yield to 20%. The substitution at N-1 has been described for the synthesis of cytidine analogues, and in many cases the yield can be quite low and is dependant on the solubility and reactivity of the electrophile.[194] Compound **188** was then deprotected in a sealed tube containing a concentrated solution of ammonia in methanol to give the amine **189** in 65% yield after purification.[195] Reaction with hexyl isocyanate in dry pyridine at 90 °C for 16 h, followed by the addition of hexane led to precipitation of crude compound **181**. Further purification using flash silica gel chromatography gave **181** as a white solid in 65% yield. Crystals of **181** were grown in order to ascertain the conformation adopted in the solid state.

5.3 Study of Compound 181 in the Solid State

Compound **181** was crystallised from chloroform as white needles. Single crystal X-ray analysis revealed a packed structure in the unit cell composed of dimer layers, spaced from each other by approximately 3.1 Å (distance between Z+1 and Z0 planes, Figure 132). See as well Appendix B for more details.

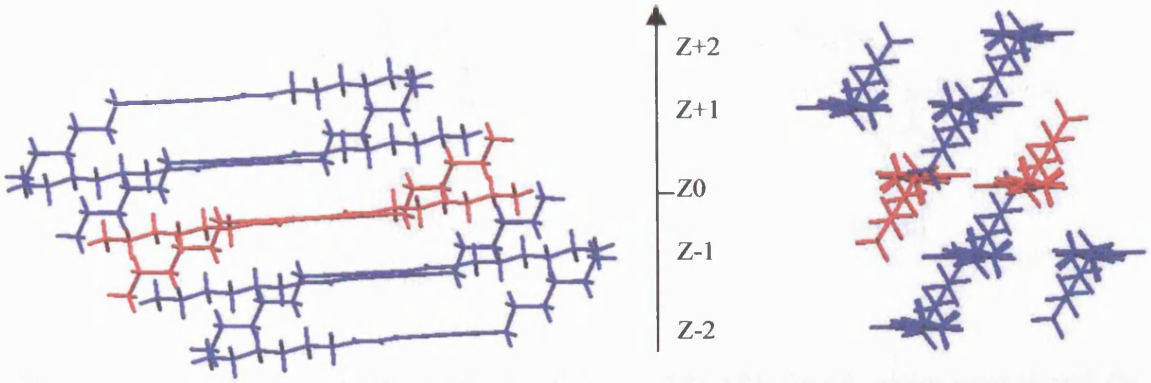

a) b)

Figure 132: a) packed structure in the unit cell, b) view along the x-axis

5.3.1 Dimer in the Plane Z0

This dimer coloured in red (Figure 132) is maintained through quadruple hydrogen bonding (Figure 133). The crystal structure clearly identified the formation of a linear DDAA motif in the solid state, and no traces of the folded conformer **C (181',** Figure 134) was observed.

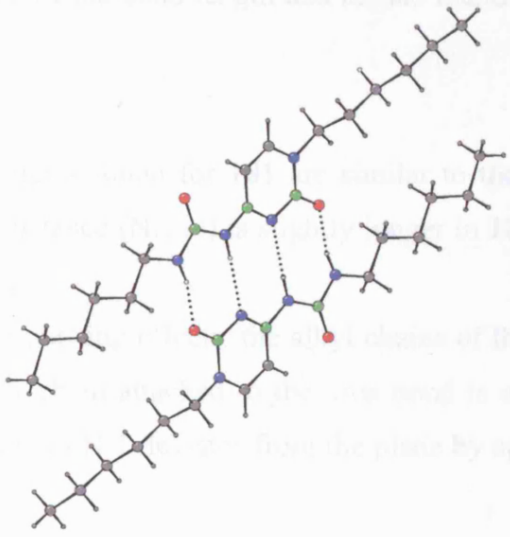

Figure 133: Quadruple hydrogen bonding (dotted lines) in the X-ray structure of dimer **181.181**

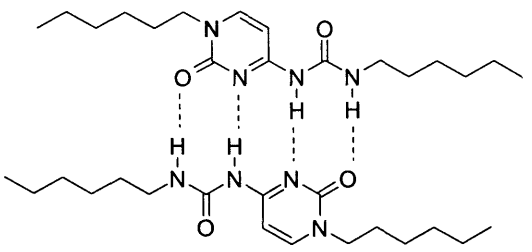

181.181

181' (C)

Figure 134: Schematic representation of dimer **181.181** found in the crystal and the folded conformer **181'** absent in the crystal structure.

As observed in the Upy system, the dimer deviates slightly from linearity since the outer hydrogen bond N-H...O (1.857 Å) is shorter than the inner one N-H...N (2.258 Å) (Table 32).

dimer	**D (d), Å**	θ, °	**Upy**	**D (Å)**	θ,°
N...N (N-H...N)	3.138 (2.258)	173.3	**N...N**	2.966	175.0
N...O (N-H...O)	2.737 (1.857)	167.7	**N...O**	2.757	163.0

Table 32: Comparison of the bond length and angles found in dimer **181.181** and in Upy

The bond lengths and angles found for **181** are similar to those reported for the Upy dimer.[111] However, the distance (N...N) is slightly longer in **181** which could influence the dimerisation constant.

Due to steric and crystal packing effects, the alkyl chains of the unit are not parallel to each other. While the C_6 chain attached to the urea bond is in the plane of the dimer unit, the C_6 chain attached to N-1 deviates from the plane by approximately 70° (Figure 135).

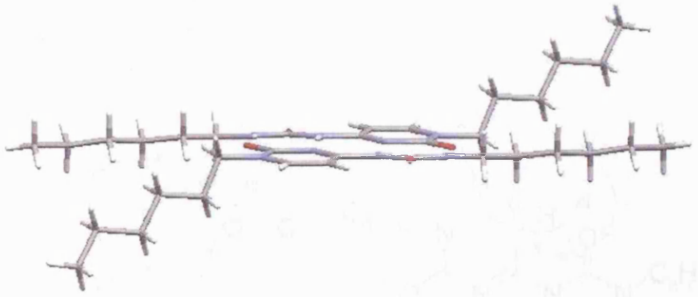

Figure 135: Side view of the **181.181** dimer highlighting the orientation of the alkyl side chains

Interestingly, the X-ray structure reveals that the side chain urea carbonyl bond and the C5-H bond directions are nearly in the same plane. The measured dihedral angle C8=O…H-C5 is ca. 13°. In principle, such geometry is in favour of a C-H…O type of hydrogen bonding (Figure 136).

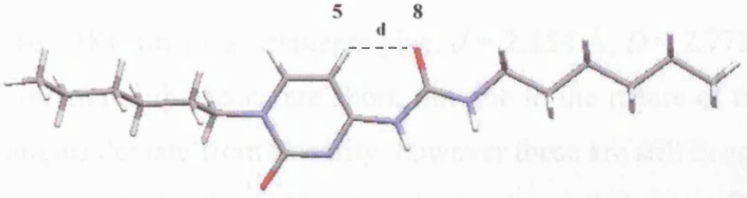

Figure 136: The view of **181** highlighting the proximity of O-8 and 5-H. The indicated distance *d* is 2.15 Å

In general, since the electronegativity of carbon is slightly greater than that of hydrogen, the C-H group may in principle act as a weak hydrogen bond donor, especially in the vicinity of a strong acceptor. This was recognised in a review by Hunter in 1947 and later by Allerhand and Schleger (1963). Sutor surveyed the crystal structures in which the C…O separations are less than 3.3 Å and suggested to view these as hydrogen bonded separations.[196] Despite scepticism in the early 1960s in response to Sutor's proposition, the existence of the C-H…O hydrogen bond is now well established. However, because this interaction is rather weak, a set of geometrical requirements has been suggested for the identification of the C-H…O hydrogen bonds. The typical

convention for the representation of the lengths (*d* and *D*) and angles (θ and φ) is shown below (Figure 137).[197]

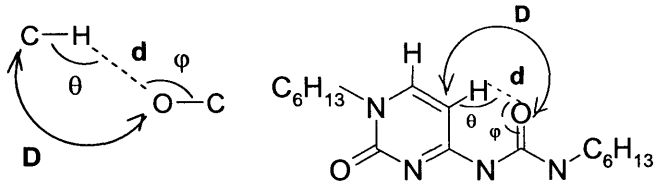

Figure 137: Geometrical parameters for the characterisation of the C-H...O hydrogen bond

While evaluating individual hydrogen bonds, the preference is given to those contacts, which occur at short distances (2.0 Å < *d* < 2.3 Å) and have nearly linear geometries (150° < θ < 180°). However, it has been shown that θ can be lower than 150°, but should be greater than 110° in order to be considered as a hydrogen bond. In general, *D* values span the range of 3.0 - 4.0 Å.

For the dimer **181.181**, the measurements give: *d* = 2.154 Å, *D* = 2.773 Å, θ = 121.7°, φ = 103.2°. The measured distances are short, but due to the nature of the intramolecular geometry the angles deviate from linearity, however these are still in agreement with the geometric requirements for the C-H...O hydrogen bond definition. This data suggests that a weak C-H...O interaction is indeed present. In analogy with the N-H...O intramolecular hydrogen bonding in 4-keto Upy's (Chapter II), the C-H...O interaction may stabilise the unfolded conformation, hence assisting the formation of the DDAA type of dimer.

5.3.1.1 *Study of the Crystal Packing*

Assessment of the crystal packing is useful for understanding the arrangement of molecules in the solid state and the non-covalent interactions that maintain the three dimensional structure.[198] Hence, the consideration of the crystal structure is further extended to the Z+1 plane (Figure 131).

Plane Z+1

The plane Z+1 gives information on the arrangement between the quadruple hydrogen bonded dimers. These units are repeated in layers separated by only 3.1Å. This suggested the presence of intermolecular interactions between the dimer units. Figure 138 shows the Z+1 plane of the packed structure in the unit cell where dotted lines indicate the quadruple hydrogen bonds when the structure is extended in the plane direction. A schematic representation of the two dimers is also drawn in Figure 138.

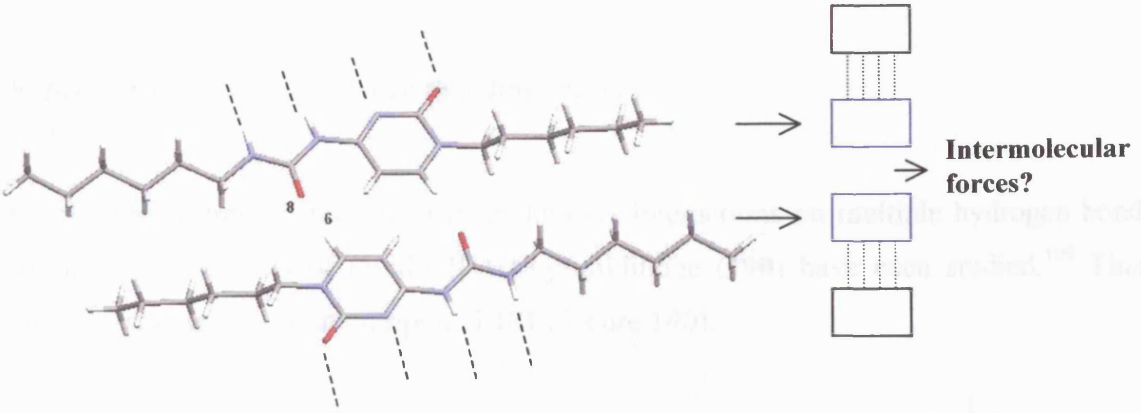

Figure 138: View of two molecules of **181** in the layer Z+1

The crystallographic data suggested a weak CH…O hydrogen bond may exist between O-8 and H-6, since the measured distances and angles were: d = 2.236 Å, D = 3.165 Å, θ = 165.7°, φ = 162° for the C6-H…O=C8. The short distances combined with a linear geometry indicated that these weak hydrogen bonds could be significant for the organisation of the crystal motif.

5.3.2 Interactions Between the Layers

In many examples, the arrangement of a crystal into layers strongly suggests the presence of interactions between them, such as π-stacking, especially when aromatic systems are present. The distance between two layers in the crystal structure of compound **181**, is approximately 3.1 Å, a short distance that is in favour of stacking interactions in the solid state (Figure 139).

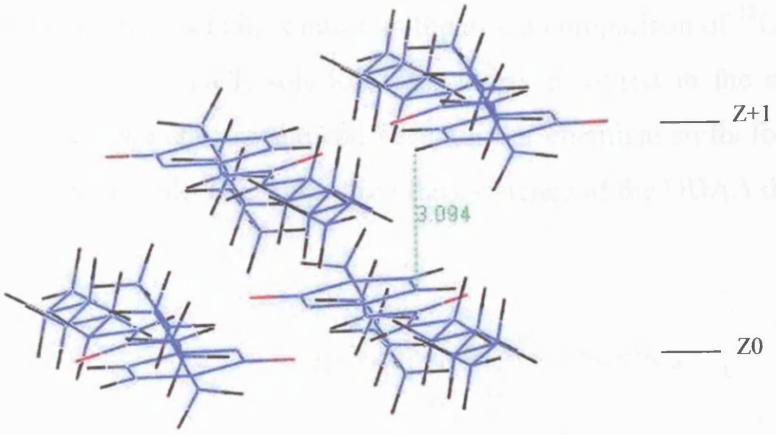

Figure 139: Distances between two dimer layers

On a relevant note, d the effect of π-stacking interactions on multiple hydrogen bond formation for dimers of ureido-4[1H]-pyrimidinone (**190**) have been studied.[199] This DDAA array is similar to compound **181** (Figure 140).

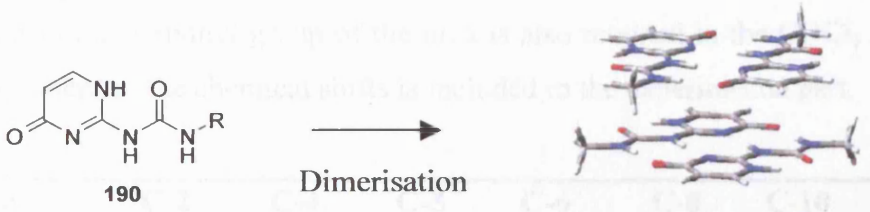

Figure 140: π-stacking between two Upy dimers

Results from DFT calculations revealed that π-stacking exists in such systems and even strengthens the hydrogen bonds in multiple hydrogen bonded dimers.[199] This observation has already been made in the DNA, where stacking interactions between adjacent base pairs provide additional stability for the helical structure.[200]

To conclude, the presence of a linear quadruple hydrogen bonded dimer has been revealed in the solid state. The layered arrangement of these dimers suggests the formation of additional non-covalent interactions such as stacking interactions as well as intra-and intermolecular C-H…O hydrogen bonds.

Although the X-ray crystallographic analysis is a valuable tool for the characterisation of the supramolecular systems, the conformational and hydrogen bonding preferences in

solution may be different from that in the solid state. One simple way of assessing the structure of **181** (Figure 141) in solution is the direct comparison of ^{13}C NMR chemical shifts measured in the $CDCl_3$ solution with those measured in the solid state. Both solution and solid-state spectra showed very similar chemical shifts for the carbons of the cytosine moiety (Table 33), suggesting the existence of the DDAA dimer in $CDCl_3$.

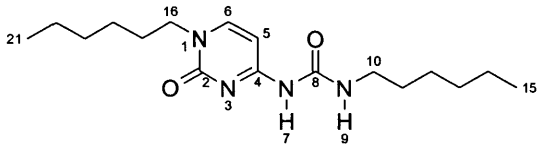

Figure 141: Compound **181** with atom numbering

In particular, carbon C-2, which is in close proximity of the quadruple hydrogen bonding system, has a distinctive chemical shift at 157.2 ppm in solution and 157.4 ppm in the solid state, in agreement with the DDAA dimer. The chemical shift for C-5 at 97.25 ppm in solution and 96.3 ppm in the solid state suggests that the close proximity of this carbon to the carbonyl group of the urea is also retained in the $CDCl_3$ solution. The full assignment of the chemical shifts is included in the experimental part.

δ_C/ppm	C-2	C-4	C-5	C-6	C-8	C-10	C-16
$CDCl_3$ (250 mM)	**157.2**	164.9	**97.3**	146.6	154.3	40.1	50.7
Solid State	**157.4**	165.7	**96.3**	150.1	155.1	40.8	49.3

Table 33: Comparison of ^{13}C chemical shifts in $CDCl_3$ and in the solid state

In addition, solid-state ^{15}N NMR chemical shifts were also measured. Using assignments of ^{15}N resonances for compound **114** (Chapter II), peaks of **181** at -280.9, -253.8, -223.9 and -163.8 ppm (relative to $MeNO_2$) were assigned to N-9, N-7, N-1 and N-3, respectively. This assignment was further confirmed by solution ^{1}H, ^{15}N HMQC and HMBC NMR spectra of **181** in the concentrated $CDCl_3$ solution, in which three ^{15}N peaks at -282.9 (N-9), -254.0 (N-7) and -225.8 (N-1) were detected.

When compound **181** is dissolved in a solvent of relatively low polarity, such as deuterated chloroform, it is likely that the secondary interactions that persist in solution

will be the strongest, in this case the quadruple hydrogen bonds. Weaker intermolecular close contacts within the crystal such as C-H...O and stacking interactions are likely to be broken completely on dissolving. With regard to the intramolecular C-H...O bond found in the solid state, further NMR studies of **181** suggested that this interaction is retained in the $CDCl_3$ solution (see below).

5.3.3 Proton NMR Chemical Shifts

The ^1H NMR spectrum shows the two hydrogen bonded protons 7-H and 9-H at 10.9 ppm and 9.0 ppm, respectively. In the Upy dimer, 7-H and 9-H were shifted further downfield, resonating at 11.8 ppm and 10.1 ppm, respectively. Based on the well known correlation between the proton chemical shift and the strength of the hydrogen bonding, this comparison of chemical shifts suggest that the strength of the hydrogen bonding may be weaker in the cytosine dimer compared to that in the Upy dimer. Interestingly, proton 5-H is strongly deshielded with a chemical shift at 7.54 ppm. By comparison, the chemical shift at 5-H in compound **186'** (Figure 142), which adopts a folded conformation, was found at 6.06 ppm indicating that proton 5-H is close to the carbonyl group in the predominant conformation of **181** in $CDCl_3$ and that the weak intramolecular C-H...O interaction identified in the solid state might persist in the $CDCl_3$ solution.

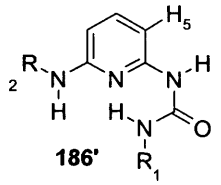

186'

Figure 142: Compound **186'** in its folded conformation

Further examination of the ^{1}H NMR spectrum revealed the presence of broad lines of very small intensity at 9.63, 9.42 and 6.17 ppm as highlighted in Figure 143.

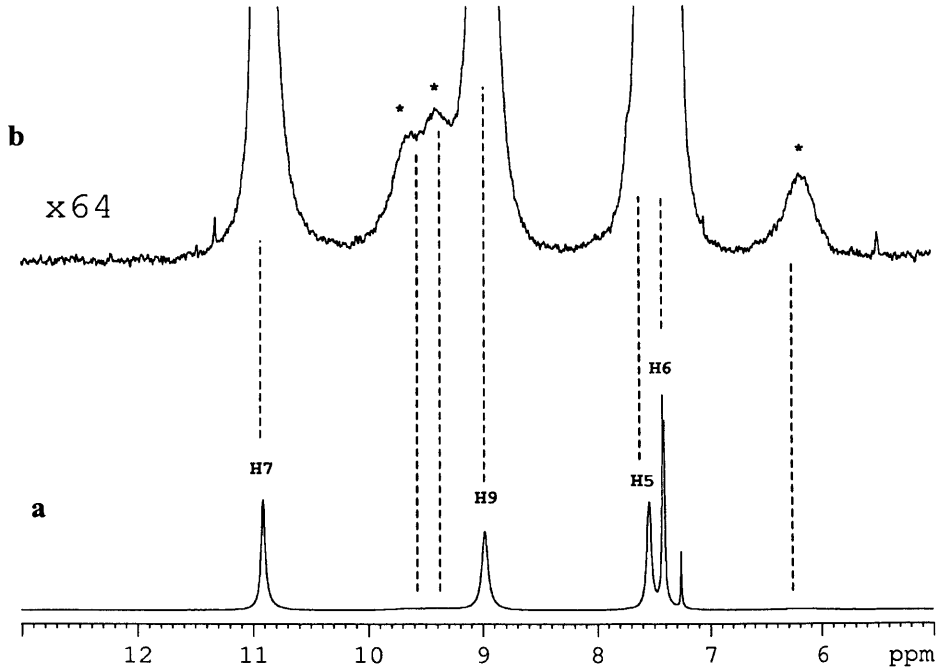

Figure 143: (a) ^{1}H NMR spectrum of the 200 mM solution of **181** in $CDCl_3$ at 298 K (b) The same spectrum with a 64-fold increase of intensity

In order to establish the origin of these peaks, a 30 mM solution of **181** in $CDCl_3$ was studied at different temperatures, since the observed line broadenings at 298 K may be caused by an exchange process (Figure 144).

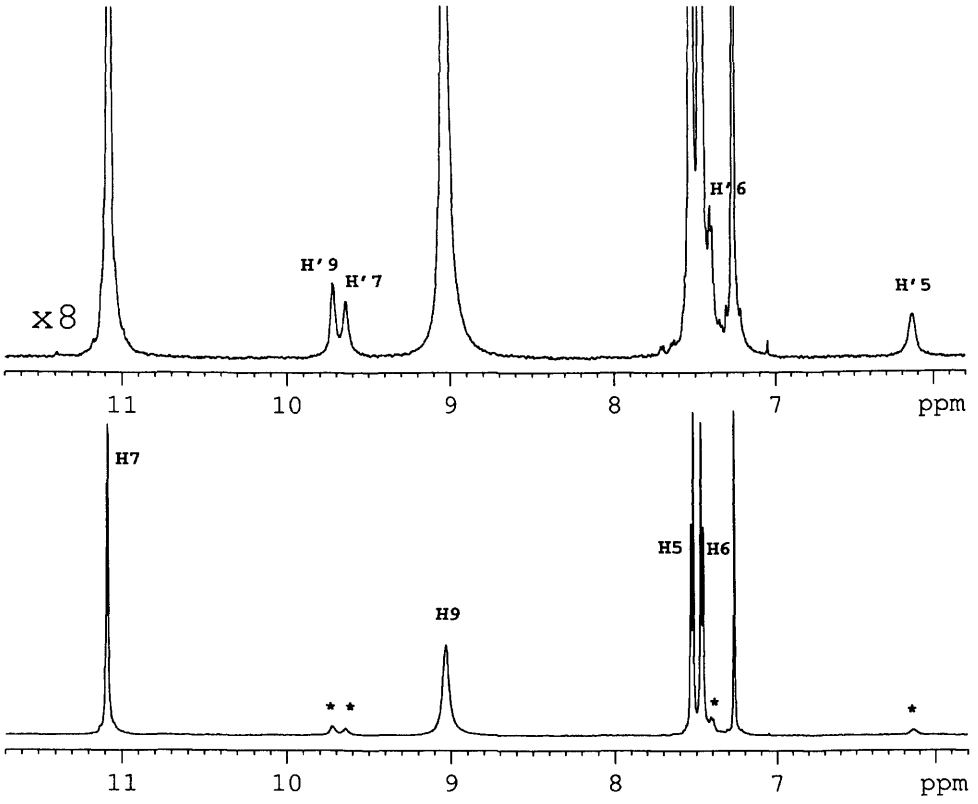

Figure 144: Bottom: ^{1}H NMR spectrum of the 30 mM solution of **181** in $CDCl_3$ at 256 K. Asterisks are used to mark the peaks due to the minor conformer **181'**. Top: the same spectrum with an eight-fold increase of intensity

At 256 K, the broad signals became much sharper and four distinct peaks at 9.55 ppm, 9.72 ppm, 7.40 ppm and 6.14 ppm were observed. The observed temperature dependence of the line widths confirms that line broadenings at 298 K are caused by an exchange process. Furthermore, the observed set of small peaks suggested that another conformer may be present such as the folded rotamer **181'**. Both the dimerisation and conformational equilibria involved are presented in Figure 145. The change of proton chemical shift of 5-H from 7.54 ppm in **181** to 6.14 ppm in **181'** is very specific in this regard since a significant low frequency shift is expected once the C_5-H...O=C_8 proximity is lost. The effect of the carbonyl group has been attributed to the magnetic anisotropy of the carbonyl group, i.e., the local magnetic fields experienced by protons can be altered by the C=O magnetic dipole and the resulting chemical shift change is dependent on whether the proton of interest is within or outside the carbonyl shielding cone.[201] However, in analogy with conventional O-H...X or N-H...X hydrogen bonding

effects on the proton chemical shift, further high-frequency shift may be expected as a result of the C-H...O hydrogen bonding.

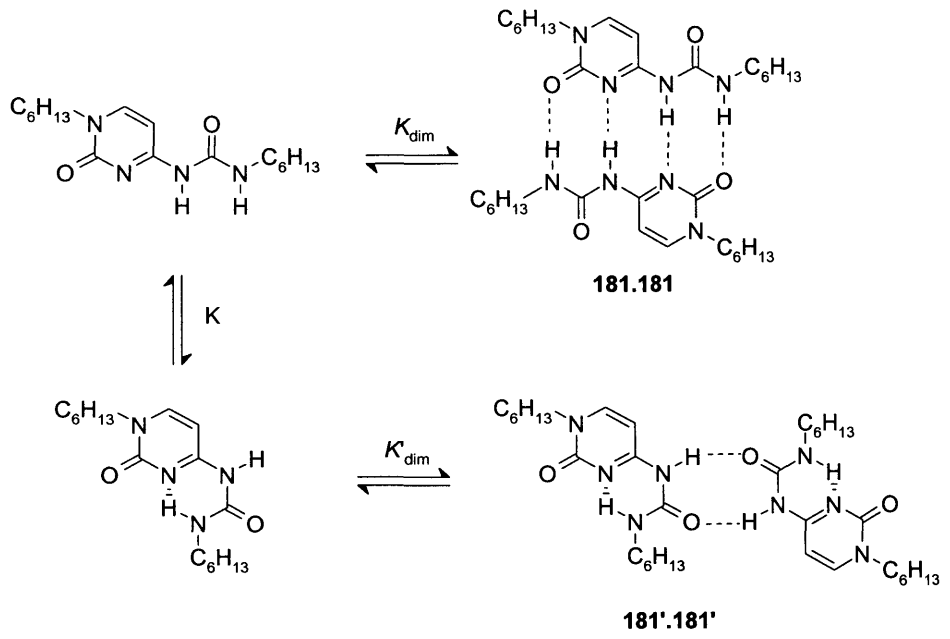

Figure 145: Dimerisation and conformational equilibria of cytosine **181** in $CDCl_3$

Overall, the observed temperature dependence suggests that there is a chemical exchange process. In order to estimate the barrier of the exchange process further variable temperature ^1H NMR spectra were recorded in $CDCl_3$ (400 MHz). Due to the overlap of the peaks and the very small content of the minor form, the coalescence temperature was determined as the temperature at which the maximum intensity decrease of the 5-H peak due to the major form (**181.181** dimer) is observed (Figure 146). The measured value was 320 K. Using the procedure described previsouly[202] the values of free energy of activation ($\Delta G^{\ddagger}$) were calculated to be 67 and 60 kJ mol^{-1} for the **181.181**→ **181'.181'** and **181'.181'** → **181.181** transitions, respectively.

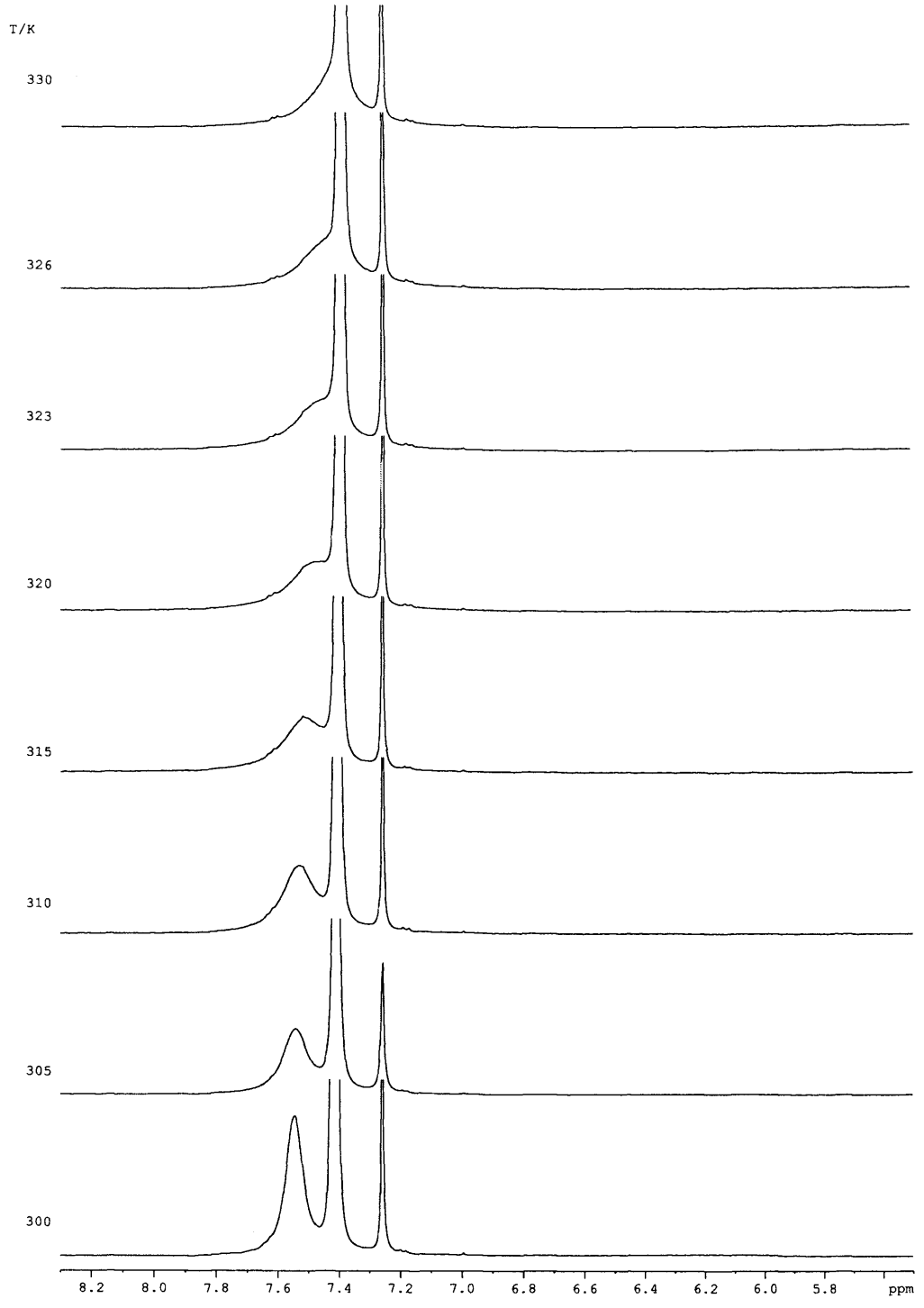

Figure 146: Variable temperature ^{1}H NMR spectra of **181** in $CDCl_3$

To further investigate the observed exchange process, NOE measurements were undertaken in order to confirm its nature, as well as to detect other peaks due to the minor form.

5.3.3.1 *NOE measurments*

NOE experiments were performed and a strong negative enhancement caused by an exchange process was observed between 7-H (the excited site) and the proton at 9.55 ppm, corresponding to 7'-H in the folded structure **181'** (Figure 147).

The signal at 9.72 ppm was attributed to proton 9'-H, which is involved in intramolecular hydrogen bonding with N-3. A positive NOE effect was observed between 7-H and 9-H (Figure 147), which is expected for the linear arrangement of these protons in the unfolded conformer of **181**.

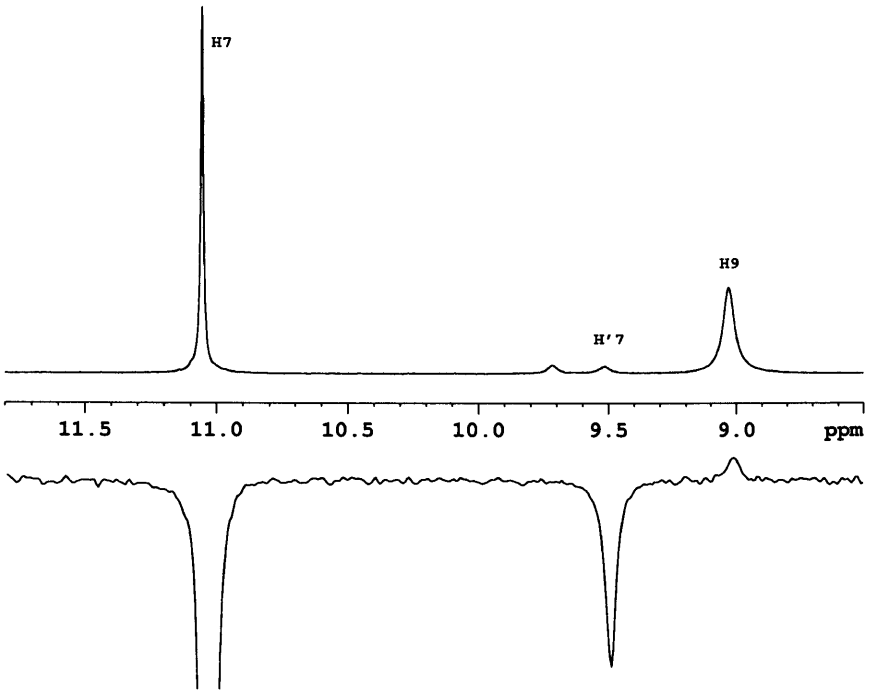

Figure 147: NOE (bottom) and ^{1}H NMR (top) spectra at 256 K

The NOESY spectrum was also recorded. The observed negative cross-peaks allowed an easy identification of the peaks due to protons 5′-H, 7′-H and 9′-H of the folded form.

These experiments confirmed the presence of the folded conformer **181'** as the minor species in solution, and integration of peaks suggested a population ratio of 19:1 in favour of **181** at 256 K. The exchange rate between the two conformers was sufficiently slow in the NMR timescale at low temperatures, allowing observation of the two distinct species. The broad signal for 5-H at 298 K becomes sharper at 256 K as the exchange between **181** and **181'** slows down on cooling. Back at room temperature the exchange rate became faster approaching the intermediate regime in the NMR timescale

and hence leading to a broader signal for proton 5-H, which showed the largest chemical shift difference between **181** and **181'** due to its proximity to the carbonyl group in **181** and the absence of such in **181'**. Note that the NMR timescale in these experiments is determined by the chemical shift difference for a given proton in **181** and **181'**.

In addition, a strong temperature dependence of the chemical shift of 7-H was observed for **181'**: 8.84 ppm at 298K and 9.62 ppm at 256 K. This observation favours an increase of the population of the double hydrogen bonded dimer (Figure 148) on lowering the temperature.

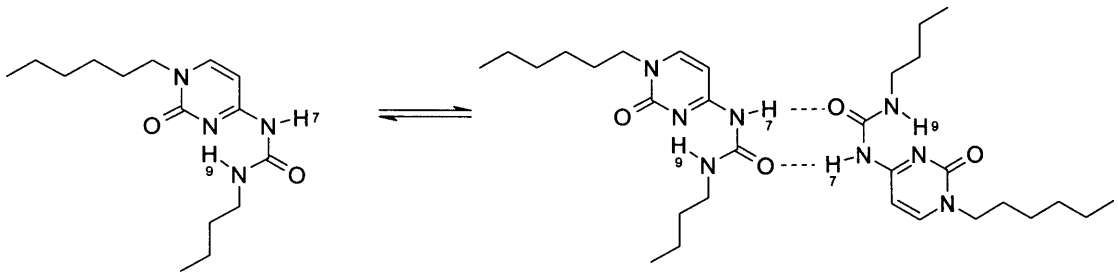

Figure 148: Monomer/dimer equilibrium for **181'**

The observed strong temperature dependence of 7-H also suggests that the double hydrogen bonded dimerisation of **181'** is not strong. For a similar type of dimerisation in $CDCl_3$, Corbin and Zimmerman have reported K_{dim} values in the range of ~ 15-95 M^{-1}, suggesting that the double hydrogen-bonded dimerisation is relatively weak.

Further evidence in favour of the equilibrium shown in Figure 148 was obtained by diffusion coefficient measurements. The measured values for the 20 mM solution in $CDCl_3$ at 256 K were 2.7×10^{-10} m^2/s for the fully dimerised **181** and 3.1×10^{-10} m^2/s for **181'**. Since the "monomer/dimer" equilibrium is fast in the NMR timescale, the observed diffusion coefficient for **181'** is the weighted average of the diffusion coefficients observed for the monomer and for the dimer, hence, faster diffusion of **181'** relative to **181** is observed.

Finally, in some of the very dilute solutions of **181** in $CDCl_3$ (~0.5 mM) additional peaks at 14.5, 13.23 and 6.59 ppm were observed. Appearance of these peaks in $CDCl_3$ was attributed to the presence of the residual water (~10 mM) in $CDCl_3$ and the acidity of the solvent may hydrolyse **181**. A possible hydrolysis scheme of **181** is shown in Figure 149):

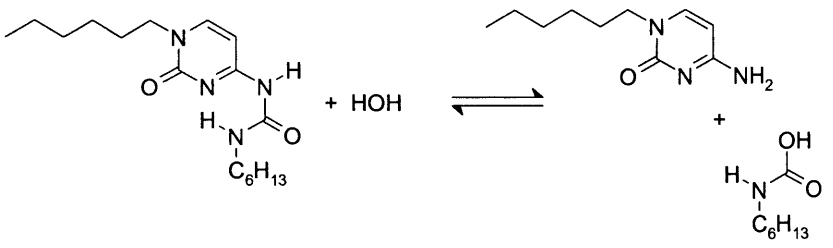

Figure 149: Possible hydrolysis of compound **181**

5.3.3.2 *^{1}H NMR in DMSO-d_6*

Compound **181** was dissolved in DMSO-d_6 and the ^{1}H and ^{13}C spectra suggested that the folded molecule **181'** was the only conformer present in solution. In particular, at 298 K the chemical shift of proton 5'-H at 6.15 ppm in the DMSO-d_6 solution was similar to that measured in the $CDCl_3$ solution at 6.08 ppm (Figure 150).

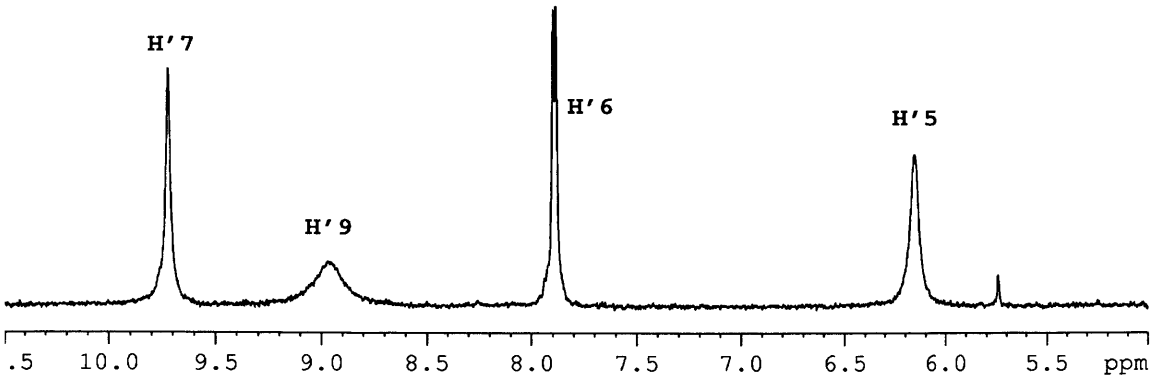

Figure 150: ^{1}H NMR spectrum of compound **181** in DMSO-d_6

One issue to address was whether **181'** existed as a dimer or a monomer in such a polar solvent. For this purpose, dilution experiments were performed at 333 K (Table 34). No changes in chemical shifts were observed on dilution. In addition, no changes in the diffusion coefficients were found for 5 and 17 mM solutions. The measured values were within $(5.0 \pm 0.1) \times 10^{-10}$ m^2/s at 333 K. These results indicated that compound **181'** existed as a monomer in DMSO, which is not surprising since DMSO is not only a highly polar solvent, but also is a strong hydrogen bond acceptor. Therefore, weak hydrogen bonds of the double hydrogen bonded dimer of **181'** are easily disrupted in DMSO. The relatively high chemical shift found for 7'-H can be attributed to a hydrogen bonding of this proton with DMSO.

Proton	δ_H (ppm), Saturated solution	δ_H (ppm), 5 mM
5'-H	6.22	6.20
6'-H	7.85	7.84
7'-H	9.55	9.53
9'-H	8.81	8.81

Table 34: Concentration dependence of ^{1}H NMR chemical shifts in DMSO-d_6 at 333K

The ^{13}C spectrum in DMSO-d_6 showed the chemical shifts of C-1 and C-5 at 153.4 ppm and 93.8 ppm, respectively, while in $CDCl_3$ the corresponding signals for the unfolded form **181** were downfield at 157.2 ppm and 97.3 ppm. These results agreed further with the presence of conformer **181'** in DMSO-d_6.

5.3.3.3 *Temperature Dependence*

Variable temperature studies in toluene-d_8 were performed to assess the strength of the hydrogen bonding network (Table 35). Upon increasing the temperature from 298 K to 353 K, protons 7-H and 9-H shifted towards lower frequencies by 0.33 ppm, which is normal for relatively strong hydrogen bonds. Indeed, for the Upy system, a decrease of 0.2 ppm and 0.3 ppm was observed for 7-H and 9-H, respectively, on increasing temperature from 296 K to 363 K. A comparison of these values suggested that the hydrogen bond N7-H...N was weaker for compound **181**. This was already apparent from the comparison of the hydrogen bond lengths measured by X-ray.

The interpretation of the shifts for protons 5-H and 6-H is more complex, since 6-H shows an increase of chemical shift by 0.24 ppm on heating from 298 K to 353 K, while 5-H shows a decrease of chemical shift by 0.15 ppm. Moreover, the peak due to 5-H becomes broader on heating. Such behaviour of both the chemical shift and the line width is similar to that observed in $CDCl_3$ and agrees with the existence of the exchange process between **181.181** and **181'.181'**, although no 5-H peak due to the minor **181'.181'** was detected in toluene-d_8, presumably due to the overlap with the 6-H peak of **181.181** or much lower content of the minor form in toluene compared to the $CDCl_3$ solution. The temperature dependence of the 6-H chemical shift is less clear. However,

comparison with the value in $CDCl_3$ at 298K suggests that solvation in toluene is such that proton 6-H is within the shielding cone of the toluene aromatic ring, possibly due to a specific solvent-solute interaction. On heating, the population of solvated species are expected to decrease, leading to the observed high frequency shift at higher temperatures.

Temperature (K)	5-H	6-H	7-H	9-H
298	7.79	6.21	11.11	9.72
330	7.75	6.38	10.95	9.53
343	7.71	6.42	10.86	9.46
353	7.65	6.45	10.76	9.39

Table 35: Variation of chemical shifts (δ_H, ppm) in toluene-d_8 depending on temperature.

5.4 Dimerisation Studies by NMR

To estimate the dimerisation constant of the DDAA array, dilution experiments were performed in $CDCl_3$, which was dried over molecular sieves and de-acidified through basic alumina (Table 36).

C (mM)	5-H	7-H	9-H
250	7.54	10.91	8.98
200	7.55	10.91	8.98
170	7.53	10.90	8.96
51	7.55	10.92	8.98
0.51	7.53	10.92	9.00

Table 36: Chemical shifts of 5-H and hydrogen bonded protons 7-H and 9-H as a function of concentration in $CDCl_3$ (298 K, 500 MHz)

There were no significant changes in the ^1H NMR spectrum upon diluting the sample from 250 mM to 0.51 mM, suggesting that the dimerisation constant was above 3×10^5 M^{-1}. NMR dilution measurements were also carried out in C_6D_6. Due to the poor

solubility in benzene the highest concentration used was 4 mM, which was then diluted to 0.73 and 0.008 mM (Table 37). Again no low frequency shifts of peaks were observed. Based on these measurements, the value of K_{dim} in benzene-d_6 was estimated as $> 2 \times 10^7\ M^{-1}$.

C (mM)	5-H	6-H	7-H	9-H
4.0	7.869	6.166	11.332	9.816
0.73	7.870	6.159	11.338	9.828
0.008	7.869	11.337	11.337	9.830

Table 37: Chemical shifts of the high-frequency peaks in benzene-d_6 as a function of concentration (296 K, 400 MHz)

Further NMR measurements were also undertaken in order to assess K_{dim} for a double-hydrogen bonded analogue of **181**. The particular focus here was to compare the association constants of double and quadruple hydrogen bonded cytosine derivatives.

5.4.1 Synthesis of a Mimetic Dimeric Array

One approach considered was to synthesise compound **191** in which proton 9-H was replaced by a CH_2 group. This would give an approximate value for dimerisation *via* two hydrogen bonds and allow assessing the significance of two additional hydrogen bonds in the quadruple hydrogen bonded systems. Compound **192** was first synthesised through the reaction between hexanoic acid and *N*-hydroxysuccinimide in the presence of DCC in THF and was obtained in 80% yield after purification (Scheme 53).[203] The synthesis of **191** was then achieved through the reaction of **189** with the activated acid **192** to afford **191** in 70% yield (Scheme 54).

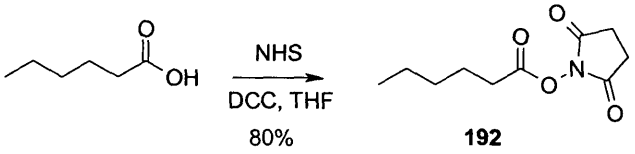

Scheme 53: Activation of hexanoic acid

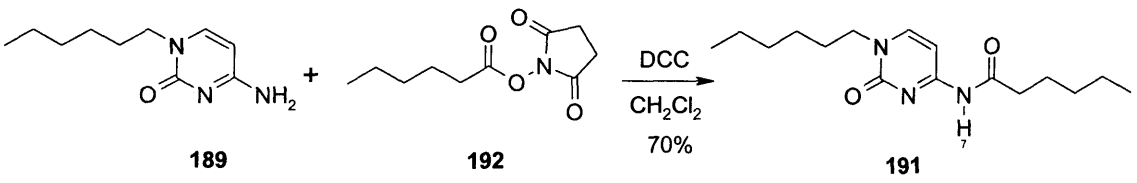

189 192 191

Scheme 54: Synthesis of compound **191**

In analogy with **181**, the occurrence of proton 5-H at 7.58 ppm was in favour of unfolded conformer as in **191.191** and a possibility of an alternative dimer **191'.191'** involving folded conformers can be ruled out (Figure 151). No trace of the folded conformer **191'** was detected in the ^{1}H NMR spectra, for which 5-H is expected to resonate at ca. 6.2 ppm. In terms of structure, unlike **181'**, conformer **191'** is not stabilised *via* intramolecular hydrogen bonding involving N-3, hence the observation of the predominantly unfolded conformer in the $CDCl_3$ solution is not surprising.

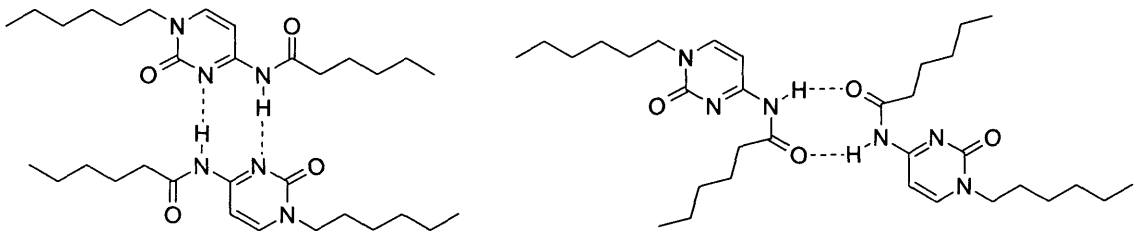

191.191 **191'.191'**

Figure 151: Representation of the dimers **191.191** and **191'.191'**

Dilution experiments were performed on this sample, and evaluation of the chemical shifts and diffusion coefficients at different concentrations agreed with the presence of dimers in solution (Table 38). The association decreased upon dilution from 190 mM to 4.7 mM and the ^{1}H NMR signal shifted upfield from 9.77 ppm to 8.20 ppm. Such a strong dependence of the chemical shift on concentration is typical for weakly hydrogen bonded dimers. More pronounced concentration-dependent chemical shift changes for 7-H than for the other protons, suggests that dimerisation of **191** occurs *via* hydrogen bonding of proton 7-H, hence larger high-frequency shifts for this proton is observed when the concentration is increased.

Concentration, mM	δ(7-H), ppm	D, $\times 10^{-10}$ m^2/s
190.0	9.766	6.66
182.5	9.724	6.70
159.4	9.617	6.90
128.7	9.476	7.13
92.5	9.249	7.50
58.3	9.007	7.75
28.8	8.700	8.03
15.3	8.423	8.30
6.8	8.206	8.64
4.7	8.199	8.90

Table 38: Diffusion coefficients and ^{1}H NMR chemical shift of proton 7-H of **191** as a function of concentration in $CDCl_3$ solution at 298 K

The measured chemical shifts were plotted against the concentration of **191**, and the dimerisation constant K_{dim} was calculated using the non-linear least squares fitting. The estimated value of K_{dim} was found to be 4 ± 1 M^{-1} with the boundary chemical shift values of 8.06 ± 0.03 ppm and 11.80 ± 0.20 ppm for the mono- and dimeric species. The dimerisation constant calculated from the diffusion coefficients was 3 ± 2 M^{-1} with boundary D values of (8.9 ± 1.1) × 10^{-10} m^2/s and (3.8 ± 1.0) × 10^{-10} m^2/s for the mono- and dimeric species. The vey low value of K_{dim} for **191** did not allow to draw any conclusive evidence regarding the importance of the quadruple hydrogen bonding compared to the double hydrogen bonding. Other models need to be considered for this purpose.

5.4.2 Dimerisation Studies in Chloroform by Fluorescence Spectroscopy

In order to quantify the strength of the dimerisation, compound **193** was synthesised and studied by fluorescence spectroscopy (Figure 152). Meijer and Zimmerman have previously used this technique in the determination of K_{dim}. The excimer signal of the

pyrene dimer exhibits an emission band at ca. 480 nm that is separate from that of the monomer at ca. 400 nm.

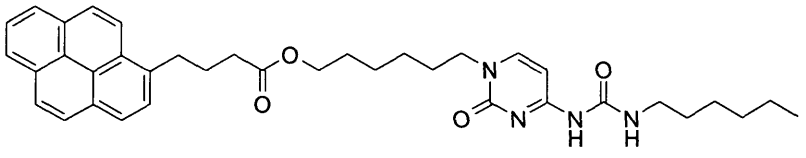

193

Figure 152: Targeted fluorescent molecule

5.4.2.1 *Synthesis of the pyrene derivative*

Compound **194** was first synthesised *via* THP protection of 6-bromohexanol[204] (Scheme 55).[205] Reaction of N^4-acetyl cytosine **187** with compound **194** was carried out using K_2CO_3 in DMF affording **195** in 70% yield (Scheme 56).

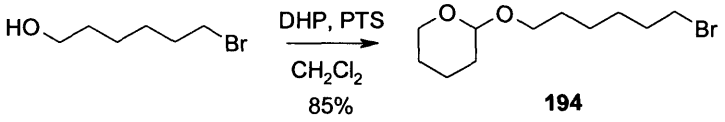

194

Scheme 55: Synthesis of compound **194**

Compound **195** was then deprotected using a concentrated solution of ammonia in methanol. The reaction was carried out using the same conditions as for compound **189** previously described and gave **196** in 65% yield. Further reaction with hexyl isocyanate in dry pyridine at 90 °C afforded an intermediate, which was not purified. Deprotection of the THP group under acidic conditions then gave **197** in 30% yield after flash column chromatography. The low yield was attributed to the very poor solubility of **197** in organic solvents, which caused partial loss of the product during the work up and the purification step (Scheme 56).

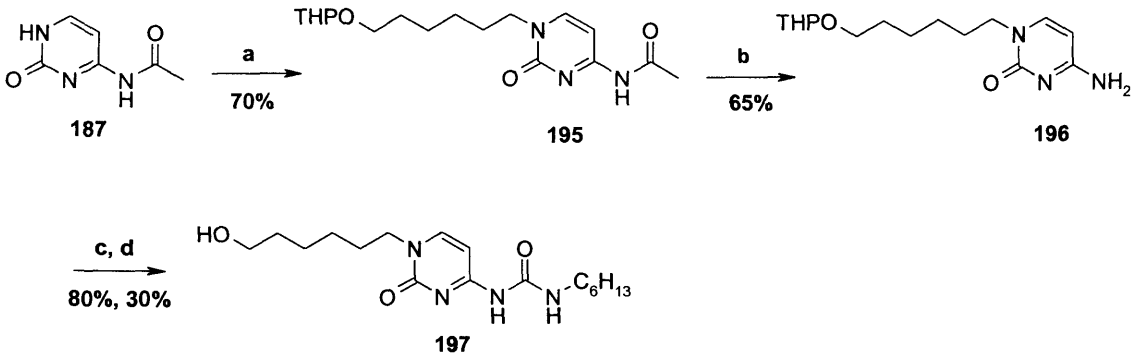

Reagents and conditions:(a) Compound **194**, K_2CO_3, DMF, 70%; **(b)** NH_3/MeOH, 65%; **(c)** $C_6H_{13}NCO$, Pyridine, 90 °C, 80% ;**(d)** HCl conc., MeOH, THF, 30%.

Scheme 56: Synthetic strategy towards the formation of compound **197**

The final step consisted in the reaction between **197** and an activated pyrene unit. Two different methods of activation of the pyrene were explored as acyl chloride **198** or as *N*-hydroxysuccinamide group **199** (Scheme 57).[206]

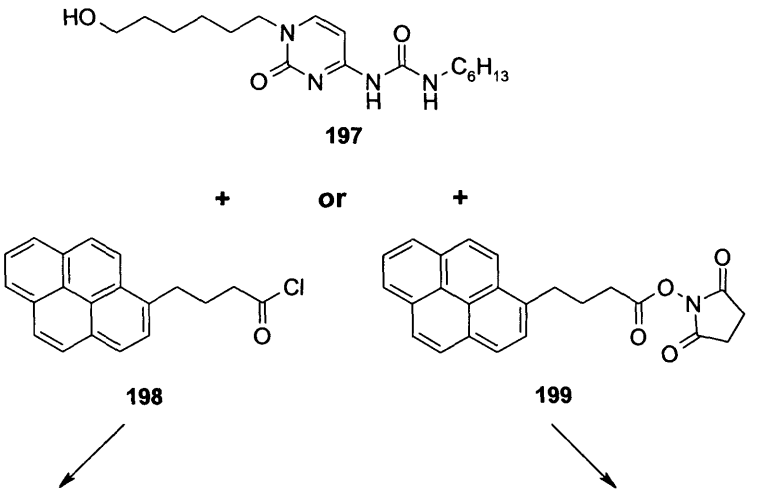

Scheme 57: Reaction of compound **197** with two activated pyrene derivatives

Mainly due to insolubility problems with **197** in solvents such as CH_2Cl_2 or THF, neither reaction with the activated acids gave the desired compound **193**. Therefore, a second strategy involving the direct reaction of **197** with pyrene acid **200** in the presence of DCC was then investigated. This method, which is frequently used to form ester bonds, was not considered at first due to insolubility of both compounds in organic solvents. Nevertheless, after optimisation of the reaction conditions, DCC and HOBt

were used in CH_2Cl_2 first at 0 °C for 1 h, then at room temperature for 16 h.[112] The desired compound **193** was isolated in 25% yield and was then used in fluorescence studies.

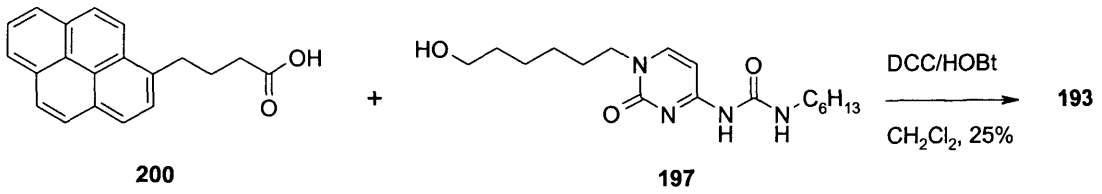

200 **197**

Scheme 58: Coupling reaction between compounds **200** and **197**

5.4.3 Fluorescence Measurements

Fluorescence spectroscopic studies were carried out in chloroform (with amylene stabiliser) dried over molecular sieves, and de-acidified through neutral alumina.

The emission fluorescence was measured on a series of diluted samples. As shown in Graph 2, the concentrated sample (16.4 mM) showed a strong emission band characteristic of the excimer band of the pyrene between 450-500 nm, suggesting the dimerisation of the molecule (Graph 2). Upon dilution to 0.0328 mM, the bands of the monomer emission gradually increased as the excimer emission band decreased in intensity (Graph 3).

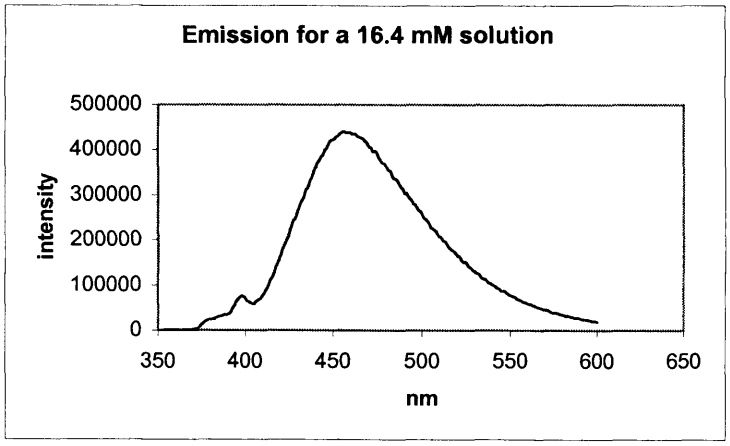

Graph 2: Emission for a 16.4 mM solution of **193**

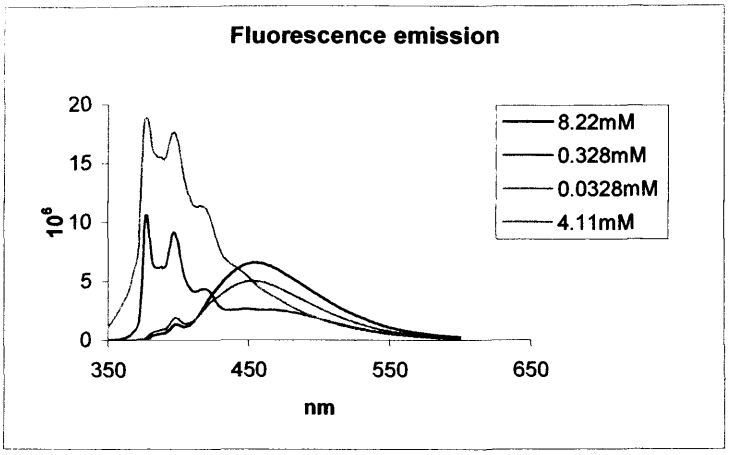

Graph 3: Emission bands for diluted samples of **193**

The procedure described previsouly[207] was used for the determination of K_{dim}. In particular, the following equation was used for non-linear least square curve fitting :

$$r = C\,(1 - (8\,K_{dim}\,[Pyr] + 1)^{1/2})\,/\,4$$

where r is the integral intensity ratio of the excimer emission (I_2) and the monomer emission (I_1) at 476 and 376 nm respectively. C is a constant and [Pyr] is the total concentration of the pyrene labelled compound **193**. This equation is derived on the assumption that $K_{dim}=[Pyr_{dim}]/[Pyr_{mono}]^2$ and $[Pyr]=2[Pyr_{dim}]+[Pyr_{mono}]$. In addition, it is also assumed that the emission intensities I_1 and I_2 are proportional to the concentration of monomeric ($[Pyr_{mono}]$) and dimeric ($[Pyr_{dim}]$) forms, respectively.

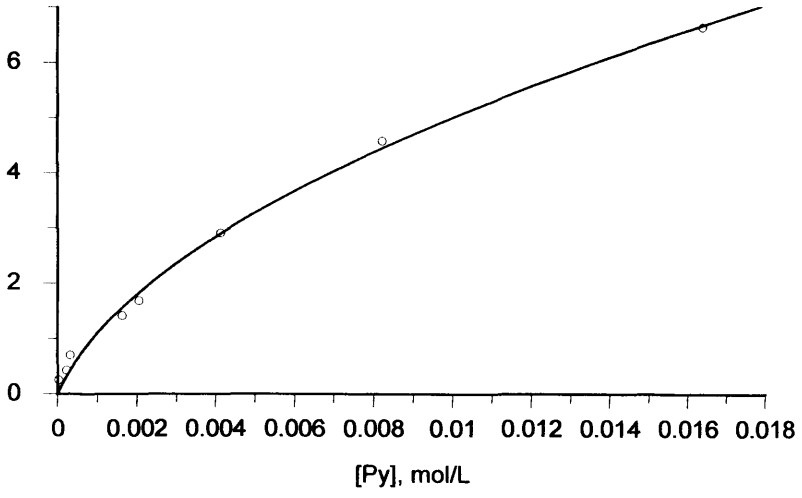

Graph 4: The ratio of the intensities I_2 / I_1 as a function of the concentration

From these calculations, the value of K_{dim} was found to be rather low with a large error margin: 365 ± 178 M^{-1}. This result did not correlate with the ^1H NMR chemical shift measurements, according to which the value of K_{dim} is higher than 10^5 M^{-1}. Although the fluorescence emission shows the excimer band which is in favour of dimerisation in solution, the determination of the dimerisation constant could not be established with reliable accuracy, and this left some doubts concerning the strength of the DDAA array. It is possible that the minor double-hydrogen bonded species **181'** influence the pyrene-pyrene stacking and decrease the value of K_{dim}. Other factors, such as overlap of the excimer and monomer bands, further limit the accuracy of the K_{dim} measurements. Another simple reason could be that the hydrolysis of **181** at very low concentrations (see above) is possible. Although dried chloroform was used, the measurements were nevertheless carried out under normal atmospheric conditions.

Conclusions

The linear quadruple hydrogen bonded array DDAA (**181.181**) found in the solid state by X-ray diffraction was also observed in the $CDCl_3$ solution. In addition, the population of the other folded conformer **181'** was approximately 5% in the $CDCl_3$ solution. NMR dilution experiments suggest that the dimerisation constant is higher than 3×10^5 M^{-1} in $CDCl_3$ and 2×10^7 M^{-1} in C_6D_6 since no changes of chemical shifts were observed down to 0.6 mM. In DMSO, however, the dimer breaks exclusively into the folded monomer **181'**.

One of the next challenges was to use this new DDAA array in the design and synthesis of new new hydrogen bonded materials, as well its binding to other DDAA modules, such as 4-keto tautomer of Upy.

5.5 Complexation with Ureidopyrimidinone

Ureidopyrimidinones have been used in numerous applications though mainly in the synthesis of supramolecular polymers. Recently, the synthesis of copolymers incorporating Upy units has shown some significant potential for the design of new materials. Li *et al.* have reported the strong and selective complexation of the 6-[1H] pyrimidinone tautomeric form of **114** with 2,7 diamido-1,8-naphthyridines (Napy) (**201**) *via* the complexation between ADDA and DAAD arrays[208,209] (Figure 153).

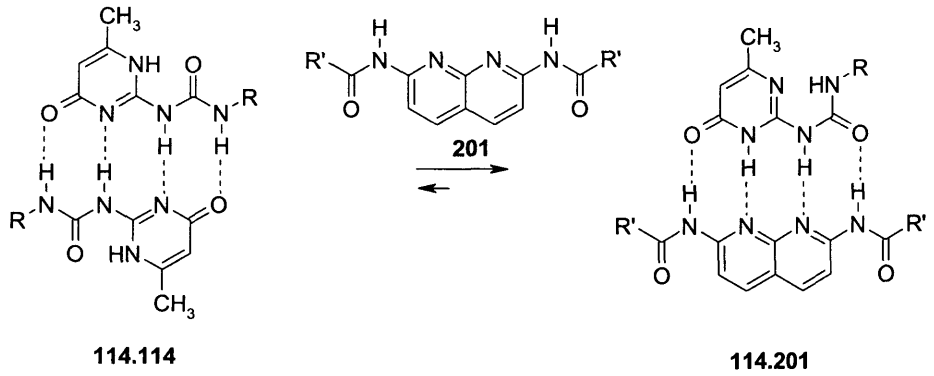

Figure 153: Complexation of Upy unit with a DAAD array **(201)**

The use of 1 equivalent of Napy in $CDCl_3$ disrupted the formation of the Upy dimer **114.114** and the use of Upy-Napy heterodimers appears attractive for the synthesis of complamentary copolymers. Note that the Upy unit undergoes a 4-keto-to-6-keto tautomeric transformation on binding with Napy.

Following a similar approach, the disruption of the Upy dimer **114.114** was explored with the addition of compound **181** in solution. A solution of a 1:1 mixture of compound **181** and **114** (Upy) in $CDCl_3$ was then prepared and the resulting solution was studied using ^1H NMR spectroscopy (Figure 154).

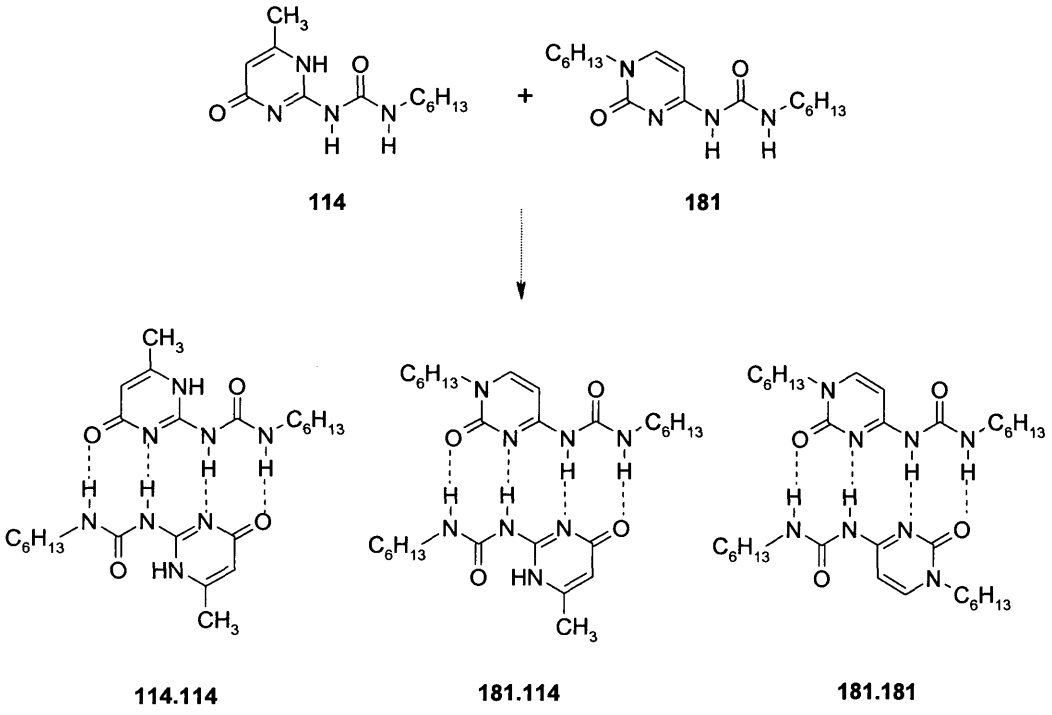

Figure 154: Complexation between Upy **114** and compound **181** in a 1:1 ratio

The ^{1}H NMR spectrum (at 298 and 283 K) revealed a set of broad peaks. In order to obtain a better resolution for assignment, a ^{1}H NMR spectrum was run at 256 K (Figure 155). As expected all the peaks became sharper and 10 different hydrogen bonded protons were identified.

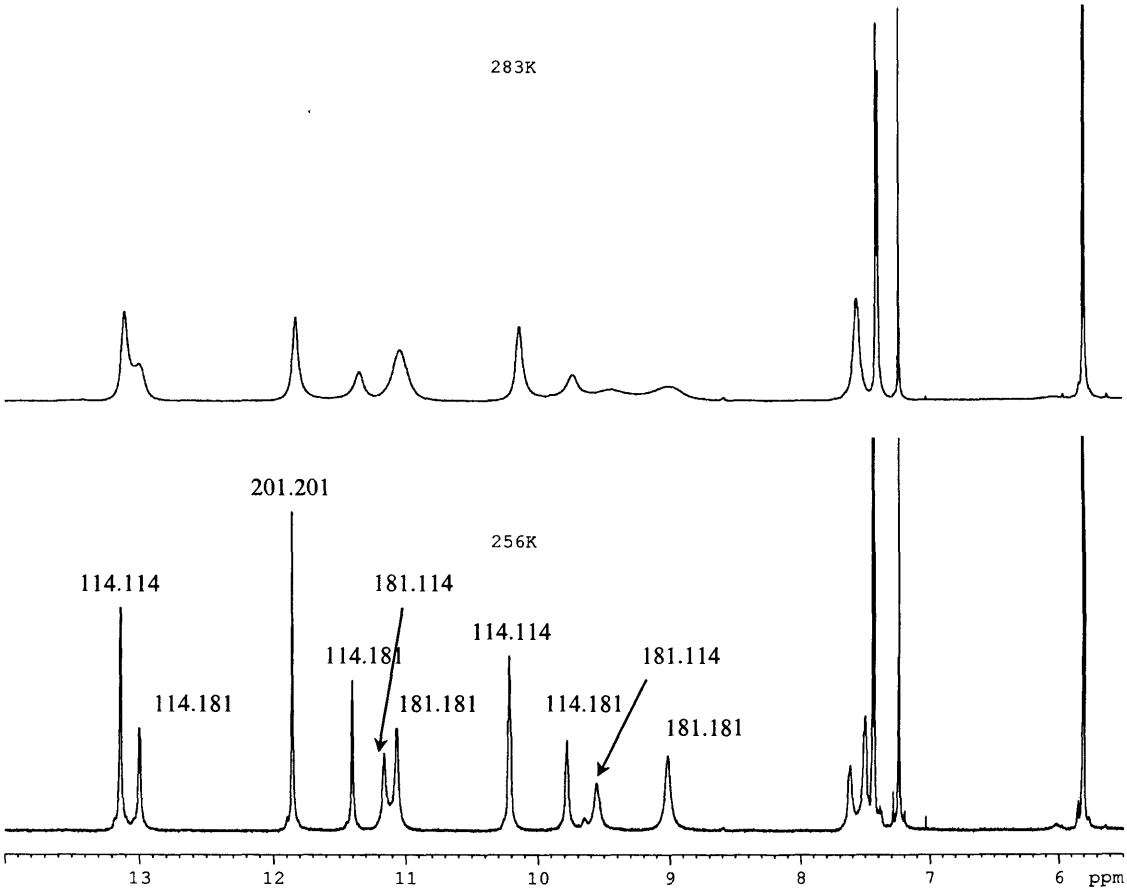

Figure 155: ^{1}H NMR spectra of a 1:1 mixture of **181** and **201** at 283 K and 256 K

The assignment of these peaks was straightforward since the chemical shifts for the hydrogen bonded protons found in the homodimers **114.114** and **181.181** have been already established. Therefore, the new peaks at 13.0 ppm, 11.40 ppm, 9.78 ppm, 11.16 ppm and 9.78 ppm were attributed to the heterodimer. A summary of the chemical shifts for 1-H, 7-H and 9-H is included in Table 39. For the equimolar solution of **114** and **181**, the ratio **114.114**:**181.181**:**114.181** was approximately 5:5:6.

dimer	1-H	7-H	9-H
114.114	13.16	11.88	10.24
114.181 (114)	13.03	11.42	9.80
181.181	-	11.09	9.04
114.181 (181)	-	11.18	9.58

Table 39: Proton chemical shifts (δ_H, ppm) for the hydrogen bonded protons found in the homodimers and heterodimer.

In summary, the new DDAA array based on cytosine partially disrupts the strong Upy-Upy dimer and this result may be of critical importance for the synthesis of new co-polymers.

5.6 Synthesis of supramolecular incorporating the cytosine module

To further evaluate the ability of the new module to polymerise *via* intermolecular quadruple hydrogen bonds, a bifunctional derivative **202** was synthesised (Figure 156). A structurally similar UPy derivative **203** was also made for comparison (Figure 157). In analogy with other UPy derivatives, **203** is expected to form mainly cyclic dimers at millimolar concentrations, with an equilibrium between cyclic dimers and higher molecular weight species on increasing the concentration. For a straightforward synthesis, an amine terminated polyethyleneglycol (~ 3400 g mol^{-1}) was reacted with the corresponding imidazole (**131**) activated units to prepare **202** and **203**.

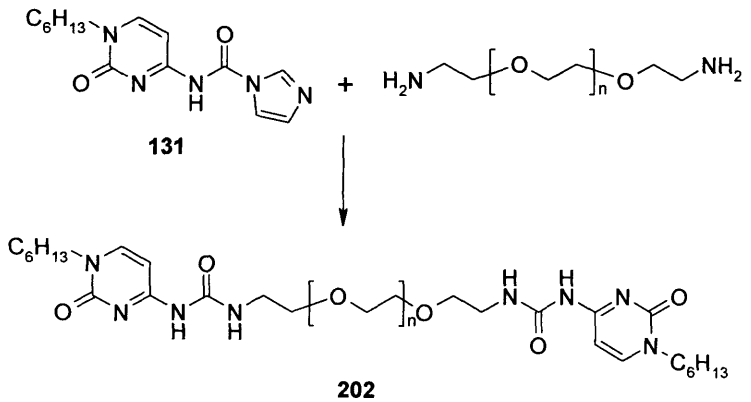

Figure 156: Synthesis of polymer **202**

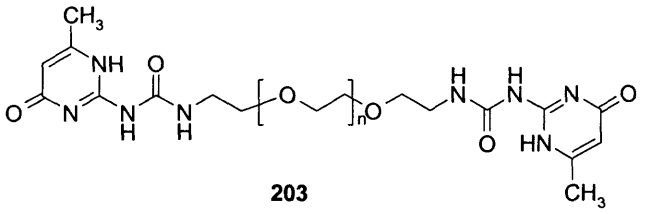

203

Figure 157: Polymer **203** synthesised using the same procedure as for **202**

Both materials are solids with close melting points (46 °C and 43 °C for **202** and **203**, respectively). Proton NMR analysis of **202** revealed the presence of the two hydrogen bonded protons (at 10.7 and 9.2 ppm) as found in dimer **181.181** suggesting that the linear DDAA array was preserved. Diffusion coefficient (D) measurements in the 6.5 mM $CDCl_3$ solutions were undertaken in order to compare the degree of self-association of **202** and **203**. The measured values were 7.0×10^{-11} m^2 s^{-1} for **202** and 1.11×10^{-10} m^2 s^{-1} for **203**. Both the ^1H spectra and the high diffusion rates are therefore consistent with the presence of presumably cyclic oligomers of **202** and **203** in dilute chloroform solutions. As expected, further polymerisation occurred on increasing the concentration and this was confirmed by a considerable slow down of diffusion in 37 mM solutions: 1.9×10^{-11} m^2s^{-1} for **202** and 4.4×10^{-11} m^2s^{-1} for **203**. This and other similarities of bifunctional derivatives suggested that a new cytosine module could be used successfully for the generation of new supramolecular materials. Further investigations are currently underway aimed at preparation of linear polymers and cyclic dimers based on the cytosine module.

Chapter VI

6 Experimental Part

6.1 Materials and reagents

Unless otherwise specified, all regeants, were purchased from commercial suppliers and used without further purification. Acetonitrile was distilled over phosphorous pentoxide. THF was distilled over sodium and benzophenone. Triethylamine and dichloromethane were distilled over calcium hydride. Chloroform was dried over molecular sieves (4 Å). Hexane is described as a fraction boiling between 67-70 °C. Water used in reactions and for washings was deionised water. All reactions using anhydrous solvents were carried out under a nitrogen atmosphere.

Melting points were determined using a Gallenkamp melting point apparatus and are uncorrected.

DSC were measured on a V2.4F TA instrument.

Infra-red (I.R) spectra were recorded on a FT-IR Shimidasu 8700 spectrophotometer. IR spectra were obtained either using a neat film on KBr discs for liquid compounds or KBr pellets for solids.

Solution ^{1}H, ^{13}C and ^{15}N spectra were recorded on Bruker NMR spectrometers AMX300, AMX400 and AVANCE500 spectrometer. Data acquisition and processing was performed using standard Bruker XwinNMR software (version 2.6). ^{1}H and ^{13}C chemical shifts are given relative to TMS and ^{15}N chemical shifts are given relative to $MeNO_2$.. Coupling constants *J* were measured in Hertz (Hz). Multiplicities for 1H are shown as a s (singlet), d (doublet), t (triplet), dd (doublet of doublets), dt (doublet of triplets), m (complex multiplet). Variable temperature NMR measurements were carried out using either AMX400 or AVANCE500 spectrometers. Deuterated solvents were used as received unless specified.
Solid-state ^{13}C and ^{15}N spectra were recorded at 75.5 MHz and 30.1 MHz, respectively, using a standard 7 mm double-resonance magic-angle spinning (MAS) probe on MSL300 (Bruker).

Mass spectra (EI, FAB) were recorded using the spectrometer UG70FE. Electrospray (ES+) were performed on a Micromass Quattro LC electrospray (MassLynx software). High resolution mass spectra (HRMS) were recorded on a MAT 900 XP.

Microanalysis were determined, where possible, using a Perkin Elmer 2400 Elemental Analyser (CHN). However, for the majority of the compounds, the purity was determined by accurate mass NMR spectroscopy analysis.

Optical Rotations were recorded on Optical Activity: PolAAR2000 polarimeter, with concentration (c.) in g/100 ml.

Fluorescence measurements were performed on a FluoroMax3. The excited wavelength was fixed at 341 nm.

Flash Silica Chromatography was performed using silica gel for flash chromatography Si60, purchased from Merck Ltd.

TLC were performed using TLC aluminium sheets, silica gel 60 F_{254} purchased from Merck Ltd., and were visualised using UV (254 nm), Phosphomolybdic acid hydrate (PMA 12 g, ethanol 250 ml, conc. Sulphuric acid) and potassium permanganate (6.25 g sodium bicarbonate in 125 ml water, 1.25 g potassium permanganate in 125 ml water) and Ninhydrin (100 ml ethanol, 0.2 g ninhydrin, 4.5 ml water, 0.5 ml acetic acid).

6.2 Ureidopyrimidinone Derivatives

2-Amino-6-(4-nitro-phenyl)-1H-pyrimidin-4-one (110)[111]

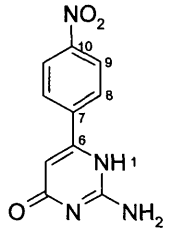

Guanidine carbonate (2.43 g, 13.50 mmol) and *p*-nitrobenzoylacetate (5.93 g, 25.0 mmol) were dissolved in absolute ethanol (25 ml) and heated at reflux for 18 h. The brown solid formed was then filtered off and washed thoroughly with cold acetone (20 ml), water (20 ml) and finally cold ethanol (20 ml). The solid was then triturated from a mixture of water/ethanol (1:1) to afford compound **110** as yellow micro-needles (0.95 g, 30%).

mp > 300 °C (ethanol);

ν_{max} **/cm^{-1} (KBr pellets)** 3500 (N-H, *s*, NH_2), 3379 (N-H, *s*, NH_2), 3089 (C=*C-H*, *s*);

^{1}H NMR (300 MHz; DMSO-*d*$_6$) δ 10.96 (1H, s, NH), 8.29 (2H, d, *J* 8.9 Hz, 9-H), 8.18 (2H, d, *J* 8.9 Hz, 8-H), 6.70 (2H, broad s, NH_2), 6.27 (1H, s, 5-H);

^{13}C NMR (75 MHz; DMSO-*d*$_6$) δ 163.0 (C=O), 160.2 (C-2), 155.9 (C-6), 148.1 (C-10), 143.5 (C-7), 127.8 (C-8), 123.4 (C-9), 99.5 (C-5);

m/z (ES+) 233 [(MH^+), 25%], 136 [(MH^+- 97), 100%];

HRMS calculated for $C_{10}H_8N_4O_3$ (MNa^+) 255.04945, found 255.04944.

N-Hexyl-*N*-(1,4-dihydro-4-oxo-6-*p*-nitrophenyl-2-pyrimidinyl)-urea (111)

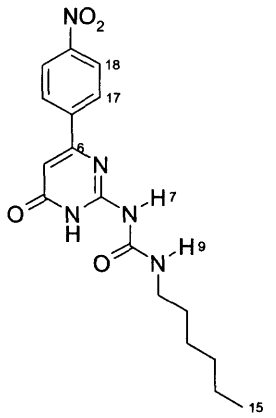

A suspension of 6-(*p*-nitrophenyl)isocytosine **110** (0.840 g, 3.62 mmol) and hexyl isocyanate (1.01 g, 7.90 mmol) in dry pyridine (15 ml) was heated at reflux for 4 h. After cooling, acetone (10 ml) was added and the product was collected by filtration to give ***111*** (1.16 g, 88%).

mp > 300 °C (pyridine);

ν_{max} /cm^{-1} (KBr pellets) (enol tautomer C) 3495 (O-H, *s*), 3386 (N-H, *s*), 3134 (C=C-H, *s*), 3075-2932 (C-H, *s*), 1660 (C=O, *s*);

^{1}H NMR (500 MHz; DMSO-d_6) (6[1H]-pyrimidinone tautomer A) δ 12.05 (1H, s, 3-H), 10.04 (1H, s, 7-H), 8.31 (2H, d, *J* 8.8 Hz, 18-H), 8.21 (2H, d, *J* 8.8 Hz, 17-H), 7.38 (1H, s, 9-H), 6.66 (1H, s, 5-H), 3.16 (2H, m, CONHCH_2), 1.47 (2H, m, NHCH$_2$CH_2), 1.28 (2H, m, NH(CH$_2$)$_2$CH_2)), 1.27 (4H, m, NH(CH$_2$)$_3$CH_2CH_2), 0.85 (3H, t, *J* 6.2 Hz, CH$_3$);

^{13}C NMR (125 MHz; DMSO-d_6) δ 161.9 (C-4), 159.1 (NH*C*ONH), 152.3 (C-2), 148.3 (C-19), 142.5 (C-16), 127.9 (C-17), 123.6 (C-18), 104.0 (C-5), 39.0 (CONH*C*H$_2$), 30.8 (NH(CH$_2$)$_3$*C*H$_2$), 29.0 (NHCH$_2$*C*H$_2$), 25.8 (NH(CH$_2$)$_2$*C*H$_2$), 21.9 (NH(CH$_2$)$_4$*C*H$_2$), 13.7 (CH$_3$);

^{15}N NMR (51 MHz, DMSO-d_6) δ -182.3 (N-1), -223.5 (N-3), -285.6 (N-9);

^{13}C CPMAS NMR (75 MHZ) (pyrimidin-4-ol tautomer C) δ 172.5 (C-4), 160.5 (C-6), 157.0 (br, C-2), 156.0 (br, NH*C*ONH), 146.3 (C-19), 139.5 (C-16), 126.0 (C-17), 124.5 (C-18), 42.0 (br, CONH*C*H$_2$), 16.1 (CH$_3$);

^{15}N CPMAS NMR (30 MHZ) δ -167.7 (N-5), -257.5 (N-7), -275.6 (N-9), -14.8 (NO_2);
m/z (ES+) 383.03 [(MNa^+), 50%];
HRMS calculated for $C_{17}H_{21}O_4N_5$ (MNa^+) 382.14912, found 382.13981;
Elemental analysis calculated for $C_{17}H_{21}O_4N_5$ C, 56.82%; H, 5.89%; N, 19.49%; found C, 55.88%; H, 5.80%; N, 19.08%.

N-Hexyl-*N*-(1,4-dihydro-4-oxo-6-*p*-aminophenyl-2-pyrimidinyl)-urea (112)

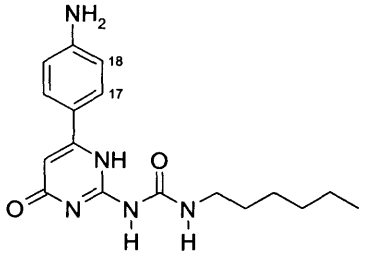

B

in chloroform

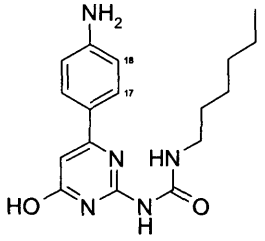

C

in DMSO and solid state

Tin (II) chloride (1.88 g, 8.30 mmol) was added to a solution of **111** (0.50 g, 1.39 mmol) in conc. HCl (15 ml) and absolute ethanol (7 ml). After stirring the mixture at r.t. for 15 min, the solution was heated at reflux for 1 h. When cooled down to r.t. The product precipitated out of solution. The product was collected by filtration and washed with (5 N) NaOH (5 ml) and water (5 ml) to give ***112*** as a yellow solid (0.25 g, 55%).

mp > 300 °C (Methanol);
ν_{max} **/cm^{-1} (KBr pellets)** 3340 & 3320 (N-H, NH_2, *s*), 1677 (C=O, *s*);
^{1}H NMR (500 MHz; $CDCl_3$; 328K) (4-keto tautomer B) δ 13.72 (1H, s, 1-H), 12.00 (1H, s, $CH_2NHCONH$), 10.17 (1H, s, $CH_2NHCONH$), 7.49 (2H, d, *J* 8.4 Hz, 17-H), 6.75 (2H, d, *J* 8.4 Hz, 18-H), 6.22 (1H, s, 5-H), 4.00 (2H, broad s, NH_2), 3.30 (2H, broad q, $CH_2NHCONH$), 1.66 (2H, m, $CH_2CH_2NHCONH$), 0.90 (3H, t, *J* 7.1 Hz, CH_3);
^{1}H NMR (500 MHz; DMSO-d_6) (pyrimidin-4-ol tautomer C) δ 10.13 (1H, s, $NHCONHCH_2$), 8.01 (1H, s, $NHCONHCH_2$), 7.51 (2H, d, *J* 8.4 Hz, 17-H), 6.57 (2H, d, *J* 8.4 Hz, 18-H), 5.87 (1H, s, 5-H), 5.34 (2H, s, NH_2), 3.20 (2H, m, $NHCONHCH_2$), 1.51 (2H, m, $NHCONHCH_2CH_2$), 1.35 (2H, m, $NH(CH_2)_2CH_2$), 1.28 (4H, m, $NH(CH_2)_3CH_2CH_2$), 0.85 (3H, m, CH_3);

^{13}C NMR (125 MHz; DMSO-d_6) δ 174.5 (C-4), 159.5 (C-6), 158.5 (C-2), 155.4 (NH*C*ONH), 149.7 (C-19), 126.9 (C-17), 125.8 (C-16), 113.3 (C-18), 98.6 (C-5), 38.8 (NHCONH*C*H_2), 31.1 (NH (CH_2)$_3$*C*H_2)), 29.6 (NHCH$_2$*C*H_2), 26.3 (NH(CH_2)$_2$*C*H_2), 22.1 (NH(CH_2)$_4$*C*H_2), 13.9 (CH_3);

^{15}N (500 MHz; DMSO-d_6) δ -186.5 (N-1), -286.0 (N-9), -319.7 (NH_2)

^{13}C CPMAS NMR (75 MHZ) δ 176.4 (C-4), 159.3 (C-6), 157.2 (NH*C*ONH), 146.5 (C-4'), 130.0 (C-1'), 129.0 (C-2'), 115.0 (C-3'), 98.5 (C-5), 41.7 (CONH*C*H_2), 33.1 (NH(CH_2)$_3$*C*H_2), 28.0 (NHCH$_2$*C*H_2), 24.5 (NH(CH_2)$_2$*C*H_2), 23.9 (NH(CH_2)$_4$*C*H_2), 16.0 (CH_3);

^{15}N CPMAS NMR (30 MHZ) δ -164.6 (N-3), -178.3 (N-1), -260.3 (N-7), -280.5 (N-9), -324.0 (NH_2);

m/z (ES+) 352 [(MNa^+), 100%];

HRMS calculated for $C_{17}H_{24}O_2N_5$ (MH^+) 330.19299, found 330.19288.

1-{6-[4-(4-Dimethylamino-phenylazo)-phenyl]-4-oxo-1,4-dihydro-pyrimidin-2-yl}-3-hexyl-urea (113)

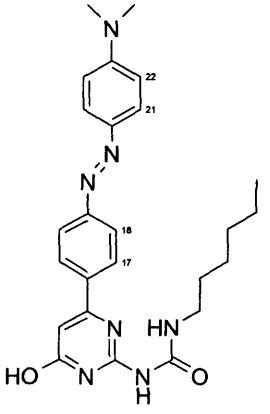

The amino compound **112** (0.10 g, 0.30 mmol) was dissolved in a mixture of acetic acid (2 ml) and conc. HCl (0.7 ml). The solution was then cooled to 5 °C. To this solution was added sodium nitrite (0.03 g, 0.03 mmol) in water (0.6 ml) at 0 °C, resulting in the formation of a yellow solution. The reaction was stirred for 15 min at 0 °C. A solution of *N,N*-dimethylaniline (0.036 g, 0.30 mol) in acetic acid (0.1 ml) at 0 °C was then added resulting in the formation of a red solution. The mixture was stirred for 30 min at r.t. A saturated sodium acetate solution was then added to the mixture in order to

increase the pH close to 6, resulting in the precipitation of the azo compound. Recrystallisation from methanol afforded ***113*** (0.030 g, 20%).

^{1}H NMR (400 MHz; DMSO-d_6) (pyrimidin-4-ol tautomer C) δ 10.21 (1H, s, N*H*CONHCH$_2$), 7.96 (2H, d, *J* 7.9 Hz, 17-H), 7.80 (2H, d *J* 9.1 Hz, 21-H), 7.78 (2H, d, *J* 7.9 Hz, 18-H), 6.83 (2H, d, *J* 9.1 Hz, 22-H), 6.04 (1H, s, 5-H), 3.18 (2H, m, NHC*H*$_2$CH$_2$), 3.06 (6H, s, NC*H*$_3$), 1.51 (2H, m, NHCH$_2$C*H*$_2$), 1.34 (2H, m, NH(CH$_2$)$_2$C*H*$_2$), 1.26 (4H, m, NH(CH$_2$)$_3$C*H*$_2$C*H*$_2$), 0.82 (3H, m, CH$_2$C*H*$_3$);

^{13}C NMR (100 MHz; DMSO-d_6) δ 175.5 (C-4), 159.5 (C-6), 158.7 (C-2), 155.8 (NH*C*ONH), 153.0, 152.97, 143.1, 140.1, 127.1, 125.1, 122.2, 112.0, 102.0 (C-5), 39.0 (NH*C*H$_2$), 30.0, 26.7, 22.4, 14.2 (CH$_2$*C*H$_3$);

m/z (ES+) 461 [(MH$^+$), 30%], 484 [(MNa$^+$), 100%];

HRMS calculated for $C_{25}H_{31}O_2N_7$ (MNa$^+$) 484.24368, found 484.17341.

N-Hexyl-*N*-(1,4-dihydro-4-oxo-6-methyl-2-pyrimidinyl)-urea (114)

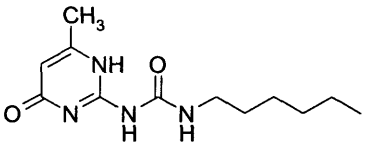

A suspension of 6-methyl-4-hydroxyl-2-amino pyrimidinone (0.50g, 4.0 mmol) and hexyl isocyanate (0.76 g, 6.0 mmol) in dry pyridine (15 ml) was heated at reflux for 16 h. After cooling, the addition of hexane resulted in the precipitation of the product, which was isolated and washed with hexane to give ***114*** (0.826 g, 82%).

mp: 184-185 °C (Hexane);

ν_{max} / cm^{-1} (KBr pellets) 3338 (N-H, *s*), 3213 (N-H, *s*), 3100 (C=C-H, *s*), 2952 (C-H, *s*), 2860 (C-H, *s*), 1706 (C=O, *s*), 1664 (C=O, *s*), 1581 (C=C, *s*);

^{1}H NMR (500 MHz; CDCl$_3$) (4[1H]-pyrimidinone tautomer B) δ 13.13 (1H, s, 1-H), 11.85 (1H, s, N*H*CONHCH$_2$), 10.14 (1H, broad t, NHCON*H*CH$_2$), 5.81 (1H, s, 5-H), 3.23 (2H, m, CONHC*H*$_2$), 2.22 (3H, s, CH$_3$), 1.59 (2H, m, NHCH$_2$C*H*$_2$), 1.32 (2H, m, NH(CH$_2$)$_2$C*H*$_2$), 1.30 (4H, m, C*H*$_2$C*H*$_2$CH$_3$), 0.87 (3H, t, *J* 6.2 Hz, CH$_2$C*H*$_3$);

^{13}C NMR (125 MHz; $CDCl_3$) 173.0 (C-4), 156.5 (NHCONH), 154.7 (C-2), 148.1 (C-6), 106.6 (C-5), 40.0 ($CONHCH_2$), 31.5 ($NH(CH_2)_3CH_2$), 29.5 ($NHCH_2CH_2$), 26.6 ($NH(CH_2)_2CH_2$), 22.5 ($NH(CH_2)_4CH_2$), 18.9 (CH_3), 14.0 (CH_2CH_3);
m/z (ES+) 253 [(MH^+), 45%], 275 [(MNa^+), 100%];
HRMS calculated for $C_{12}H_{21}O_2N_4$ (MNa^+) 275.14785, found 275.14704.

Methanesulfonic acid 2-[2-(2-methoxy-ethoxy)-ethoxy]-ethyl ester (116)[148]

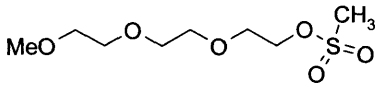

To a cooled solution of methyltriethylene glycole (0.98 g, 6.0 mmol) and triethylamine (1.87 ml, 13.38 mmol) in CH_2Cl_2 (10 ml) was added dropwise at 0 °C, a solution of methanesulfonylchloride (0.93 ml, 12.0 mmol) in CH_2Cl_2 (5 ml). After addition, the reaction mixture was stirred at r.t. until completion of the reaction. Dichloromethane (20 ml) was then added to the solution and the mixture was washed with saturated solution of $NaHCO_3$ (2 × 30 ml) and a saturated sodium chloride solution (2 × 30 ml). The organic phases were combined together and dried ($MgSO_4$). The solvent was evaporated *in vacuo* and water was removed *via* azeotropic distillation with toluene to afford **116** as an oil (1.24 g, 85%), which was used directly in the next step without further purification.

^{1}H NMR (300 MHz; $CDCl_3$) δ 4.32 (2H, m, CH_2OSO_2), 3.73 (2H, m, CH_2OMe), 3.62 (6H, m, CH_2O), 3.57 (2H, m, $CH_2CH_2OSO_2$), 3.49 (3H, s, CH_3SO_2), 3.03 (3H, s, OCH_3);

1-[2-(2-Azido-ethoxy)-ethoxy]-2-methoxy-ethane (117)[149]

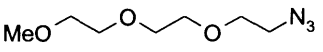

To a solution of **116** (3.82 g, 15.70 mmol) in anhydrous DMF (45 ml) was added sodium azide (6.15 g, 94.7 mmol). The mixture was stirred at r.t. until completion of the reaction. After 5 days, the solvent was evaporated and washed with water (20 ml) then with a saturated solution of sodium chloride (20 ml). The organic phase was dried ($MgSO_4$) and the solvent evaporated. Compound **117** was obtained as an oil (2.31 g, 78%).

ν_{max}/cm^{-1} (KBr film) 2160 (N=N=N, *s*);
^{1}H NMR (300 MHz; $CDCl_3$) δ 3.64-5.59 (8H, m, CH_2O), 3.52 (2H, m, CH_2OMe), 3.33-3.35 (5H, m, CH_3, CH_2N_3);
^{13}C NMR (75 MHz; $CDCl_3$) δ 71.9 (*C*H_2O), 70.7 (2 × CH_2O), 70.6 (CH_2O), 69.9 (CH_2O), 58.9 (*C*H_2O), 50.7(CH_2N_3);
HRMS calculated for $C_7H_{15}O_3N_3$ (MNa^+) 212.10056, found 212.10071.

2-[2-(2-Methoxy-ethoxy)-ethoxy]-ethylamine (115)[151]

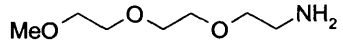

Compound **117** (2.31g, 12.2 mmol) was hydrogenated over Pd/C (10% w/w) in ethanol (45 ml) at r.t. under 1 atm. The reaction was monitored by TLC and after two days the reaction was completed. The catalyst was filtered off through celite and the solvent was evaporated to afford compound **115** as an oil (1.86 g, 93%).

ν_{max}/cm^{-1} (KBr film): 3400 (N-H, NH_2, *s*), 2877 (C-H, *s*), 1103 (C-O, *s*);
^{1}H NMR (300 MHz; $CDCl_3$) δ 3.55-3.60 (6H, m, C*H*$_2$$CH_2NH_2$, 2 × CH_2O), 3.45 (4H, m, CH_2O), 3.28 (3H, s, OMe), 2.75 (2H, t, *J* 5.2 Hz, C*H*$_2$$NH_2$), 2.27 (2H, s, NH_2);
^{13}C NMR (75 MHz; $CDCl_3$) δ 73.0 (CH_2O), 71.8 (*C*H_2O), 70.5 (CH_2O), 70.4 (CH_2O), 70.2 (CH_2O), 58.8 (OCH_3), 41.5 (CH_2NH_2);
m/z (ES+) 164 [(MH^+), 100%], 186 [(MNa^+), 20%];
HRMS calculated for $C_7H_{17}O_3N$ (MH^+) 164.12812, found 164.12794.

2-[2-(2-Methoxy-ethoxy) ethoxy]-ethanoic acid (119)[155]

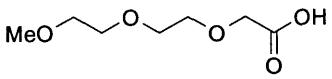

2-[2-(2-Methoxy-ethoxy)-ethoxy]-ethanol (2.0 g, 12.1 mmol), KOH (1.36 g, 24.3 mmol) and $KMnO_4$ (3.84 g, 24.3 mmol) were mixed together in water (100 ml) and stirred at r.t. for 18 h. The reaction mixture was then filtered and the distillat was acidified with conc. HCl until pH ~ 2-3. The aqueous layer was evaporated under reduced pressure and the remaining solid was dissolved in a saturated sodium chloride solution (100 ml). The aqueous phase was then extracted with chloroform (3 × 100 ml). The organic phase was then dried over $NaSO_4$ and evaporated *in vacuo*. Fractionated distillation afforded compound **119** as an oil (0.875 g, 40%).

ν_{max}/cm^{-1} (KBr film) 4300 (O-H, *s*);
^{1}H NMR (300 MHz; $CDCl_3$) δ 8.81 (1H, broad s, COOH), 4.16 (2H, s, CH_2COOH)), 3.74 (2H, m, CH_2OCH_2COOH)), 3.67 (4H, m, 2 × CH_2O), 3.55 (2H, m, CH_2OMe), 3.37 (3H, s, OCH_3);
^{13}C NMR (75 MHz; $CDCl_3$) δ 173.2 (COOH), 71.7 (CH_2COOH), 71.3 (CH_2OMe), 70.5 (CH_2O), 70.2 (CH_2O), 68.6 (CH_2O), 59.0 (OCH_3);
m/z (ES+) 133.03 [(M-COOH), 100%],179.03 [(MH^+), 20%];
HRMS calculated for $C_7H_{14}O_5$ (MH^+) 201.07334, found 201.07308.

2-[2-(2-Methoxy-ethoxy)ethoxy]-acylchloride (120)

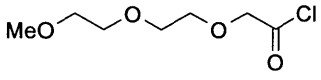

Thionyl chloride (0.90 ml, 0.12 mol) was added dropwise to a solution of 2-[2-(2-methoxy-ethoxy)ethoxy]-ethanoic acid (0.50g, 2.80 mmol) in dichloromethane (5 ml) and the solution was heated at reflux for 12 h. The solvent and excess thionyl chloride were removed *in vacuo* to afford compound **120** in quantitative yield as an oil.

ν_{max}/cm^{-1} **(KBr film)** 1803 (C=O, *s*);

^{1}**H NMR (300 MHz; CDCl$_3$)** δ 4.48 (2H, s, CH_2COCl), 3.78 (2H, m, CH_2OCH_2COCl), 3.68 (2H, m, CH_2O), 3.63 (2H, m, CH_2OCH_2OMe), 3.55 (2H, m, CH_2OMe), 3.38 (3H, s, OCH_3);

^{13}**C NMR (75 MHz; CDCl$_3$)** δ 172.0 (COCl), 71.7 (CH_2COCl), 71.2 (CH_2OCH_2COCl), 70.7 (CH_2O), 70.5 (CH_2O), 58.9 (OCH_3).

1-(2-Isocyanatomethoxy-ethoxy)-2-methoxy-ethane (122)

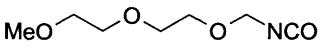

To a solution of the acid chloride (**120**) (2.81 mmol) in freshly distilled acetone (3 ml) was added, dropwise at 0 °C, a solution of sodium azide (0.728 g, 11.2 mmol) in water (5 ml). The solution was stirred for 30 min at 5 °C. The mixture was then extracted with chloroform (3 × 10 ml) and the organic phase washed with water (5 ml) and saturated sodium chloride solution (5 ml). Anhydrous toluene (3 ml) was added to the organic phase, which was dried ($MgSO_4$) for 1 h. The filtrate was partially concentrated *in vacuo* to give [2-(2-methoxy-ethoxy)]-actetyl azide (**121**) (ν_{max} 2140 cm^{-1}). The solution was directly heated at reflux for 30 min until the evolution of the nitrogen had ceased, then the solvent was evaporated *in vacuo* to give the isocyanate ***122*** (ν_{max} 2260 cm^{-1}) which was then used immediately in the next step.

1-[2-(2-Methoxy-ethoxymethyl]-3-(1,4-dihydro-4-oxo-6-*p*-nitrophenyl-2-pyrimidinyl)-urea (123)

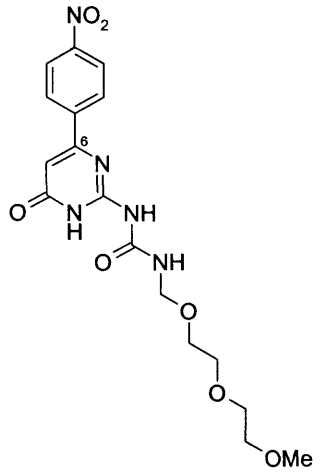

A suspension of 6-(*p*-nitrophenyl)isocytosine (**110**) (150 mg, 0.645 mmol) and **122** (2.80 mmol) in dry pyridine (10 ml) and DMF (15 ml) was heated at 90 °C for 16 h. The solvent was removed *in vacuo* and the product purified using flash silica gel chromatography ($CHCl_3$/MeOH, 35:1) to give ***123*** as a solid (32 mg, 28%).

^{1}H NMR (300 MHz; DMSO-d_6) (6 [1H]-pyrimidinone monomeric A) δ 11.92 (1H, s, 3-H), 10.30 (1H, s, N*H*CONHCH$_2$), 8.32 (2H, d, *J* 9.1 Hz, Ar 3-H), 8.23 (2H, d, *J* 9.1 Hz, Ar 2-H), 7.86 (1H, broad s, CON*H*CH$_2$), 6.72 (1H, s, 5-H), 4.67 (2H, d, *J* 6.6 Hz, NHC*H*$_2$O), 3.48-3.55 (6H, m, CH$_2$O), 3.42 (2H, m, CH$_2$O), 3.21 (3H, s, OCH$_3$);
^{13}C NMR (100 MHz; DMSO-d_6) δ 164.0 (C-4), 155.2 (NHCONH), 148.5 (Ar C-4), 142.4 (Ar C-1), 128.1 (Ar C-2), 123.8 (Ar C-3), 104.8 (C-5), 74.6 (NH*C*H$_2$O), 71.3 (CH$_2$O), 69.7(CH$_2$O), 69.6 (CH$_2$O), 67.0 (CH$_2$O), 58.0 (OCH$_3$);
m/z (ES+) 408 [(MH$^+$), 10%], 430 [(MNa$^+$), 90%].

(4-{2-[2-(2-Methoxy-ethoxy)-ethoxy]-ethoxy}-phenyl)-ethanoic acid methyl ester (126)

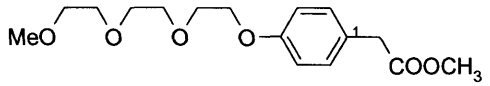

Methyl-4-hydroxy phenyl ethanoate (3.33 g, 20 mmol), 1-(2-bromo ethoxy)-2-(methoxy ethoxy)-ethane (9.07 g, 40 mmol) and potassium carbonate (11.04 g, 0.08 mol) were heated at reflux in acetonitrile (100 ml) for 18 h. The solvent was evaporated *in vacuo* and the residue was redissolved in EtOAc (100 ml) and washed with (1 N) HCl solution (100 ml) and (5 N) NaOH solution (50 ml). The organic phase was dried over ($MgSO_4$) and the solvent evaporated *in vacuo*. The crude product was purified using flash chromatography column (Hexane/EtOAc, 1:1) to give compound ***126*** as an oil (4.28 g, 77%).

ν_{max}/cm^{-1} (KBr film) 2880 (C-H, *s*), 1736 (C=O, *s*), 1614 (C=C-H, *s*), 1514 (C-O, *s*);
^{1}H NMR (400 MHz; $CDCl_3$) δ 7.15 (2H, d, *J* 8.7 Hz, Ar 2-H, 6-H), 6.90 (2H, d, *J* 8.7 Hz Ar 3-H, 5-H), 4.08 (2H, t, *J* 5.1 Hz, C*H*$_2$OAr), 3.82 (2H, t, *J* 8.7 Hz, C*H*$_2$CH$_2$OAr), 3.71 (2H, m, CH_2O), 3.53-3.65 (11H, m, CO_2CH_3, 4 × CH_2), 3.35 (3H, s, OCH_3);
^{13}C NMR (100 MHz; $CDCl_3$) δ 172.3 (COO), 157.9 (Ar C-4), 130.2 (Ar C-2, Ar C-6), 126.2 (C-1), 114.7 (Ar C-3, Ar C-5), 71.9 (*C*H_2OMe), 70.8 (CH$_2$*C*H$_2$OAr), 70.6 (*C*H_2CH$_2$O), 70.6 (*C*H_2CH$_2$O), 69.7 (*C*H_2CH$_2$O), 67.4 (*C*H_2CH$_2$O), 59.0 (OCH_3), 52.0 (COO*C*H_3), 40.3 (*C*H_2COOCH$_3$);
m/z (ES+) 335 [(MNa^+), 100%];
HRMS calculated for $C_{16}H_{25}O_6$ (MH^+) 313.16511, found 313.16512.

1-Bromo-2-[2-(2-methoxy-ethoxy)-ethoxy]-ethane (125)[158]

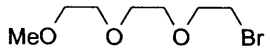

To a solution of mesylate (2.904 g, 0.012 mol) in acetone (30 ml) was added portion-wise lithium bromide (1.56 g, 0.018 mol). The solution was heated under reflux conditions for 18 h. To this solution was added a saturated sodium chloride solution (60 ml). The solution was then extracted with chloroform (60 ml) followed by diethyl ether (60 ml). The combined organic phases were dried over $MgSO_4$ and the solvents evaporated *in vacuo*. The crude product was then purified using flash chromatography column to afford ***131*** as an oil (1.843 g, 68%).

ν_{max}/cm^{-1} (KBr film) 2875 (C-H, s), 663 (C-Br);
^1H NMR (400 MHz, $CDCl_3$) δ 3.77 (2H, t, *J* 6.3 Hz, OCH_2CH_2Br), 3.66-3.63 (8H, m, CH_2CH_2O), 3.54 (2H, m, CH_2Br), 3.36 (3H, s, CH_3O);
^{13}C NMR (75 MHz, $CDCl_3$) δ 71.9 ($BrCH_2CH_2O$), 71.2 (CH_2O), 70.6 (CH_2O), 70.5 (CH_2O), 59.0 (OCH_3), 30.3 (CH_2Br);
m/z (ES+) 249 [(MNa^+), 100%];
HRMS calculated for $C_7H_{15}BrO_3$ (MNa^+) 249.00968, found 249.00965.

(4-Hexyloxy-phenyl)-acetic acid methyl ester (126a)

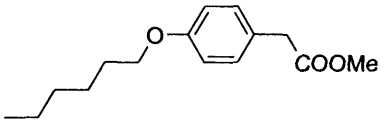

To a solution of 4-hydroxyphenylacetate (1 g, 6 mmol) in DMF (30 ml) and methanol (6 ml) was added bromohexane (1.98 g, 12 mmol) and potassium carbonate (3.31 g, 24 mmol). The solution was heated at 100 °C for 16 h. The solid was filtered off and the filtrate was evaporated *in vacuo*. The residue was redissolved in a mixture of (EtOAc/$CHCl_3$/hexane/1N HCl). The organic phase was then washed with water (20 ml) then with 5N NaOH (20 ml) and the organic phase was dried ($MgSO_4$). Evaporation of the solvents under reduced pressure afforded crude **126a,** which was purified using flash silica gel chromatography (hexane/EtOAc, 3:1). Compound ***126a*** was obtained as an oil (1.05 g, 70%).

ν_{max}/cm^{-1} **(KBr film)** 2931(C-H, *s*), 2856 (C-H, *s*), 1740 (C=O, *s*), 1610 (C=C-H, *s*), 1514 (C=C-H, *s*), 1153 (C-O, *s*);

^{1}H NMR (400 MHz, $CDCl_3$) δ 7.16 (2H, d, *J* 8.5 Hz, Ar 2-H, 6-H), 6.86 (2H, d, *J* 8.5 Hz, Ar 3-H, 5-H), 3.93 (2H, t, *J* 6.6 Hz, $ArOCH_2$), 3.68 (3H, s, $COOCH_3$), 3.56 (2H, s, CH_2COOMe), 1.76 (2H, m, CH_2CH_2OAr), 1.45-1.31 (6H, m, CH_2CH_2), 0.91 (3H, s, CH_2CH_3);

^{13}C NMR (100 MHz, $CDCl_3$) δ 172.4 (*C*OOMe), 158.3 (Ar C-4), 130.2 (Ar C-2, C-6), 125.8 (Ar C-1), 114.6 (Ar C-3, C-5), 68.0 (CH_2OAr), 52.0 ($COOCH_3$), 40.3 (CH_2COOMe), 31.6 (CH_2CH_2OAr), 29.2 (CH_2), 25.7 (CH_2), 22.6 (CH_2CH_3), 14.0 (CH_3);

HRMS calculated for $C_{15}H_{22}O_3$ (MNa^+) 273.14612, found 273.14579.

(4-Hexyloxy-phenyl)-acetic acid (126a (b))

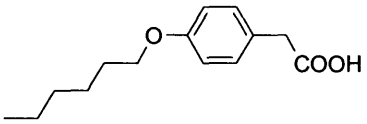

Compound **126a** (0.7 g, 2.8 mmol) was dissolved in a solution of MeOH (10 ml) and (1N) NaOH (5.6 ml). The solution was heated at reflux for 1 h 30 min. The solvent was then evaporated *in vacuo* and the residue was redissolved in water. A solution of (1N) HCl was added to the mixture in order to bring the pH to ~ 2 which led to the precipitation of a white solid. The solid was filtered off *in vacuo* and dried carefully affording compound ***126a(b)*** (0.362 g, 55%).

mp: 90-91 °C (methanol);

ν_{max}/cm^{-1} **(KBr pellet)** 2950 (C-H, *s*), 2860 (C-H, *s*), 1700 (C=O, *s*);

^{1}H NMR (300 MHz, $CDCl_3$) δ 7.15 (2H, d, *J* 8.5 Hz, Ar 2-H, 6-H), 6.88 (2H, d, *J* 8.5 Hz, Ar 3-H, 5-H), 3.93 (2H, t, *J* 6.6 Hz, CH_2OAr), 3.57 (2H, s, CH_2COOH), 1.76 (2H, m, CH_2CH_2OAr), 1.47-1.30 (6H, m, CH_2CH_2), 0.91 (3H, t, *J* 7.0 Hz, CH_3CH_2);

^{13}C NMR (75 MHz, $CDCl_3$) δ 177.9 (COOH), 158.4 (Ar C-4), 130.4 (Ar C-2, C-6), 125.1 (Ar C-1), 114.6 (Ar C-3, C-5), 68.0 (CH_2OAr), 40.1 (CH_2COOH), 31.6 (CH_2CH_2OAr), 29.2 (CH_2), 25.7 (CH_2), 22.6 (CH_2CH_3), 14.0 (CH_3);

m/z (ES+) 259 [(MNa^+), 100%];

HRMS calculated for $C_{14}H_{20}O_3$ (MH^+) 236.14124, found 236.14230.

1-Hexyloxy-4-isocyanatomethyl-benzene (127a)

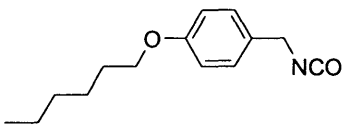

Thionyl chloride (0.46 ml, 6.3 mmol) was added dropwise to a solution of (4-hexyloxy-phenyl)-acetic acid (0.30 g, 1.27 mmol) and the solution was heated at reflux for 12 h. The excess of thionyl chloride was removed *in vacuo* to afford the acid chloride (ν_{max} 1800 cm^{-1}) in quantitative yield. To the acid chloride (0.323 g, 1.27 mmol) in freshly distilled acetone (1.3 ml) was added, dropwise at 0 °C, a solution of sodium azide (0.33 g, 5.08 mmol) in water (4 ml). The solution was stirred for 30 min at 5 °C. The mixture was then extracted with chloroform (3 × 5 ml) and the organic phase washed with cold water (5ml) and with a saturated sodium chloride solution (5 ml). Anhydrous toluene (6 ml) was added to the organic phase, which was dried ($MgSO_4$) for 30 min. This was directly heated at reflux until gas evolution ceased, then the solution was evaporated *in vacuo* to give the isocyanate ***127a*** (ν_{max} 2260 cm^{-1}), which was used directly in the next step.

1-(4-Hexyloxy-benzyl)-3-[4-(4-nitro-phenyl)-6-oxo-1,6-dihydro-pyrimidin-2-yl]-urea (128a)

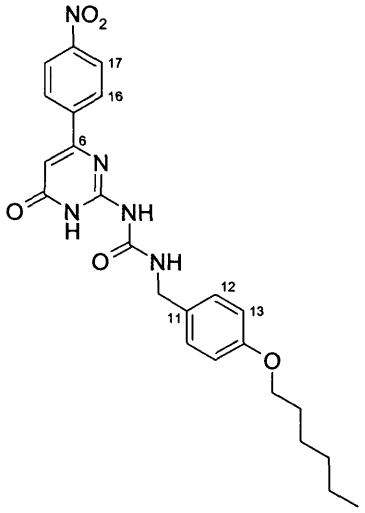

The isocyanate **127a** (1.27 mmol) was added to a solution of the amine **110** (0.1 g, 0.43 mmol) in dry pyridine (5 ml). The mixture was then heated at reflux for 16 h. The product was precipitated by addition of hexane and filtration afforded ***128a*** as a pale yellow solid (0.153 g, 77%).

mp: 274 °C (hexane);

ν_{max}/cm^{-1} (KBr pellet) 3230 (N-H, *s*), 3125 (N-H, *s*), 3100 (C=C-H, *s*), 3000 (C-H, *s*), 2943 (C-H, *s*), 1663 (C=O, *s*), 1610 (C=C, *s*), 1560 (C=C, *s*), 1520 (NO_2, *s*);

^{1}H NMR (300 MHz; DMSO-*d*$_6$) (6[1H]-pyrimidinone tautomer A) δ 11.87 (1H, s, 3-H), 10.03 (1H, s, N*H*CONHCH$_2$), 8.25 (2H, d, *J* 8.8 Hz, 17-H), 8.13 (2H, d, *J* 8.8 Hz, 16-H), 7.74 (1H, broad t, NHCON*H*CH$_2$), 7.26 (2H, d, *J* 8.5 Hz, 12-H), 6.93 (2H, d, *J* 8.5 Hz, 13-H), 6.67 (1H, s, 5-H), 4.30 (2H, d, *J* 5.4 Hz, CONHC*H*$_2$), 3.92 (2H, t, *J* 6.5 Hz, C*H*$_2$OAr), 1.68 (2H, m, C*H*$_2$CH$_2$OAr), 1.40-1.25 (6H, m, CH$_2$C*H*$_2$), 0.85 (3H, t, *J* 7.0 Hz, CH$_2$C*H*$_3$);

^{13}C NMR (100 MHz; DMSO-*d*$_6$) δ 163.1 (C-4), 157.8 (Ar C-14), 154.1 (NHCONH), 148.2 (Ar C-18), 142.2 (Ar C-15), 130.1 (Ar C-11), 128.5 (Ar C-12), 127.6 (Ar C-16), 123.3 (Ar C-17), 114.4 (Ar C-13), 103.9 (C-5), 67.4 (CH$_2$OAr), 42.3 (NHCH$_2$Ar), 30.6 (CH$_2$), 28.3 (CH$_2$), 24.8 (CH$_2$), 21.6 (CH$_2$), 13.4 (CH$_3$);

Elemental analysis calculated for $C_{24}H_{27}O_5N_5$ C, 61.92%; H, 5.85%; N, 15.04%; found C, 61.95 %; H, 6.01%; N, 14.69%.

(4-{2-[2-(2-methoxy-ethoxy)-ethoxy]-ethoxy}-phenyl)-ethanoic acid (126 (b))

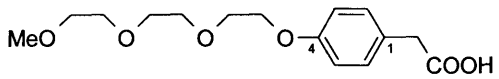

The methyl ester (0.560 g, 1.80 mmol) was mixed with a solution of (1N) NaOH (3.6 ml, 3.60 mmol) in methanol (10 ml). The solution was heated at reflux for 3 h, then the solvent was removed *in vacuo*, and the solid was redissolved in water. The aqueous phase was then acidified with (1N) HCl (15 ml) and extracted with chloroform (5 × 10 ml). The combined organic phase was dried over $MgSO_4$ and the solvent was evaporated *in vacuo* to give ***126(b)*** as an oil (0.37 g, 69%).

ν_{max}/cm^{-1} (KBr film) 3400 (O-H, *s*), 2880 (C-H, *s*), 1720 (C=O, *s*), 1614 (C=C-H, *s*), 1585 (C-O, *s*), 1514 (C-O, *s*);

^{1}H NMR (400 MHz; $CDCl_3$) δ 7.15 (2H, d, *J* 6.6 Hz, Ar 2-H, 6-H), 6.90 (2H, d, *J* 6.6 Hz, Ar 3-H, 5-H), 4.08 (2H, t, *J* 5.1 Hz, C*H*$_2$OAr), 3.82 (2H, t, *J* 5.1 Hz, C*H*$_2$CH$_2$OAr), 3.70 (2H, m, CH_2O), 3.63 (4H, m, 2 × CH_2O), 3.54 (4H, m, CH_2O + CH_2COOH), 3.35 (3H, s, OCH_3);

^{13}C NMR (100 MHz; $CDCl_3$) δ 177.2 (CO), 158.0 (C-4), 130.4 (C-2), 125.7 (C-1), 114.8 (C-3), 71.9 (CH_2OAr), 70.8 (OCH_2), 70.6 (OCH_2), 70.5 (OCH_2), 69.7 (OCH_2), 67.4 (OCH_2), 59.0 (OCH_3), 40.1 (CH_2COOH);

m/z (ES+) 321 [(MNa^+), 100 %].

HRMS Calculated for $C_{15}H_{22}O_6$ (MNa^+) 321.13086, found 321.13094.

1-Isocyanatomethyl-4-{2-[2-(2-methoxy-ethoxy)-ethoxy]-ethoxy}-benzene (127)

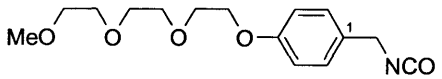

Thionyl chloride (1.44 ml, 19.8 mmol) was added slowly to a solution of (4-{2-[2-(2-methoxy-ethoxy)-ethoxy]-ethoxy}-phenyl)-ethanoic acid (1.00 g, 3.36 mmol) in dichloromethane (5 ml) and the solution was heated at reflux for 18 h. The solvent and excess thionyl chloride were removed *in vacuo* to afford (4-{2-[2-(2-methoxy-ethoxy)-ethoxy]-ethoxy}-phenyl)-acetyl chloride (ν_{max} 1800 cm^{-1}) in quantitative yield. To the acid chloride (1.05 g, 3.30 mmol) in freshly distilled acetone (3 ml) was added, dropwise at 0 °C, a solution of sodium azide (0.858 g, 13.2 mmol) in water (10 ml). The resulting red solution was stirred for 30 min at 5 °C. The mixture was then extracted with chloroform (3 × 10 ml) and the organic phase was washed with water (10 ml) and saturated sodium chloride solution (10 ml). Anhydrous toluene was added to the organic phase, which was dried ($MgSO_4$) for 1 h. The filtrate was partially concentrated *in vacuo* to give (4-{2-[2-(2-methoxy-ethoxy)-ethoxy]-ethoxy}-phenyl)-ethanoyl azide (ν_{max} 2140 cm^{-1}). This was directly heated at reflux for 30 min until the evolution of nitrogen had ceased, then evaporated *in vacuo* to give the isocyanate ***127*** (ν_{max} 2260 cm^{-1}), which was used immediately in the next step.

1-(4-{2-[2-(2-Methoxy-ethoxy)-ethoxy]-ethoxy}-benzyl)-3-[6-(4-nitro-phenyl)-4-oxo-1,4 dihydro-pyrimidin-2-yl]-urea (128)

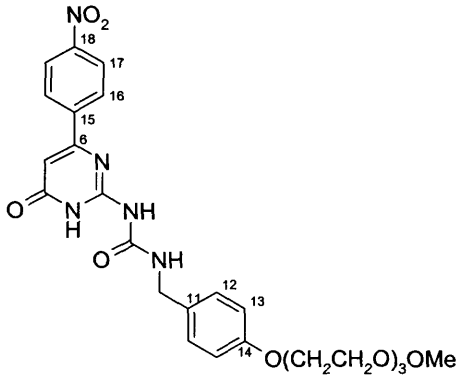

The isocyanate **127** (3.30 mmol) was added to a solution of the amine **110** (0.255 g, 1.10 mmol) in dry pyridine (10 ml). The mixture was then heated at reflux for 18 h. The product was precipitated with the addition of hexane and filtration of the solid afforded compound ***128*** as a colourless solid (0.469 g, 81%).

mp: 238-240 °C (hexane);

ν_{max} / cm^{-1} (KBr film) 3216 (N-H, *s*), 3079 (C=*C-H*, *s*), 2979 (C-H, *s*), 2931 (C-H, *s*), 1667 (C=O, *s*), 1613 (C=C, *s*), 1559 (C=C, *s*);

^{1}H NMR (400 MHz; DMSO-d_6) (6[1H]-pyrimidinone tautomer A) δ 11.92 (1H, s, 3-H), 10.07 (1H, s, N*H*CONHCH$_2$), 8.25 (2H, d, *J* 8.8 Hz, 17-H), 8.13 (2H, d, *J* 8.8 Hz, 16-H), 7.74 (1H, broad t, CON*H*CH$_2$), 7.26 (2H, d, *J* 8.5 Hz, 12-H), 6.93 (2H, d, *J* 8.5 Hz, 13-H), 6.67 (1H, s, 5-H), 4.31 (2H, d, *J* 5.4 Hz, CONHC*H*$_2$), 4.06 (2H, m, C*H*$_2$OAr), 3.73 (2H, m, C*H*$_2$O), 3.56 (2H, m, C*H*$_2$O), 3.51 (4H, m, 2 × C*H*$_2$O), 3.42 (2H, m, C*H*$_2$O), 3.35 (3H, s, OCH$_3$);

^{13}C NMR (125 MHz; DMSO-d_6) δ 161.6 (C-4), 159.1 (C-6), 157.7 (C-14), 154.5 (NH*C*ONH), 152.1 (C-2), 148.4 (C-18), 142.3 (C-15), 130.7 (C-11), 128.9 (C-12), 127.9 (C-16), 123.7 (C-17), 114.5 (C-13), 104.2 (C-5), 71.3 (*C*H$_2$OAr), 69.9 (CH$_2$O), 69.8 (CH$_2$O), 69.6 (CH$_2$O), 68.9 (CH$_2$O), 67.1 (CH$_2$O), 58.1 (OCH$_3$), 42.4 (NH*C*H$_2$Ar);

m/z (+FAB) 550 [(MNa$^+$), 100%];

HRMS calculated for $C_{25}H_{29}N_5O_8$ (MNa$^+$) 550.19083, found 550.19059.

1-(4-{2-[2-(2-Methoxy-ethoxy)-ethoxy]-ethoxy}-benzyl)-3-[6-(4-aminophenyl)-4-oxo-1, 4-dihydro-pyrimidin-2yl]-urea (129)

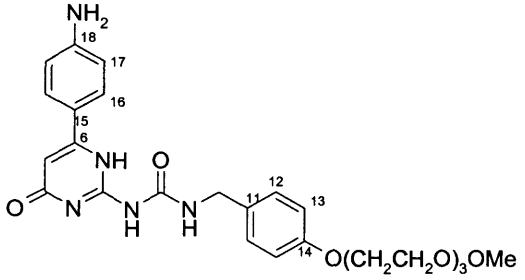

B

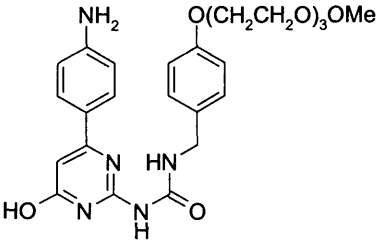

C

Tin II chloride (0.857 g, 3.80 mmol) was added to a solution of **128** (0.334 g, 0.634 mmol) in conc. HCl (7.5 ml) and absolute ethanol (3.75 ml). The solution was heated at 90 °C for 2 h. The yellow solution was then poured into ice and the pH adjusted to 8-9 by addition of sodium hydrogen carbonate. The aqueous layer was then extracted with chloroform (5 × 10 ml) and the organic phase was washed with saturated sodium chloride solution (10 ml) and then dried (MgSO$_4$). The solvents were evaporated *in*

vacuo and the product was purified using flash silica gel chromatography ($CHCl_3$/MeOH, 7:1) to give ***129*** as an oil (200 mg, 63%).

ν_{max} / cm^{-1} (KBr film) 3448 (N-H, *s*, NH_2), 3363 (N-H, *s*, NH_2), 3219 (N-H, *s*), 2937 (C-H, *s*) 1693 (C=O, *s*), 1667 (C=O, *s*), 1623 (C=C, *s*), 1600 (C=C, *s*), 1512 (C-O, *s*);
^{1}H NMR (500 MHz; $CDCl_3$) (4[1H]-pyrimidinone, tautomer B) δ 13.66 (1H, s, 1-H), 12.17 (1H, s, N*H*CONHCH$_2$), 10.89 (1H, s, CON*H*CH$_2$), 7.45 (2H, d, *J* 7.3 Hz, 12-H), 7.31 (2H, d, *J* 8.2 Hz, 16-H), 6.87 (2H, d, *J* 7.3 Hz, 13-H), 6.73 (2H, d, *J* 8.2 Hz, 17-H), 6.21 (1H, s, 5-H), 4.46 (2H, s, CONHC*H*$_2$), 4.16-3.44 (12H, m, C*H*$_2$O), 3.36 (3H, s, OCH_3); **(pyrimidin-4-ol, tautomer C)** δ 13.24 (1H, s, OH), 11.41 (1H, s, N*H*CONHCH$_2$), 10.19 (1H, s, CON*H*CH$_2$), 7.37 (2H, d, *J* 8.2 Hz, 16-H), 7.13 (2H, d, *J* 8.2 Hz, 17-H), 4.43 (2H, s, CONHC*H*$_2$), 4.16-3.44 (12H, m, C*H*$_2$O), 3.41 (3H, s, OCH_3);
^{13}C NMR (125 MHz, $CDCl_3$) (4[1H]-pyrimidinone, tautomer B) δ 173.1 (CO), 157.9 (C-14), 157.0 (NH*C*ONH), 149.7 (C-18), 131.3 (C-11), 128.7 (C-12), 127.1 (C-16), 120.0 (C-15), 115.2 (C-18), 114.6 (C-13), 101.7 (C-5), 71.9-67.4 (CH_2O) (signal overlap), 60.4-38.7 (several signals not assignable to each tautomer);
^{13}C NMR (100 MHz; DMSO-d_6) (pyrimidin-4-ol, DADA, tautomer C) 165.5 (C-OH), 161.0 (C-6), 157.7 (C-14), 154.6 (NH*C*ONH), 153.2 (C-2), 151.0 (C-18), 131.0 (C-11), 129 (C-12), 127.7 (C-16), 123 (C-15), 114.5 (C-13) 113.3 (C-18), 98.0 (C-5), 71.3 (CH_2O), 67.0 (CH_2O), 69.8 (CH_2O), 69.0 (CH_2O), 67.2 (CH_2O), 58.1 (OCH_3), 42.4 (NH*C*H$_2$);
HRMS calculated for $C_{15}H_{22}O_6$ (MH^+) 498.23471, found 498.23376.

6.3 Synthesis of polymers and energetic precursors

2(6-Isocyanatohexylaminocarbonylamino)-6-methyl-4[1H]pyrimidone (131)[127]

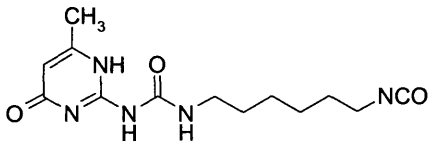

A solution of 2-amino-4-hydroxy-6-methyl-pyrimidine (0.20 g, 1.60 mmol) in hexyldiisocyanate (2.77 g, 11.0 mmol) was heated at 100 °C under a nitrogen atmosphere for 16 h. Hexane was added and the resulting precipitate was filtered and washed thoroughly with hexane in order to remove the unreacted diisocyanate. The white powder was dried at 50 °C under reduced pressure for 24 h to give **131** (3.75 g, 80%).

mp: 210 °C (chloroform, lit. 215 °C);

ν_{max} **/cm^{-1} (KBr pellets)** 3100-3350 (N-H, *s*), 2277 (N=C=O, *s*), 1702 (C=O, *s*), 1668 (C=O, *s*, urea);

^{1}H NMR (300 MHz; $CDCl_3$) δ 13.10 (1H, s, 1-H), 11.85 (1H, s, N*H*CONHCH$_2$), 10.16 (1H, s, NHCHN*H*CH$_2$), 5.81 (1H, s, 5-H), 3.28 (4H m, NHCONHC*H*$_2$, C*H*$_2$NCO), 2.28 (3H, s, CH$_3$), 1.62 (4H, m, NHCH$_2$C*H*$_2$, C*H*$_2$CH$_2$NCO), 1.40 (4H, m, CH$_2$);

^{13}C NMR (75 MHz; $CDCl_3$) δ 172.4 (C-4), 157.0 (NHCONH), 155.1 (C-2), 148.6 (C-6), 121.5 (N=C=O), 107.1 (C-5), 43.3 (*C*H$_2$NCO), 40.2 (*C*H$_2$NH), 31.6 (*C*H$_2$CH$_2$NH), 29.7 (CH$_2$), 26.6 (CH$_2$), 26.5 (CH$_2$), 19.3 (CH$_3$);

m/z (ES+) 294 [(MH$^+$), 100%];

HRMS calculated for $C_{13}H_{19}O_3N_5$ (MH$^+$) 316.13855, found 316.13470.

6.3.1 Synthesis of Polymer

General procedure

To a solution of polyethyleneglycol (n = 6) (48.0 mg, 0.17 mmol) in chloroform (12 ml), was added compound **131** (0.20 g, 0.68 mmol) with the addition of one drop of

dibutyltindilaurate, and the reaction mixture was heated at reflux for 20 h. Chloroform (10 ml) was then added and the mixture was filtered off *in vacuo* to remove the excess of isocyanate. The filtrate was concentrated down to 10 ml, and silica gel (200 mg) was added together with a drop of dibutyldilaurate. The solution was heated to 60 °C for 1 h. The silica gel was then removed by filtration and the chloroform was evaporated *in vacuo*. Precipitation of the polymer from chloroform with hexane gave polymer ***132,*** which was then dried *in vacuo* at 50 °C (95 mg, 63%). The absence of isocyanate in the final compound was confirmed by IR.

ν_{max} **/cm^{-1} (KBr pellets)** 3500 (N-H, s), 3440 (N-H, *s*), 3000 (C=*C-H, s*), 1700 (C=O, *s*, amide), 1667 (C=O, *s*, urea);

T_g: -26.7 °C;

^{1}H NMR (300 MHz; $CDCl_3$) δ 13.10 (1H, s, 1-H), 11.82 (1H, s, N*H*CONHCH$_2$), 10.24 (1H, s, NHCON*H*CH$_2$), 5.84 (1H, s, H-5), 5.14 & 4.84 (1H, s, NHCOO), 4.16 (2H, m, COOC*H*$_2$CH$_2$O), 3.59 (10H, m, CH$_2$O), 3.24 (2H, m, CH$_2$C*H*$_2$NHCO) 3.14 (2H, m, C*H*$_2$NHCOO), 2.21 (3H, s, CH$_3$), 1.56-1.26 (8H, m, CH$_2$);

^{13}C NMR (75 MHz; $CDCl_3$) δ 173.1 (C-4), 156.9 (NHCONH), 156.8 (NHCOO), 155.7 (C-2), 148.6 (C-6), 107.0 (C-5), 73.0 (NHCOOCH$_2$), 70.9 (NHCOOCH$_2$CH$_2$), 70.9 (OCH$_2$), 70.6 (OCH$_2$), 62.0 (OCH$_2$), 41.2 (NHCONHCH$_2$), 40.0 (CH$_2$NHCOO), 30.1 (NHCONHCH$_2$CH$_2$), 29.6 (CH$_2$), 26.5 (CH$_2$), 19.2 (CH$_3$);

m/z (ES+) 869.66 [(MH$^+$), 15%], 891.66 [(MNa$^+$), 20%].

Polymer **133**

T_g: -24.9 °C;

ν_{max} **/cm^{-1} (KBr pellet)** 1699 (C=O, *s*), 1667 (C=O, *s*);

^{1}H NMR (300 MHz; $CDCl_3$) δ 13.10 (1H, s, 1-H), 11.82 (1H, s, N*H*CONHCH$_2$), 10.09 (1H, s, NHCON*H*CH$_2$), 5.81 (1H, s, 5-H), 5.11 & 4.85 (1H, s, NHCOO), 4.17 (2H, m, COOC*H*$_2$CH$_2$O), 3.57 (26H, m, CH$_2$O), 3.25 (2H, m, CH$_2$C*H*$_2$NHCO), 3.15 (2H, m, C*H*$_2$NHCOO), 2.20 (3H, s, CH$_3$), 1.48-1.25 (8H m, CH$_2$).

Polymer **134**

T_g: -44 °C;

ν_{max} /cm^{-1} (KBr pellet) 1694 (C=O, *s*), 1661 (C=O, *s*);

^{1}H NMR (300 MHz; $CDCl_3$) δ 13.10 (1H, s, 1-H), 11.83 (1H, s, N*H*CONHCH$_2$), 10.11 (1H, s, NHCON*H*CH$_2$), 5.81 (1H, s, 5-H), 5.0 & 4.89 (1H, s, NHCOO), 4.17 (2H, m, COOC*H*$_2$CH$_2$O), 3.61 (62H, m, CH$_2$O), 3.21 (2H, m, CH$_2$C*H*$_2$NHCO), 3.08 (2H, m, C*H*$_2$NHCOO), 2.20 (3H, s, CH$_3$), 1.48-1.25 (8H m, CH$_2$).

Polymer **135**

ν_{max} /cm^{-1} (KBr pellet) 3342 (N-H, *s*), 1700 (C=O, *s*), 1660 (C=O, *s*, urea);

^{1}H NMR (300 MHz; $CDCl_3$) δ 13.10 (1H, s, 1-H), 11.82 (1H, s, N*H*CONHCH$_2$), 10.09 (1H, s, NHCON*H*CH$_2$), 5.81 (1H, s, 5-H), 4.94 & 4.71 (1H, s, NHCOO), 4.17 (2H, m, COOC*H*$_2$CH$_2$O), 3.50 (178H, m, CH$_2$O), 3.36 (2H, m, CH$_2$C*H*$_2$NHCO), 3.12 (2H, m, C*H*$_2$NHCOO), 2.19 (3H, s, CH$_3$), 1.48-1.24 (8H m, CH$_2$);

^{13}C NMR (75 MHz; $CDCl_3$) 172.5 (C-4), 156.5 (NHCONH), 154.7 (NHCOO), 148.2 (C-6), 106.1 (C-5), 70.5 (OCH$_2$), 69.6 (OCH$_2$), 69.6 (OCH$_2$), 29.7 (CH$_2$), 29.3 (CH$_2$), 26.1 (CH$_2$), 18.8 (CH$_3$);

Polymer **136**

T_g: -60.4 °C;

^{1}H NMR (300 MHz; $CDCl_3$) δ 13.10 (1H, s, 1-H), 11.84 (1H, s, N*H*CONHCH$_2$), 10.11 (1H, s, NHCON*H*CH$_2$), 5.83 (1H, s, 5-H), 4.95 & 4.76 (1H, s, NHCOO), 4.19 (2H, m, COOC*H*$_2$CH$_2$O), 3.63 (12H, m, CH$_2$O), 3.59 (21H, m, C*H*$_2$CHCH$_3$), 3.38 (12H, m, C*H*CH$_3$), 3.31 (2H, m, NHCONHC*H*$_2$CH$_2$), 3.15 (2H, m, CH$_2$NHCOO), 2.21 (3H, s, CH$_3$), 1.59-1.26 (8H, m, CH$_2$), 1.13 (33H, m, C*H*$_3$CHCH$_2$O);

Polymer **137**

T_g: -63.7 °C;

^{1}H NMR (300 MHz; $CDCl_3$) δ 13.10 (1H, s, 1-H), 11.84 (1H, s, N*H*CONHCH$_2$), 10.11 (1H, s, NHCON*H*CH$_2$), 5.83 (1H, s, 5-H), 4.96 & 4.73 (1H, s, NHCOO), 4.19 (2H, m, COOC*H*$_2$CH$_2$O), 3.63 (60H, m, CH$_2$O), 3.59 (38H, m, C*H*$_2$CHCH$_3$), 3.41 (22H, m, C*H*CH$_3$), 3.30 (2H, m, NHCONHC*H*$_2$CH$_2$), 3.14 (2H, m, CH$_2$NHCOO), 2.21 (3H, s, CH$_3$), 1.49-1.26 (8H, m, CH$_2$), 1.13 (57H, m, C*H*$_3$CHCH$_2$O);

^{13}C NMR (75 MHz; $CDCl_3$) δ 173.0 (C-4), 156.5 (NHCONH), 155.7 (NHCOO), 148.2 (C-6), 106.6 (C-5), 75.5 (*C*HCH$_2$O), 75.3, 75.1, 73.3, 72.8, 70.5, 69.6, 68.5, 41.7, 39.6, 30.1, 29.7, 29.2, 18.8, 17.4, 17.3.

Polymer **138**

T_g: -64.5 °C;

^{1}H NMR (500 MHz; $CDCl_3$) δ 13.10 (1H, s, 1-H), 11.85 (1H, s, NHCONHNH$_2$), 10.11 (1H, s, NHCONHCH$_2$), 5.83 (1H, s, 5-H), 4.94 (1H, s, NHCOO), 4.11 (32H, m, OCOCH$_2$), 3.43 (64H, m, OCH$_2$), 3.24 (2H, m, NHCONHCH$_2$), 3.13 (2H, m, CH$_2$NHCO), 2.21 (3H, s, CH$_3$), 1.73-1.62 (96H, m, OCH$_2$CH$_2$CH$_2$), 1.36-1.22 (8H, m, CH$_2$);

^{13}C NMR (125 MHz; $CDCl_3$) δ 173.0 (C-4), 156.6 (NHCOO), 156.4 (NHCONH), 155.2 (OCOO), 154.6 (C-2), 148.2 (C-6), 106.5 (C-5), 70.2 (CH$_2$O), 70.1 (CH$_2$), 70.0 (CH$_2$O), 69.9 (CH$_2$O), 67.8 (CH$_2$O), 67.6, 67.2, 67.0, 64.3, 40.5 (*C*H$_2$NHCOO), 39.5 (NHCONH*C*H$_2$), 29.6 (*C*H$_2$CH$_2$NHCOO), 29.2 (NHCONHCH$_2$*C*H$_2$), 26.4 (CH$_2$), 25.9 (NHCONHCH$_2$CH$_2$*C*H$_2$), 25.8 (CH$_2$), 25.5 (CH$_2$), 18.8 (CH$_3$).

Pyrrole-1-carboxylic acid (6-methyl-4-oxo-1,4-dihydro-pyrimidin-2-yl)-amide (139)[131]

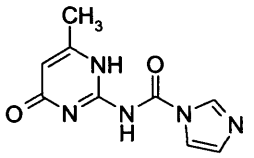

4-hydroxy-methyl-pyrimidinone (0.5 g, 4.0 mmol) and CDI (1.03 g, 6.40 mmol) were suspended in anhydrous DMSO (10 ml) and the solution was heated at 60 °C for 2 h. To this solution was then added acetone, and the solid was filtered *in vacuo*, and washed thoroughly with acetone to afford compound **139** as an insoluble solid (0.840 g, 96%).

ν_{max}/cm^{-1} (KBr pellets) 3176 (N-H, *s*), 3089 (C=*C-H*, *s*), 2933 (C-H, *s*), 1708 (C=O, s), 1653 (C=N, s)), 1608, 1508 (N-H, *d*), 1481, 1377.

6-Amino-hexanoic acid methyl ester hydrochloride (143)[162]

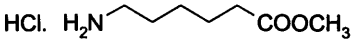

Thionyl chloride (0.55 ml, 7.6 mmol) was added slowly to anhydrous MeOH (10 ml) at -10 °C. After 15 min, 6-aminohexanoic acid was added dropwise and the mixture was stirred at r.t. for 16 h. The solution was then concentrated *in vacuo* and the residue was dissolved in MeOH (5 ml). To this was added ether (25 ml) to precipitate the salt. Filtration of the solid afforded pure compound **143** as white crystals (0.560 g, 81%).

mp: 116-118 °C (methanol, lit. 118-122°C);

ν_{max}/cm^{-1} (KBr pellet) 3100-2900 (NH_3^+, *s*), 2530 (NH_3^+, *s*), 1996 (NH_3^+, *s*), 1732 (C=O, *s*), 1620 (NH_3^+, *d, asym*), 1581 (NH_3^+, *d, sym*), 1521 (NH_3^+, *d*);

^{1}H NMR (300 MHz; CD_3OD) δ 3.65 (3H, s, $COOCH_3$), 2.91 (2H, t, *J* 7.4 Hz, CH_2NH_2), 2.35 (2H, *J* 7.3 Hz, CH_2COOCH_3), 1.66 (4H, m, $CH_2CH_2COOCH_3$, $CH_2CH_2NH_2$), 1.42 (2H, m, CH_2);

^{13}C NMR (75 MHz; CD_3OD) δ 175.6 (*C*$OOCH_3$), 52.0 ($COOCH_3$), 40.6 (*C*H_2NH_2), 34.4 (*C*H_2COOCH_3), 28.2 (*C*$H_2CH_2NH_2$), 26.9 (*C*$H_2CH_2CH_2NH_2$), 25.4 (*C*$H_2CH_2COOCH_3$);

m/z (ES+) 216 [($MH^+ + Cl^-$), 100%].

6-[3-(6-Methyl-4-oxo-1,4-dihydro-pyrimidin-2-yl)-ureido]-hexanoic acid methyl ester (140)

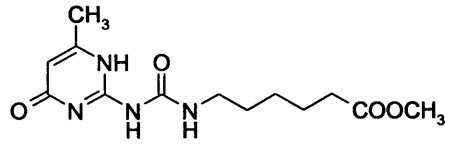

Compound **143** (0.248 g, 1.36 mmol) was dissolved in THF (15 ml) and triethylamine (0.141 g, 1.4 mmol). To this solution was added compound **139** (0.20 g, 0.91 mmol) and the reaction mixture was heated at reflux for 16 h. The solution was cooled down to r.t. and the solvents were evaporated *in vacuo*. The residue was redissolved in chloroform and the organic phase was washed with water (2 × 15 ml) then saturated sodium chloride solution (15 ml) and the organic phase was dried ($MgSO_4$). The solvent was evaporated *in vacuo* and the residue was purified through flash silica gel chromatography ($CHCl_3$/MeOH, 7:1) to afford compound ***140*** as a solid (0.220 g, 81%).

mp: 140-142 °C (methanol);

ν_{max}/cm^{-1} (KBr pellets) 3213 (N-H, *s*), 3151 (N-H, *s*), 3020 (C=C-H, *s*), 2960 (C-H, *s*), 2866 (C-H, *s*), 1726 (C=O, *s*), 1700 (C=O, *s*), 1664 (C=O, *s*, urea), 1583 (C=C, *s*).

^{1}H NMR (400 MHz; $CDCl_3$) δ 13.08 (1H, s, 1-H), 11.83 (1H, s, 7-H), 10.16 (1H, s, 9-H), 5.83 (1H, s, 5-H), 3.63 (3H, s, $COOCH_3$), 3.21 (2H, q, *J* 7.1 Hz, $NHCONHCH_2$), 2.29 (2H, t, *J* 7.5Hz, CH_2COOCH_3), 2.21 (3H, s, CH_3), 1.61 (4H, m, $NHCH_2CH_2$, $NHCH_2CH_2CH_2$), 1.36 (2H, m, CH_2);

^{13}C NMR (100 MHz; $CDCl_3$) 174.0 (C-4), 173.0 (*C*$OOCH_3$), 156.6 (NH*C*ONH), 154.7 (C-2), 148.1 (C-6), 106.7 (C-5), 51.4 ($COOCH_3$), 39.8 ($NHCH_2$), 34.0 (*C*H_2COOCH_3), 29.1 ($NHCH_2CH_2$), 26.5 ($NHCH_2CH_2CH_2$), 24.6 (*C*$H_2CH_2COOCH_3$), 18.9 (CH_3);

m/z (ES+) 297 [(MH^+), 70%], 319 [(MNa^+), 100%], 593 [($2MH^+$), 20%], 615 [($2MNa^+$), 65%];

HRMS calculated for $C_{13}H_{20}N_4O_4$ (MH^+) 297.15573, found 297.15522.

6-[3-(6-Methyl-4-oxo-1,4-dihydro-pyrimidin-2-yl)-ureido]-hexanoic acid (141)

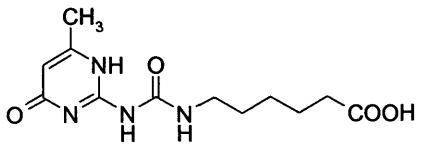

Compound **140** (0.60 g, 2.0 mmol) was dissolved in THF (2.5 ml) and (2 N) HCl (4 ml). The solution was heated at reflux for 2h and then cooled down to r.t. allowing the precipitation of a white solid. The solid was filtrated and washed with water then acetone affording compound ***141***, which was used directly without further purification (0.33 g, 58%).

mp: 216-218 °C (acetone);
ν_{max}/cm^{-1} (KBr pellets) 3400 (O-H, *s*), 3215 (N-H, *s*), 3142 (N-H, *s*), 3041 (C=C-H, *s*), 2931 (C-H, *s*), 2858 (C-H, *s*), 1726 (C=O, *s*), 1703 (C=O, *s*), 1662 (C=O, *s*), 1595 (C=C, *s*);
m/z (ES+) 283 [(MH^+), 100%], 305 [(MNa^+), 80%], 565 [($2MH^+$), 20%];
HRMS calculated for $C_{12}H_{18}O_4N_4$ (MH^+) 283.14008, found 283.13933.

6-[3-(6-Methyl-4-oxo-1,4-dihydro-pyrimidin-2-yl)-ureido]-hexanoic acid 4-{6-[3-(6-methyl-4-oxo-1,4-dihydro-pyrimidin-2-yl)-ureido]-hexanoyloxy-butyl ester (144)

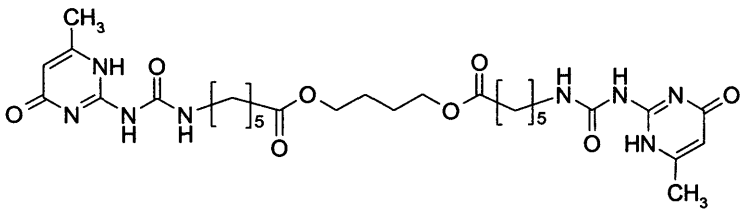

To a solution of **141** (0.22 g, 0.78 mmol) in CH_2Cl_2 was added thionyl chloride (0.34 ml, 4.7 mmol). The solution was stirred at r.t. for 4 h, and the solvent and excess of thionyl chloride were evaporated *in vacuo*. The formation of the acid chloride was

confirmed by IR (ν_{max} ~ 1800 cm^{-1}). The crude acid azide (0.78 mmol) was dissolved in THF (1 ml) and a solution of 1,4-butanediol (0.26 mmol) in CH_2Cl_2 (1 ml) was added. To this solution was added a drop of triethylamine and the solution was stirred at r.t. for 16 h. The solvents were evaporated *in vacuo* and the crude material was purified through flash silica gel chromatography ($CHCl_3$/MeOH, 9:1) affording compound ***144*** (0.230 g, 48%) as a solid.

mp: 114-115 °C (methanol);

ν_{max} **/cm^{-1} (KBr pellets)** 3211 (N-H), 3149 (N-H), 3030 (C=*C-H*), 2958 (C-H), 1733 (C=O), 1703 (C=O), 1666 (C=O);

^{1}H NMR (500 MHz; $CDCl_3$) δ 13.09 (1H, s, 1-H), 11.82 (1H, s, 7-H), 10.15 (1H, s, 9-H), 5.81 (1H, s, 5-H), 4.07 (2H, t, $COOCH_2CH_2$), 3.23 (2H, m, $NHCONHCH_2$), 2.30 (2H, t, CH_2COO), 2.23 (3H, s, CH_3), 1.67 (2H, m, $COOCH_2CH_2$), 1.65 (2H, m, CH_2CH_2COO), 1.62 (2H, $NHCONHCH_2CH_2$), 1.41 (2H, m, $NHCH_2CH_2CH_2$);

^{13}C NMR (125 MHz; $CDCl_3$) δ 173.5 (COO), 172.9 (C-4), 156.4 (NHCONH), 154.6 (C-2), 148.2 (C-6), 63.6 ($COOCH_2$), 39.7 ($NHCH_2$), 34.1 (CH_2COO), 29.1 ($NHCH_2CH_2$), 26.4 ($NHCH_2CH_2CH_2$), 25.2 ($COOCH_2CH_2$), 24.5 (CH_2CH_2COO), 18.8 (CH_3);

m/z (ES+) 144 [(MH^+), 100%];

HRMS calculated for $C_{28}H_{42}O_8N_8$ (MNa^+) 641.30178, found 641.30229.

4-Benzyloxy-3-oxo-butyric acid ethyl ester (145)[165]

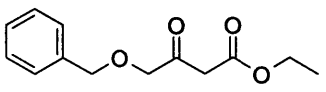

To a suspension of sodium hydride (60% in parrafine oil, 0.210 g, 5.29 mmol) in toluene (5 ml) was added dropwise over 1 h, benzyl alcohol (0.50 g, 4.60 mmol) in toluene (2 ml). The solution was stirred at r.t. for 2 h. To this slurry solution was then added chloroacetoacetate (0.377 g, 2.3 mmol) in toluene (2 ml) over 30 min. The reaction mixture was stirred at r.t. for 16 h. To this reaction was then added (2 N) citric acid (8 ml). The organic phase was then separated and the aqueous phase was extracted with toluene (3 × 10 ml). The organic phases were combined and dried ($MgSO_4$) to give

an orange oil. The crude material was further purified using flash silica gel chromatography (hexane/EtOAc, 4:1) to afford compound **145** as a yellow oil (0.43 g, 80%).

ν_{max}/cm^{-1} (KBr film) 2979 (C-H, *s*), 2923 (C-H, *s*), 2867 (C-H, *s*), 1744 (C=O, *s*), 1726 (C=O, *s*), 1657 (C=O, *s*), 1452, 1317, 1262 (C-H, *d*);
^{1}H NMR (400 MHz; $CDCl_3$) δ 7.31 (5H, m, Ar-H), 4.56 (2H, s, CH_2Ar), 4.16-4.12 (4H, m, $COOCH_2CH_3$, OCH_2CO), 3.51 (2H, s, $COCH_2COOCH_2CH_3$), 1.20 (3H, t, *J* 7.7 Hz, $COOCH_2CH_3$);
^{13}C NMR (100 MHz; $CDCl_3$) δ 201.8 (CO), 167.1 (COO), 136.9 (Ar C-1), 128.6 (Ar), 128.1 (Ar), 127.0 (Ar), 74.8 (OCH_2CO), 73.5 (CH_2Ar), 61.5 ($COOCH_2CH_3$), 46.1 ($COCH_2COOCH_2CH_3$), 14.1 (CH_3);
m/z (ES+) 259.07 [(MNa^+), 100%];
HRMS calculated for $C_{13}H_{16}O_4$ (MNa^+) 259.09408, found 259.09422.

2-Amino-6-benzyloxymethyl-1H-pyrimidin-4-one (146)

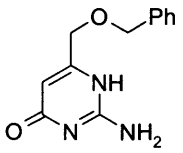

β–keto ester **145** (0.358 g, 1.51 mmol) and guanidine carbonate (0.136 g, 0.758 mmol) were dissolved in ethanol (5ml) and the mixture was heated at reflux for 18 h. The solution was then cooled down to r.t. and the product crystallised from the solution. Crystals were filtered off and washed thoroughly with cold water and acetone. The crude product was then purified through flash silica gel chromatography ($CHCl_3$/MeOH, 5:1) to afford compound ***146*** as a solid (0.175 mg, 50%).

mp: 182-184 °C (methanol);
ν_{max}/cm^{-1} (KBr pellet) 3342 (N-H, *s*, NH_2), 3142 (N-H, *s*), 2951 (C-H, *s*), 2857 (C-H, *s*), 1675 (C=C, *s*), 1619, 1596, 1475, 1447, 1350, 1119, 989;
^{1}H NMR (300 MHz; DMSO-d_6) δ 7.33 (5H, m, Ar-H), 6.49 (2H, broad s, NH_2), 5.61 (1H, s, 5-H), 4.53 (2H, s, CH_2Ar), 4.15 (2H, s, CH_2OCH_2Ar);

^{13}C NMR (75 MHz; DMSO-d_6) δ 166.4 (C-6), 162.8 (C-2), 155.6 (C-4), 138.0 (Ar C-1), 128.2 (Ar C-3), 127.4 (Ar C-2, Ar C-4), 97.7 (C-5), 71.9 (CH_2Ph), 71.1 (CH_2OCH_2Ph);

m/z (ES+) 232 [(MH^+), 100%], 254 [(MNa^+), 60%];

HRMS (FAB) calculated for $C_{12}H_{13}O_2N$ (MH^+) 3232.10805, found 232.10750.

1-(6-Benzyloxymethyl-4-oxo-1,4-dihydro-pyrimidin-2-yl)-3-hexyl-urea (147)

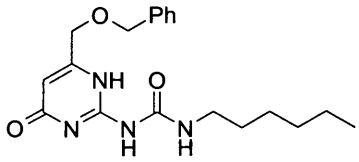

To a solution of the amine **146** (0.034 g, 0.15 mmol) in dry pyridine (1 ml) was added hexyl isocyanate (0.043 g, 0.22 mmol). The solution was then heated at 90 °C for 18 h. The solution was cooled down to r.t. and a white solid precipitated out of the solution. The solid was then filtered off and washed thoroughly with hexane to afford compound *147* as a solid (0.042 g, 80%).

mp: 186-187 °C (hexane);

ν_{max}/cm^{-1} (KBr pellet): 3203 (N-H, *s*), 3137 (N-H, *s*), 3035 (C=*C-H*, *s*), 2960 (C-H, s), 2856 (C-H, *s*), 1696 (C=O, *s*), 1667 (C=O, urea, *s*);

^{1}H NMR (300 MHz; $CDCl_3$) (4-keto tautomer) δ 13.47 (1H, s, 1-H), 11.82 (1H, s, 7-H), 10.03 (1H, s, 9-H), 7.4 (5H, m, Ar-H), 5.91 (1H, s, 5-H), 4.67 (2H, s, CH_2Ar), 4.39 (2H, s, CH_2OCH$_2$Ar), 3.28 (2H, m, NHCONHCH_2), 1.61 (2H, m, NHCONHCH$_2$CH_2), 1.32 (6H, m, CH_2), 0.90 (3H, m, CH_2CH_3);

m/z (ES+) 381 [(MNa^+), 100%], 740 [($2MNa^+$), 10%];

HRMS (FAB) calculated for $C_{19}H_{26}O_3N_4$ (MNa^+) 381.18971, found 381.18900;

Elemental analysis calculated for $C_{19}H_{26}O_3N_4$ C, 63.67%; H, 7.31%; N, 15.63%; found C, 63.44%; H, 7.37%; N, 15.44%.

1-Hexyl-3-(6-hydroxymethyl-4-oxo-1,4-dihydro-pyrimidin-2-yl)-urea (148)

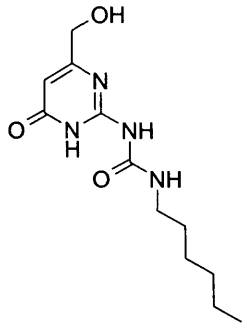

To a suspension of compound **147** (0.120 g, 0.335 mmol) in CH_2Cl_2 (12 ml) was added slowly at -50 °C a solution of BCl_3 (1N, in CH_2Cl_2, 0.67 ml, 0.67 mmol). The solution was stirred at low temperature for 1 h. The solution was then warmed to r.t. and hexane was added. The resulting precipitate was then filtered off. The crude material was purified using flash silica gel chromatography ($CHCl_3$/MeOH, 7:1) to afford compound ***148*** as a solid (0.03 g, 90%).

mp > 250 °C (methanol);

ν_{max}/cm^{-1} (KBr pellet) 3375 (O-H), 3209 (N-H), 3051 (C=*C-H*), 2937 (C-H), 1706 (C=O), 1664 (C=O), 1584 (C=O), 1520 (C=C);

^{1}H NMR (400 MHz; DMSO-*d*$_6$) (6-keto tautomer A) δ 7.84 (1H, t broad, NHCON*H*CH_2), 6.13 (1H, s, 5-H), 4.35 (2H, s, CH_2Ar), 3.13 (2H, q, *J* 6.6 Hz, NHCONHC*H*$_2$), 1.40 (2H, m, NHCONHCH$_2$C*H*$_2$), 1.26 (6H, m, CH_2), 0.85 (3H, t, *J* 6.8 Hz, CH_3);

^{13}C NMR (100 MHz; DMSO-*d*$_6$) δ 164.7 (C-6), 163.0 (C-4), 154.5 (NHCONH), 151.7 (C-2), 100.6 (C-5), 61.0 (CH_2OH), 39.7(NHCONH*C*H_2), 30.8 (*C*$H_2CH_2CH_3$), 28.9 (NHCONHCH$_2$*C*H_2), 25.8 (NHCONHCH$_2$CH$_2$*C*H_2), 21.9 (*C*H_2CH_3), 13.8 (CH_3);

m/z (ES+) 269 [(MH^+), 100%];

HRMS calculated for $C_{12}H_{20}O_3N_4$ (MH^+) 269.16082, found 269.16062.

4-(2,2-Dimethyl-[1,3] doxolan-4-ylmethoxy)-3-oxo-butyric acid ethyl ester (149)[165]

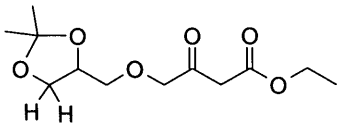

To a suspension of sodium hydride (60% in parrafine oil, 1.32 g, 33.0 mmol) in dry toluene (32 ml) was added slowly over 1.5 h a solution of solketal (4.0 g, 30.0 mmol) in toluene (8 ml). The solution was stirred at r.t. for 1 h, and chloroacetoacetate (2.48 g, 15.13 g) in toluene (8 ml) was added. The solution was stirred at r.t. over 16 h. The solution was acidified with (2 N) citric acid and the organic phase was separated. The aqueous phase was extracted with toluene (3 × 50 ml) and the organic phases were combined together and dried ($MgSO_4$). The solvent was evaporated *in vacuo* and the crude material was purified through flash silica gel chromatography ($CHCl_3$/EtOAc, 4:1) to afford compound **149** as an oil (1.8 g, 46%).

ν_{max}/cm^{-1} (KBr film) 2985 (C-H, *s*), 2935 (C-H, *s*), 2879 (C-H, *s*), 1750 (C=O, *s*), 1724 (C=O, *s*), 1456, 1371, 1217;

^{1}H NMR (300 MHz; $CDCl_3$) δ 4.26 (1H, m, C*H*CH_2O)), 4.21-4.19 (4H, m, OCH_2CO, $COOCH_2CH_3$), 4.08 (1H, dd, *J* 6.5 Hz, *J* 8.3 Hz, C*H*HOC$(CH_3)_2$), 3.79 (1H, dd, *J* 6.4 Hz, *J* 8.3 Hz, C*H*HOC$(CH_3)_2$), 3.56 (2H, d, *J* 5.3 Hz, $CHCH_2OCH_2CO$), 3.50 (2H, s, $COCH_2COOCH_2CH_3$), 1.40 (3H, s, C-CH_3), 1.34 (3H, s, C-CH_3), 1.24 (3H, t, *J* 7.1 Hz, $COOCH_2CH_3$);

^{13}C NMR (75 MHz; $CDCl_3$) δ 201.4 (CO), 166.9 ($COOCH_2CH_3$), 109.6 (*C*-CH_3), 76.3 (CH), 74.6 (OCH_2CO), 72.5 ($CH_2O(CH_3)_2$), 66.5 (OCH_2CH_3), 61.4 ($CHCH_2O$), 45.9 ($COCH_2COO$), 26.7 (C-CH_3), 25.3 (C-CH_3), 14.1 ($COOCH_2CH_3$);

m/z (ES+) 283 [(MNa^+), 100%].

2-Amino-6-(2,2-dimethyl-[1,3]dioxolan-4-ylmethoxymethyl)-1H-pyrimidin-4-one (150)

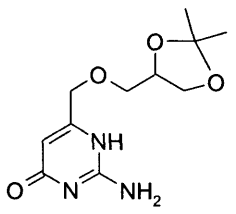

Compound **149** (1.74 g, 6.7 mmol) and guanidine carbonate (0.605 g, 3.3 mmol) were mixed together in ethanol (20 ml) and heated a reflux for 16 h. The solution was cooled down to r.t. leading to precipitation of a white solid, which was filtered off and washed thoroughly with cold water, acetone and cold ethanol. The product was further purified using flash silica gel chromatography ($CHCl_3$/MeOH, 7:1) to afford compound ***150*** (1.51 g, 68%).

mp: 125-126 °C (methanol);

ν_{max}/cm^{-1} (KBr pellets) 3377 (N-H, *s*, NH_2), 3118 (N-H, *s*), 2987 (C-H, *s*), 2870 (C-H, s);

^{1}H NMR (300 MHz; $CDCl_3$) δ 6.60 (2H, broad s, NH_2), 5.83 (1H, s, 5-H), 4.28 (3H, m, CH=CC*H*$_2$O, OCH$_2$C*H*O), 4.04 (1H, dd, *J* 6.1 Hz, *J* 8.3 Hz, C*H*HOC(CH$_3$)$_2$), 3.72 (1H, dd, *J* 6.3 Hz, *J* 8.3 Hz, C*H*HOC(CH$_3$)$_2$), 3.55 (2H, dd, *J* 2.9 Hz, *J* 5.7 Hz, CH$_2$OC*H*$_2$CH), 1.40 (3H, s, C-CH$_3$), 1.34 (3H, s, C-CH$_3$);

^{13}C NMR (75 MHz; $CDCl_3$) δ 168 (broad, C-6), 160.5 (C-4), 156.0 (C-2), 109.7 (*C*-CH$_3$), 100.0 (C-5), 74.6 (CH), 72.1 (*C*H$_2$OCH$_2$CH, CH$_2$O*C*H$_2$CH), 66.4 (CH*C*H$_2$O), 26.7(CH$_3$), 25.3 (CH$_3$);

HRMS calculated for $C_{11}H_{17}O_4N_3$ (MH^+) 256.12918, found 256.12919.

1-[6-(2,2-Dimethyl-[1,3]dioxolan-4-ylmethoxymethyl)-4-oxo-1,4-dihydro-pyrimidin-2-yl]-3-hexyl-urea (151)

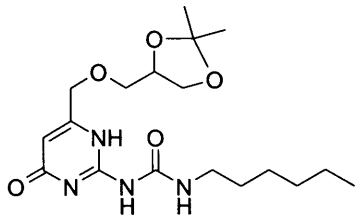

To a solution of compound **150** (1.30 g, 5.09 mmol) in dry pyridine (20 ml) was added hexyl isocyanate (1.52 g, 7.1 mmol) and the solution was heated at 90 °C for 16 h. The solution was cooled down leading to the precipitation of a white solid, which was filtered off. The solid was thoroughly washed with hexane and dried *in vacuo* to give compound ***151*** as a white solid (1.547 g, 80%).

mp: 141-143 °C (hexane);

ν_{max}/cm^{-1} **(KBr pellets)** 3203 (N-H, s), 3142 (N-H, s), 3034 (C=*C-H*, s), 2960 (C-H, s), 2933 (C-H, s), 2860 (c-H, s), 1697 (c=O, s), 1662 (C=O, urea, s);

^{1}**H NMR (300 MHz; CDCl$_3$)** δ 13.38 (1H, s, 1-H), 11.76 (1H, s, N*H*CONHCH$_2$), 9.91 (1H, s, NHCON*H*CH$_2$), 5.88 (1H, s, 5-H), 4.45 (2H, d, *J* 3.7 Hz, CH=CC*H*$_2$O), 4.31 (1H, m, CH$_2$C*H*O), 4.08 (1H, dd, *J* 6.4 Hz, *J* 8.4 Hz, C*H*HOC(CH$_3$)$_2$), 3,78 (1H, dd, *J* 6.3 Hz, *J* 8.4 Hz, C*H*HOC(CH$_3$)$_2$), 3.60 (2H, d, *J* 5.3 Hz, CH$_2$OC*H*$_2$CH), 3.23 (2H, q, *J* 6.6 Hz, NHCONHC*H*$_2$), 1.58 (2H, m, C*H*$_2$CH$_2$NH), 1.41 (3H, s, CHC*H*$_3$), 1.36 (3H, s, CHC*H*$_3$), 1.30 (6H, m, C*H*$_2$CH$_2$), 0.86 (3H, t, *J* 6.4 Hz, CH$_2$C*H*$_3$);

^{13}**C NMR (75 MHz; CDCl$_3$)** δ 172.6 (C-2), 156.3 (NH*C*ONH), 154.7 (C-2), 109.6 148.4 (C-6), 109.6 (*C*-CH$_3$), 105 (C-5), 74.5 (CH$_2$*C*HO), 72.1 (CH$_2$O*C*H$_2$CH), 68.3 (*C*H$_2$OCH$_2$CH), 66.5 (*C*H$_2$OC(CH$_3$)$_2$), 40.1 (CH$_2$NH), 31.5 (*C*H$_2$CH$_2$NH), 29.4 (*C*H$_2$), 26.7 (C-*C*H$_3$), 26.6 (C-*C*H$_3$), 25.3 (*C*H$_2$), 22.6 (*C*H$_2$), 14.0 (CH$_2$*C*H$_3$);

HRMS calculated for $C_{18}H_{30}N_4O_5$ (MNa$^+$) 405.21084, found 405.21155.

1-[6-(2,3-Dihydroxy-propoxymethyl)-4-oxo-1,4-dihydro-pyrimidin-2-yl]-3-hexyl-urea (152)

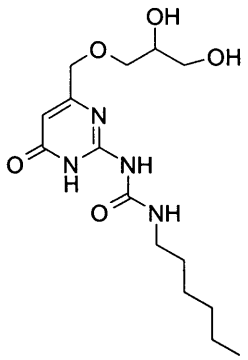

Compound **151** (0.200 g, 0.523 mmol) was dissolved in methanol (6 ml), THF (3 ml) and (1 N) HCl solution (1.5 ml). The mixture was heated at reflux for 1 h. To this cooled mixture was added (1 N) NaOH to bring the pH close to 7. The solvents were then evaporated *in vacuo* to afford compound ***152*** as a solid (0.160 g, 80%).

mp: 126-127 °C (chloroform);

ν_{max}/cm^{-1} (KBr pellets) 3367 (O-H), 3253 (N-H), 3042 (C=*C-H*), 2929 (C-H), 1706 (C=O), 1663 (C=O, urea), 1567 (C=C);

^{1}H NMR (400 MHz; DMSO-d_6) (6-keto tautomer A) δ 10.13 (1H, broad s, N*H*CONHCH$_2$), 8.03 (1H, s, NHCON*H*CH$_2$), 5.95 (1H, s, 5-H), 4.21 (2H, s, C*H*$_2$OCH$_2$CH) 4.02 (2H, broad s, OH), 3.60 (1H, m, C*H*OH), 3.50 (1H, dd, *J* 4.4 Hz, *J* 9.8 Hz, CHC*H*HOH), 3.39 (1H, dd, *J* 6.1 Hz, *J* 9.8 Hz, CHC*H*HOH), 3.35 (2H, d, *J* 5.7 Hz, CH$_2$OC*H*$_2$CH), 3.10 (2H, q, *J* 6.7 Hz, NHCONHC*H*$_2$), 1.41 (2H, m, NHCH$_2$C*H*$_2$), 1.24 (6H, m, CH$_2$), 0.84 (3H, t, *J* 6.2 Hz, CH$_3$);

^{13}C NMR (100 MHz; DMSO-d_6) δ 165.1 (C-2), 161.0 (broad, C-4), 102.1 (C-5), 72.6 (*C*H$_2$OH), 71.4 (*C*H$_2$OCH$_2$CH)), 70.5 (CH), 62.8 (CH$_2$O*C*H$_2$CH), 30.8 (NHCH$_2$), 29.0 (CH$_2$), 25.9 (NHCH$_2$*C*H$_2$), 22.0 (CH$_2$), 13.8 (CH$_3$);

m/z (ES+) 343 [(MH$^+$), 50%], 365 [(MNa$^+$), 100%], 685 [(2MH$^+$), 80%], 707 [(2MNa$^+$), 100%].

6.4 Synthesis towards the formation of cyclic dimers

2-Benzyloxycarbonylamino-3-hydroxy-propionic acid (154)[169]

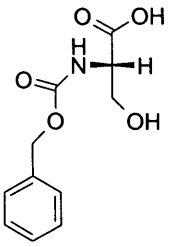

Benzylchloroformate (4.86 ml, 2.80 mmol) in toluene (9.6 ml) was added to a solution of L-serine (2.00 g, 1.90 mmol) in a saturated aqueous sodium hydrogen carbonate solution (80 ml). The mixture was stirred vigorously for 4h. Water (80 ml) was then added and the aqueous phase was extracted with ether (2 × 100 ml) and acidified with conc. HCl to pH 3. The acidified solution was extracted with ethyl acetate (3 × 100 ml) and the organic phase was dried (Na_2SO_4) and concentrated *in vacuo* to afford crude compound **154** as an oil (0.74 g, 90%).

ν_{max} /cm^{-1} (KBr film) 3450 (O-H, *s*), 3320 (O-H, *s*), 3190 (N-H, *s*), 1747 (C=O, *s*, COOH), 1685 (C=O, *s*, ester);

^{1}H NMR (300 MHz; DMSO-d_6) δ 7.45 (5H, m, Ar-H), 5.15 (2H, s, CH_2Ar), 4.20 (1H, m, C*H*COOH), 3.80 (2H, m, CH_2OH);

^{13}C NMR (75 MHz; DMSO-d_6) δ 171.1 (COOH), 156.0 (NH*C*OOBz), 138.0 (Ar C-1), 128.32 (Ar C-3), 127.65 (Ar C-2, Ar C-4), 65.44 (*C*H_2Ar), 61.31 (*C*HCOOH), 56.63 (*C*H_2OH);

m/z (ES+) 262 [(MNa$^+$), 100%];

HRMS calculated for $C_{11}H_{13}O_5N$ (MNa$^+$) 262.06914, found 262.06965.

2-(2-Benzyloxycarbonylamino-3-hydroxy-propionil amino)-3-hydroxy-propionic acid methyl ester (155)[169]

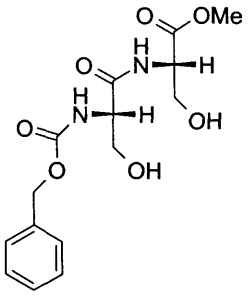

Compound **154** (1.00 g, 4.18 mmol) and triphenylphosphine (1.32 g, 5.01 mmol) were dissolved in acetonitrile (15 ml) together with L-serine methyl ester (0.98 g, 6.30 mmol). Triethylamine (1.20 ml, 8.82 mmol) and carbon tetrachloride (0.50 ml, 5.20 mmol) for 16h. The solvents were evaporated and the residue was dissolved in EtOAc (50 ml) and water (10 ml). The organic layer was washed with citric acid (10% solution, 3 × 5 ml) then with a sodium hydrogen carbonate solution (3 × 5 ml) and saturated sodium chloride solution (5 ml). The organic phase was dried (Na_2SO_4) and the solvent was evaporated *in vacuo*. The crude material was then purified by flash silica gel chromatography ($CHCl_3$/MeOH, 40:1) to afford **155** as a white solid (0.68 g, 50%).

mp: 137 °C (methanol);

ν_{max}/**cm^{-1} (KBr pellets)** 3445-3405 (O-H, *s*), 3307 (N-H, *s*), 3272 (N-H, *s*), 3084 (C-H, *s*), 2949 (C-H, *s*), 1745 (C=O, *s*), 1670 (C=O, *s*);

^{1}H NMR (300 MHz; DMSO-d_6) δ 8.07 (1H, d, *J* 7.7 Hz, N*H*COOCH$_2$Ph), 7.31 (5H, m, Ar-H), 7.18 (1H, d, *J* 8.0 Hz, N*H*CHCOOMe), 5.26 (3H, m, C*H*$_2$Ph, CH*H*CHNHCOO), 4.83 (1H, broad t, C*H*HCHCOOMe), 4.32 (1H, m, C*H*NHCOO), 4.12 (1H, m, C*H*NHCOOMe), 3.68 (1H, m, CH*H*CHNHCOO), 3.60 (3H, s, CH_3OCO), 3.56 (1H, m, C*H*HCHNHCOO);

^{13}C NMR (75 MHz; DMSO-d_6) δ 170.8 (CH*C*ONH), 170.3 (COOMe), 157.6 (COOBz), 136.9 (Ar C-1), 128.3 (Ar C-3), 127.7 (Ar C-2, Ar C-4), 65.5 (*C*H$_2$Ph), 61.7 (COBzCH*C*H$_2$OH), 61.7 (COOMeCH*C*H$_2$OH), 57.0 (*C*HNHCOOBz), 54.8 (C*H*COOMe), 51.8 (CH_3);

m/z (ES+) 363.12 [(MNa$^+$), 100%];

HRMS calculated for $C_{15}H_{18}O_7N_2$ (MNa$^+$) 363.11682, found 363.11744.

(S)- *cis*-3,6-Bis hydroxyl methyl-piperazine-2,5-dione (153)[169]

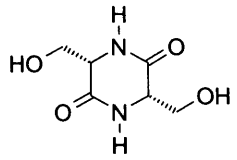

Dipeptide **155** (0.20 g, 0.59 mmol) in methanol (3 ml) was added to a suspension of Pd/C (0.02 g, 10% w/w) in methanol (4 ml). The mixture was hydrogenated with a ballon of H_2 at r.t. for 2 d. The catalyst was removed by filtration through Celite and washed with methanol. The filtrate was then evaporated *in vacuo* and the crude material was redissolved in MeOH (13 ml). The solution was heated at reflux for ca. 5 d. The solvent was evaporated *in vacuo* and the product was recrystallised from MeOH/Et_2O to give compound **153** as colourless crystals (15.30 mg, 15%).

^{1}H NMR (300 MHz; DMSO-d_6) δ 7.95 (2H, broad s, NH), 4.96 (2H, t, *J* 5.2 Hz, OH), 3.76 (2H, m, C*H*CH_2OH), 3.66 (2H, m, C*H*HOH), 3.64 (2H, m, CH*H*OH);
^{13}C NMR (75 MHz; DMSO-d_6) δ 166.3 (C=O), 63.7 (CH), 57.5 (CH_2OH);
m/z (ES+) 106.94 [(MH^+ – 97), 100%);
HRMS calculated for $C_6H_{10}O_4N_2$ (MNa^+) 197.05382, found 197.05386.

N,N'-Dibutyl-2,3-dihydroxy-succinamide

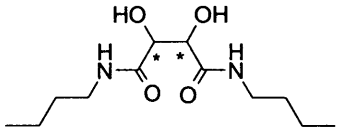

Method A [174]

To a solution of L-tartaric acid (0.427 g, 2.8 mmol) in dry DMF (8 ml) was added at 0 °C EDCI (1.18 g, 6.2 mmol) followed by HOBt (0.83 g, 6.2 mmol). To the cooled solution was then added butylamine (0.5 g, 6.8 mmol) and the solution was stirred at r.t. for 16 h. The solvent was then evaporated *in vacuo* and the residue was redissolved in chloroform (10 ml) and washed with water (10 ml) then with a saturated sodium chloride solution (10 ml). The organic phase was then dried ($MgSO_4$), and the solvent

was evaporated *in vacuo*. The solid was purified using flash silica gel chromatography ($CHCl_3$/MeOH, 8:1) to afford the desired compound as a solid (0.332 g, 45%).

Method B [173]

Tartaric acid (0.10 g, 0.66 mmol) and butylamine (0.12 g, 1.66 mmol) were mixed together in a special vessel. The tube was then placed in the microwave reactor (temperature reached 180 °C and held for 9 min. max power).
The brown solid was then redissolved in chloroform and washed with water (10 ml) then saturated sodium chloride solution (10 ml). The organic phase was then dried ($MgSO_4$) and the solvent was evaporated *in vacuo*. The crude sample was then purified using flash silica gel chromatography ($CHCl_3$/MeOH, 8:1) to afford the tartramide (0.10 g, 60%).

^{1}H NMR (400 MHz; $CDCl_3$; 313 K) δ 7.09 (2H, s, NH), 5.43 (2H, broad s, OH), 4.24 (2H, s, C*H*OH), 3.25 (4H, q, *J* 6.9 Hz, CH_2NHCO), 1.49 (4H, q, *J* 7.2 Hz, $NHCH_2CH_2$), 1.35 (4H, q, *J* 7.4 Hz, CH_3CH_2), 0.91 (6H, t, *J* 7.3 Hz, CH_3);
^{13}C NMR (100 MHz; $CDCl_3$; 313 K) δ 173.7 (CO), 70.2 (CH), 38.8 ($NHCH_2$), 31.4 ($NHCH_2CH_2$), 19.9 (CH_2CH_3), 13.6 (CH_3);
HRMS calculated for $C_{12}H_{24}O_4N_2$ (MNa^+) 283.16283, found 283.16228.

(6-Amino-hexyl)-carbamic acid *tert*-butyl ester (159)[175]

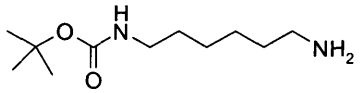

To a solution of hexanediamine (5.0 g, 43.0 mmol) in chloroform (25 ml) was added dropwise at 0 °C, Boc_2O (1.0 g, 4.3 mol) in chloroform (25 ml). The solution was stirred at r.t. for 16 h, then washed with water (30 ml). Saturated sodium chloride solution (30 ml) and the organic phases were combined together and dried ($MgSO_4$). The solvents were removed *in vacuo*. The crude oil was then purified through flash silica gel chromatography ($CHCl_3$/MeOH/Et_3N (5:1:0.4)) to afford **159** as an oil (0.786 mg, 85%).

ν_{max} /cm^{-1} (KBr film) 3361(N-H, *s*, NH_2), 3242 (N-H, *s*), 2933 (C-H, *s*), 2856 (C-H, *s*), 1700 (C=O, *s*), 1520;

NMR ^{1}H (400 MHz; $CDCl_3$) δ 4.57 (1H, s, NH), 3.07 (2H, m, CH_2NH), 2.54 (2H, t, *J* 6.8 Hz, CH_2NH_2), 1.45-1.40 (13H, m, 3 × CH_3, 2 × CH_2), 1.3 (4H, m, CH_2), 1.22 (2H, s, NH_2);

NMR ^{13}C (100 MHz; $CDCl_3$) δ 155.8 (CO), 78.9 (CCH_3), 42.0 (CH_2NH), 40.4 (CH_2NH_2), 33.6 ($CH_2CH_2NH_2$), 29.9 (CH_2CH_2NH), 28.3 (CH_3), 26.5 (CH_2), 26.4 (CH_2).

{6-[3-(6-*tert*-Butoxycarbonylamino-hexylcarbamoyl)-2,3-dihydroxy-propionylamino]-hexyl}-carbamic acid *tert*-butyl ester (160)

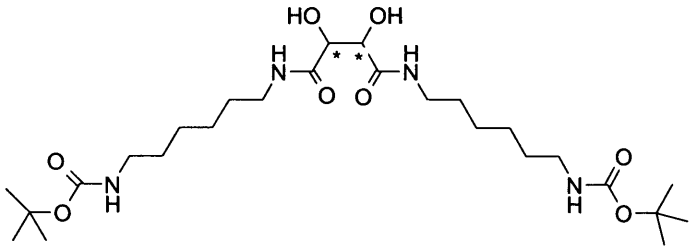

To a solution of L-tartaric acid (0.231 g, 1.50 mmol) in dry DMF (10 ml) was added at 0 °C, EDCI (0.690 g, 3.6 mmol) followed by HOBt (0.486 g, 3.6 mmol). To the cooled solution was then added compound **159** (0.8 g, 3.7 mmol) and the reaction was stirred at r.t. for 16 h. The solvent was then evaporated *in vacuo* and the residue was redissolved in chloroform (10 ml) and washed with water (10 ml) then saturated sodium chloride solution (10 ml). The organic phase was then dried ($MgSO_4$), and the solvent was evaporated *in vacuo*. The solid was purified using flash silica gel chromatography ($CHCl_3$/MeOH, 10:1) to afford compound ***160*** as a solid (0.609 g, 74%).

mp: 148-149 °C (chloroform);

ν_{max} /cm^{-1} (KBr pellets): 3365 (O-H, s), 2982 (C-H, s), 2930, 1690;

^{1}H NMR (400 MHz; $CDCl_3$) δ 7.03 (2H, broad t, N*H*COCH), 5.31 (2H, broad s, OH), 4.66 (2H, broad t, NHCOO), 4.30 (2H, s, CH), 3.22 (4H, q, *J* 6.4 Hz, C*H*$_2$NHCOCH), 3.08 (4H, broad q, C*H*$_2$NHCOO), 1.47 (4H, m, C*H*$_2$CH$_2$NHCOO, C*H*$_2$CH$_2$NHCOOCH), 1.41 (9H, m, CH_3), 1.30 (4H, m, 2 × CH_2);

^{13}C NMR (100 MHz; $CDCl_3$) δ 173.5 (*C*ONHCH$_2$), 156.0 (NHCOO), 79.0 (*C*-CH$_3$), 70.5 (CHOH), 40.2 (*C*H$_2$NHCOO), 38.9 (*C*H$_2$NHCOCH), 29.8 (*C*H$_2$CH$_2$NHCOO), 29.2 (*C*H$_2$CH$_2$NHCOCH), 28.4 (CH_3), 26.2 (CH_2);
m/z (ES+) 547 [(MH^+), 100%], 569 [(MNa^+), 98%], 1116 [($2MNa^+$), 60%].

N,N'-Bis-(6-amino-hexyl)-2,3-dihydroxy-succinamide (158)

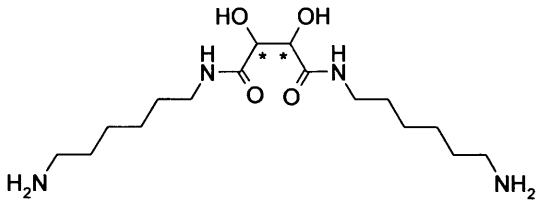

Compound **160** (0.540 g, 0.98 mmol) was dissolved in CH_2Cl_2 (10 ml) and TFA was added (10 ml). The solution was stirred at r.t. for 2 h. The solvents were evaporated *in vacuo* and the residue was redissolved in THF. Triethylamine was added and the solution was heated allowing precipitation of compound ***158*** (0.374 g, 100%).

mp: 143-144 °C (methanol);
ν_{max} /cm^{-1} (KBr pellets) 3409 (N-H, *s*, NH_2), 3294 (O-H, *s*), 3124 (N-H, *s*), 2935 (C-H, *s*), 2856 (C-H, *s*), 1705 (C=O, *s*);
^{1}H NMR (400 MHz; CD_3OD) δ 4.42 (2H, s, CH), 3.25 (4H, t, *J* 7.0 Hz, C*H*$_2$NHCO), 2.90 (4H, t, *J* 7.7 Hz, C*H*$_2$NH$_2$), 1.63 (4H, q, *J* 7.1 Hz, C*H*$_2$CH$_2$NHCO), 1.57 (4H, q, *J* 6.8 Hz, C*H*$_2$CH$_2$NH$_2$), 1.37 (8H, m, CH_2);
^{13}C NMR (100 MHz; CD_3OD) δ 174.6 (CO), 74.0 (CH), 49.6 (*C*H$_2$NHCO), 39.8 (CH_2NH_2), 30.2 (*C*H$_2$CH$_2$NHCO), 28.5 (*C*H$_2$CH$_2$NH$_2$), 27.1 (CH_2), 27.0 (CH_2);
HRMS calculated for $C_{16}H_{34}O_4N_4$ (MH^+) 347.26526, found 347.26499.

2,3-Bis-{6[3-(6-methyl-4-oxo-1,4-dihydro-pyrimidin-2-yl)-ureido]-hexylcarbamoyloxy}-succinic acid diethyl ester (163)

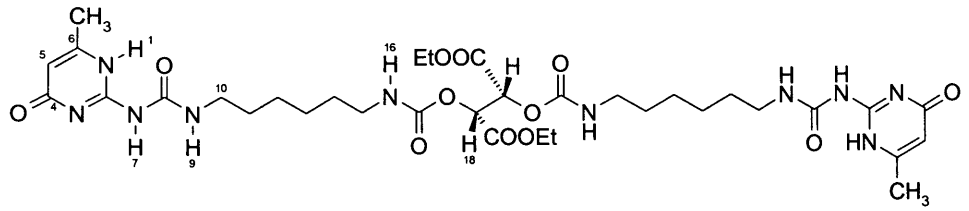

Diethyl L-tartrate (0.3 g, 1.4 mmol) was dissolved in dry chloroform (15 ml) (amylene stabiliser) in the presence of tinbutyldilaurate as catalyst (0.5% w/w). Compound **131** (1.0 g, 3.5 mmol) was then added and the solution was heated at 60 °C under a flux of nitrogen. The reaction vessel was opened to the air allowing a slow evaporation of the solvent over 2-3 h. The residue was redissolved in chloroform (30 ml) and the solution was then filtered off. The filtrate was concentrated *in vacuo* until 10 ml and 0.20 g of silica was added to the solution together with a drop of catalyst. The mixture was heated at reflux for 2 h. The solution was then filtered off to remove the silica and the filtrate was concentrated *in vacuo*. The crude product was then purified using flash silica gel chromatography ($CHCl_3$/MeOH, 7:1) to afford compound ***163*** as a glassy solid (220 mg, 30%).

mp: 142-143 °C (chloroform);

ν_{max} **/cm^{-1} (KBr pellet)** 3333 (N-H, *s*), 3220 (N-H, *s*), 2925 (C-H, *s*), 2850 (C-H, *s*), 1738 (C=O ester, *s*), 1700 (C=O amide, *s*), 1669 (C=O urea, *s*);

^{1}H NMR (500 MHz; $CDCl_3$) (4-keto tautomer B) δ 13.41 (1H, s, 1-H), 11.68 (1H, s, 7-H), 10.21 (1H, s, 9-H), 7.68 (1H, s, 16-H), 6.41 (1H, s, 5-H), 5.92 (1H, s, 18-H), 4.17 & 4.34 (2H, m, $COOCH_2$), 3.68 (1H, m, 10-H), 3.40 (1H, m, 15-H), 2.86 (1H, m, 15-H), 2.78 (1H, m, 10-H), 2.23 (3H, s, CH_3), 1.72 (1H, m, 11-H), 1.66 (1H, m, 14-H), (1H, m, 13-H), 1.51 (2H, m, 12-H, 13-H), 1.37 (1H, m, 11-H), 1.30 (1H, m, 14-H), 1.26 (3H, t, *J* 7.1 Hz, $COOCH_2CH_3$) 1.12 (2H, m, 12-H, 13-H);

^{13}C NMR (125 MHz; $CDCl_3$) δ 174.0. (C-4), 167.4 (COOEt), 156.5 (NHCONH), 155.0 (NHCOO), 154.5 (C-2), 148.6 (C-6), 107.0 (C-5), 71.1 (C-18), 61.7 ($COOCH_2$), 38.4 (C-10), 37.1 (C-15), 28.9 (C-11), 28.7 (C-14), 22.84 (C-12), 22.81 (C-13), 18.20 (CH_3), 14.0 ($COOCH_2CH_3$);

^{15}N NMR (500 MHz; $CDCl_3$) δ -299.2 (N-17), -284.1 (N-9), -266.5 (N-7), -246.3 (N-1), -172.2 (N-3);

^{1}H NMR (500 MHz; DMSO-d_6) (6-keto tautomer A) δ 11.4 (1H, s, 3-H), 9.8 (1H, s, 7-H), 7.44 (1H, s, 9-H), 7.38 (1H, s, 17-H), 5.44 (1H, s, 18-H), 4.08 (4H, m, $COOCH_2CH_3$), 3.10 (2H, m, 10-H), 2.95 (2H, m, 15-H), 2.09 (3H, s, CH_3), 1.41 (2H, m, 11-H), 1.36 (2H, m, 14-H), 1.24 (4H, m, 12-H, 13-H), 1.12 (3H, t, *J* 7.1 Hz, $COOCH_2CH_3$);

^{13}C NMR (125 MHz; DMSO-d_6) δ 166.8 (COOEt), 164.8 (C-6), 161.9 (C-4), 155.0 (NHCONH), 154.8 (NHCOO), 151.6 (C-2), 104.6 (C-5), 71.0 (C-18), 39.2 (C-10), 38.7 (C-15), 29.2 (C-11, C-14), 26.0 (C-12), 25.8 (C-13), 23.2 (CH_3);

^{15}N NMR (500 MHz; DMSO-d_6) δ -296.2 (N-17), -285.8 (N-9), -174.8 (N-1);

^{13}C CPMAS NMR (75 MHZ) δ 174.4 (C-4), 168.0 (COOEt), 156.6 (NHCONH), 155.0 (C-18, C-2), 149.3 (C-6), 107.5 (C-5), 37.8 (C-10, C-15), 29.8 (C-11, C-14), 23.7 (C12, C13), 18.4 (CH_3);

^{15}N CPMAS NMR (30 MHZ) δ -299.0 (N-17), -283.8 (N-9), -266.4 (N-7), -245.9 (N-1), -172.1 (N-3);

m/z (ES+) 793.28 [(MH^+), 100%], 815.26 [(MNa^+), 40%];

$[\alpha]_D$ for L-tartrate: + 365 (c = 0.1, 21 °C, chloroform), for D-tartrate: -339 (c = 0.54, 21 °C, chloroform).

Mixture of Compounds 161 and 162

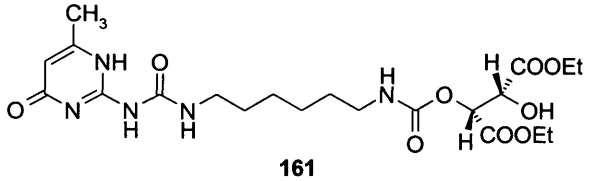

161

+

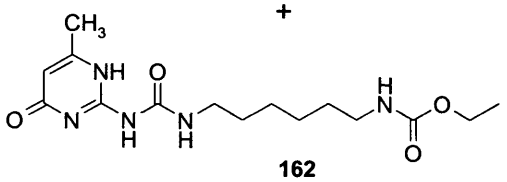

162

ν_{max} /cm^{-1} (KBr pellet) 3342 (N-H), 3415 (N-H), 1700 (C=O), 1669 (C=O urea);

^{1}H NMR (500 MHz; $CDCl_3$) δ 13.09 (2H, s, CH_3CNH), 11.82 (2H, s, $CH_2NH(C{=}O)NH$), 10.08 (2H, s, $CH_2NH(CO)NH$), 5.82 (2H, s, $CH{=}CCH_3$), 5.40 (1H, s, CH(COOEt) (**161**)), 5.34 (1H, s, CH_2NHCOO), 4.82 (1H, s, $CH_2NH(CO)O$), 4.68 (1H, s, CH(COOEt) (**162**)), 4.24 (2H, q, *J* 7.2 Hz, CH_3CH_2OCO), 4.10 (2H, q, *J* 6.8 Hz, CH_3CH_2OCO), 3.23 (4H, m, $NH(CO)CH_2CH_2$), 3.14 (4H, m, CH_2NCO), 2.20 (6H, s, $CH_3C{=}CH$), 1.56-1.34 (16H, m, $CH_2CH_2CH_2CH_2CH_2$), 1.26 (3H, t, CH_3CH_2 (CO)O), 1.20 (3H, t, CH_3CH_2 (CO)O (**162**));
^{13}C NMR (125 MHz; $CDCl_3$) δ 173.0, 170.9, 156.7, 154.61, 148.2, 106.6, 73.1, 71.8, 62.7, 62.2, 41.1, 39.9, 30.1, 29.7, 26.5, 19.2, 14.4, 14.4;
m/z (ES+) 340 [(MH^+), 50%] for (**162**)

2,3-Bis-hexylcarbamoyloxy-succinic acid diethyl ester (164)

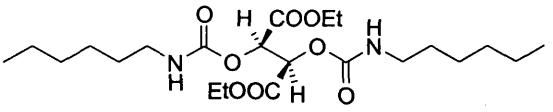

Hexyl isocyanate (0.20 g, 1.57 mmol) was added to a solution of diethyl L-tartrate (0.80 mg, 0.49 mmol) in chloroform (10 ml). Tinbutyl dilaureate was added as catalyst (1% w/w diethyl L-tartrate). The solution was heated at reflux for 16 h. The excess hexyl isocyanate was reacted with silica gel (0.2 g) for 2 h at reflux temperature. The solution was then filtered and the solvent removed *in vacuo* to afford a white solid which was purified using flash silica gel chromatography ($CHCl_3$/MeOH, 15:1) to give ***164*** (0.74 g, 56%).

mp: 40-42 °C (methanol);
ν_{max} /cm^{-1} (KBr pellets) 3348 (N-H, *s*), 1739 (C=O ester, *s*), 1722 (C=O amide, *s*);
^{1}H NMR (300 MHz; $CDCl_3$) δ 6.00 (1H, t, NH), 5.65 (1H, s, CHCOOEt), 4.13-4.23 (2H, m, $COOCH_2$), 3.13 (2H, m, CH_2NHCOO), 1.39 (2H, m, CH_2CH_2NHCOO), 1.23 (9H, m, 4 × CH_2, $COOCH_2CH_3$), 0.83 (6H, m, CH_3);
^{13}C NMR (75 MHz; $CDCl_3$) δ 167.6 ($COOCH_2CH_3$), 154.8 (NHCOO), 71.1 (CHCOOEt), 62.0 (OCH_2CH_3), 41.2 (CH_2NHCOO), 31.4 ($CH_2CH_2CH_3$), 29.6 (CH_2CH_2NHCO), 26.9 ($CH_2CH_2CH_3$), 26.3 (CH_2CH_3), 22.5 (CH_3CH_2OCO), 13.9 (CH_2CH_3);

m/z (ES+) 483.21 [(MNa^+), 100%];

HRMS calculated for $C_{22}O_8N_2H_{40}$ (MNa^+) 483.26822, found 483.26911.

{6-[3-(6-Methyl-4-oxo-1,4-dihydro-pyrimidin-2-yl)-ureido]-hexyl}-carbamic acid 1-methyl-2-{6-[3-(6-methyl-4-oxo-1,4-dihydro-pyrimidin-2-yl)-ureido]-hexylcarbamoyloxy}-propyl ester (166)

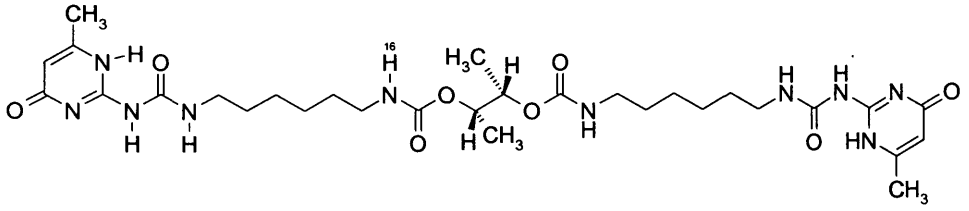

Same procedure used for compound **163.** Compound ***166*** was obtained in 25% yield.

mp: 122-124 °C ;

ν_{max}/cm^{-1} (KBr pellets) 3338 (N-H), 3220 (N-H), 3035 (C=C-H), 2935 (C-H), 2856 (C-H), 1701 (C=O), 16662 (C=O, urea), 1582 (C=C) ;

^{1}H NMR (400 MHz; $CDCl_3$) δ 13.50 (1H, s, 1-H), 11.66 (1H, s, N*H*CONHCH$_2$), 10.14 (1H, s, NHCON*H*CH$_2$), 7.13 (1H, s, NHCOO), 6.06 (1H, s, 5-H), 5.20 (1H, q, *J* 5.68 Hz, C*H*CH$_3$) 3.61(1H, m, NH(CO)CH*H*CH$_2$), 3.31 (2H, m, C*H*HNHCOO), 2.96 (2H, m, CH*H*NHCOO, NH(CO)CH*H*CH$_2$), 2.23 (3H, s, C*H*$_3$C=CH), 1.0-1.80 (11H, m, C*H*$_2$CH$_2$, CHC*H*$_3$);

^{13}C NMR (125 MHz, $CDCl_3$) δ 173.6 (C-4), 156.4 (NHCONH), 156.3 (NHCOO), 154.6 (C-2), 148.3 (C-6), 106.6 (C-5), 71.4 (*C*HCH$_3$), 38.8 (C-10), 37.4 (C-15), 28.9 (C-11), 28.4 (C-14), 23.3 (C-12), 22.4 (C-13), 18.7 (CH_3), 18.0 (CH_3)

HRMS calculated for $C_{30}H_{48}N_{10}O_8$ (MNa^+) 699.35488, found 699.35678;

$[\alpha]_D$: + 217 (c = 0.34, 21 °C, chloroform).

Dimethyl 2,3-*O*-isopropylidene L-tartrate (168)[177]

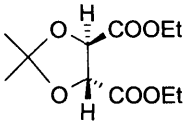

Diethyl L-tartrate (5.30 g, 0.025 mmol), 2,2-dimethoxypropane (3.00 g, 0.028 mmol) and PTS (0.03g, 25% w/w) were dissolved in toluene (20 ml) and the mixture was heated at reflux temperature. The methanol generated was removed *via* a Deans stark apparatus. The advance of the reaction was followed by TLC analysis (EtOAc/Hexane, 1:1) and the reaction was completed after 3-4 hours. Toluene and excess of 2,2-dimethyl propane were removed *in vacuo*. A mixture of the diesters was obtained during the reaction and the material was carried directly through to the next step.

^{1}H NMR (300 MHz; $CDCl_3$) δ 4.81-4.73 (2H, m, CH), 4.28 (4H, q, *J* 7.1 Hz, CH_2CH_3), 3.78 (3H, s, $COOCH_3$), 1.50 (6H, s, C-CH_3), 1.20 (6H, t, *J* 7.1 Hz, $COOCH_2CH3$);
^{13}C NMR (75 MHz; $CDCl_3$) δ 170.45 (COOEt), 170.00 (COOMe), 114.18 (*C*-CH_3), 62.23 (*C*HCOOEt), 26.74 ($COOCH_2CH_3$), 21.75 ($COOCH_3$), 14.44 (C-CH_3);

2,3-*O*-isopropylidene D-threitol (169)[178]

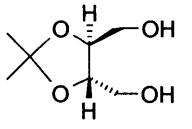

A solution of **168** (7.35 g, 0.02 mol) in anhydrous ethanol (15 ml) was added dropwise to a mixture of $NaBH_4$ (3.41 g, 0.09 mol) in anhydrous ethanol (40 ml) under vigourous stirring at such rate to maintain reflux and evolution of H_2. The mixture was then heated at reflux temperature for 4 h. The reaction was monitored by TLC analysis (EtOAc/hexane, 1:1). The reaction was concentrated *in vacuo* and chloroform (20 ml) was added, followed by the addition of water (dropwise) with vigorous stirring until the solution became clear. The solution was then stirred for an additional hour. The organic phase was separated and dried ($MgSO_4$). The solvent was evaporated and the product

was purified through flash silica gel chromatography with (CH_2Cl_2/MeOH, 8:1) to give **169** as colourless oil (1.86 g, 57%).

ν_{max} / **cm^{-1}(KBr film)** 3400 (O-H, *s*) 2950 (C-H, *s*);

^{1}H NMR (300 MHz; $CDCl_3$) δ 3.92 (2H, m, C*H*CH_2), 3.73 (4H, m, C*H*$_2$OH), 2.77 (2H, s, OH), 1.38 (6H, s, CH_3);

^{13}C NMR (75 MHz; $CDCl_3$) δ 109.6 (*C*-CH_3), 78.6 (CH), 62.5 (CH_2), 27.3 (CH_3);

m/z (CI+) 147 [(MH^+- CH_3), 40%], 163 [(MH^+), 10%];

$[\alpha_D]^{22}$ + 3 (c = 0.1, methanol).

(4S, 5S)-4,5-Bis benzyloxymethyl-2,2-dimethyl-[1,3] dioxolane (170)[181]

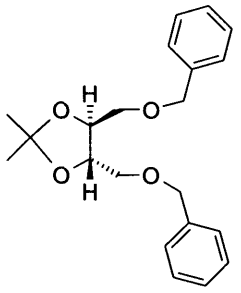

To a solution of compound **169** (0.530 g, 3.30 mmol) dissolved in dry THF (10 ml) was added slowly at 0 °C, sodium hydride (60% in parafine oil, 0.330 g, 8.00 mmol). The solution was stirred for 30 min and benzyl bromide (0.4 ml, 9.9 mmol) was added. The reaction mixture was stirred at r.t. for 16 h. The solvent was evaporated *in vacuo*, and the residue was redissolved in chloroform. The organic phase was washed with water (10 ml) then saturated sodium chloride solution (10 ml), and the organic phase was then dried ($MgSO_4$). The solvent was evaporated *in vacuo* and the product was purified through flash silica gel chromatography ($CHCl_3$/EtOAc, 1:10) to afford compound **170** as pale oil (0.442 g, 40%).

ν_{max} **/cm^{-1}**: 3065 (C-H, Ar), 3028 (C-H, Ar), 2984 (C-H), 2868 (C-H), 1498 (C=C), 1454, 1373 (C-H, $C(CH_3)_2$);

^{1}H NMR (300 MHz; $CDCl_3$) δ 7.31 (5H, m, Ar-H), 4.39 (2H, d, *J* 2.7 Hz, CH_2Ar), 4.04 (1H, m, CHO), 3.61 (2H, m, C*H*$_2$OCH_2Ar), 1.43 (3H, s, CH_3);

^{13}C NMR (75 MHz; $CDCl_3$) δ 137.9 (Ar C-1), 128.3 (Ar C-3), 127.6 (Ar C-2, C-4), 109.6 (*C*CH_3), 77.4 (CHO), 73.4 (CH_2Ar), 70.6 (*C*H_2OCH_2Ar), 26.9 (CH_3);
HRMS calculated for $C_{21}H_{26}O_4$ (MNa^+) 365.17233, found 365.17190.

(2S, 3S)-1,4-Bis-benzyloxy-butane-2,3-diol (171)[181]

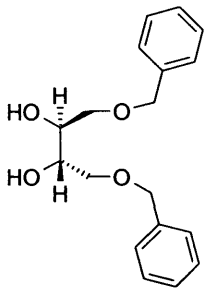

Compound **170** (0.440 g, 1.31 mmol) was dissolved in a THF/MeOH/HCl (1 N) (5 ml:10 ml:5 ml) and heated at reflux for 16 h. The solution was cooled down and (5 N) NaOH was added to bring the pH close to 8. The solvents were then evaporated and the residue was redissolved in chloroform. The organic phase was washed with water (2 × 10 ml) and then dried ($MgSO_4$). The solvent was evaporated to afford compound **171** as a solid (0.38 g, 90%).

mp: 40-50 °C (methanol);
ν_{max} /cm^{-1} (KBr pellets) 3316 (O-H, *s*), 2926 (C-H, *s*), 2857 (C-H, *s*), 1451, 1387;
^{1}H NMR (300 MHz; $CDCl_3$) δ 7.32 (5H, m, H-Ar), 4.55 (2H, s, CH_2Ar), 3.87 (1H, broad t, C*H*OH), 3.60 (2H, m, CH_2OCH_2Ar), 2.85 (1H, broad s, OH);
^{13}C NMR (75 MHz; $CDCl_3$) δ 137.8 (Ar C-1), 128.5 (Ar), 127.9 (Ar), 127.8 (Ar), 73.6 (CH_2Ar), 72.0 (*C*H_2OCH_2Ar), 70.6 (CHOH);
HRMS calculated for $C_{18}H_{22}O_4$ (MNa^+) 325.14103, found 325.14131.

(2S, 3S)-2,3-Bis-benzyloxymethyl-1,4,7,10,13 pentaoxa-cyclopentadecane (172)[181]

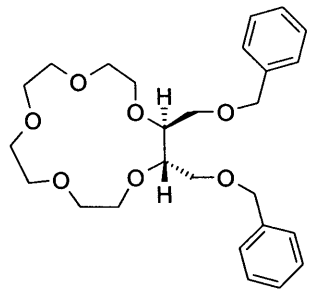

To a suspension of sodium hydride (60% in parafine oil, 0.30 g, 7.5 mmol) in dry THF (45 ml) was added compound **171** (0.52 g, 1.72 mmol) and the solution was heated at 70 °C for 1 h. A solution of bis toluene-4-sulfonic acid 2-{2-[2-(2-ethoxy)-ethoxy]-ethoxy}-ethyl ester (0.90 g, 1.79 mmol) was then added at once, and the solution was stirred at 75 °C for 3 days. The solution was then filtered off and the filtrate vaporated *in vacuo*. The crude material was purified through (neutral) alumina chromatography (gradient: petrol ether/propan 2-ol (50:1) then (10:1)). A second flash silica gel chromatography in EtOAc was performed to afford **172** (0.20 g, 25%).

^{1}H NMR (400 MHz; $CDCl_3$) δ 7.28-7.24 (5H, m, Ar-H), 4.49 (2H, d, *J* 7.9 Hz, CH_2Ar), 3.83 (2H, m, CH_2OCH_2Ar), 3.62-3.68 (8H, m, CH_2CH_2O), 3.47 (1H, m, CHO);

^{13}C NMR (100 MHz; $CDCl_3$) δ 138.3 (Ar C-1), 128.2 (Ar C-3), 127.5 (Ar C-2, Ar C-4), 79.6 (CH_2Ar), 73.2 (CHO), 71.3 (CH_2O), 71.0 (CH_2O), 70.5 (CH_2O), 70.2 (CH_2O), 69.8 (CH_2O);

m/z (ES+) 483.4 [(MNa^+), 100%];

HRMS calculated for $C_{26}H_{36}O_7$ (MNa^+) 483.23667, found 483.23532.

((2S, 3S)-3-hydroxymethyl-1,4,7,10,13 pentaoxa-cyclopentadec-2-yl)-methanol (173)[181]

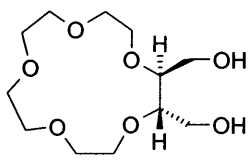

Compound **172** (0.085 g, 0.17 mmol) was dissolved in MeOH (5 ml) and was hydrogenated over Pd/C (20 mg) at r.t. for 16 h. The solution was then filtered through celite and the solvent was evaporated to afford compound **173** as an oil (0.040 g, 85%).

ν_{max} /cm^{-1} (KBr film) 3338 (O-H, s), 3217 (O-H, s), 3043 (C-H, s), 2933 (C-H, s), 2856, 1585, 1251;

^{1}H NMR (400 MHz; $CDCl_3$) δ 3.75 (2H, m, CH_2OH), 3.68-3.60 (7H, m, CH_2CH_2O, CHO), 3.3 (1H, broad s, OH);

^{13}C NMR (125 MHz; $CDCl_3$) δ 80.1 (CHO), 72.5 (CH_2CH_2OCH), 71.3 (CH_2CH_2OCH), 70.3 (CH_2O), 70.0 (CH_2O), 69.4 (CH_2O), 60.8 (CH_2OH);

m/z (ES+) 303.2 [(MNa^+), 100%];

HRMS calculated for $C_{12}H_{24}O_7$ (MNa^+) 303.14142, found 303.14179.

Bis-toluene-4-sulfonic acid-2-{2-[2-(2-ethoxy)-ethoxy]-ethoxy}-ethyl ester [181]

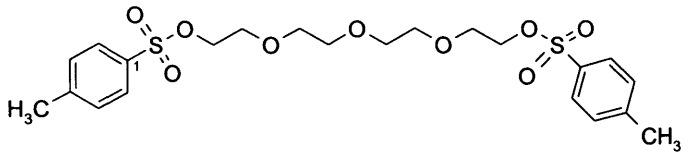

PEG_4 (1.0 g, 5.1 mmol) was dissolved in CH_2Cl_2 (10 ml) with triethylamine (4 ml). The solution was cooled at 0 °C and a solution of tosyl chloride (5.9 g, 30.1 mmol) in CH_2Cl_2 (5 ml) was added dropwise. The mixture was then stirred at r.t. for 16 h. The organic phase was then washed with water (2 × 20 ml) followed by a saturated sodium chloride solution (20 ml). The organic phase was dried ($MgSO_4$) and the solvent evaporated *in vacuo*. The crude material was purified through flash silica gel chromatography (EtOAc/hexane, 2:1) and the final compound was azeotroped with toluene to afford the desired compound as an oil (1.87 g, 84%).

ν_{max} /cm^{-1} (KBr film) 3022 (C-H, *s*), 2875 (C-H, *s*), 1597 (C=C, *s*), 1452 (C=C, *s*), 1360;

^{1}H NMR (400 MHz; $CDCl_3$) δ 7.53 (2H, d, *J* 8.0 Hz, Ar 2-H), 7.30 (2H, d, *J* 8.0 Hz, Ar 3-H), 4.13 (2H, t, *J* 4.7 Hz, CH_2OSO_2Ar), 3.65 (2H, t, *J* 4.7 Hz, $CH_2CH_2OSO_2Ar$), 3.55 (4H, m, CH_2CH_2O), 2.41 (3H, s, CH_3Ar);

^{13}C NMR (125 MHz; $CDCl_3$) δ 144.7 (Ar C-4), 132.8 (Ar C-1), 129.8 (Ar C-3), 127.8 (Ar C-2), 70.6 (CH_2O), 70.4 (CH_2O), 69.2 ($CH_2CH_2OSO_2Ar$), 68.6 (CH_2SO_2Ar), 21.5 (CH_3);

HRMS calculated for $C_{22}H_{30}O_4S_2$ (MNa^+) 525.12235, found 525.12268.

{6-[3-(6-Methyl-4-oxo-1,4-dihydro-pyrimidin-2-yl)-ureido]-hexyl}-carbamicacid 1,1,2-trimethyl-2-{6-[3-(6-methyl-4-oxo-1,4-dihydro-pyrimidin-2-yl)-ureido]-hexylcarbamoyloxy}-propyl ester (175)

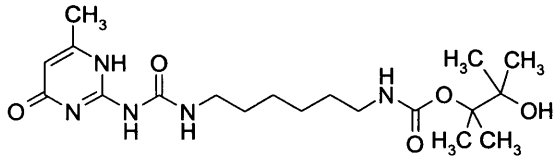

Same procedure as for compound **163**. Compound ***175*** was obtained in 52% yield.

mp: 117-119 °C (chloroform);

ν_{max}/cm^{-1} (KBr pellets) 3419 (O-H, *s*), 2925 (C-H, *s*), 2854, 1701 (C=O, *s*), 1670 (C=O, *s*), 1585 (C=C, *s*), 1525 (C=C, *s*) ;

^{1}H NMR (400 MHz; $CDCl_3$) δ 13.12 (1H, s, 1-H), 11.83 (1H, s, N*H*CONHCH$_2$), 10.12 (1H, s, NHCON*H*CH$_2$), 5.83 (1H, s, H-5), 5.10 (1H, s, NHCOO), 3.24 (2H, m, NH(CO)NHC*H*$_2$), 3.10 (2H, m, C*H*$_2$NHCOO), 2.21 (3H, s, C*H*$_3$C=CH), 1.60-1.28 (8H, m, CH_2), 1.16 (6H, s, C-C*H*$_3$);

^{13}C NMR (125 MHz; $CDCl_3$) δ 173.1 (C-4), 156.9 (NHCONH), 156.5 (NHCOO), 154.7 (C-2), 148.3 (C-6), 106.6 (C-5), 88.7 (*C*-CH_3), 40.7 (C-10), 39.6 (C-15), 29.7 (CH_2), 29.3 (CH_2), 29.2, 26.1, 25.5 (CH_3), 23.0 (CH_2), 18.9 (CH_3);

HRMS calculated for $C_{10}H_{33}O_5N_4$ (MNa^+) 434.23739 found, 434.23831.

8-*tert*-Butoxycarbonylamino-octanoic acid (177)[183]

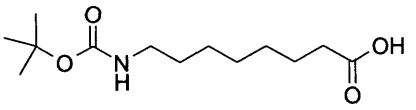

To a solution of aminocaprilic acid (1.5 g, 9.4 mmol) in water (5ml) and CH_2Cl_2 (5 ml) was added sodium hydroxide (0.752 g, 18.8 mmol). The solution was cooled to 0 °C and a solution of Boc_2O (2.05 g, 9.4 mmol) in CH_2Cl_2 (10 ml) was added slowly. The solution was stirred at r.t. for 16 h. The mixture was acidified with conc. HCl. The organic layer was separated and the aqueous phase was extracted with CH_2Cl_2 (2 × 20 ml). The organic phase were combined and dried ($MgSO_4$). The solvent was evaporated *in vacuo* and the crude material was purified through flash silica gel chromatography ($CHCl_3/CH_3CN/CH_3OH$, 18:1:1) to afford compound **177** as a solid (0.733 g, 30%).

mp: 54-56 °C (chloroform);

ν_{max} /cm^{-1} (KBr pellets) 3365 (O-H, *s*, COOH), 2934 (C-H, *s*), 2843, 1714 (C=O, s, COOH), 1683 (C=O, s), 1520;

^{1}H NMR (400 MHz; $CDCl_3$) δ 11.5 (1H, broad s, COOH), 4.56 (1H, broad t, NHCOO), 3.07 (2H, m, C*H*$_2$NHCOO), 2.32 (2H, t, *J* 7.4 Hz, C*H*$_2$COOH), 1.60 (2H, q, *J* 7.2 Hz, C*H*$_2$CH$_2$NHCOO), 1.41 (11H, m, CH_3, CH_2), 1.30 (6H, m, CH_2);

^{13}C NMR (100 MHz; $CDCl_3$) δ 179.3 (COOH), 155.9 (NHCOO), 79.0 (*C*-CH_3), 40.4 (*C*H$_2$NHCOO), 33.9 (*C*H$_2$COOH), 29.8 (*C*H$_2$CH$_2$NHCOO), 28.9 (*C*H$_2$CH$_2$COOH, CH_2), 28.3 (CH_3), 26.5 (CH_2), 24.5 (CH_2);

HRMS calculated for $C_{13}H_{25}O_4N$ (MNa^+) 282.16758, found 282.16736.

(2R, 3S)-2,3-Bis-(8-tert-butoxycarbonylamino-octanoyloxy)-succinic acid diethyl ester (178)

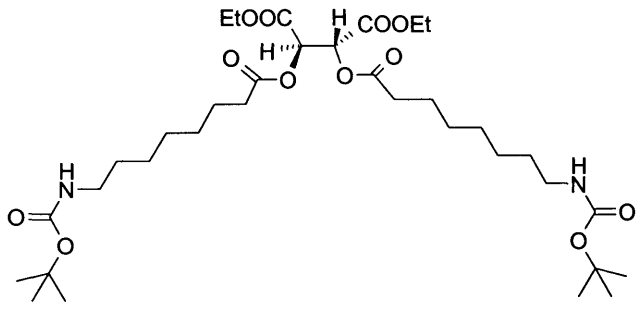

To a solution of **177** (0.30 g, 1.16 mmol) in CH_2Cl_2 (12 ml) was added at 0 °C, DCC (0.262 g, 1.27 mmol) and DMAP (0.052 g). The solution was stirred at 0 °C for 1 h and diethyl L-tartrate (0.103 g, 0.50 mmol) in CH_2Cl_2 (3 ml) was added. The resulting solution was stirred at r.t. for 16 h. The solution was filtered off and the filtrate was evaporated *in vacuo*. The residue was washed with water (10 ml) and saturated sodium chloride solution (10 ml) and the organic phase was dried ($MgSO_4$). The solvent was evaporated *in vacuo* and the crude material was purified through flash silica gel chromatography ($CHCl_3$/MeOH, 10:1) to give compound *177* as an oil (0.140 g, 50%)

ν_{max} /cm^{-1} (KBr film): 3370-3360 (N-H, *s*), 2930 (C-H, *s*), 1858 (C-H, *s*), 1755 (C=O, s, ester), 1697 (C=O, *s*), 1529, 1365;

^{1}H NMR (300 MHz; $CDCl_3$) δ 4.55 (1H, broad t, NHCOO), 4.18 (2H, q, *J* 7.1 Hz, $COOCH_2CH_3$), 3.01 (2H, q, *J* 6.4 Hz, CH_2NHCOO), 2.42 (2H, q, *J* 8.1 Hz CH_2COO), 1.60 (2H, m, CH_2CH_2COO), 1.41-1.42 (12H, m, CH_2CH_2NHCOO, C-CH_3), 1.28 (6H, m, $CH_2CH_2CH_2COO$, CH_2), 1.22 (3H, t, *J* 7.1 Hz, CH_2CH_3);

^{13}C NMR (75 MHz; $CDCl_3$) δ 172.4 (*C*OOCH), 165.9 ($COOCH_2CH_3$), 156.0 (NHCOO), 79.0 (*C*-CH_3), 70.6 (CH), 62.1 (CH_2CH_3), 40.5 (CH_2NH), 33.6 (CH_2COOCH), 30.0 (CH_2CH_2NHCOO), 28.8 ($CH_2CH_2CH_2COO$), 28.4 (C-CH_3), 26.5 (CH_2), 24.6 (CH_2), 14.1 (CH_2CH_3);

m/z (ES+) 689.7 [(MH^+), 100%], 711.7 [(MNa^+), 20%];

HRMS calculated for $C_{34}H_{60}O_{12}N_2$ (MNa^+) 711.40385, found 711.4048.

2,3-Bis-{8-[3-(6-methyl-4-oxo-1,4-dihydro-pyrimidin-2-yl)-ureido]-octanoyloxy}-succinic acid diethyl ester (176)

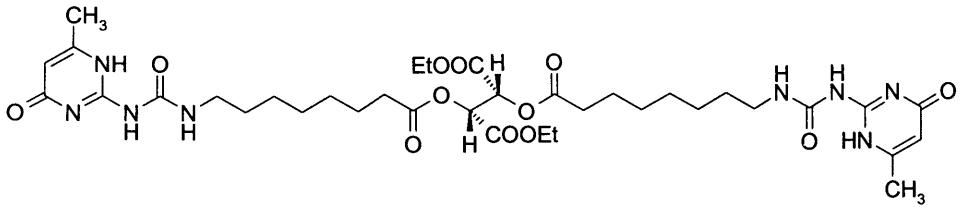

Compound **178** (0.131 g, 0.19 mmol) was dissolved in CH_2Cl_2 (10 ml) and TFA (10 ml). The solution was stirred at r.t. for 2h, and the solvents were evaporated *in vacuo*. The remaining salt (**179**) was dried under reduced pressure for 16 h. Compound **179** (0.121 g, 0.17 mmol) was dissolved in THF (15 ml) and triethylamine (0.2 ml). To this solution was added diethyl L-tartrate (0.192 g, 1.0 mmol), and the solution was heated at reflux for 16 h. The solid was filtered off and the filtrate was evaporated under reduced pressure. The residue was purified through flash silica gel chromatography ($CHCl_3$/MeOH, 10:1) to give ***176*** as a solid (0.107 g, 80%);

mp: 100-102 °C;

ν_{max} /cm^{-1} (KBr pellets) 3478 (N-H, *s*), 3415 (N-H, *s*), 3227 (N-H, *s*), 2935 (C-H, *s*), 2856 (C-H, *s*), 1751 (C=O, *s*, ester), 1701 (C=O, *s*, ester), 1666 (C=O, *s*, urea), 1589, 1521, 1256;

^{1}H NMR (500 MHz; $CDCl_3$) δ 13.11 (1H, s, 1-H), 11.83 (1H, s, 7-H), 10.15 (1H, s, 9-H), 5.80 (1H, s, 5-H), 5.69 (1H, s, CH), 4.21 (2H, q, *J* 7.1 Hz, $COOCH_2CH_3$), 3.21 (2H, broad t, $NHCONHCH_2$), 2.38 (2H, m, CH_2COO), 2.22 (3H, s, CH_3), 1.62 (2H, m, CH_2CH_2COO), 1.58 (2H, m, $CH_2CH_2NHCONH$), 1.33 (6H, m, CH_2), 1.24 (3H, t, *J* 7.2 Hz, $COOCH_2CH_3$);

^{13}C NMR (75 MHz; $CDCl_3$) δ 172.9 (C-4), 172.4 (COO), 165.9 ($COOCH_2CH_3$), 156.5 (NHCONH), 154.7 (C-2), 148.2 (C-6), 106.6 (C-5), 70.6 (CH), 62.2 ($COOCH_2CH_3$), 39.9 ($NHCONHCH_2$), 33.8 (CH_2COO), 29.4 ($CH_2CH_2NHCONH$), 28.9 ($CH_2CH_2CH_2COO$), 28.8 ($CH_2CH_2CH_2CH_2NHCONH$), 26.7 ($CH_2CH_2CH_2NHCONH$), 24.7 (CH_2CH_2COO), 18.9 (CH_3), 14.1 (CH_2CH_3);

m/z (ES+) 791.6 [(MH^+), 100%], 813.5 [(MNa^+), 40%];

HRMS calculated for $C_{36}H_{54}O_{12}N_8$ (MNa^+) 813.37534, found 813.37343.

6.5 Synthesis of Cytosine Derivatives

N-(2-Oxo-1, 2-dihydro-pyrimidin-4-yl)-acetamide (187)[191]

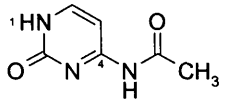

Cytosine (2.0 g, 1.8 mmol) was mixed with acetic anhydride (8.2 ml, 8.7 mmol) in pyridine (10 ml) and the solution was heated at 125 °C for 2.5 h. The solution was then cooled down to r.t. and EtOAc (15 ml) was added. The resulting mixture was stirred at r.t. for an additional 3 h and the solid was filtered off *in vacuo*. The white powder was washed thoroughly with EtOAc and dried *in vacuo* to afford **187** as a white solid (2.97 g, 93%).

mp > 300 °C (EtOAC);

ν_{max}**/cm^{-1} (KBr pellet)** 3140 (N-H, *s*), 3130 (N-H, *s*), 3025 (C=*C-H, s*), 2969 (C-H, *s*), 2838 (C-H, *s*), 1722 (C=O, *s*), 1702 (C=O, *s*), 1610 (N-H amide, *d*), 1503, 1462 (C-H, *d*);

^{1}H NMR (400 MHz; DMSO-d_6) δ 11.49 (1H, s, N*H*), 10.75 (1H, s, N*H*COCH$_3$), 7.80 (1H, d, *J* 7.0 Hz, C*H*CHNH), 7.08 (1H, d, *J* 7.0 Hz, C*H*NH), 2.23 (3H, s, CH$_3$);

^{13}C NMR (100 MHz; DMSO-d_6, 353 K) δ 170.1 (NHCOCH$_3$), 162.6 (C-4), 155.5 (NHCONH), 146.3 (C-6), 94.1 (C-5), 23.7 (CH$_3$);

m/z (ES-) 152.02 [(M-H$^+$), 100%];

HRMS calculated for $C_6H_7O_2N_2$ (MNa$^+$) 176.04305, found 176.04279.

N-(1-Hexyl-2-oxo-1,2-dihydro-pyrimidin-4-yl)-acetamide (188)

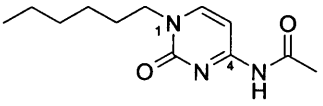

To a solution of compound **187** (0.5 g, 3.2 mmol) in dry DMF (15 ml) was added portionwise anhydrous potassium carbonate (0.675 g, 4.9 mmol) followed with

bromohexane (0.70 ml, 4.9 mmol). The solution was heated at 80 °C for 16 h. The residual solid was then filtered off and the filtrate evaporated under reduced pressure. The solid was then redissolved in $CHCl_3$ and washed with (1 N) HCl (10 ml) then water (10 ml) and finally with saturated sodium chloride solution (10 ml) and the organic phase was dried over $MgSO_4$. The solvents were evaporated *in vacuo* and the crude solid was purified over flash chromatography ($CHCl_3$/EtOAc, 5:1) to give compound ***188*** as a white solid (0.57 g, 75%).

mp: 129-130 °C (chloroform);

ν_{max}/**cm^{-1} (KBr pellets)** 3232 (N-H, *s*), 2950-2920 (C-H, *s*), 2848 (C-H, *s*), 1704 (C=O, *s*), 1660 (C=O, *s*);

^{1}H NMR (400 MHz; $CDCl_3$) δ 10.34 (1H, s, N*H*), 7.56 (1H, d, *J* 7.2 Hz, 5-H,), 7.38 (1H, d, *J* 7.2 Hz, 6-H), 3.84 (2H, t, *J* 7.0 Hz, CH_2CH_2N), 2.33 (3H, s, $COCH_3$), 1.74 (2H, m, CH_2CH_2N), 1.32 (6H, m, 3 × CH_2CH_2), 0.85 (3H, t, *J* 7.1 Hz, CH_3CH_2);

^{13}C NMR (75 MHz; $CDCl_3$) δ 171.3 ($COCH_3$), 162.9 (C-4), 155.8 (C-2), 148.6 (C-6), 96.8 (C-5), 51.0 (CH_2N), 31.3 ($CH_3CH_2CH_2$), 29.0 (CH_2CH_2N), 26.1 ($CH_2CH_2CH_2N$), 24.8 (CH_3CO), 22.4 (CH_3CH_2), 13.9 (CH_3CH_2);

m/z (ES+) 238 [(MH^+), 20%], 260 [(MNa^+), 50%], 497 [($2MNa^+$), 100%];

HRMS calculated for $C_{12}H_{19}N_3O_2$ (MH^+) 238.1500 found 238.15544.

4-Amino-1-hexyl-1*H*-pyrimidin-2-one (189)

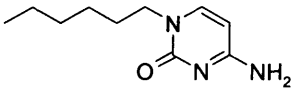

Compound **188** (0.10 g, 0.40 mmol) was dissolved in a solution of ammonia in MeOH (7N) (15 ml). The solution was stirred at r.t. in a sealed tube for 48 h. The completion of the reaction was followed by TLC ($CHCl_3$/MeOH, 5:1) and the solution was evaporated *in vacuo* to afford a crude solid. Purification over flash chromatography ($CHCl_3$/MeOH, 7:1) afforded compound ***189*** (0.052 g, 63%).

mp: 216-217 °C (methanol);

ν_{max}/**cm^{-1}(KBr pellets)** 3350 (N-H, primary amine, *s*), 3105 (C=*C-H*, *s*), 2930 (C-H, *s*), 2856, 1664 (C=O, *s*), 1620 (N-H, *d*);

^{1}H NMR (300 MHz; $CDCl_3$) δ 7.22 (1H, d, *J* 7.2 Hz, C*H*CHN), 5.68 (1H, d, *J* 7.2 Hz, CHC*H*N), 5.67 (2H, broad s, NH_2), 3.73 (2H, t, *J* 7.3 Hz, CH_2N), 1.68 (2H, m, CH_2CH$_2$N), 1.28 (6H, m, CH_2CH$_3$), 0.88 (3H, t, *J* 7.2 Hz, CH$_3$);

^{13}C NMR (75 MHz; $CDCl_3$) δ 165.4 (C-4), 156.4 (C=O), 145.8 (C-6), 93.7 (C-5), 50.3 (*C*H$_2$N), 31.4 (CH$_3$CH$_2$*C*H$_2$), 29.1 (*C*H$_2$CH$_2$N), 26.2 (*C*H$_2$CH$_2$CH$_2$N), 22.6 (CH$_3$*C*H$_2$), 14.0 (*C*H$_3$);

m/z (ES+) 196.15 [(MH$^+$), 100%], 218.15 [(MNa$^+$), 95%], 391.5 [(2MH$^+$), 80%], 413.5 [(2MNa$^+$), 85%], 586.74 [(3MH$^+$), 5%], 508.74 [(3MNa$^+$), 20%];

HRMS calculated for $C_{10}H_{17}ON_3$ (MH$^+$) 196.14444, found 196.14486.

1-Hexyl-3-(1-hexyl-2-oxo-1,2-dihydro-pyrimidin-4-yl)-urea (181)

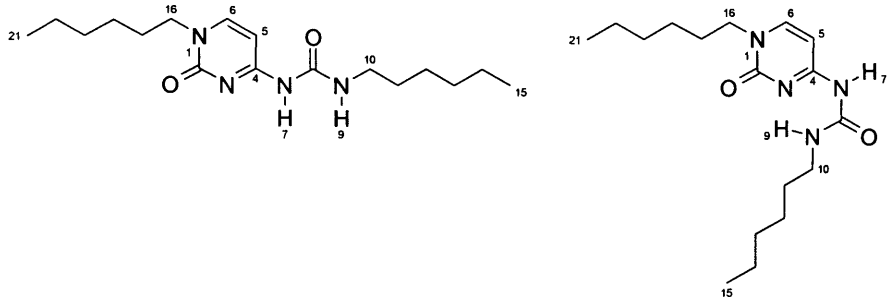

To a solution of compound **189** (0.10 g, 0.51 mmol) in dry pyridine (5 ml) was added hexylisocyanate (0.110 ml, 0.769 mmol). The resulting yellow solution was heated at 90 °C for 16 h. The solution was then cooled down to r.t. and addition of hexane (5 ml) allowed precipitation of a white solid which was then filtered off *in vacuo*. The solid was purified through flash chromatography column ($CHCl_3$/MeOH, 15:1) to give compound ***181*** as white needles (0.128 g, 78%).

mp: 210-211 °C (chloroform);

ν_{max}/**cm^{-1} (KBr pellet)** 3221 (N-H, *s*), 3057 (C=*C-H*, *s*), 2925 (C-H, *s*), 2856, (C-H, s), 1701 (C=O, *s*), 1658 (C=O, *s*), 1620 (N-H, *d*), 1564 (N-H, *d*);

^{1}H NMR (500 MHz; $CDCl_3$; 298 K) (conformer 181) δ 10.90 (1H, s, 7-H), 8.98 (1H, s, 9-H), 7.54 (1H, broad d, 5-H), 7.42 (1H, d, *J* 7.4 Hz, 6-H), 3.79 (2H, t, *J* 7.2 Hz, 16-

H), 3.22 (2H, broad q, 10-H), 1.71 (2H, m, 17-H), 1.54 (2H, m, 11-H), 1.33 (2H, m, 18-H), 1.32 (2H, m, 12-H), 1.29 (12H, m, 13-H, 14-H, 19-H, 20-H), 0.87 (3H, m, 15-H), 0.85 (3H, m, 21-H);

^{1}H NMR (500 MHz; $CDCl_3$; 254.6 K) (conformer 181 (19:1)) δ 11.08 (1H, s, 7-H), 9.03 (1H, s, 9-H), 7.53 (1H, broad d, 5-H), 7.46 (1H, d, *J* 7.4 Hz, 6-H), 3.81 (2H, t, *J* 7.2 Hz, 16-H), 3.21 ((2H, broad q, 10-H), 1.70 (2H, m, 17-H), 1.28 (8H, m, 13-H, 14-H, 19-H, 20-H), 0.86 (3H, m, 15-H), 0.84 (3H, m, 21-H); **(conformer 181' (1:19))** δ 9.72 (1H, s, 9-H), 9.65 (1H, s, 7-H), 7.40 (1H, broad d, 6-H), 6.14 (1H, broad d, 5-H);

^{13}C NMR (125 MHz; $CDCl_3$; 298 K) (conformer 181) δ 164.9 (C-4), 157.2 (C-2), 154.3 (NH*C*ONH), 146.6 (C-6), 97.2 (C-5), 50.7 (C-16), 40.1 (C-10), 31.53 (C-13), 31.3 (C-19), 29.3 (C-11), 28.9 (C-17), 26.6 (C-12), 26.10 (C-18), 22.6 (C-14), 22.4 (C-20), 14.0 (C-21), 13.9 (C-15);

^{1}H NMR (500 MHz; DMSO-d_6; 333 K) (conformer 181') δ 9.55 (1H, s, 7-H), 8.81 (1H, s, 9-H), 7.85 (1H, d, 6-H), 6.22 (1H, broad d, 5-H), 3.72 (2H, t, 16-H), 3.16 (2H, m, 10-H), 1.60 (2H, m, 17-H), 1.47 (2H, m, 11-H), 1.31 (4H, m, 12-H, 18-H), 1.29 (4H, m, 13-H, 14-H), 1,27 (4H, m, 19-H, 20-H), 0.86 (6H, m, 15-H, 21-H);

^{15}N NMR (51 MHz, $CDCl_3$) (conformer 181) δ –282.9 (N-9), -254.0 (N-7), -225.8 (N-1);

^{13}C NMR (125 MHz; DMSO-d_6; 333 K) (conformer 181') δ 162.1 (C-4), 153.8 (NH*C*ONH), 153.3 (C-2), 147.9 (C-6), 93.8 (C-5), 48.9 (C-16), 38.8 (C-10), 30.5 (C-13), 30.4 (C-19), 28.9 (C-11), 27.9 (C-17), 25.6 (C-12), 25.1 (C-18), 21.6 (C-14), 21.5 (C-20), 13.4 (C-21), 13.3 (C-15);

^{13}C CPMAS NMR (75 MHZ) (conformer 181) δ 165.7 (C-4), 157.4 (C-2), 155.1 (NH*C*ONH), 150.1 (C-6), 96.3 (C-5), 49.3 (C-16), 40.8 (C-10), 34.1 (C-13, C-19), 32.3 (C-11), 31.8 (C-17), 29.5 (C-12, C-18), 24.7 (C-14), 24.2 (C-20), 15.0 (C-15, C-21);

^{15}N CPMAS NMR (30 MHZ) (relative to $MeNO_2$) δ -280.9 (N-9), -253.8 (N-7), -223.9 (N-1), -163.8 (N-3);

m/z (ES+) 323 [(MH^+), 100%], 280 [(MH^+-C_3H_7), 55%];

HRMS calculated for $C_{17}H_{30}O_2N_4$ (MH^+) 323.24469, found 323.24362.

6-Bromo-hexan-1-ol [203]

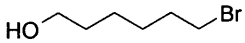

To a solution of borane sulfide (2 N in THF, 1.6 ml, 3.3 mmol) was added at 0 °C a solution of 6-bromohexanoic acid (0.5 g, 2.5 mmol) in THF (5 ml). The solution was stirred at r.t. for 16 h. The solution was quenched by addition of EtOH (10 ml) followed by water (10 ml). The solution was then extracted with CH_2Cl_2 (3 × 10 ml) and the combined organic phases were dried ($MgSO_4$). The solvent was evaporated *in vacuo* and the crude material was then purified through flash chromatography column (hexane/EtOAc, 8:1) to afford the desired compound as an oil (0.36 g, 80%).

ν_{max}/cm^{-1} (KBr film) 3300 (O-H, *s*), 2922-2850 (C-H, *s*), 1460 (C-H, *d*), 561 (C-Br, *s*);
^{1}H NMR (300 MHz; $CDCl_3$) δ 3.60 (2H, t, *J* 6.5 Hz, C*H*$_2$OH), 3.39 (2H, t, *J* 6.8 Hz, C*H*$_2$Br), 1.85 (2H, m, C*H*$_2$CH$_2$OH), 1.65 (1H, s, O*H*), 1.56 (2H, m, C*H*$_2$CH$_2$Br), 1.41 (4H, m, C*H*$_2$C*H*$_2$);
^{13}C NMR (75 MHz; $CDCl_3$) δ 62.7 (CH_2OH), 33.8 (CH_2Br), 32.7 (*C*H$_2$CH$_2$OH), 32.5 (*C*H$_2$CH$_2$Br), 27.9 (*C*H$_2$CH$_2$CH$_2$Br), 24.9 (*C*H$_2$CH$_2$CH$_2$OH);
HMRS calculated for $C_6H_{14}OBr$ (MH^+) 181.02280, found 181.02316.

2-(6-Bromo-hexyloxy)-tetrahydro-pyran (194)[204]

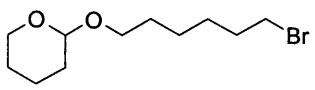

To a solution of 6-bromo hexan-ol (2 g, 11 mmol) in CH_2Cl_2 (50 ml) was added dropwise DHP (1.6 ml, 16.5 mmol) followed by PTS (0.075 g). The reaction mixture was stirred at r.t. for 16 h. The dark blue solution was then washed with water (2 × 25 ml) then saturated hydrogen carbonate solution (25 ml) and finally with a saturated sodium chloride solution (25 ml). The organic phase was then dried ($MgSO_4$) and the solvent was evaporated under reduced pressure. The crude material was then purified

through flash silica gel chromatography (hexane/EtOAc, 10:1) to afford compound **194** as an oil (0.5 g, 70%).

ν_{max}/cm^{-1} **(KBr film)** 2937-2864 (C-H, *s*), 1136 (C-O, *s*), 1118 (C-O, *s*);
^{1}H NMR (300 MHz; $CDCl_3$) δ 4.52 (1H, dd, *J* 4.3 Hz, OC*H*O), 3.81 (1H, ddd, CH*H*OCH), 3.67 (1H, dt, CH*H*OTHP), 3.41 (1H, ddd, CH*H*OCH), 3.36 (3H, m, CH*H*OTHP, C*H*$_2$Br), 1.82 (2H, m, C*H*$_2$CH$_2$Br), 1.36-1.56 (12H, m, CH$_2$C*H*$_2$CH$_2$);
^{13}C NMR (75 MHz; $CDCl_3$) δ 98.8 (O*C*HO), 67.3 (*C*H$_2$OTHP), 62.5 (*C*H$_2$OCH), 34.6 (*C*H$_2$Br), 33.8 (*C*H$_2$CH$_2$Br), 31.5 (*C*H$_2$CHO), 30.7, 29.5, 27.9, 25.4, 20.7;
m/z (ES+) 287.08 [(MNa$^+$), 100%];
HMRS calculated for $C_{11}H_{21}O_2Br$ (MNa$^+$) 287.06171, found 287.06140.

N-{2-Oxo-1-[6-(tetrahydro-pyran-2-yloxy)-hexyl]-1,2-dihydro-pyrimidin-4-yl}-acetamide (195)

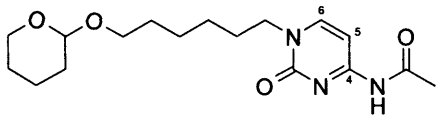

To a suspension of compound **187** (0.56 g, 3.00 mmol) in DMF (40 ml) was added anhydrous potassium carbonate (0.62 g, 4.50 mmol). The mixture was stirred at r.t. for 30 min and compound **194** (1.2 g, 4.5 mol) was added. The solution was then heated at 80 °C for 48 h. The solution was cooled down, the residue was filtered off and the filtrate was concentrated *in vacuo*. The residue was redissolved in chloroform (50 ml) and washed with water (2 × 30 ml), then saturated sodium chloride solution (2 × 30 ml). The solution was dried ($MgSO_4$) and the solvent was evaporated under reduced pressure. The crude material was then purified through flash silica gel chromatography ($CHCl_3$/MeOH, 10:1) to afford compound ***195*** as a yellow oil (0.690 g, 68%).

ν_{max}/cm^{-1} **(KBr film)** 3014 (C=C-H, *s*), 2862 (C-H, *s*), 1712 (C=O, *s*), 1660 (C=O, *s*);
^{1}H NMR (300 MHz; $CDCl_3$) δ 10.57 (1H, s, N*H*), 7.56 (1H, d, *J* 7.3 Hz, 5-H), 7.36 (1H, d, *J* 7.2 Hz, 6-H), 4.50 (1H, m, OC*H*O), 3.82 (3H, m, C*H*HOCH, C*H*$_2$N), 3.63

(1H, m, C*H*H_2OTHP), 3.40 (1H, m, C*H*HOCH), 3.30 (1H, m, CH*H*OTHP), 2.20 (3H, s, CH3), 1.70 (4H, m, CH_2CH_2N, CH_2 (THP)), 1.50-1.30 (10H, m, CH_2CH_2);

^{13}C NMR (75 MHz; $CDCl_3$) δ 171.56 (*C*OCH_3), 163.04 (C-4), 155.82 (C-2), 148.6 (C-6), 98.8 (O*C*HO), 96.9 (C-5), 67.28 (*C*H_2OTHP), 62.41 (*C*H_2OCHO), 50.91 (CH_2N), 30.74 (*C*H_2CHO), 29.50, 28.84, 26.29, 25.83, 25.42, 24.76, 19.70 (CH_3);

m/z (ES+) 360.28 [(MNa^+), 100%], 697.69 [($2MNa^+$), 20%];

HRMS calculated for $C_{17}H_{28}N_3O_4$ (MNa^+) 360.18938, found 360.18940.

4-Amino-1-[6-(tetrahydro-pyran-2-yloxy)-hexyl]-1H-pyrimidin-2-one (196)

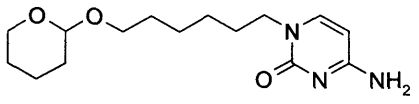

Compound **196** (0.44 g, 1.3 mmol) was dissolved in a solution of ammonia in MeOH (7 N) (50 ml). The mixture was stirred at r.t. for 16 h. After completion of the reaction the solvent was evaporated under reduced pressure and the crude material was purified over flash silica gel chromatography ($CHCl_3$/MeOH, 10:1) to give compound ***196*** as a semi-solid (0.25 g, 65%).

ν_{max}/cm^{-1} (KBr film) 3480 (N-H, primary amine, *s*), 3400 (N-H, primary amine, *s*), 2950 (C-H, *s*) 2860 (C-H, *s*), 1651 (C=O, *s*);

^{1}H NMR (400 MHz; $CDCl_3$) δ 7.14 (1H, d, *J* 7.2 Hz, 6-H), 5.76 (1H, d, *J* 7.2 Hz, 5-H), 4.51 (1H, m, OC*H*HO), 3.80 (1H, m, C*H*HOCH), 3.68 (3H, m, C*H*HOTHP, CH_2N), 3.41 (1H, m, CH*H*OCH), 3.33 (1H, m, CH*H*OTHP), 1.29-1.66 (14H, m, $CH_2CH_2CH_2$);

^{13}C NMR (125 MHz; $CDCl_3$) δ 166.0 (C-4), 156.8 (C-2), 145.1 (C-6), 98.8 (CH), 94.5 (C-5), 67.3 (*C*H_2OTHP), 62.4 (*C*H_2OCH), 50.3 (*C*H_2N), 30.6 (*C*H_2CHO), 29.4, 29.0, 26.3, 25.8, 25.3, 19.6;

m/z (ES+) 296.21 [(MH^+), 20%], 318.21 [(MNa^+), 100%], 591.49 [($2MH^+$), 60%];

HRMS calculated for $C_{15}H_{26}N_3O_3$ (MNa^+) 360.17881, found 360.17997.

1-Hexyl-3-[1-(6-hydroxy-hexyl)-2-oxo-1,2-dihydro-pyrimidin-4-yl]-urea (197)

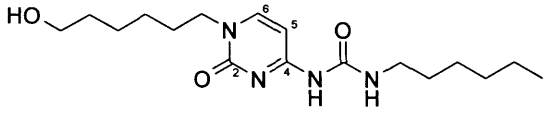

To a solution of compound **196** (0.50 g, 1.70 mmol) in dry pyridine (6 ml) was added dropwise hexylisoycanate (0.32 g, 2.5 mmol). The solution was heated at 90 °C for 16 h. The solvent was then evaporated *in vacuo*. The crude solid was redissolved in $CHCl_3$ (10 ml), washed with water (5 ml) then saturated sodium chloride solution (5 ml) and dried ($MgSO_4$). The solvent was evaporated under reduced pressure to afford a crude solid (0.50 g). The solid was dissolved in a mixture of MeOH (15 ml), THF (3 ml) and conc. HCl (3 ml). The solution was stirred at rt. for 16 h and the solvents were evaporated *in vacuo*. The residue was purified through flash silica gel chromatography ($CHCl_3$/MeOH, 9:1) to afford compound ***197*** (0.170 g, 30%).

mp: 166 °C (methanol);

ν_{max}/cm^{-1} (KBr pellet) 3219 (O-H, *s*), 3055 (C=*C-H*, *s*), 2929 (C-H, *s*), 2856 (C-H, *s*), 1701 (C=O, *s*), 1654 (C=O, *s*), 1622 (C=C, *s*), 1430 (O-H, *d*), 1053 (C-O *s*, OH);

^{1}H NMR (400 MHz; $CDCl_3$) δ 10.91 (1H, s, 7-H), 8.94 (1H, s, 9-H), 7.54 (1H, d broad, 5-H), 7.42 (1H, d, *J* 7.4 Hz, 6-H), 3.81 (2H, t, *J* 7.2 Hz, C*H*$_2$N), 3.62 (2H, t, *J* 6.4 Hz, C*H*$_2$OH), 3.23 (2H, broad q, C*H*$_2$NHCONH), 1.74 (2H, m, C*H*$_2$CH$_2$N), 1.55 (4H, m, C*H*$_2$CH$_2$NHCONH, C*H*$_2$CH$_2$OH), 1.41-1.28 (12H, m, C*H*$_2$CH$_2$), 0.86 (3H, t, *J* 6.6 Hz, CH$_3$);

^{13}C NMR (**100 MHz; $CDCl_3$)** not concentrated enough

m/z (ES+) 362.46 [(MH$^+$) 100%];

HRMS calculated for $C_{17}H_{30}N_4O_3$ (MH$^+$) 361.22101, found 361.22137.

4-Pyren-1-yl-butyric acid 6-[4-(3-hexyl-ureido)-2-oxo-2H-pyrimidin-1-yl]-hexyl ester (193)

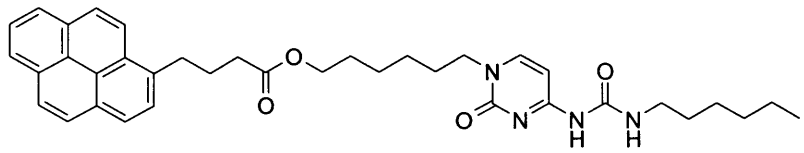

To a solution of pyrene butyric acid (0.05 g, 0.17 mmol) in CH_2Cl_2 (5 ml) was added at 0 °C, DCC (0.044 g, 0.210 mmol) and DMAP (4 mg). The mixture was stirred for 1 h. Compound **197** was then added to the mixture and the solution was stirred at r.t. for 16 h. The solid was filtered off and the filtrate washed with water (2 × 10 ml) then saturated sodium chloride solution (5 ml). The organic phase was then dried ($MgSO_4$) and the solvent evaporated *in vacuo*. The crude solid was purified using flash silica gel chromatography using a gradient: 1) ($CHCl_3$) 2) ($CHCl_3$/EtOAc, 5:1) and 3) ($CHCl_3$/EtOAc/Et_3N, 5:1:0.2). Compound ***193*** was obtained as a yellow solid (0.025 mg, 23%).

mp: 114-115 °C (chloroform);

ν_{max}/cm^{-1} (KBr pellet) 3212 (N-H, *s*), 3047 (C=*C-H*, *s*), 2927 (C-H, *s*), 2857 (C-H, *s*), 1736 (C=O, *s*), 1702 (C=O, *s*), 1659 (C=O, *s*), 1620 (C=C, *d*);

^{1}H NMR (400 MHz; $CDCl_3$) δ 10.87 (1H, s, 7-H), 8.97 (1H, s, 9-H), 8.28-7.82 (10H, m, Pyrene-H), 7.50 (1H, broad d, 5-H), 7.27 (1H, d, *J* 7.2 Hz, 6-H), 4.05 (2H, t, *J* 6.6 Hz, C*H*$_2$OCO), 3.70 (2H, t, *J* 7.2 Hz, CH_2N), 3.38 (2H, t, *J* 7.6 Hz, C*H*$_2$-pyrene), 3.23 (2H, m, C*H*$_2$NHCONH), 2.44 (2H, t, *J* 7.4 Hz, C*H*$_2$COO), 2.18 (2H, t, *J* 7.6 Hz, C*H*$_2$CH$_2$COO), 1.66-1.55 (6H, m, C*H*$_2$CH$_2$OCO, C*H*$_2$CH$_2$N, C*H*$_2$CH$_2$NHCONH), 1.32-1.27 (10H, m, C*H*$_2$CH$_2$), 0.85 (3H, t, *J* 6.7 Hz, CH_3);

^{13}C NMR (100 MHz; $CDCl_3$) δ 173.5 (*C*OO), 165.0 (C-4), 154 (NHCONH), 146.4 (C-6), 135.6 (C-33), 131.3, 130.7, 129.9, 128.6, 127.4, 127.3, 127.2, 126.6, 125.8, 125.0, 124.0, 124.8, 124.7, 124.6, 123.2, 98.9 (C-5), 64.1(COO*C*H$_2$), 50.4 (CH_2N), 40.0 (*C*H$_2$NHCONH), 33.8 (CH_2-Ar), 32.6 (CH_2COO), 31.5 (NHCONHCH$_2$CH$_2$*C*H$_2$), 29.3 (*C*H$_2$CH$_2$N), 28.7 (CH_2), 28.3 (CH_2), 26.7 (CH_2), 26.6 (CH_2), 26.0 (*C*H$_2$CH$_2$CH$_2$N), 25.5 (CH_2), 22.5 (CH_2), 14.0 (CH_3);

HRMS calculated for $C_{37}H_{44}O_4N_4$ (MH^+) 631.32548 found 631.32640.

Hexanoic acid 2,5-dioxo-pyrrolidin-1-yl ester (192)[202]

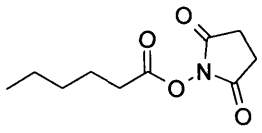

To a solution of hexanoic acid (0.2 g, 1.7 mmol) in THF (5 ml) was added at 0 °C DCC (0.391 g, 1.890 mmol). The solution was stirred for 30 min and NHS (0.215 g, 1.870 mmol) was added to the cooled solution. The mixture was stirred at r.t. for and 16 h. The solid was filtered off *in vacuo*. Ether (15 ml) was added to the filtrate solution to precipitate residual urea and the solid was filtered off. The solvent was evaporated *in vacuo* to give crude compound ***192*** (0.290 g, 80%) as a white solid, which was used in the next step without further purification.

ν_{max}/cm^{-1} (KBr pellet) 2935 (C-H, *s*), 2860 (C-H, *s*), 1728 (C=O, *s*), 1787 (*C*=*O*-N, *s*); **^{1}H NMR (CDCl$_3$; 300 MHz)** δ 2.72 (4H, s, C*H*$_2$CON), 2.50 (2H, t, q *J* 7.4 Hz, C*H*$_2$COO), 1.64 (2H, q, *J* 7.4 Hz, C*H*$_2$CH$_2$COO), 1.30 (4H, m, C*H*$_2$C*H*$_2$CH$_3$), 0.83 (3H, t, *J* 7.0 Hz, CH$_3$).

Hexanoic acid (1-hexyl-2-oxo-1,2-dihydro-pyrimidin-4-yl)-amide (191)

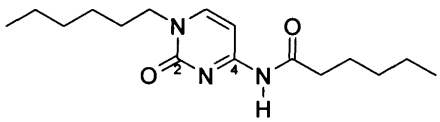

Compound **189** (0.22 g, 1.13 mmol) was added to a solution of **192** (0.29 g, 1.36 mmol) in CH_2Cl_2 (8 ml). The solution was stirred at r.t. for 16 h. The solvent was evaporated *in vacuo* and the residue was redissolved in chloroform and washed with water (10 ml) then saturated sodium chloride solution (10 ml). The organic phase was dried ($MgSO_4$) and the solvent evaporated *in vacuo*. The crude material was purified through flash silica gel chromatography ($CHCl_3$/MeOH, 7:1) to give compound ***191*** as a white solid (0.33 g, 70%).

mp: 178-180 °C;

ν_{max}/cm^{-1} (KBr pellet) 3276 (N-H, *s*), 3236 (N-H, *s*), 3045 (C=*C-H*, *s*), 2953 (C-H, *s*), 2923 (C-H, *s*), 2856 (C-H, *s*), 1701 (C=O, *s*), 1650 (C=O, *s*), 1570 (C=C-H, *d*);

^{1}H NMR (CDCl$_3$; 400 MHz) δ 10.21 (1H, s, NH), 7.56 (1H, d, *J* 7.3 Hz, 5-H), 7.37 (1H, d, *J* 7.2 Hz, 6-H), 3.81 (2H, t, *J* 7.4 Hz, C*H*$_2$N), 2.50 (2H, t, *J* 7.6 Hz, C*H*$_2$CONH), 1.68 (2H, m, C*H*$_2$CH$_2$N), 1.60 (2H, m, C*H*$_2$CH$_2$CONH), 1.25 (12H, m, C*H*$_2$CH$_2$), 0.81 (6H, m, CH$_2$C*H*$_3$);

^{13}C NMR (CDCl$_3$; 75 MHz) δ 174.4 (CONH), 162.8 (C-4), 155.7 (C-2), 148.6 (C-6), 96.6 (C-5), 49.9 (*C*H$_2$N), 37.1 (*C*H$_2$CONH), 31.2 (CH$_2$), 31.1 (CH$_2$), 28.7 (*C*H$_2$CH$_2$N), 26.0 (CH$_2$), 24.4 (*C*H$_2$CH$_2$CONH), 22.3 (CH$_2$), 22.2 (CH$_2$), 13.9 (CH$_3$), 13.7 (CH$_3$);

m/z (ES+) 294 [(MH$^+$), 100%];

HRMS calculated for $C_{16}H_{27}N_3O_2$ (MNa$^+$) 316.19955, found 316.1999.

4- Pyren-1-yl-butyric acid 2,5-dioxo-pyrrolidin-1-yl ester (199)[205]

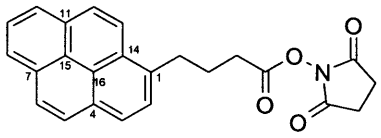

To a solution of pyrene butyric acid (0.50 g, 1.73 mmol) in DMF (8 ml) was added at 0 °C DCC (0.357 g, 1.73 mmol) and NHS (0.219 g, 1.90 mmol). The solvent was evaporated under reduced pressure. The residue was purified through flash silica gel chromatography (EtOAc) to give compound **199** as a pale yellow solid (0.40 g, 60%).

mp: 128-130 °C (EtOAc);

ν_{max}/cm^{-1} (KBr pellets) 3030 (C-H, s), 2935 (C-H, s), 1818, 1788 (C=O, s), 1728 (C=O, s);

^{1}H NMR (300 MHz; CDCl$_3$) δ 8.30-7.80 (9H, m, pyrene-H), 3.47 (2H, t, *J* 7.3 Hz, C*H*$_2$-Ar), 2.84 (4H, broad s, C*H*$_2$CON), 2.74 (2H, t, *J* 7.3 Hz, C*H*$_2$COO), 2.28 (2H, q, *J* 7.3 Hz, C*H*$_2$CH$_2$COO);

^{13}C NMR (75 MHz; CDCl$_3$) δ 169.2 (NCO), 168.6 (COO), 134.9 (Ar C-1), 131.4, 130.9, 130.2, 128.7, 127.6, 127.5, 126.9, 125.9, 125.1, 125.0, 124.9, 124.8, 123.2, 33.8 (CH$_2$-Ar), 32.2 (CH$_2$COO), 26.4 (*C*H$_2$CH$_2$COO), 25.6 (*C*H$_2$CON);

HRMS calculated for $C_{25}H_{21}O_4N$ (MNa$^+$) 408.12063, found 408.12073.

Polymer incorporating the cytosine moiety (202)

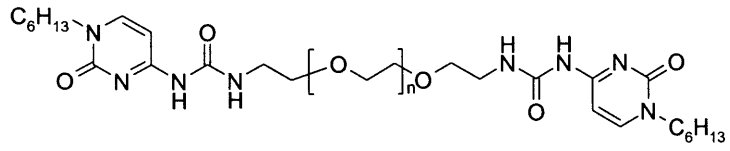

To a solution of compound **189** (0.400 g, 2.0 mmol) in dry CH_2Cl_2 (35 ml) was added *N,N*-carbonyldiimidazole (0.52 g, 2.05 mmol). The solution was stirred at r.t. for 16h. The solvent was evaporated and the residue was redissolved in dry chloroform. Hexane was added to precipitate the final material, which was dried *in vacuo* and was used directly without further purification. PEG terminated amine (0.58 g, 0.17 mmol) was dissolved in dry THF (35 ml) and the imidazole intermediate (0.200, 0.70 mmol) was added. The solution was stirred at reflux for 16 h. The solvent was evaporated and the residue was redissolved in chloroform. The organic phase was washed with water (25 ml), followed with saturated sodium chloride solution (25 ml). The organic phase was dried over $MgSO_4$ and the solvent evaporated *in vacuo*. Purification over flash silica gel chromatography ($CHCl_3$/MeOH, 7:1) gave polymer ***202*** (0.380 g, 60%).

mp: 46 °C;

ν_{max}/cm^{-1} (KBr pellets): 3230 (N-H, *s*), 3010, 2880 (C-H), 1721 (CO, *s*), 1651 (CO, urea), 1568 (C-H), 1504;

^{1}H NMR ($CDCl_3$, 500MHz) δ 10.73 (1H, s, N*H*CONHCH$_2$), 9.15 (1H, s, NHCON*H*CH$_2$), 7.42 (1H, d, *J* 7.3 Hz, 6-H), 3.78 (2H, t, *J* 7.4 Hz, CH_2N), 3.75-3.60 (170H, m, CH_2CH_2O), 1.70 (2H, m, CH_2CH_2N), 1.30 (6H, m, CH_2CH_2), 0.87 (3H, t, CH_3);

^{13}C NMR ($CDCl_3$, 125 MHz) δ 164.2 (C-4), 156.7 (C-2), 154.3 (NH*C*ONH), 146.7 (C-6), 96.7 (C-5), 70.4 (CH_2O), 70.3 (CH_2O), 69.4 (CH_2O), 50.5 (CH_2N), 39.4 (NHCONHCH$_2$), 31.1 (CH_2), 28.7 (CH_2), 25.9 (CH_2), 22.2 (CH_2O), 13.98 (CH_3);

Polymer incorporating the Upy moiety (203)

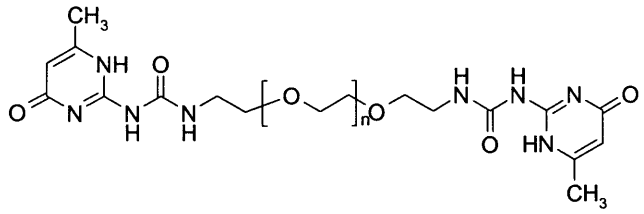

Compound **139** (0.5 g, 2.3 mmol) was suspended in dry THF (30 ml) and PEG terminated amine was added (1.94 g, 0.57 mmol). The solution was heated under reflux conditions for 16 h, and the solvent was evaporated *in vacuo*. The residue was redissolved in chloroform and washed with water (30 ml) then with a saturated sodium chloride solution (20 ml). The organic phase was then dried over $MgSO_4$ and the solvent evaporated *in vacuo* to give compound ***203*** (0.80 g, 40%).

mp: 43 °C;

ν_{max}/cm^{-1} (KBr pellets): 3223 (N-H, *s*), 2883 (C-H, *s*), 1721 (CO, *s*), 1662 (CO, urea, *s*), 1620, 1589, 1465;

^{1}H NMR (CDCl$_3$, 500 MHz) δ 13.0 (1H, s, 1-H), 11.9 (1H, s, N*H*CONHCH$_2$), 10.2 (1H, s, NHCON*H*CH$_2$), 5.79 (1H, s, 5-H), 3.75-3.60 (m, 170 H, CH$_2$C*H*$_2$O), 3.46 (4H, m, NHCONHC*H*$_2$, NHCONHCH$_2$C*H*$_2$O), 2.22 (3H, s, CH$_3$);

^{13}C NMR (CDCl$_3$, 125 MHz) δ 172.9 (C-4), 156.8 (NHCONH), 154.6 (C-2), 148.2 (C-6), 106.7 (C-5), 70.5-68.4 (CH$_2$O), 39.6 (NHCONH*C*H$_2$), 29.6 (CH$_2$), 18.9 (CH$_3$);

6.6 Specific Physical methods

6.6.1 Fluorescence Measurements

Fluorescence spectra were recorded on a Fluoro Max3 spectrophotometer (Birkbeck College) equipped with a thermostated cell, using quartz cuvett with a path length of 1 cm. The excited wavelength was fixed at 341 nm.

Chloroform used as solvent was of analytical grade, passed through basic alumina and dried over molecular sieves. The fluorescence cells were cleaned thoroughly with water, acetone and chloroform until a clear baseline without residual pyrene emission was obtained. The sample was diluted several times, from 16.4 mM to 0.033 mM. The ratio of the intensities at 476 nm and 376 nm were then calculated for each concentration and the data was analysed using a non-linear least square fitting technique:[207]

$$r = C\,(1 - (8\,K_{dim}\,[Pyr] + 1)^{1/2}) / 4$$

where r is the integral intensity ratio of the excimer emission (I_2) and the monomer emission (I_1) at 476 and 376 nm, respectively. C is a constant and [Pyr] is the total concentration of the pyrene labelled compound **193**. The results of fitting are shown in Graph 4 in the text. The data used in Graph 4 is listed below.

Concentration, mol/L	Ratio r
0.00033	0.250
0.00023	0.426
0.00033	0.703
0.00164	1.412
0.00206	1.682
0.00411	2.906
0.00822	4.572
0.01640	6.631

6.6.2 Diffusion Coefficient Measurements

All diffusion NMR experiments were carried out on a Bruker Avance 500 NMR spectrometer, equipped with *z*-gradient facilities. The convection compensated pulse sequence was used in this work.[210] Convection in solution is usually caused by small changes of temperature along the NMR sample tube and its effect is similar to that of fast diffusion. Therefore, for accurate measurements of diffusion coefficients the effects of convection must be suppressed, especially in the case of non-viscous solutions (e.g., in $CDCl_3$). The standard Bruker pulse sequence *dstegs3s* was used for the convection suppression.

In the diffusion NMR experiment used, the change of the NMR signal depends on the gradient strength according to:

$$I_i = I_0 \exp\left[-D(2\pi\gamma g_i\delta)^2\left(\Delta - \frac{\delta}{3}\right)\right] \qquad (1)$$

where γ is the gyromagnetic ratio, g_i is the amplitude of the gradient pulse (in the range from 0.7 to 33 G cm^{-1}), δ is the duration of the gradient pulse pair (3-4 ms for small molecular weight species, up to 12 ms for polymers), I_i is the signal intensity in the NMR spectrum measured for a given g_i, I_o is the signal intensity in the absence of gradient pulses, Δ is the diffusion delay [$\Delta = (200 + \delta)$ / ms in our experiments] and D is the diffusion coefficient. In each D measurement, a set of 16 or 32 separate spectra were acquired as a function of gradient amplitude. The majority of the diffusion measurements were performed for solutions in DMSO-d_6 or $CDCl_3$ at 298K. Data acquisition and processing were performed using standard Bruker XwinNMR software (version 2.6). The diffusion coefficients were determined from Eq. (1) using T_1/T_2 utility of XwinNMR. The mean deviation was in the range ±0.03 - ±0.08× 10^{-10} m^2 s^{-1} for the diffusion coefficient measurements.

In order to account for viscosity changes due to concentration changes, the solvent corrected D values are reported in the text: $D=D_{meas} \times (D^{sol}_{pure} / D^{sol}_{meas})$, where D_{meas} and D^{sol}_{meas} are the measured values for the solute and the residual solvent peak (e.g., $CHCl_3$), respectively, and D^{sol}_{pure} is the diffusion coefficient measured for the residual $CHCl_3$ in pure $CDCl_3$ (D^{sol}_{pure}=23.66 × 10^{-10} m^2 s^{-1}) or for the residual DMSO-d_5 in pure DMSO-d_6 (D^{sol}_{pure}=6.43 × 10^{-10} m^2 s^{-1}).

The value of the dimerization constant (K_{dim}) for **112** was obtained from the concentration dependence of the diffusion coefficients using the non-linear least squares fitting as implemented in the ASSOCIATE program (provided by Dr B R Peterson, Pennsylvania State University).[145, 211]

Chapter VII

7 Conclusions and Future Work

7.1 Conclusions

The synthesis of an ureidopyrimidinone compound incorporating an electron-donating group ($PhNH_2$) at the C-6 position has led to the formation of the dimeric form DADA in DMSO-d_6. It was the first time that dimeric species were observed in such polar a solvent. The polarity of the solvent combined with its ability to act as a hydrogen bond acceptor appeared to be the main reason for the tautomeric change towards the enol form. Further work has been conducted to incorporate a solubilizing side chain at the ureido position. Finally, the analysis has revealed the presence of both the 4-keto and the enol form in $CDCl_3$. These results highlighted the complexity of the Upy systems in solution in terms of the prediction of the tautomeric distribution. It is clear that factors such as polarity of the solvent, nature of the substituent at C-6 have a strong influence on the tautomeric equilibrium and that a combination of these factors can sometimes lead to unpredictable results. The formation of dimeric species that exist in a polar solvent appears particularly interesting for the design of materials that are intended to survive in biological media.

Futhermore, the use of Upy modules for the synthesis of supramolecular polymers has been achieved with the particular objective to synthesise a new class of energetic supramolecular polymers based on PolyGlyn, for use as energetic binders. In addition, the development of an alternative synthetic approach avoiding the use of isocyanate has been successfully developed leading to supramolecular polymers of appreciable quality. The synthesis of energetic precursors based on Upy has been investigated with the intention of forming supramolecular polymers incorporating these energetic modules.

In addition, the synthesis of bifunctional Upys incorporating small chiral spacers has been achieved. Notably, it was found that the use of diethyl L-tartrate or butane diol led to the formation of extremely stable cyclic dimers in chloroform with a dimerisation constant greater than 10^8 M^{-1}. The formation of new intramolecular hydrogen bonds within the cyclic species was observed in the crystal structure and was found to stabilise the dimer in solution. Upon increasing the concentration up to 500 mM in chloroform, no trace of polymeric species were observed, which suggested that the critical concentration was well above 500 mM. The incorporation of a more crowded spacer (crown ether derivative) generated the formation of cyclic species as well, although the

results were less clear due to poor solubility. These examples clearly showed how the "cyclic dimer/polymer" equilibrium can be controlled by only minor adjustments of the structure.

Finally, the design of a new quadruple hydrogen bonded DDAA array based on cytosine has been successfully achieved *via* a straightforward synthetic strategy. The structure of the linear DDAA/AADD dimer was revealed in the solid state with the observation of a weak intramolecular C-H...O close contact, which is believed to stabilise the dimer in addition to a strong quadruple hydrogen bonding network. A similar dimer was also observed in chloroform, with the presence of 5% of the folded conformer. Dilutions experiments suggested that the dimerisation constant K_{dim} is greater than 10^7 M^{-1} and 10^5 M^{-1} in benzene and chloroform, respectively. In addition, when mixed with Upy in a 1:1 ratio, the formation of heterodimer was observed, which showed that the new DDAA array compete well with very strong dimers in solution, such as Upy. This result is especially important for the design of supramolecular co-polymers. In order to investigate further the use of the new DDAA module, a supramolecular polymer incorporating a PEG chain (M_n ~ 3400 g/mol) was synthesised. On comparison with the Upy analogue, it was found that both supramolecular polymers adopted very similar behaviour both in solution and in the solid state. This last result is especially promising for the generation of novel materials based on the novel cytosine module.

7.2 Future Work

The potential of Upy units has been well studied by various research groups in the past few years. A new challenge in the field of quadruple hydrogen bonded modules is therefore the design of new arrays that can offer similar or better advantages than the Upy module. In this regard the cytosine module can play an important role in the synthesis of supramolecular materials with useful properties. Therefore, the synthesis of supramolecular polymers based on the cytosine unit is of particular interest, and especially for the AWE if energetic supramolecular polymers can be made.

The cytosine unit is particularly attractive since it only exists as one tautomer in solution. Furthermore, the possibility of functionalisation at N-1 can be very interesting since it can lead to the design of material with desired properties. Besides, it could form supramolecular polymers with two different DDAA-linker attachments (Figure 158 **A** and **B**).

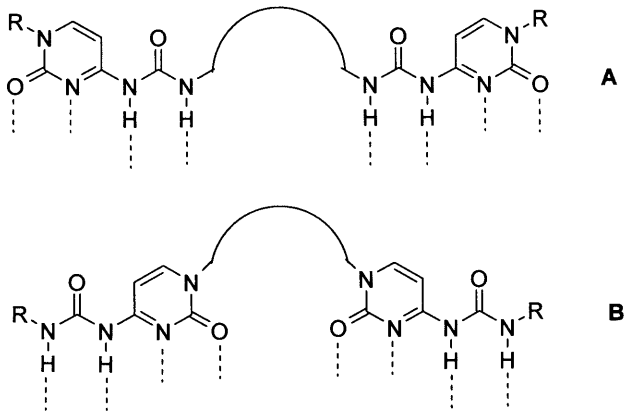

Figure 158: Possible ways of linking cytosine modules to generate bifunctional derivatives

Also, since the cytosine unit can efficiently dimerise with the Upy unit, the next challenge would be to synthesis a bifunctional system possessing different units at each end (Figure 159). This may be useful for adjustments of polymer properties.

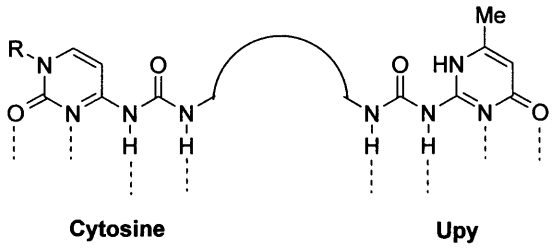

Figure 159: Supramolecular polymer incorporating both cytosine and Upy units

Futhermore, it would be interesting to study the ring/chain equilibrium with this new cytosine system and design arrays that could form exclusively cyclic species both in solution and solid state.

Clearly, the development of supramolecular arrays around the cytosine or DNA base units is one of the most promising directions of studies in the forthcoming furture. Indirectly, these studies could allow to advance our understanding of the structure and function of DNA and other related systems.

APPENDIX A

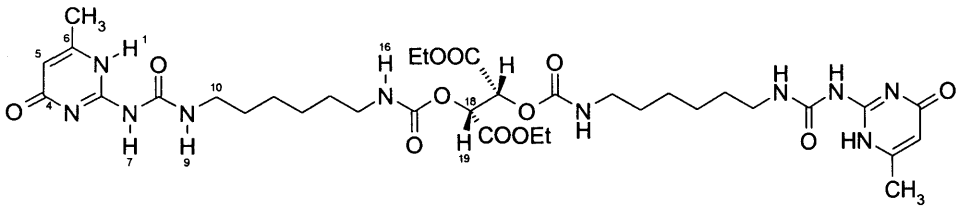

163

Crystal data and structure refinement of compound 163

Identification code	**04src0614**	
Empirical formula	$C_{34}H_{52}N_{10}O_{12}$	
Formula weight	792.86	
Temperature	120(2) K	
Wavelength	0.71073 Å	
Crystal system	Monoclinic	
Space group	$P2_1$	
Unit cell dimensions	a = 20.776(5) Å	α = 90°
	b = 19.800(4) Å	β = 90.05(2)°
	c = 21.001(7) Å	γ = 90°
Volume	8639(4) Å^3	
Z	8	
Density (calculated)	1.219 Mg / m^3	
Absorption coefficient	0.093 mm^{-1}	
F(000)	3376	
Crystal	Slab; Colourless	
Crystal size	0.44 x 0.18 x 0.08 mm^3	
θ range for data collection	2.94 – 27.48°	
Index ranges	$-26 \le h \le 25$, $-25 \le k \le 25$, $-27 \le l \le 26$	
Reflections collected	56139	
Independent reflections	36135 [R_{int} = 0.0480]	
Completeness to θ = 27.48°	95.6 %	
Absorption correction	Semi-empirical from equivalents	
Max. and min. transmission	0.9926 and 0.9600	
Refinement method	Full-matrix least-squares on F^2	
Data / restraints / parameters	36135 / 2664 / 2029	
Goodness-of-fit on F^2	1.536	
Final R indices [$F^2 > 2\sigma(F^2)$]	$R1$ = 0.1900, $wR2$ = 0.4517	
R indices (all data)	$R1$ = 0.2493, $wR2$ = 0.4766	
Absolute structure parameter	0(2)	
Largest diff. peak and hole	0.719 and –0.841 e Å^{-3}	

Diffractometer: *Nonius KappaCCD* area detector (ϕ scans and ω scans to fill *asymmetric unit* sphere). **Cell determination:** DirAx (Duisenberg, A.J.M.(1992). J. Appl. Cryst. 25, 92-96.) **Data collection:** Collect (Collect: Data collection software, R. Hooft, Nonius B.V., 1998). **Data reduction and cell refinement**: *Denzo* (Z. Otwinowski & W. Minor, *Methods in Enzymology* (1997) Vol. **276**: *Macromolecular Crystallography*, part A, pp. 307–326; C. W. Carter, Jr. & R. M. Sweet, Eds., Academic Press). **Absorption correction**: *SORTAV* (R. H. Blessing, Acta Cryst. A**51** (1995) 33–37; R. H. Blessing, J. Appl. Cryst. **30** (1997) 421–426). **Structure solution**: *SHELXS97* (G. M. Sheldrick, Acta Cryst. (1990) A**46** 467–473). **Structure refinement**: *SHELXL97* (G. M. Sheldrick (1997), University of Göttingen, Germany). **Graphics:** Cameron - A Molecular Graphics Package. (D. M. Watkin, L. Pearce and C. K. Prout, Chemical Crystallography Laboratory, University of Oxford, 1993).

APPENDIX B

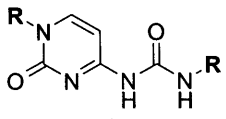

181

$R = C_6H_{13}$

Crystal data and structure refinement of compound 181

Identification code	**04src0943**	
Empirical formula	$C_{17}H_{30}N_4O_2$	
Formula weight	322.45	
Temperature	120(2) K	
Wavelength	0.71073 Å	
Crystal system	Triclinic	
Space group	*P*–1	
Unit cell dimensions	$a = 4.5636(12)$ Å	$\alpha = 81.10(3)°$
	$b = 9.979(3)$ Å	$\beta = 86.46(2)°$
	$c = 20.116(6)$ Å	$\gamma = 88.48(3)°$
Volume	903.2(5) $Å^3$	
Z	2	
Density (calculated)	1.186 Mg / m^3	
Absorption coefficient	0.079 mm^{-1}	
F(000)	352	
Crystal	Plate; Colourless	
Crystal size	0.15 × 0.10 × 0.02 mm^3	
θ range for data collection	3.08 – 27.48°	
Index ranges	$-5 \le h \le 5, -12 \le k \le 12, -26 \le l \le 26$	
Reflections collected	15490	
Independent reflections	3976 [$R_{int} = 0.0511$]	
Completeness to $\theta = 27.48°$	96.5 %	
Absorption correction	Semi–empirical from equivalents	
Max. and min. transmission	0.9984 and 0.9882	
Refinement method	Full-matrix least-squares on F^2	
Data / restraints / parameters	3976 / 0 / 211	
Goodness-of-fit on F^2	1.077	
Final *R* indices [$F^2 > 2\sigma(F^2)$]	*R1* = 0.0586, *wR2* = 0.1424	
R indices (all data)	*R1* = 0.0808, *wR2* = 0.1584	
Extinction coefficient	0.023(8)	
Largest diff. peak and hole	0.249 and –0.271 e $Å^{-3}$	

REFERENCES

1. Lehn, J. -M. *Comprehensive Supramolecular Chemistry*, Pergamin: Oxford, **1996**

2. Lehn, J. -M. *Angew. Chem., Int. Ed. Engl.* **1988**, *27*, 89-112

3. Vögtle, F. *Supramolecular Chemistry*, John Wiley and Sons: New York, **1991**

4. Lehn, J. -M. *Supramolecular Chemistry: Concepts and perspectives*, VCH: Weinheim, **1995**

5. Whitesides, G. M.; Simanek, E. E.; Mathias, J. P.; Seto, C. T.; Chim, D. N.; Mameen, M.; Gordon, D. M. *Acc. Chem., Res.* **1995**, *28*, 37-44

6. Behr, J. P. *The Lock and Key Principle. The State of the Art-100 years on*, J. Wiley & Sons: Chichester, **1994**

7. Pedersen, C. J. *Angew. Chem., Int. Ed. Engl.* **1988**, *27*, 1021-1027

8. Pedersen, C. J. *J. Am. Chem. Soc.* **1967**, *89*, 7017

9. Dietrich, B.; Lehn, J. -M.; Sauvage, J. -P. *Tetrahedron. Lett.* **1969**, *10*, 2889

10. Dietrich, B.; Lehn, J. -M.; Sauvage, J. -P.; Blanzat, J. *Tetrahedron*, **1973**, *29*, 1647

11. Dietrich, B.; Lehn, J. -M.; Sauvage, J. -P. *Tetrahedron*, **1973**, 29, 1647

12. Cram, D. J., Cram, J. M. *Science*, **1974**, *183*, 803

13. Dietrich, B.; Viout, P.; Lehn, J. -M. *Macrocyclic Chemistry*, VCH, Weinheim, **1993**

14. *Macrocycle Synthesis*, Ed. D.Parker, Oxford University Press, Oxford, **1996**

15. Cram, D. J.; Cram, J. M.; Stoddart, J. F. *The Royal Society of Chemistry*, Cambridge, **1994**

16. Lehn. J. -M. *Rep. Prog. Phys.* **2004**, *67*, 249-265

17. Blokzijil, W.; Engberts, J. B. F. N. *Angew. Chem.* **1993**, *105*, 1610-1644

18. Rekharsky, M.; Inoue, Y. *Chem. Rev.* **1998**, *98*, 1975-1917

19. Hossain, M. A.; Schneider, H. -J. *Chem. Rev.* **1997**, *97*, 2005-2062

20. Hunter, C. A.; Sanders, J. K. M. *J. Am. Chem. Soc.* **1990**, 5525-5534

21. Claessens, C. G.; Stoddart, J. F. *J. Phys. Org. Chem*, **1997**, *10*, 254-272

22. Steiner, T. *Angew. Chem., Int. Ed. Engl.* **2002**, *41*, 48-76

23. Hibber, F.; Emsley, C. *J. Adv. Phys. Org. Chem*, **1990**, *26*, 255-379

24. Jeffrey G. A. *An introduction to hydrogen bonding*, New York, Oxford University Press, **1997**

25. Kollman, P. A.; Allen, L. C. *Chem. Rev.* **1972**, 72, 283-303

26. Dingley, A. J.; Cordier, F.; Grzesiek, S. *Concepts in Magnetic Resonance* **2001**, *13* (2), 103-127

27. Schuster, P.; Zundel, G., Sandorfy, C. *The Hydrogen Bond: Recent Developments in Theory and Experiments,* vol. 1-3, North-Holland: Amsterdam, **1976**

28. Pople, J. A.; Schneider, W. G.; Bernstein, H. J. *High resolution Nuclear Magnetic Resonance,* McGraw-Hill, New York, **1959**, Chap.15

29. *Hydrogen Bonding: A Theoretical Perspective*, Oxford University, Press: New York, **1997**

30. Seebach, B.; Matthews J. L. *Chem. Commun.* **1997**, 2015-2022

31. Philp, D.; Stoddart, J. F. *Angew. Chem., Int. Ed. Engl.* **1996**, *35*, 1154-1196

32. Stryer, L. *Biochemistry*, Fouth Ed. W. H. Freeman and Co: New York, **1995**

33. Voegel, J. J.; Benner, S. A. *J. Am. Chem. Soc.* **1994**, *116*, 6929, a) www. Acessexcellence.org/.../dna_molecule.html

34. Klug, A. *Angew.Chem., Int. Ed. Engl.* **1983**, *22*, 565-583

35. Prins, L. J.; Reinhoudt, D. N.; Timmerman, P. *Angew. Chem., Int. Ed. Engl.* **2001**, *40*, 2382, 24-26

36. Terfort, A. Kiedrowski, von G. *Angew. Chem.* **1992**, *104*, 626-628; *Angew. Chem., Int. Ed. Engl.* **1992**, *31*, 654-656

37. Vötgle, F.; Dűnnuald, T.; Schmidt, T. *Acc. Chem. Res. 1996, 29*, 451-460

38. Breault, G. A.; Hunter, C. A.; Mayers, P. C. *Tetrahedron* **1999**, *55*, 5265-5293

39. Jäger, R.; Vötgle, F. *Angew. Chem.* **1997**, *109*, 966-980; *Angew. Chem., Chem. Int. Ed. Engl.* **1997**, *36*, 930-944

40. Gibson, H. W.; Hamilton, L.; Yamaguchi, N. *Polym. Adv. Technol.* **2000**, *11*, 791-797

41. Johnston, A. G.; Leigh, D. A.; Pritchard, R. J.; Deegan, M. D. *Angew. Chem.* **1995**, *107*, 1324-1327; *Angew. Chem., Int. Ed. Engl.* **1995**, *34*, 1209-1212

42. Johnston, A. G.; Leigh, D. A.; Nezhat, L.; Smart, J. P.; Deegan, M. D. *Angew. Chem.* **1995**, *107*, 1327-1331; *Angew. Chem., Int. Ed. Engl.* **1995**, *34*, 1209-1212. (a) www.chem.ed.ac.uk/leigh/

43. Ashton, P. R.; Chrystal, E. J. T.; Glink, P. T.; Menzer, S.; Schiavo, C.; Spencer, N.; Stoddart, J. F.; Taker, P. A.; White, A. J. P.; Williams, D. J. *Chem. Eur. J.* **1996**, *2*, 709-726

44. Glink, P.T.; Stoddart, J. F. *Pure & Appl. Chem.* **1996**, *70*, 2, 419-424

45. Conn, M. M.; Rebek, J. Jr. *Chem. Rev.* **1997**, *97*, 1647-1668

46. Wyler, R.; de Mendoza, J.; Rebek, J. Jr. *Angew. Chem., Int. Ed. Engl* **1993**, *32*, 1969- 1701

47. Meissner, R. S.; Rebek, J. Jr.; de Mendoza J. *Science* **1995**, *270*, 1485-1488

48. Ghadiri, M. R.; Granja, J. R.; Milligan, R. A.; McRee, D. E.; Khazanovich, N. *Nature* **1993**, *366*, 324-237

49. Ghadiri, M. R. *Adv. Mater.* **1995**, *7*, 675-677

50. Hartgerink, J. D.; Granja, J. R.; Milligan, R. A.; Ghadiri, M. R. *J. Am. Chem. Soc*, **1996**, *118*, 43-50

51. Hartgerink, J. D.; Clark, T. D.; Ghadiri, M. R. *Chem. Eur. J.* **1998**, *4*, 1367-1370

52. Khazanovich, N.; Granja, J. R.; McRee, D. R.; Milligan, R. A.; Ghadiri, M. R. *J. Am. Chem. Soc.* **1994**, *116*, 6011-6012

53. Bisson, A. P.; Hunter, C. A. *Chem. Commun.* **1996**, 1723-1724

54. Adams, H.; Carver, F. J.; Hunter, C. A.; Morales, J. C.; Seward, E. M. *Angew. Chem.* **1996**, *108*, 1628-1631; *Angew. Chem., Int. Ed. Engl.* **1996**, *35*, 1542-1544

55. Bisson, A. P.; Carver, F. J.; Eggleston, D. S.; Haltiwanger, R. C.; Hunter, C. A.; Livingstone, D. L.; McCabe, J. F. Rotger, C.; Rowan, A. E. *J. Am. Chem. Soc.* **2000**, *122*, 8856-8868. Hunter, C. A.; Jones, P. S.; Tiger, P. M. N.; Tomas, S. *Chem. Commun.*, **2003**, 1642-1643

56. Gong, B.; Yang, Y.; Zeng, H.; Skrypezak-Jankunn, E.; Kim, Y. W.; Zhu, J.; Ickes, H. *J. Am. Chem. Soc.* **1999**, *121*, 5607-5608

57. Zeng, H.; Miller, R. S.; Flowers, R. A.; Gong, H. B. *J. Am. Chem. Soc.* **2000**, *122*, 2635-2644

58. Sanford, A. R.; Yamato, K.; Yang, X.; Yuan, L.; Han, Y.; Gong, B. *Eur. J. Biochem.* **2004**, *271*, 1416-1425

59. Zhao, X.; Chang, Y. -L.; Fowler, F.; Lauher, J. W. *J. Am. Chem. Soc.* **1990**, *112*, 6627-6634

60. Hammes, G. C.; Spivey, H. O. *J. Am. Chem. Soc.* **1996**, *88*, 1621-1625

61. Etter, M. C.; Urbańczyk-Lipkowska, Z.; Zia-Ebrahimi, M.; Panunto, T. W. *J. Am. Chem. Soc.* **1990**, *112*, 8415-8426

62. Sartorius, J.; Schneider, H. -J. *Chem. Eur. J.* **1996**, *2*, 1446-1452

63. Ducharme, Y.; Wuest, J. D. *J. Org. Chem.* **1998**, *53*, 5787-5789

64. Gallant, M.; Viet, M. T. P.; Wuest, J. D. *J. Am. Chem . Soc.* **1991**, *113*, 721-723

65. Boucher, E.; Simard, M.; Wuest, J. D. *J. Org. Chem.* **1995**, *60*, 1408-1412

66. Müller, M.; Dardin, A.; Seidel, U.; Balsamo, V.; Iván, B.; Spiess, M. W.; Stadler, R. *Macromolecules* **1996**, *258*, 2566

67. delucc Freitas, L.; Stadler, R. *Colloid Polym. Sci.* **1988**, *266*, 1095-1101

68. Zimmerman, S. C.; Corbin, P. S. *Structure and Bonding* **2000**, *96*, 64-87

69. Park, T. K.; Schroeder, J.; Rebek, J. Jr. *J. Am. Chem. Soc.* **1991**, *113*, 5125

70. Schneider, J.; Juvena, R. K.; Simona, S. *Chem. Ber.* **1989**, *122*, 8024

71. Kelly, T. R.; Bidger, G. J.; Zhao, C. *J. Am. Chem. Soc.* **1990**, *112*, 8024

72. Beijer, H.; Sijbesma, R. P.; Vekemans, J. A. J. M.; Meijer, E. W.; Koojman, H.; Spek, A. L. *J. Org. Chem.* **1996**, *61*, 6371

73. Kirnos, M. D.; Khudyakov, I. Y.; Alexandrushikina, N. I.; Vanyushin, B. F. *Nature* **1997**, *270*, 369

74. Kyogoku, Y.; Lord, R. C.; Rich, A. *Proc. Natl. Acad, Sci USA* **1967**, *57*, 250

75. Murray, T. J.; Zimmerman, S. C. *J. Am. Chem. Soc.* **1992**, *114*, 4010-4011

76. Fenlon, E. E.; Murray, T. J.; Baloga, M. H.; Zimmerman, S. C. *J. Org. Chem.* **1993**, *58*, 6625-6628

77. Berstein, J.; Sterns, B.; Shaw, E.; Lott, W. A. *J. Am. Chem. Soc.* **1947**, *69*, 115

78. Murray, T. J.; Zimmerman, S. C.; Kolotuchin, S. V. *Tetrahedron* **1994**, *51*, 635

79. Fenlon, E. E.; Murray, T. J.; Baloga, M. H.; Zimmerman, S. C. *J. Org. Chem.* **1993**, *58*, 6625-6628

80. Jorgensen, W. L.; Pranata, J. *J. Am. Chem. Soc.* **1990**, *112*, 2008-2010

81. Pranata, J.; Wierschke, S. G.; Jorgensen, W. L. *J. Am. Chem. Soc.* **1991**, *113*, 2810-1819

82. Sherrington, D. C.; Taskinen, K. A. *Chem. Soc. Rev.* **2001**, *30*, 83-93

83. Kolotuchin, S. V.; Zimmerman, S. C. *J. Am. Chem. Soc.* **1998**, *120*, 9092-9093

84. Whitesides, G. M.; Simanek, E. E.; Mathias, J. P.; Seto, C. T.; Chin, D. N.; Mammen, M.; Gordon, D. *Acc. Chem. Res.* **1995**, *28*, 37-44

85. Zerkowski, J. A.; Seto, C. T.; Wierda, D. A.; Whitesides, G. M.; *J. Am. Chem. Soc.* **1990**, *112*, 9025-9026

86. Lehn, J. -M.; Mascal, M.; Decian, A.; Fisher, J. *J. Chem. Soc.; Chem. Commun.* **1990**, 479-480

87. Zerkowski, J. A.; Seto, C. T.; Whitesides, G. M. *J. Am. Chem. Soc.* **1992**, *114*, 5473-5475

88. Mathias, J. P.; Simanek, E. E.; Zerkowski, J. A.; Seto, C. T.; Whitesides, G. M. *J. Am. Chem. Soc.* **1996**, *118*, 12614-12623

89. Seto, C. T.; Whitesides, G. M. *J. Am. Chem. Soc.* **1993**, 115, 905-916

90. Seto, C. T.; Whitesides, G. M. *J. Am. Chem. Soc.* **1990**, 112, 6409-6411

91. Lehn, J. -M. *J. Chem. Soc., Perkin Trans 2* **1992**, 460-467

92. Sijbsema, R. P.; Meijer.E. W. *Curr. Opin. Colloid Interface. Sci.* **1999**, *4*, 24

93. Farnik, D.; Kluger, C.; Kunz, M. J.; Machl, D.; Petraru, L.; Binder, W. H. *Macromol. Symp.* **2004**, *217*, 247-266

94. Brunsveld, L.; Folmer, B. J. B.; Meijer, E. W.; Sijbersma, R. P. *Chem. Rev.* **2001**, *101*, 4071-4097

95. Martin, B. R. *Chem. Rev.***1996**, 3043-3064

96. Fouquey, C.; Lehn, J.-M; Levelut, A.-M. *Adv. Mater.* **1990**, *2*, 254-257

97. Kotera, M.; Lehn J.-M., Vigneron, J.-P. *J. Chem. Soc., Chem. Commun.* **1994**, 197-200

98. Kotera, M.; Lehn, J.-M.; Vigneron, J.-P. *Tetrahedron* **1995**, *51*, 1953-1972

99. Berl, V.; Schmutz, M.; Krische, M. J.; Khoury, R. G.; Lehn, J.-M. *Chem. Eur. J.* **2002**, *8*, 1227-1244

100. Sijbesma, R. P.; Meijer, E. W. *Chem. Commun.* **2003**, 5-16

101. Schmuck, C.; Wienand, W. *Angew. Chem. Int. Ed.* **2001**, *40*, 4363

102. Corbin, P. S.; Zimmerman, S. C. *J. Am. Chem. Soc.* **1998**, *120*, 9710

103. Lüning, U.; Kühl, C. *Tetrahedron Lett.* **1998**, *39*, 5735

104. Zhoa, X.; Wang, X. H.; Jiang, X. K.; Chen, Y. Q.; Li, Z. T.; Chen, G. J. *J. Am. Chem. Soc.* **2003**, *125*, 15128-15139

105. Sõntjens, S. H. M.; Meijer, J. T.; Kooijman, H.; Spek, A. L.; van Genderen, M. H. P.; Sijbesma, R. P.; Meijer, E. W. *Org. Lett.* **2001**, *24*, 3887-3889

106. Brammer, S.; Lüning, U.; Kühl, C. *Eur. J. Org. Chem.* **2002**, 4054-4062

107. Lüning, U.; Kühl, C.; Uphoff, A. *Eur, J. Org. Chem.* **2002**, 4063-4070

108. Beijer, F. H.; Kooijman, H.; Spek, A. L.; Sijbesma, R. P.; Meijer, E. W. *Angew. Chem. Int. Ed.* **1998**, *37*, 75-78

109. Hirschberg, J. H. K. K.; Brunsveld, L.; Ramzi, A.; Vekemans, J. A. J. M.; Sijbesma, R. P.; E. W. Meijer. *Nature* **2000**, *407*, 167-170

110. Schenning, A. P. H. J.; Jonkheijm, P.; Peeters, E.; Meijer, E. W. *J. Am. Chem. Soc.* **2001**, *123*, 409-416

111. Beijer, F. H.; Sijbesma, R. P.; Kooijman, H.; Spek, A. L.; Meijer, E. W. *J. Am. Chem. Soc.* **1998**, *120*, 6761- 6769

112. Sontjens, S. H. M.; Sijbesma, R. P.; van Genderen, M. H. P.; Meijer, E. W. *J. Am. Chem. Soc.* **2000**, *122*, 7487-7493

113. Söntjens, S. H. M.; Sijbesma, R. P.; van Genderen, M. H. P.; Meijer, E. W. *Macromolecules* **2001**, *34*, 3815-3818

114. Sijbesma, R. P.; Beijer, F. H.; Brunsveld, L.; Folmer, B. J. B.; Hirschberg, J. H. K. K., Lange, R. F. M.; Lowe, J. K. L.; Meijer, E. W. *Science* **1997**, *278*, 1601-1604

115. Folmer, B. J. B.; Sijbesma, R. P.; Versteegen, R. M.; van der Rijt J. A. J.; Meijer, E. W. *Adv. Mater.* **2000**, *12*, 874-878

116. Keizer, H. M.; Sijbesma, R. P.; Jansen, J. F. G. A.; Pasternack, G.; Meijer, E. W. *Macromolecules* **2003**, *36*, 5602-5606

117. El-Ghayoury A.; Peeters, E.; Schenning A. P. H. J.; Meijer, E. W. *Chem. Commun.* **2000**, 1969-1970

118. Schenning, A. P. H. J.; Jonkheijm, P.; Peeters, E.; Meijer, E. W. *J. Am. Chem. Soc.* **2001**, *123*, 409-416

119. Gonzalez, J. J.; de Mendoza, J.; Gonzalez, S.; Priego, E. M.; Martin, N.; Luo, C. D. Guldi, M. *Chem. Commun.* **2001**, 163-164

120. Rispens, M. T.; Sanchez, L.; Knol, J.; Hummelen, J. C. *Chem. Commun.***2001**, 161-162

121. Sanchez, L.; Rispens, M. T.; Hummelen, J. C. *Angew. Chem., Int. Ed. Engl.* **2002**, *41*, 838-840

122. Rieth, L. R.; Eaton, R. F.; Coates, G. W. *Angew. Chem. Int. Ed. Engl.* **2001**, *40*, 2153-2156

123. Guan, Z.; Roland, J. T.; Bai, J. Z.; Ma, S. X.; McIntire, T. M.; Nguyen, M. *J. Am. Chem. Soc.* **2004**, *126*, 2058-2065

124. Lange, R. F. M.; Van Gurp, M.; Meijer, E. W. *Polymer Sci. A: Polymer Chem.* **1999**, *37*, 3657-3670

125. Jacobson, H.; Stockmayer, W. H. *J. Chem. Phys.* **1950**, *18*, 1600-1606

126. Tessa ten Cate, A.; Sijbesma, R. P.; Meijer E. W. *Polym. Prepr. Am. Chem. Soc., Div. Polym. Chem.* **2002**, *43*, 333-334

127. Söntjens, S. H. M.; Sijbesma, R. P.; van Genderen, M. H. P.; Meijer, E. W. *Macromolecules* **2001**, *34*, 3815-381

128. Folmer, B. J. B.; Sijbesma, R. P.; Kooijman, H.; Spek, A. L.; Meijer, E. W. *J. Am. Chem. Soc.* **1999**, *121*, 9001-9007

129. Gonzalez, J. J.; Prados, P.; de Mendoza, J. *Angew. Chem., Int. Ed. Engl.* **1999**, *38*, 525-528

130. Hoffmann, R. W. *Angew. Chem., Int. Ed. Engl.* **2000**, *39*, 2055-207

131. Tessa ten Cate, A.; Sijbesma, R. P.; Meijer, E. W. *Polym. Prepr. Am. Chem. Soc., Div. Polym. Chem.* **2002**, *43*, 333-334

132. Sijbesma, R. P.; Beijer, F. H.; Brunsveld, L.; Folmer, B. J. B.; Hirschberg, J. H. K. K.; Lange, R. F. M.; Lowe, J. K. L.; Meijer, E. W. *Science* **1997**, *278*, 1601-1604

133. Folmer, B. J. B.; Sijbesma R. P.; Meijer, E. W. *J. Am. Chem. Soc.* **2001**, *123*, 2093-2094

134. Corbin P. S.; Zimmerman, S. C. *J. Am. Chem. Soc.* **1998**, *120*, 9710-9711

135. Davis, A. P.; Draper, S. M.; Dunne, G.; Ashton, P. *Chem. Commun.* **1999**, 2265-2266

136. Bauser, M.; Delapierre, G.; Hauswald, M.; Flessner, T.; D'Urso, D.; Hermann, A.; Beyreuther, B.; Vry, J.; Spreyer, P.; Reissmueller, E.; Meier, H. *Bioog. Med. Chem. Lett.* **2004**, *14*, 1997-2000

137. Wang, X-J.; Tan, J.; Zhang, L. *Org. Lett.* **2000**, *20*, 3107-3110

138. Hird, M.; Toyne, K.; Goodby, J. W.; Gray, G. W.; Minter, V.; Tuffin, R. P.; Mc Donnell, D. G. *J. Mat. Chem.* **2004**, *14*, 1731-1743

139. von Gersdoff, J.; Huber, M.; Schubert, H.; Niethamner, D.; Kirste, B. *Angew. Chem.* **1990**, *102*, 690-692

140. Coco, S.; Espinet, P.; Marcos, E.; *J. Mater. Chem.* **2000**, *6*, 1297-1302

141. Hemstra, J. M.; Moor, J. S. *Tetrahedron*, **2004**, *60*, 7287-7292

142. Hartman, H.; Zug, I. J. *J. Chem. Soc., Perkin Trans.1* **2000**, *24*, 4316-4320

143. Singh, A. K.; Das, J.; Majumdar, N. *J. Am. Chem. Soc.* **1996**, *118*, 6185-6191

144. Szczepaniak, K.; Szczepaniak, M. *J. Mol. Struct.* **1984**, *115*, 221

145. Peterson, B. R.; Wallimann, P.; Carcanague, D.R.; Diederich, F. *Tetrahedron* **1995**, *29*, 769-771

146. Atkinson, C. E.; Aliev, A. E.; Motherwell, W. B. *Chem. Eur. J.* **2003**, *9*, 1714-1723

147. Reddy, G. V.; Rao, G. V.; Subramanyam, R. V. K.; Lyengar, D .S. *Synth. Commun.* **2000**, *30*, 2233-2238

148. Keil.S.; Claus, C.; Dippold, W.; Kunz, H. *Angew. Chem., Int. Ed. Engl.* **2001**, *40*, 366-369

149. Schmidt, M.; Amstutz, R.; Crass, G.; Seebach, D. *Chem. Ber.* **1980**, *113*, 1691-1707

150. Jain, A.; Huang, S. G.; Whitesides, G. M. *J. Am. Chem. Soc.* **1994**, *116*, 5057-5062

151. Brouwer, A. J.; Mulders, S. J. E.; Liskamp, R. M. J. *Eur. J. Org. Chem.* **2000**, *10*, 1903-1916

152. Gunzenhauser, S.; Biala, E.; Strazewski, P. *Tetrahedron Lett.* **1998**, *39*, 6277-6280

153. Gunzenhauser, S.; Biala, E.; Strazewski, P. *Nucleosides Nucleotides* **1999**, *18*, 1223-1224

154. Mironov, V. F.; Sheludyakov, V. D; Kozyukov, V. P. *Zh. Obshch. Khim.***1969**, *39*, 2598 (Russ.); CA 1970, 72:66300r (Eng.)

155. Heimann, U.; Voegtle, F.; *Liebigs Ann. Chem.* **1980**, *6*, 858-862

156. Greco, M. N.; Hageman, W. E.; Powell, E. T.; Tighe, J. J.; Persico, F. J. *J. Med. Chem.* **1992**, *35*, 3180-3183

157. Yus, M.; Radivoy, G.; Alonso, F. *Synthesis* **2001**, *6*, 914-918

158. Rabouin, D.; Perron, V.; N'Zemba, B.; C.-Gaudreault, R.; Derube, G. *Bioorg. Med. Chem. Lett.* **2003**, *13*, 557-560

159. Von Gizycki, U. *Angew. Chem., Int. Ed., Engl.* **1971**, *10*, 402-406

160. Staab, H. A.; *Angew. Chem.* **1956**, *68*, 754-755

161. Staab, H. A.; Rohr, W.; Mannschreck, A.; *Angew. Chem.* **1961**, *73*, 143

162. Lin, Y-M .; Miller, M. J. *J. Org.Chem.* **2001**, *86*, 8282-8286

163. Chen, A.; Wu, D.; Johnson, C. S. Jr. *J. Am. Chem. Soc.* **1995**, *117*, 7965-7970

164. a) Provatas, A. DSTO-TR-0966, b) Urbanski, T. *Chemistry and Technology of Explosives* **1984**, Vol 4, Pergamon Press: New York

165. Yasohara, Y.; Kizaki, N.; Haseyawa, J.; Wada, M.; Kataoka, M.; Shimizu, S. *Tetrahedron: Asymmetry* **2001**, *12*, 1713-1718

166. Beck, G.; Jendralla, H.; Kesseler, K. *Synthesis* **1995**, *8*, 1014-1018

167. Gillaizeau, I.; Charamon, S.; Agrofoglio, L. A. *Tetrahedron Lett.* **2001**, *42*, 8817-8820

168. Liu, W.; Wise, D. S; Townsend, L. B. *J. Org. Chem.* **2001**, *66*, 44, 4783-4786

169. Toshihita, U.; Morinobu, S.; Tetsu, K.; Nobuo, I. *Bull. Chem. Soc. Jpn.* **1983**, *68-56*, 2, 572

170. Scheurer, A.; Mosset, P.; Bauer, W.; Saalfrank, R. W. *Eur. J. Org. Chem.* **2001**, 3067-3074

171. Appel R.; Baume, G.; Struver, W.; *Chem. Ber.* **1975**, 2680-2692

172. Tessa ten Cate, A.; Kooijman, H.; Spek, A. L.; Sijbesma, R. P.; Meijer, E. W. *J. Am. Chem. Soc.* **2004**, *126*, 3801

173. Massicot, F.; Plantier-Royon, R.; Portella, C.; Saleur, D.; Sudha, A. V. R. L. *Synthesis* **2001**, *16*, 2441-2444

174. Marastoni, M.; Bergonzoni, M.; Bortolotti, F.; Tomatis, R. *Arzneim Forsch.* **1997**, *47*, 7, 889-894

175. Montero, A.; Goya, P.; Jagerovic, N.; Gallado, L. F.; Meana, J. J.; Giron. R.; Goicoechea, C.; Martin, I. *Bioorg. Med. Chem.* **2002**, *10*, 4, 1009-1018

176. Schlecht, M. F. *Molecular Modelling on the PC.* Wiley-VCH: New York, **1998.** The software used for the force field calculatation was PCMODEL [version 8.5, Serena Software]

177. Tessa ten Cate, A.; Dankers, P. Y. W.; Kooijman, H.; Spek, A. L.; Sijbesma, R. P.; Meijer, E. W. *J. Am. Chem. Soc.* **2003**, *125*, 6860-6861

178. Horvath, A.; Benner, J.; Baeckvall, J-E. *Eur. J. Org. Chem.* **2004**, *15*, 3240-3243

179. Towmsend, J. M.; Blount, J.-F.; Sun, R. C.; Zawoiski, S.; Valentine, D. *J. Org. Chem.* **1980**, *15*, 2995-2999

180. Dehmlow, E. V.; Sauerbier, C. *Liebigs Ann. Chem.* **1989**, 181-186

181. Kaky, R.; Nicholson, P. E.; Parker, D. *J. Chem. Soc., Perkin. Trans 2* **1990**, *2*, 321-327

182. Johansson, G.; Percec, V.; Ungar, G.; Abramic, D. *J. J. Chem. Soc., Perkin Trans 1.* **1994**, *4*, 447-460

183. Chenevert, R.; Voyer, N.; Plante, R. *Synthesis* **1982**, *9*, 782

184. Dardonville, C.; Jagerovic, N.; Callado, L.F.; Meana, J. *J. Bioog. Med. Chem. Lett.* **2004**, *14*, 491-494

185. Chabner, B. A. *Cytidine analogues. In: Cancer Chemotherapy and Biotherapy-Principles and Practice.* Eds Chabner, B. A. and Longo, D. L. Lippincott-Raven, Philadelphia, **1996**, 213–234.

186. Rueda, M.; Luque, F. J.; López, J. M.; Orozco, M.; *J. Phys. Chem. A.* **2001**, *105*, 6575-6580

187. Ogretir, C.; Yaman, M. *J. Mol. Struct.* **1999**, *458*, 217-226

188. Shoup, R. R.; Miles, H. T.; Becker, E. D. *J. Phys. Chem.* **1972**, *76*, 64

189. Parthasarathy, R.; Ginell, S. L.; De, N. C.; Chheda, G. B. *Biochem. Biophys. Res. Commun.* **1974**, 83, 657

190. Kawai, G.; Hashizume, T.; Yasuda, M.; Miyazawa, T.; McCloskey, J. A.; Yokoyama, S. *Nucleosides and Nucleotides* **1972**, *11*, 759

191. Corbin, P. S.; Zimmerman, S. C. *J. Am. Chem. Soc.* **2000**, *122*, 3779-3780

192. Okabe, M.; Sun, R-C.; Zenchoff, G. B. *J. Org. Chem.* **1991**, *56*, 4392-4397

193. Lindsell, W. E.; Murray, C.; Preston, P. N.; Woodman, T. A. J. *Tetrahedron* **2000**, *56*, 1233-1245

194. Sun, F.; Darbre, T.; Keese, R. *Tetrahedron* **1999**, *55*, 9777-9786

195. Schroeder, A. C.; Hughes, R. G.; Bloch, Jr. A. *J. Med. Chem.* **1981**, *24*, 1078-1083

196. Sutor, D. J. *J. Chem. Soc.* **1963**, 1105-1110

197. Desiraju, G. R. *Acc. Chem. Res.* **1996**, *29*, 444-449

198. Aakeroy, C. B.; Beatty, A. M. *Aust. J. Chem.* **2001**, *54*, 409-421

199. Guo, D.; Sijbesma, R.P.; Zuilhof, H. *Org. Lett.* **2004**, *6*, 3667-3670

200. Rebek, J. Jr.; Askew, B.; Ballester, P.; Buhr, C.; Jones, S.; Nemeth, D.; Williams, K. *J. Am. Chem. Soc.* **1987**, *109*, 5033-5035

201. Günther, H. *NMR Spectroscopy. Basic Principles, Concepts, and Applications in Chemistry. 2nd edition*, John Wiley & Sons, Chichester, **1995**, 581

202. Shanan-Atidi, H.; Bar-Eli, K.H. *J. Phys. Chem.* **1970**, *74*, 961-962

203. Danklmaier, J.; Hoenig, H. *Liebigs Ann. Chem.* **1990**, 145-150

204. Mattes, H.; Benezra, C. *J. Org. Chem.* **1988**, *53*, 2732-2737

205. Clyne, D. S.; Weiler, L. *Tetrahedron* **1999**, *55*, 13659-13682

206. Tong, G.; Lawlor, J. M.; Tregear, G. W.; Haralambidis, J. *J. Am. Chem. Soc.* **1995**, *117*, 12151-12158

207. Hossain, M. A.; Matsumura, S.; Kanai, T.; Hamasaki, K.; Mihara H.; Ueno, A. *J. Chem. Soc., Perkin Trans. 2* **2000**, 1527-1533

208. Li, X-Q.; Feng, D-J.; Jiang, X-K.; Li, Z-T. *Tetrahedron* **2004**, *60*, 8275-8284

209. Wang, X-Z.; Li, X-Q.; Shao, X-B.; Zhao, X.; Deng, P.; Jiang,X-K.; Li, Z-T.; Chen, Y-Q. *Chem. Eur. J.* **2003**, *9*, 2904-2913

210. Jerschow, A.; Müller, N. *J. Magn. Reson.* **1997**, *125*, 372–375

211. Carcanague, D. R.; Diederich, F. *Angew. Chem., Int. Ed. Engl.* **1990**, *29*, 769–771